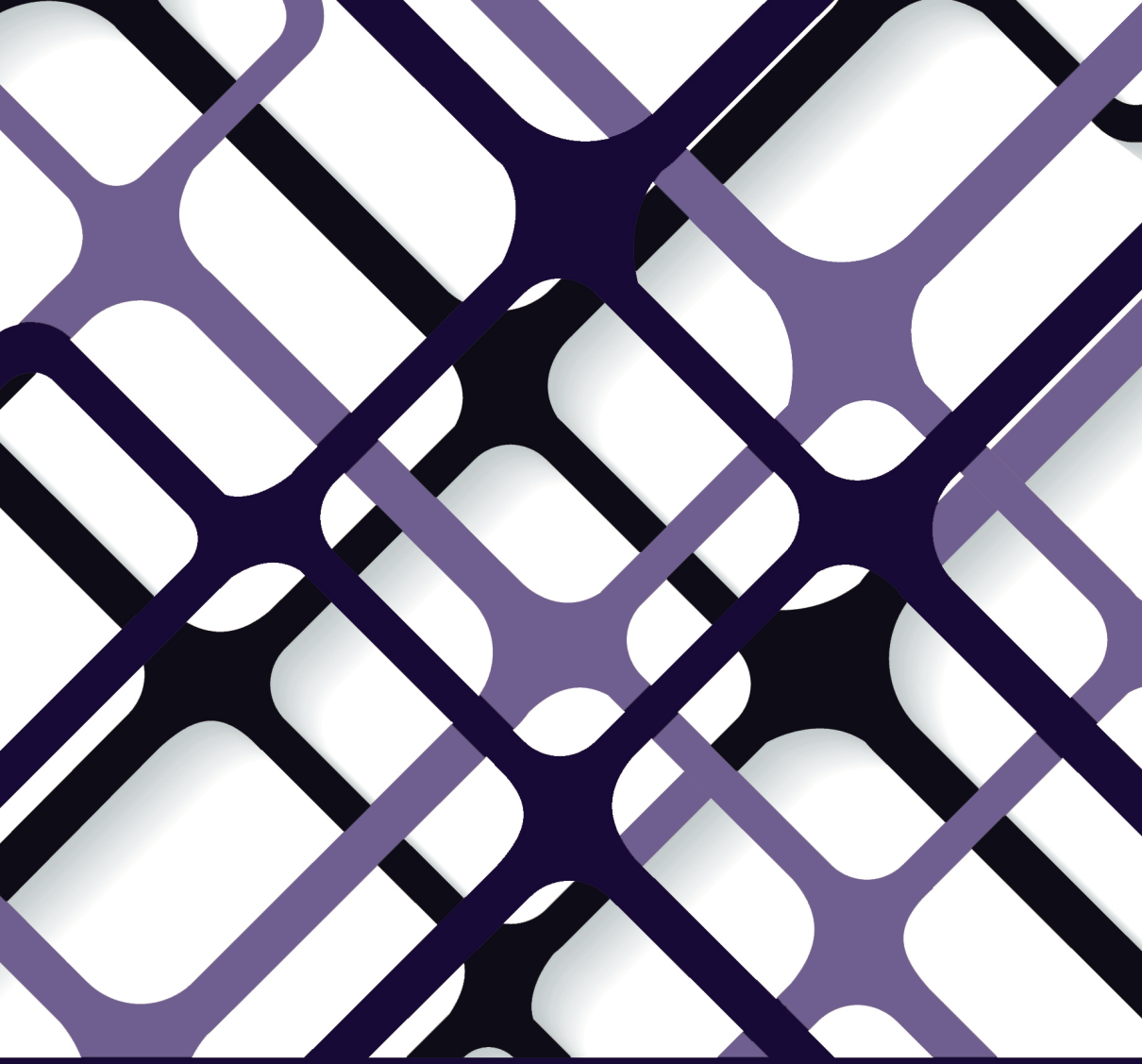

RESEARCH & REVIEWS IN ENGINEERING - I

SEPTEMBER/2021

EDITORS
PROF. DR. BANU NERGİS
ASSOC. PROF. DR. SELAHATTİN BARDAK
ASSOC. PROF. DR. MAHMUT KAYAR
DR. ARİF FURKAN MENDİ

gece kitaplığı

İmtiyaz Sahibi / Publisher • Yaşar Hız
Genel Yayın Yönetmeni / Editor in Chief • Eda Altunel
Kapak & İç T asarım / Cover & Interior Design • Gece Kitaplığı
Editörler / Editors • Prof. Dr. Banu NERGİS
Assoc. Prof. Dr. Selahattin BARDAK
Assoc. Prof. Dr. Mahmut KAYAR
Dr. Arif Furkan MENDİ
Birinci Basım / First Edition • © Eylül 2021
ISBN • 978-625-8002-44-7

Gece Kitaplığı / Gece Publishing
Türkiye Adres / Turkey Address: Kızılay Mah. Fevzi Çakmak 1. Sokak Ümit Apt. No: 22/A Çankaya / Ankara / TR
Telefon / Phone: +90 312 384 80 40
web: www.gecekitapligi.com
e-mail: gecekitapligi@gmail.com

Baskı & Cilt / Printing & Volume
Sertifika / Certificate No: 47083

RESEARCH & REVIEWS IN ENGINEERING - I

September / 2021

EDITORS
PROF. DR. BANU NERGİS
ASSOC. PROF. DR. SELAHATTİN BARDAK
ASSOC. PROF. DR. MAHMUT KAYAR
DR. ARİF FURKAN MENDİ

gece kitaplığı

CONTENTS

Chapter 1

MITIGATION OF HARMONIC DISTORTION IN A THREE-PHASE FULL-WAVE CONTROLLED RECTIFIER

Süleyman ADAK[1]
Hasan CANGI[2]

1 Assistant Professor Süleyman Adak, suleymanadak@yahoo.com, ORCID:0000-0003-1436-2830, Mardin Artuklu University, Vocational School, Electrical and Energy Department, Mardin, Turkey
2 Dr.Hasan Cangi, HASCAN Engineering and contracting company,cangihasan@gmail.com ORCID: 0000-0003-1436-2830, HASCAN Engineering and contracting company, Mardin, Turkey, Reducing harmonic distortion in energy systems, Supervisor :Prof.Dr. Celal Kocatepe, Yildiz Technical University, Graduate School of Natural and Applied Sciences

1. Introduction

Non-linear loads that increasing use of with the development of technology, caused disorders in the sinusoidal form of current and voltage signals. Non-linear waveform contains harmonic components. These harmonic components occur in integer multiples of the main components (50 Hz), such as 150Hz, 250Hz, 350Hz and 750Hz are the 3rd 5th, 7th,.., and 15th harmonic components of a 50Hz fundamental waveform. Harmonic distortion is generally caused by a nonlinear waveform in electrical power systems networks. Harmonic components in the power system will cause in the following hazards at electricity networks:

- Overheating in power lines.
- Resonance in power systems.
- Shortening of life transformers and electrical devices.
- Drilling of the compensation capacitor.
- Protective devices in power systems open timeless due to the harmonic components.
- Parasites in communication facilities.

Converters, rectifiers and frequency drives are used in power electronics. They are the most important sources of harmonic sources. Today, renewable energy sources have great importance in power system. These systems do not have hazards to the environment. In contrast, they are environment friendly. DC/AC converter and inverter are used in these systems Converters and inverters are accomplished by power transistors.

During the production, transmission and distribution of electrical energy, it is desired that the waveform of current and voltage magnitudes be in sinusoidal form. This condition is one of the main factors that determine the quality of electrical energy. However, for many reasons, these fundamental sizes lose their basic properties, causing unwanted harmonics to occur in the system. Harmonic components disrupt the sinusoidal current and voltage waveforms. These waves are called non-sinusoidal waves. The non-linear wave consists of the basic component and sinusoidal waves. Non-sinusoidal waves are expressed in terms of fundamental component and other harmonic components with the help of Fourier analysis.

Also most electronic power supply switching circuits such as rectifiers, silicon controlled rectifier (SCR's), power transistors, power converters and other such solid state switches which cut and chop the power supplies sinusoidal waveform to control motor power, or to convert the sinusoidal AC supply to DC. Theses switching circuits tend to draw current only at

the peak values of the AC supply and since the switching current waveform is non-sinusoidal the resulting load current is said to contain harmonics.

Harmonic components in electrical facilities; they cause additional energy losses, additional voltage drops, resonance events in the power system, low power factor, and consumer low quality energy. Especially AC/DC converters are an important harmonic source in electrical installations. The six-pulse controlled rectifier effectively contains 5th, 7th, 11th, 13th harmonic components. The principle diagram of the power system is as given in Fig. 1.

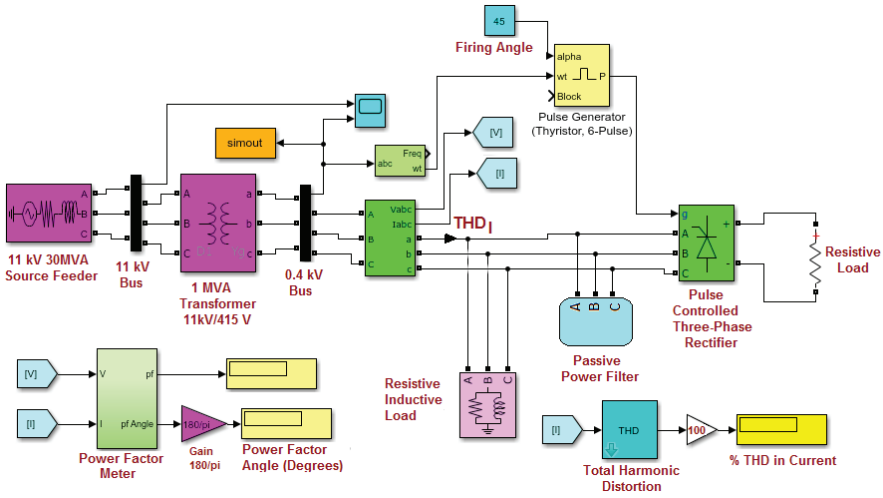

Fig.1. Principle scheme of the power system containing non-linear elements

The harmonic distortion observed in the electrical systems is gradually increasing due to the power electronics-based converters, the use of uninterrupted power supplies with their choppers and their application areas, and the resulting harmonic components cause the energy quality to decrease. As a result of increased harmonic distortion, they damage the devices and cause power losses. Harmonic components are expressed in the power system as exactly multiples of the fundamental frequency. Frequency of harmonic components is found from equation (1).

$$f_n = \mathrm{n}.\, f_1 \qquad (1)$$

Where, n is the degree of harmonic component, f_1 is basic component. According to equation (1), the third harmonic component is calculated as f_3 = 150 Hz, the fifth harmonic component, f_5 = 250Hz The six-pulse controlled rectifier effectively contains 5th, 7th, 11th, 13th harmonic components. Non-linear characteristic elements cause serious harmonic pollution in power systems and decrease the quality of the energy given to the consumer. To ensure reliable and stable operation of the power system, non-linear elements or harmonic components produced by non-sinusoidal sources should be determined.

In power systems, passive filters are used to suppress harmonic currents and decrease voltage distortion appearing in sensitive parts of the system. A passive filter component is a combination of capacitors and inductors that are tuned to resonate at a single frequency, or through a band of frequencies. In power systems, passive filters are used to suppress harmonic currents and decrease voltage distortion appearing in sensitive parts of the system. A passive filter component is a combination of capacitors and inductors that are tuned to resonate at a single frequency, or through a band of frequencies.

2. Modeling and analysis of the power system

In electrical power systems, harmonic distortion often affects the entire system at great distances from the original sources. Harmonics components are pollution in power systems. As the use of static converters and non-linear elements in energy systems, this pollution rate increases day by day. As a result, harmonic distortion for current or voltage also increases.

The purpose of passive filters is to determine the L and C values that will resonate at the harmonic component frequency that is desired to be destroyed. For each harmonic component, a separate filter arm should be placed to resonate that component. Passive filters can be adjusted to the frequency that makes inductive and capacitive reactance equal to each other. The quality factor Q determines the setting acuity. Depending on the Q factor, the filter is either high pass or low pass. Filter calculations are made by making use of the power formula to be compensated. Reactive power value required for compensation in power system;

$$QKom = P\tan(\cos{-1}\varphi_1) - \tan(\cos{-1}\varphi_2) \quad (2)$$

Where Cos φ_1 pre-compensation power factor, Cos φ_2 power factor after compensation, P the active power of the power system. The most used method for compensation of power systems is compensation made

with passive filters. Distribution of reactive power to passive filters;

$$Q_{fh} = Q_{Kom}\frac{I_h}{\sum I_h} \qquad h = 2,3.. \qquad (3)$$

Where, Q_{fh}, reactive power of the "h" harmonic component, Q_{Kom} is the reactive power required for compensation in the power system, I_h the amplitude of the "h" harmonic current component, ∑Ih shows the sum of harmonic currents. As a result of non-linear loads in the power system, the additional loss and total harmonic distortion (THD) values reach high values.Total harmonic distortion for current,

$$THD_I = \frac{\sqrt{I_2^2 + I + I + \ldots\ldots + I}}{I_1} * 100\% \qquad (4)$$

It is defined as the ratio of the effective values of the harmonic components to the main component effective value. It is usually expressed as a percentage. This value is a measure of the deviation of the non-linear waveform from the sine waveform. The amount of waveform distortion present giving a complex waveform its distinctive shape is directly related to the frequencies and magnitudes of the most dominant harmonic components whose harmonic frequency is multiples (whole integers) of the fundamental frequency. The most dominant harmonic components are the low order harmonics from 2nd to the 19th with the triplens being the worst. The principle diagram of the power system is as given in Fig. 2.

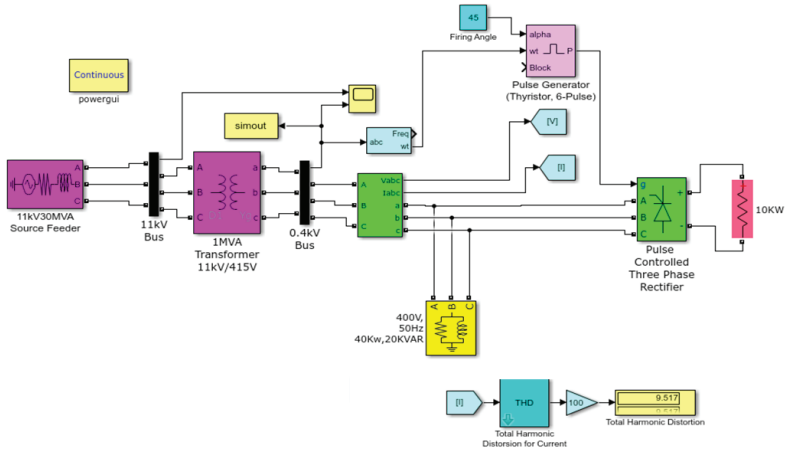

Fig.2. Simulink equivalent of power system (before filtering)

Before filtering, the total harmonic distortion was measured as 9,517%. These value is high and exceed the limit values specified in the standards. In this book, power quality indices are analyzed for an industrial three phase full wave controlled rectifier as a non-linear load. The amplitudes of the harmonic currents and voltages are inversely proportional to their order, and as the order gets larger, the harmonic amplitude decreases.

Harmonic components currents flow from the harmonic source to the lowest impedance in the power system. The impedance seen by the harmonic current source is the impedance of the system source impedance and other loads connected in parallel to the system. The principle diagram of three phase full wave controlled rectifier is given in Fig. 3.

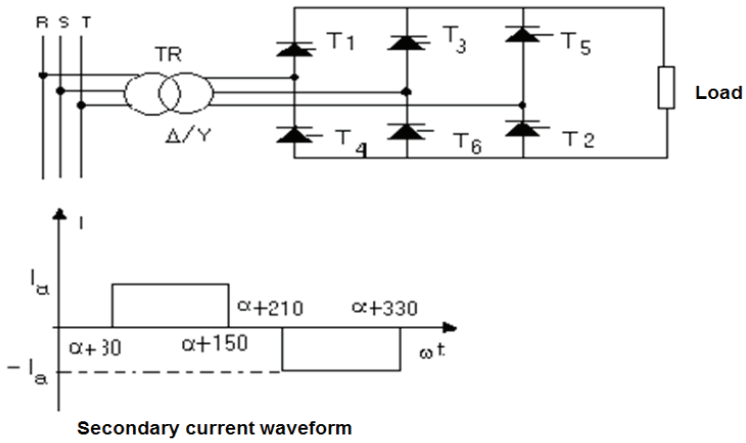

Fig. 3 Three-phase full-wave controlled rectifier and input current waveform

Fig. 3 shows the controlled rectifier circuit and the input current waveform. Fourier series for the controlled rectifier as follows:

$$I = I_d + \sum_{n=1}^{\infty} (A_n \cos(n\omega t) + B_n \sin(n\omega t)) \quad (5)$$

The direct current component is found by equation (4).

$$I_d = \frac{1}{2\pi} \int_0^{2\pi} i_1(t) d\omega t = 0 \quad (6)$$

A_n component of the Fourier series,

$$A_n = \frac{1}{\pi} \int_0^{T} i_1(t) \cos(n\omega t) d\omega t \quad (7)$$

$$A_n = \frac{1}{\pi}\left[\int_{\pi/6+\alpha}^{5\pi/6+\alpha} I_a \cos(n\omega t)d\omega t - \int_{7\pi/6+\alpha}^{1\ \pi/6+\alpha} I_a \cos(n\omega t)d\omega t\right] \quad (8)$$

$$A_n = \frac{I_a}{\pi n}\left\{\left[\sin \omega t\right]_{\pi/6+\alpha}^{5\pi/6+\alpha} - \left[\sin \omega t\right]_{7\pi/6+\alpha}^{1\ \pi/6+\alpha}\right\} \quad (9)$$

The general expression of the An component is as follows.

$$A_n = \frac{4I_a}{\pi.n}\sin\frac{n\pi}{3}\sin n\alpha \qquad (n = 1,3,5.....) \quad (10)$$

Bn component of the Fourier series,

$$B_n = \frac{1}{\pi}\int_0^{2\pi} i_1(t)\sin(n\omega t)d\omega t \quad (11)$$

(12)

$$B_n = \frac{1}{\pi}\left[\int_{\pi/6+\alpha}^{5\pi/6+\alpha} I_a \sin(n\omega t)d\omega t - \int_{7\pi/6+\alpha}^{1\ \pi/6+\alpha} I_a \sin(n\omega t)d\omega t\right]$$

$$B_n = \frac{I_a}{n.\pi}\left\{\left[-\cos n\omega t\right]_{\pi/6+\alpha}^{5\pi/6+\alpha} - \left[-\cos n\omega t\right]_{7\pi/6+\alpha}^{1\ \pi/6+\alpha}\right\} \quad (13)$$

$$B_n = \frac{4I_a}{n.\pi}\sin\frac{n\pi}{3}\cos n\alpha \qquad (n = 1,\ 3,\ 5.....) \quad (14)$$

is found. Effective value of input current,

$$I_n = \frac{\sqrt{A_n^2 + B_n^2}}{\sqrt{2}} = \frac{2\sqrt{2}I_a}{n\pi}\sin\frac{n\pi}{3} \quad (15)$$

Analytical equation of input current,

$$i_n(t) = \frac{4.I_a}{n\pi}\sin\frac{n\pi}{3}\sin(n\omega t - n\alpha) \quad (16)$$

is found. In short, harmonics are undesirable quantities in energy systems, as they affect all elements in the system. The forms of non-sinusoidal waves consist of the sum of other sinusoidal waves with different frequency and amplitude. Sinusoidal waves other than the basic wave are called "harmonic components". The graph of the nonlinear load current is as given in Fig. 4.

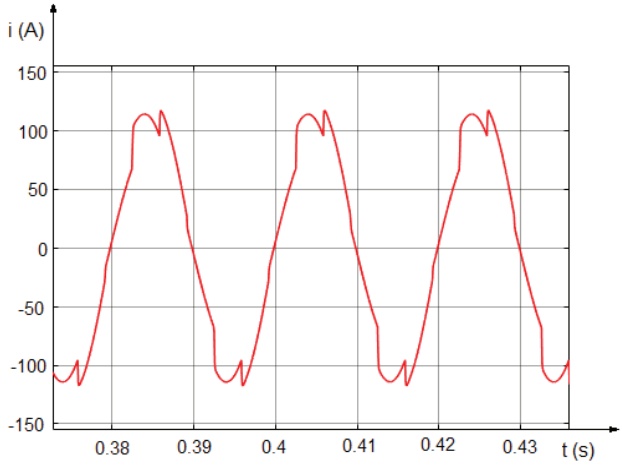

Fig. 4. Non-linear characteristic load current waveform

Power electronics-based choppers, transformers and inverters used in power systems are harmonic sources. Because of their operating characteristics, deviations occur in the sinusoidal waveform of current and voltage. High pulse rectifiers should be used to reduce harmonic components in power systems. As the number of pulses at the rectifier output increases, the waveform resembles the sine curve and the THD value decreases.

Table 1 Harmonic components in the power system (without filter)

Harmonic components	The amplitude of harmonic components (A)	Phase angle of harmonic components (Degrees)
h1	116.4	-0.0459
h3	0	0
h5	8.374	144.2
h7	4.129	21.47
h9	0	0
h11	3.347	-133
h13	2.327	104.4
h15	0	0
h17	2.081	-50.1
h19	1.6	-172.5
h21	0	0
h23	1.499	32.83
h25	1.204	-89.33

h27	0	0
h29	1.162	115.9
h31	0.9541	-5.97
h33	0	0
h35	0.9401	-161
h37	0.7812	77.56
h39	0	0
h41	0.7827	-77.66
h43	0.6544	161.3
h45	0	0
h47	0.6647	5.808
h49	0.5576	-114.8

Power electronics-based choppers, transformers and inverters used in power systems are harmonic sources. Because of their operating characteristics, deviations occur in the sinusoidal waveform of current and voltage. High pulse rectifiers should be used to reduce harmonic components in power systems. As the number of pulses at the rectifier output increases, the waveform resembles the sine curve and the THD value decreases.

Even if non-linear characteristic loads are low power, they disrupt the sinusoidal current and voltage waveform in power systems. Considering a large number of non-linear loads connected to power systems, they result in increased harmonic distortion values with additional losses. The harmonic components of the nonlinear current wave are as shown in Fig. 5.

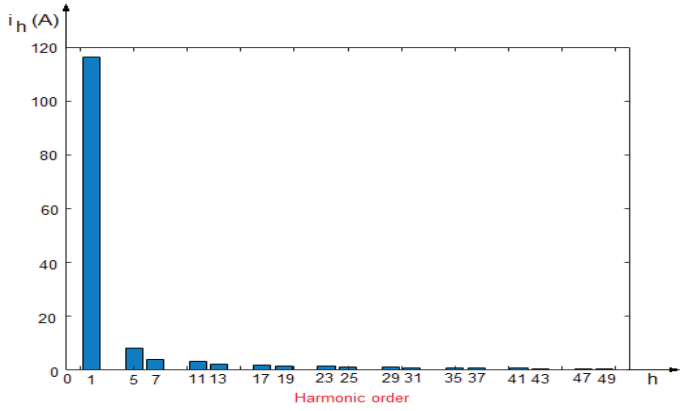

Fig. 5. Amplitude of harmonic components of the non-linear load(before filtering)

In short, harmonic components are undesirable quantities in power systems, as they affect all elements in the system. Therefore, it is absolutely

necessary to install filter circuits that will filter harmonics. Passive filters are placed in parallel in the power system. Among these filters, bandpass and highpass filters are used very often in the power system. The power transformer secondary current waveform as shown below.

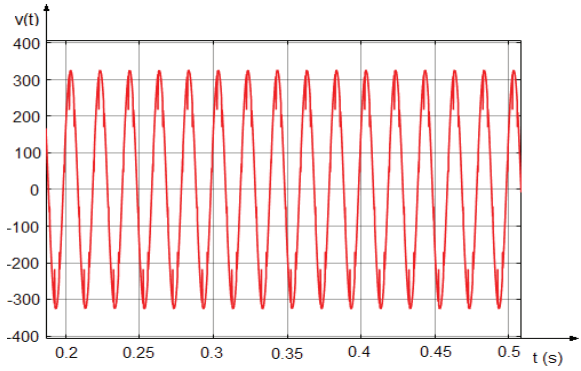

Fig. 6. Secondary voltage of the power transformer

Resonance conditions must be calculated separately for each harmonic component. It causes damage to equipment in power system. High-grade harmonic components can affect the entire power system. These effects also reduce the performance of the power system and other equipment.

3. Reducing of total harmonic distortion in power system

In power systems, it is desired that the current and voltage waveform be in sinusoidal form and at a 50 Hz frequency. This condition is one of the main factors that determine quality of energy. However, due to many reasons, the waveform of this current and voltage loses its basic properties and harmonic components are occured in the power system.

To operate electric energy system and their loads reliably, the waveform of the system magnitudes should be in the form of sinusoidal with 50 Hz . However, owing to elements connected to the power system and some events the voltage and current waveform are deviated from pure sinusoidal form, which cause to undesired harmonics. It has long been known that nonlinear loads cause to voltage and current waveform distortion in distribution networks. In addition importance of the research on this subject has recently intensified due to both the widespread use of power electronic devices and the increase in the number of sensitive electrical devices to waveform distortion. Voltage and current waveform distortion due to harmonics can make the electrical system and electrical consumer either demaged or out of order.

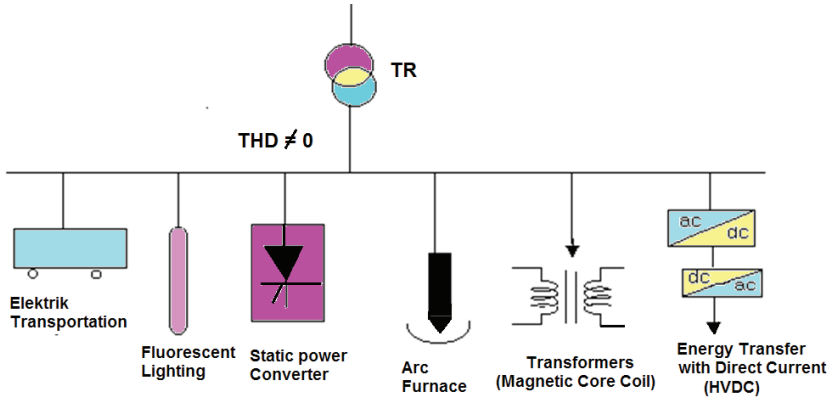

Fig.7 Non-linear loads (harmonic current sources)

Important harmonic sources that cause harmonic components in power systems are as follows;

- One and three phase transformers,
- Rotary electric machines,
- Converters,
- Arc furnaces,
- Gas discharge armatures,
- Static VAR compensators (SVC),
- Photovoltaic solar systems,
- Computers,
- Uninterruptible power supplies (UPS), :Uninterruptible Power Supply),
- High voltage energy transport with direct current,
- Electric locomotives.

The analysis of these elements, which are the source of harmonic, is great importance. Non-linear characteristic load current is as given below.

$$\begin{aligned} i(\omega t) = {} & 116.4\sin(\omega t - 0.046) + 8.374\sin(5\omega t + 144.2) + 4.129\sin(7\omega t + 21.47) \\ & + 3.347\sin(11\omega t - 133) + 2.327\sin(13\omega t + 104.4) + 2.081\sin(17\omega t - 50.1) \\ & + 1.6\sin(19\omega t - 172.5) + 1.499\sin(23\omega t + 32.83) + 1.204\sin(25\omega t - 89.33) \\ & + 1.162\sin(29\omega t + 115.9) + 0.9541\sin(31\omega t - 5.97) \\ & + 0.9401\sin(35\omega t - 161) + 0.7812\sin(37\omega t + 76.56) \\ & + 0.7827\sin(41\omega t - 77.66) + 0.6544\sin(43\omega t + 161.3) \\ & + 0.6647\sin(47\omega t + 5.8008) + 5.5576\sin(49\omega t - 114.8) \end{aligned} \quad (17)$$

The graph of this non-linear characteristic current wave is as shown in Fig. 8.

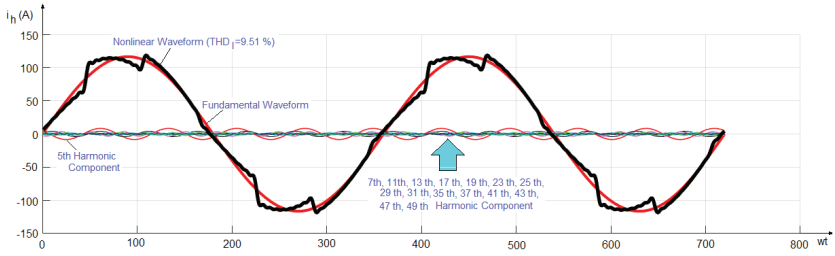

Fig. 8. *Non-linear waveform with the harmonic components*

Power electronics equipment is an important source of harmonics. In general terms, rectifiers, inverters, frequency inverters and choppers are harmonic sources. These devices produce harmonics because they work with the principle of electronic switching. One of the harmonic sources is one-phase and three-phase line commutated converters.

DC transmission systems, battery and photovoltaic systems are fed via line commanded converters. One of the uses of the big powerful converter is electric energy transfer system. The advantage of a three-phase converter over a one-phase converter is that it does not generate solid harmonics of three and three. Harmonic components produced by an ideal converter,

$$h=kp\pm1 \tag{18}$$

Here, p the number of pulse, k is any number from 1 to infinity, h indicates the harmonic order. Thus, the three-pulse rectifier generates all harmonics except the multiples of three and three. A 6-pulse rectifier generates 5th, 7th, 13th, 17th, 19th, 23rd, 25th, etc. harmonics. 12 pulse rectifier produces 11th, 13th, 23rd, 25th, 35th, 37th, etc. harmonics. Generally, six pulse rectifiers are used in industrial power system. Between the fundamental component current I1 and the harmonic component current In,

$$\frac{I_n}{I_1} = \frac{I}{h} \tag{19}$$

It is found by this analytical formula. In order to increase energy quality, the efficiency of non-linear loads in power systems should be reduced.

4. Reducing harmonic distortion with passive filters

Harmonic filter is equipment consisting of passive circuit elements such as capacitor, reactor and resistor. It is used for reactive power compensation while eliminating unwanted harmonic currents. It provides a low impedance path at one or more specified frequencies in the network, which prevents the currents at those frequencies from flowing to the grid. Moreover, since they also make reactive power compensation, they provide voltage support to the network. They are used mostly in heavy industries such as cement, textile, iron & steel factories, etc. Passive filters are generally used to eliminate harmonic components in the power system. Passive filters used in power systems are shown in Fig. 9.

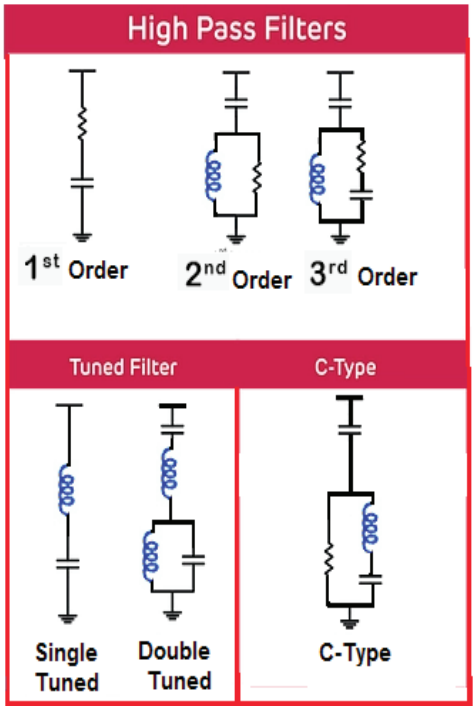

Fig. 9 Types of passive filters

Passive Filters Types:

- High pass filters are also named as damped filters.
- Generally used for the filtering of harmonics higher than 13th harmonics.

• Tuned filters are generally tuned to a specific frequencies like 3rd,5th,7th,11th and 13th to present low impedance to a particular harmonic current.

• C-type filter is generally used for attenuation of low order harmonics and inter-harmonics created by an electric arc furnace (EAF) and HVDC transmission systems.

Passive filters consist of inductance, capacity and ohmic resistance. Passive filters eliminate harmonic components other than the basic component. They are placed between the source and the load. L and C elements are brought to resonance at the frequency value of the harmonic components to be eliminated. Single-tuned filters are used for low-grade harmonic components while filter design.

A passive filter can consist of several steps which are tuned to different frequencies. It can also consist of several steps for a certain frequency. The tuning frequency, capacity and network impedance determine the effectiveness of the filter. One step is required for each harmonic up to the desired frequency. With passive filters, the tuning frequencies of the filter steps are not precisely tuned to the harmonic currents to be filtered so that extremely high filter currents are avoided.

In addition, passive filtering is not only possible in the range from the 3rd to the 25th harmonic, but also possible even beyond this. Filter steps for all possible harmonics of a lower order must be present for each filter circuit, namely for higher harmonics, to prevent their reinforcement. Passive filters are frequently implemented as tuned filters. In industrial networks, these filters are usually tuned to the harmonics of the order h = 5, 7, 11, 13, . . . which are typical for inverters. Passive filters – and reactor-protected compensation systems – are made of a series circuit of reactor and capacitor. The characteristic of series resonance is used here intentionally to divert harmonic currents for the specific frequency by using lower impedance.

This means that the network impedance/filter step current divider reduces the harmonic current flowing into the network and thus also the harmonic voltage in the network impedance. In addition to the 'fundamental frequency compensation power' (basic harmonic reactive power) that is provided, the harmonic load ability thus becomes an important characteristic for passive filtering.

4.1. The Series (Single-Tuned) filter

It is the most used filter type.Fig.10 shows the circuit schematic and a typical impedance characteristic for the series or single-tuned filter.

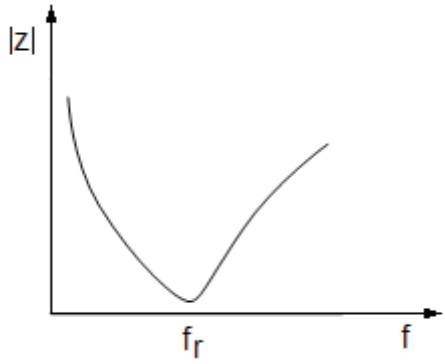

Fig.10 Series (Single-Tuned) Filter

This filter is tuned to suppress a single frequency and is designed based on three quantities: The harmonic current order that requires blocking, the capacitive reactive power that it is going to provide, and its quality factor. The voltage level and the fundamental frequency, which are given by the system, must also be considered during the design process. The quality factor is a quantity that defines the bandwidth of the filter and, in this case, is expressed as the ratio between the reactance and the resistance of the filter. A typical range for Q is between 30 and 60. The following equations can be applied for designing the filter:

$$C = \frac{Q_c}{2\pi f V^2} \tag{20}$$

$$X = \frac{1}{2\pi f h C} \tag{21}$$

$$L = \frac{X}{2hf} \tag{22}$$

$$Q = \frac{2\pi f L}{R} \tag{23}$$

$$R = \frac{1}{2\pi f C} \tag{24}$$

Where, X is the reactance of the inductor or the capacitor at the tuned frequency, h is Tuning point of the filter (harmonic order), Qc is reactive power of the filter [MVAr], Q Quality factor, f is system frequency [Hz], V System voltage [kV].

4.2Band-pass filter

This component can be used in to model high-order filters. Probably the most popular is the double-tuned filter (depicted in Fig.11), which is a combination of a band-pass filter in series with an inductor and a capacitor. This type of filter works by combining the parallel resonance of the band-pass filter, with the series-resonance of the inductor and capacitor combination. Two new resonant frequencies are optioned, as shown in the graph. This configuration makes the filter less expensive to build than the parallel combination of two independent series filters.

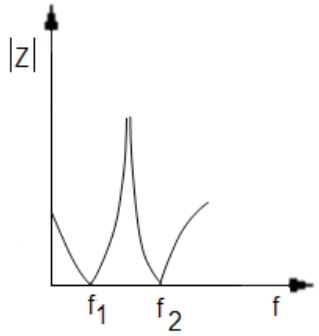

Fig.11 Impedance characteristic of a double-tuned filter

Due to tuning, filter circuits cannot be controlled like reactor power compensation. The generation of harmonics does not correlate with the compensation requirements. This means that the steps of the same tuning frequency can thus be overloaded if they are only switched on and off based on reactive power requirements.

4.3. High-pass filter

This filter is designed to have an impedance characteristic that is flat for high frequencies. Fig. 12 shows the circuit schematic and a typical impedance characteristic for a high-pass filter.

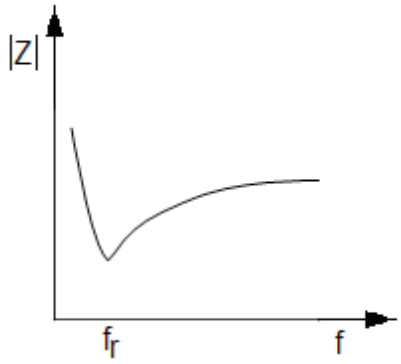

fig.12 High-pass filter

It can be shown that low resistance values will increase the losses, due to that parallel connection with the inductor, and having higher inductance is easier to achieve when designing the filter to work at high frequencies. Thus, this type of filter is applied to suppress 5th harmonic order currents or higher. The resistance also establishes an asymptotic behaviour in the impedance, limiting the maximum value at high frequencies. This means wide bandwidth that can be measured by the quality factor, which is the inverse of that for the series filter, and it is designed to have values between 0.5 and 2.

Application areas of passive harmonic filters:

- Transmission and Distribution Systems
- Metal Industry
- Mining Industry
- Textile Industry
- Commercial Facilities
- Power systems converters

As the harmonic degree grows, it is not economical to design filters for each harmonic component. In addition to the highpass filter design, bandpass filter should be designed for harmonic components above a certain frequency.

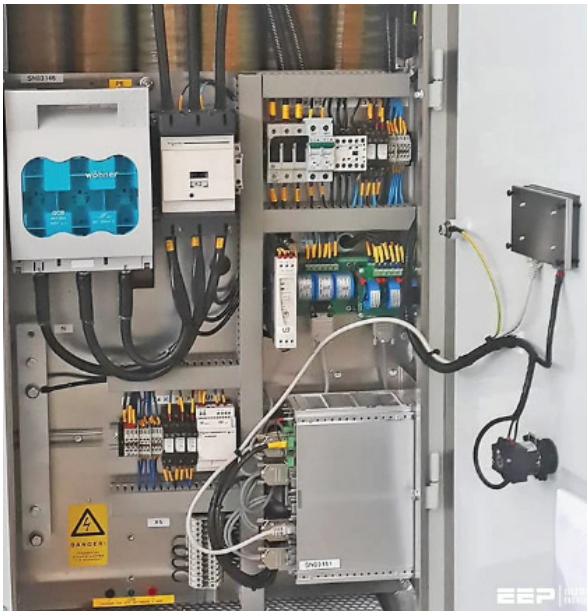

Fig.13 Passive filter

As the passive filters offer very low impedance at the resonance frequency, the corresponding harmonic current will flow in the circuit whatever its magnitude. Passive filter always provides a certain amount of reactive power. This is not desirable when the loads to be compensated are alternating current (AC) drives, which already have a good power factor (PF). In that case, the risk of overcompensation exists as a result of which the utility may impose a fine.

The degree of filtering provided by the passive filter is given by its impedance in relation to all other impedances in the network. As a result, the filtration level of a passive filter cannot be controlled and its tuning frequency may change in time due to aging of the components or network modifications.The quality of the filtration will then deteriorate. It is also important to note that a passive filter circuit may only filter one harmonic component. A separate filter circuit is required for each harmonic that needs to be filtered.

Passive filters can get overloaded under which condition they will switch off or be damaged. The overload may be caused by the presence of unforeseen harmonics on the supply system or caused by structural modifications in the plant itself (such as the installation of a new drive).

Generally, the dimensioning of the filters is as much as the load reactive power requirement for power factor correction. In this case, when the power factor correction capacitor is converted to a harmonic filter, the capacitor size is given. The principle schema of the power system after using filters is given in Fig. 14.

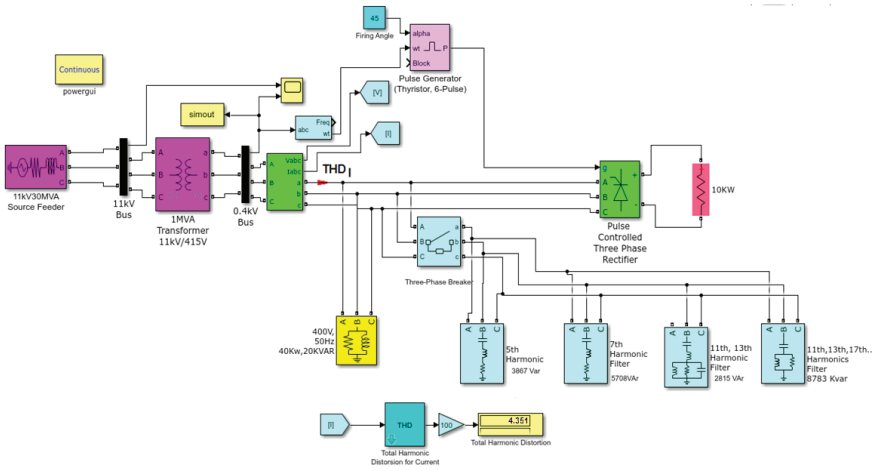

Fig. 14 Simulink equivalent of power system (after filtering)

After filtering, the total harmonic distortion was measured as 4,351%. This value overlaps with the values given in the standards. In this article, Matlab/Simulink software is used to filter the power system and filter harmonics.

In this book, various filters were used to mitigate harmonic components, such as 5th and 7th harmonic components with single tuning filters, 11th and 13th harmonic components with a double tuned filter, high harmonic components with a high pass filter. As a result of this study, it was observed that both harmonic distortions were reduced and power factor was improved.

Over-saturated magnetic circuits, arc-operated operating tools, and power electronics-based devices are harmonics in the power system. Because the current and voltage waveforms of these systems are non-linear. These harmonic components, which are formed in current and voltage waveforms, damage electrical facilities and consumers connected to these facilities and make power systems inoperable.

Table 2 Harmonic components in the power system (after filtering)

Harmonic components	Amplitude of harmonic components (A)	Phase angle of the harmonic components (Degrees)
h1	102.9	21.38
h3	0	0
h5	2.88	75.6
h7	1.427	-43.79
h9	0	0
h11	0.397	147.3
h13	0.1728	29.59
h15	0	0
h17	0.601	-51.72
h19	1.28	-174.5
h21	0	0
h23	1.216	30.11
h25	0.9919	-92.10
h27	0	0
h29	0.9504	112.4
h31	0.7905	-9.481
h33	0	0
h35	0.768	-165
h37	0.6468	73.51
h39	0	0
h41	0.636	-82.17
h43	0.54	156.8
h45	1.157	87.41
h47	0.5363	0.9027
h49	0.4579	-119.7

Harmonics cause loss of copper and iron and leakage fluxes in transformers. In rotary electrical machines, they affect the slip and moment and cause noise and vibration operation. At the same time, they cause false signals to be triggered by systems triggering the transition of the sine wave from zero. In the power system, resonance occurs due to harmonics components. This means that the fuses in the power system will open frequently, irregular operation of the protection relays and shorten the life of all devices in the power system.

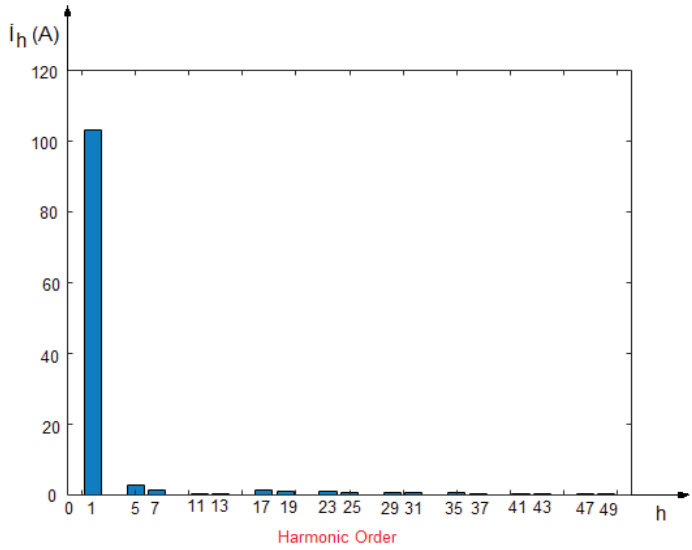

Fig. 15 Amplitude of harmonic components (after filtering)

Harmonics that are active in the power system are the fifth harmonic component, the seventh harmonic component and the eleventh harmonic components.

4.4. Comparison of harmonic components before and after filtering

Harmonic currents tend to flow from the harmonic source to the lowest impedance. The total impedance in the power system is the impedance of the system source and loads impedance which connected in parallel to the system. In the power system, the waveform of the voltage and current must be in the sinusoidal waveform.

However, the sinusoidal waveform of current and voltage lose their sinusoidal characteristics due to nonlinear loads in electrical networks. As an example of these loads; uninterruptible power supplies, AC / DC converters, soft starters and various office equipment. it is a highly preferred method to use passive harmonic filters for reduction total harmonic distortion (THD) and to improve the system power factor. The proposed power system is a combination of three-phase voltage supply, three-phase power transformer, six-pulse controlled rectifier, passive filter and resistive inductive load.

The six-pulse controlled rectifier in the power system is like a harmonic source and produce 5th, 7th, 13th, 17th, 19th, etc. harmonic components. Passive filters were used to reduce the total harmonic distortion of the load

current and to improve the power factor of the system. The power system was modeled and analyzed using the Matlab/Simulink software program. Before using the filter in the power system, the total harmonic distortion for current (THDI) value was measured as 9,517%. It was observed that the THDI value decreased by 4,351% after using the passive filter.

Table 3 Harmonic components in the power system (before and after filtering)

Order of harmonic components	Amplitude of the harmonic component (before filtering) (A)	The amplitude of the harmonic component (after filtering) (A)
h1	116.4	102.9
h3	0	0
h5	8.374	2.88
h7	4.129	1.427
h9	0	0
h11	3.347	0.397
h13	2.327	0.1728
h15	0	0
h17	2.081	0.601
h19	1.6	1.28
h21	0	0
h23	1.499	1.216
h25	1.204	0.9919
h27	0	0
h29	1.162	0.9504
h31	0.9541	0.7905
h33	0	0
h35	0.9401	0.768
h37	0.7812	0.6468
h39	0	0
h41	0.7827	0.636
h43	0.6544	0.54
h45	0	1.157
h47	0.6647	0.5363
h49	0.5576	0.4579

Some measures should be taken to overcome the technical and economic problems of harmonics in the energy system. Harmonic filters should be used in order to reduce harmonic distortion in the power system below the limit values given in the standards.

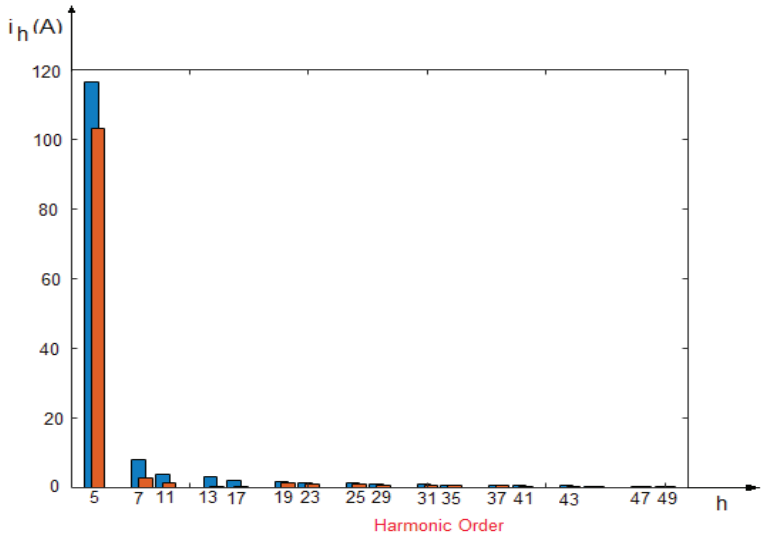

Fig. 16 Amplitude of harmonic components (before and after filtering)

As shown by Fig. 10, after 5th, 7th harmonic filters installation, the 5th harmonic content is decreased from 8.374 A to 2.88 A, and the 7th harmonic content is decreased from 4.129 A to 1.427 A. The 11th harmonic decreased from 3.347 A to 0.397 A, and the 13th harmonic decreased from 2.327 A to 0.1728 A, respectively.

Harmonic components in the power system cause additional heat losses. This additional loss increases the cost of energy used. In addition, harmonic components other than the basic harmonic on the system create additional voltage drops. Office equipment, mainly used in electrical facilities, uninterrupted power supplies and gas-discharge lamps are produced in the third harmonic component. As far as possible, three phases of these devices should be selected. The third harmonic components are zero on three-phase converters.

Harmonics have only been around in sufficient quantities over the last few decades since the introduction of electronic drives for motors, fans and pumps, power supply switching circuits such as rectifiers, power converters and thyristor power controllers as well as most non-linear electronic phase controlled loads and high frequency (energy saving) fluorescent lights. This is due mainly to the fact that the controlled current drawn by the load does not faithfully follow the sinusoidal supply waveforms as in the case of rectifiers or power semiconductor switching circuits.

5. Conclusion

(1) The increase in the use of power electronics-based devices every day causes an increase in harmonic components in the energy system. Because the characteristics of the switching elements used in these devices are nonlinear. As a result, the harmonic distortion increases for current or voltage in the power system. In electrical power systems, harmonic distortion often affects the entire system at great distances from the original sources.

(2) Harmonics are pollution in power systems. Today, with the increase of the use of static converters, this pollution rate is increasing day by day. Passive filters are widely used to filter harmonic components, because it has a simple structure, low cost, high reliability, etc. Total harmonic distortion, which was measured before filtering 9,517% and this value was reduced to 4,351% after filtering.

(3) Passive filters are connected between source and load. They destroy harmonic components other than the fundamental frequency. It consists of a combination of series connected capacitor and inductance. In some cases, ohmic resistance can also be connected. In order to filter the harmonic components in the power system, 2 single tuned filters, 1 double tuned filter and 1 second-order damped filter were used.

(4) Harmonics in the electrical power distribution system combine with the fundamental frequency (50Hz or 60Hz) supply to create distortion of the voltage and/or current waveforms. This distortion creates a complex waveform made up from a number of harmonic frequencies which can have an adverse effect on electrical equipment and power lines.

REFERENCES

Dastfan, A., Yassami, H., Rafiei, M. R. (2014). Optimum Design of Passive Harmonic Filter by Using Game Theory Concepts. Intelligent Systems in Electrical Engineering. Vol. 4, No. 4, pp. 250-256

El-Ela, A.A., Alam, S., El-Arwash, H. (2008). An Optimal Design of Single Tuned Filter in Distribution Systems, Electric Power Systems Research Vol. 78, No. 6, pp. 967-974

Napoles, J., Leon, J.I., Portillo, R., Franquelo, L.G. (2010). Aguirre, M.A. Selective Harmonic Mitigation Technique for High-Power Converters. IEEE Trans. Ind. Electron. Vol. 57, pp. 2315–2323

İzgi, E., Ay, S., (2016). A parametric study on privatization revenues of the electricity distribution companies in Turkey, Turkish Journal Of Electrical Engineering And Computer Sciences, Vol. 24, No.3, pp.979-993

Bayindir, R., Sağiroğlu, Ş., Çolak, İ., Alper Ö. (2009). Investigating Industrial Risks Based on Information Security for Observerable Electrical Energy Distribution System and Suggestions. Journal of the Faculty of Engineering and Architecture of Gazi University. Vol. 24, No. 3, pp.715-723

Rashid, H.M. (2014). Power Electronics, Circuits, Devices, and Applications, Perason Press

Adak, S., Cangi, H. (2016). Analysis and Simulation Total Harmonic Distortion of Output Voltage Three Level Diode Clamped Inverter in Photovoltaic System, Bitlis Eren University, Journal of Science. Vol. 5, No. 2, pp. 242-253

Kocatepe, C., Uzunoğlu, M., Yumurtacı, R., Karakaş, A., Arıkan, O., (2003). Harmonics in Electrical Plants, Birsen Publication, İstanbul

https://www.endoks.com/en/service/passive-harmonic-filtering-systems/

Diwan, S.P., Inamdar, H.P. , Vaidya, A. P. (2011). Simulation Studies of Shunt Passive Harmonic Filters: Six Pulse Rectifier Load - Power Factor Improvement and Harmonic Control. ACEEE International Journal on Electrical and Power Engineering. Vol. 2, No. 1, pp. 1-6

Ozdemir, A., Ferikoglu, A. (2004). Low cost mixed-signal microcontroller based power measurement technique - IEE Proceedings-Science Measurement And Technology - Vol.151, pp. 253-258 - ISSN : 1350-2344 - DOI : 10.1049/ip-smt:20040242 - WOS:000222969400004.

Yilmaz, A. S., Alkan, A., Asyali, M. (2008). Applications of parametric spectral estimation methods on detection of power system harmonics, Electric Power Systems Research. Vol. 7, No. 4, pp. 683-693

Rustemli, S., Cengiz, M.S. (2016). Passive Filter Solution and Simulation Perfornance in Industrial Plants. Bitlis Eren University J Science and Technolog. Vol. 6, No. 1, pp. 39-43

Memon, Z.A., Uquaili, M. A. and Unar, M. A. (2012). Harmonics mitigation of industrial power system using passive filters. Mehran University Research Journal of Engineering and Technology.Vol. 31,No. 2, pp. 355-360

Cho, Y. S. (2009). Analysis and Design of Passive Harmonic Filter for a Three-phase Rectifier, KIEE Magazine. Vol. 58, No. 3, pp. 316-322

Ayan, K., Arifoğlu, U. (2013). Optimizing reactive power flow of HVDC systems using genetic algorithm - International Journal of Electrical Power & Energy Systems. Vol. 55, No. 2, pp.1-12 - ISSN : 0142-0615 - DOI : 10.1016/j.ijepes

Anooja, C. L., Leena, N. (2013). Passive Filter For Harmonic Mitigation of Power Diode Rectifier And SCR Rectifier Fed Loads. International Journal of Scientific & Engineering Research. Vol. 4, No. 6, pp. 310-317

Thoma, M., Blooming, P.E., Daiel J., Camovale P.E. Application of IEEE Std 519-1992. Harmonic Linits.

Sekkeli, M., Tarkan, N. (2013). Development of a novel method for optimal use of a newly designed reactive power control relay. International Journal of Electrical Power and Energy Systems, Vol. 44,No. 2, p. 736-742

Srivastava, K. K., Shakil, S., Pandey, A. V. (2013). Harmonics & Its Mitigation Technique by Passive Shunt Filter. International Journal of Soft Computing and Engineering (IJSCE) 57(1), pp. 2231-2307

Chen, C.I., Chen, Y.C. (2014). Comparative Study of Harmonic and Interharmonic Estimation Methods for Stationary and Time-Varying Signals, IEEE Transactions on Industrial Electronics, Vol. 61, No. 1, pp. 397-404

https://electrical-engineering-portal.com/harmonic-filters

Mohan, N., Undeland, T. R., Robbins W.P. (2003). Power Electronics. Converters, applications and design. John Wiley & Sons.

Osigwe, C., Thévenin Equivalent of Solar Cell Mode, Minnesota State University, Mankato,Minnesota, Theses, Dissertations, December 2019

Vlahinic, S., Brnobic, D. (2009). Vucetic, D., Measurement and Analysis of Harmonic Distortion in Power Distribution Systems, Electric Power Systems Research. Vol. 79, No. 7, pp. 1121-1126

Chapter 2

THE EFFECT OF OVEN BAG USAGE ON THE FORMATION OF HETEROCYCLIC AROMATIC AMINES IN CHICKEN MEAT COOKED IN OVEN*

Adem SAVAŞ[1]
Fatih ÖZ[2]

1 PhD student, Atatürk University, Faculty of Agriculture, Food Engineering Department, Erzurum, Turkey, ORCID ID: 0000-0002-4365-1482

2 Prof. Dr., Corresponding author, Atatürk University, Faculty of Agriculture, Food Engineering Department, Erzurum, Turkey, ORCID ID: 0000-0002-5300-7519, fatihoz@atauni.edu.tr

* This article is produced from Adem Savaş's master thesis entitled "Determination of the formation of heterocyclic aromatic amines and the migration level of bisphenol-A in chicken meat cooked in oven with oven bag" under the supervision of Prof. Dr. Fatih Öz, Atatürk University, Graduate School of Natural and Applied Sciences, 2019, Erzurum, Turkey.

1. Introduction

Meat has significant nutritional importance due to the fact that it contains adequate and balanced levels of macro compounds (protein and fat) and micro compounds (mineral and vitamins) (Lawrie, 1991). It is known that some micro compounds that are spontaneously present in meat are not found or have a low bioavailability in plant-based foods (Oz, 2019). Of the animal-based products, chicken meat is one of the most frequently consumed products due to some reasons such as its low-fat content, high and qualified protein content, rich in vitamins (especially B complex) and minerals, preparation for consumption in a short period of time, easy to transfer and low price compared to beef meat (Soyer et al., 1998; Zorba, 2009).

Cooking is an important process to obtain a tasty and reliable product in terms of food safety. The aim of the cooking process is to provide basic characteristics such as taste-aroma and tenderness desired by consumers. The cooking process, which is usually applied immediately before consumption of meat and meat products, also increases the hygienic quality of the meat by inactivation of pathogenic microorganisms and extends the shelf life. On the other hand, many negative reactions could occur in foods during the cooking process (García-Arias et al., 2003; Tornberg, 2005; Gerber et al., 2009). For example, cooking may cause the formation of various food toxicants (Oz and Kaya, 2011). Among these food toxicants formed, heterocyclic aromatic amines (HAAs) have an important place.

HAAs were firstly detected in grilled fish and meats by Japanese scientists in 1977 (Nagao et al., 1977). It has been declared that many of HAAs are mutagenic, and almost all are carcinogenic (Sugimura, 1995; Skog et al., 1998). It has been reported that about 30 HAAs have been isolated and identified in foods until today (Savaş et al., 2021). HAAs are 100 times more mutagenic than aflatoxin B1 and 2000 times more mutagenic than benzo[a]pyrene that is an indicator for polycyclic aromatic hydrocarbons (Oz and Kaya, 2011). In addition, the International Agency for Research on Cancer (IARC) classifies some of the HAAs include MeIQ, MeIQx, PhIP, AαC, MeAαC, Trp-P-1, Trp-P-2, and Glu-P-1 as “possible human carcinogens” in class 2B and one HAA, IQ, as “probable human carcinogens” in class 2A (IARC, 1993).

HAAs are basically divided into two classes. The first one is aminoimidazoazoarenes and the second one is aminocarbolines (Puignou et al., 1997; Skog et al., 2000; Skog and Solyakov, 2002). Aminoimidazoazoarenes (IQ-type compounds, thermal HAAs) are generally formed at temperatures below 300°C as a result of reactions between creatine/creatinine, free amino acids, and hexoses (Jägerstad et al., 1983; Laser-Reuterswärd et al., 1987a and 1987b). The second group of HAAs, aminocarbolines (non-IQ-type compounds or pyrolytic HAAs), are usually formed by pyrolysis of proteins

and amino acids at temperatures above 300°C (Sugimura, 1997; Sugimura and Adamson, 2000; Knasmüller et al., 2001; Toribio et al., 2002).

Many factors such as meat type, pH, water activity, cooking conditions (temperature, duration, method, surface, etc.), free amino acids, and creatine etc. influence the formation and contents of HAAs in foods (Felton et al., 1997; Reistad et al., 1997; Pais et al., 1999; Keating and Bogen, 2001). In addition, heat and mass transfer, lipid, lipid oxidation, and antioxidants have an effect on the variety and concentration of HAAs formed (Jägerstad et al., 1998; Oz, 2019; Savaş et al., 2021; Oz, 2021a and 2021b). Oven cooking is one of the traditional cooking methods and is frequently used in cooking of meat and meat products including chicken meats. By the way, oven bags are also frequently used during the oven cooking of chicken meats due to some benefits (Savaş et al., 2021). Until now, there have been published a lot of articles showing the effect of different cooking methods on the formation of HAAs in chicken meats. However, the articles showing the effect of oven bag usage duration of oven cooking on the formation of HAAs in chicken meats are very limited (Savaş et al., 2021). Therefore, in the present study, the determination of the effect of oven bag usage on the formation of HAAs in chicken meats cooked in the oven was aimed.

2. Material and method

2.1.Materials

The chicken meats were obtained as fresh from the distributor of a nation-wide known company in Erzurum, which only sells poultry meat. We paid much attention to obtain the chicken carcasses from the same party with approximately the same size and same gender. The chicken carcasses were brought to the laboratory under the cold chain (2ºC), the breast and leg meats were properly removed from the carcasses and used as material in the present study. The oven bags belonged to five different companies were purchased from local markets.

2.1.1. Chemicals

All of the chemicals used in the present study were analytical or high performance liquid chromatography-grade. The HAAs standards were obtained from Toronto Research Chemicals (Downsview, ON, Canada).

2.2. Methods

2.2.1. The cooking of chicken meats

In the present study, the oven-cooking process was selected as a cooking method in order to determine the effect of oven bag usage on the formation of HAAs in chicken meat samples. After the meat samples were placed in the oven bags, the mouth of the oven bags was closed

with a clip given by the company, and the oven bags were pierced with a toothpick. Then, the cooking process was started. No additives and/or spices were used during the oven cooking process in order to determine the only effect of oven bag usage. The oven cooking process was done using a domestic oven (Arçelik, Turkey). The cooking temperature was selected as 200ºC due to the fact that the temperature of the oven cooking process was suggested as 200 ºC by the oven bag companies. The cooking time was determined as 75 min as a result of the preliminary tests at this temperature. At the end of the cooking, all meat samples were well cooked and consumable.

2.2.2. Determination of HAA Content

The extraction of HAAs was performed according to Messner and Murkovic (2004) with some modifications (Savaş et al., 2021). For this aim, 1 g of meat sample was mixed with 12 ml of 1 M sodium hydroxide for 1 h at 500 rpm on a magnetic stirrer. After stirring, 10 g of Extrelute NT packaging material was added and the mixture was treated with ethyl acetate, hydrochloric acid, and methanol on an Oasis MCX (3cc, 60mg, Waters, Milford, MA) cartridge connected to a vacuum manifold system. The HAAs in the samples were eluted with a solution of methanol:ammonia (95:5, v/v). The samples were kept at -18°C until HPLC analysis and dried in an oven at 45°C one day before the analysis. HPLC analysis was started by adding 100 µl of methanol (including internal standard) in the vial. To determine the HAAs in the chicken meats, a reverse phase analytic colon (Acclaim™ 120 C18, 3µm, 4.6x150 mm, Tosoh Bioscience GmbH, Stuttgart, Germany) was used in a HPLC (Thermo Ultimate 3000, Thermo Scientific, USA) containing a Diode Array Detector (DAD-3000). The separation process was conducted at 35°C, at a flow rate of 0.7 ml/min (Savaş et al., 2021).

2.2.3. Statistical analysis

The experiment was set up according to a completely randomized design and employed (in two replicates for each meat pieces, n=4). The average of the analysis results determined in the breast and leg meats were given as the analysis results in the current study. The data obtained in the present study were subjected to analysis of variance. Duncan multi comparison test was applied to data in order to determine the statistical differences between the values detected by using the Statistical Package for the Social Sciences 20.0 statistical software package (Yıldız and Bircan, 1991).

3. Results and discussion

3.1. Method validation

The standard addition method was used to determine the recoveries of HAAs and the HAA mix stock solution at known concentrations (10, 7.5, 5, 2.5, 1 and 0.5 ng/g) was added to the samples prior to the extraction. Then, the recoveries were determined. The limit of detection (LOD), limit of quantification (LOQ), and recoveries were given in Table 1. The LOD and LOQ values and recoveries of the HAAs were consistent with the data in the literature (Murkovic et al., 1998; Balogh et al., 2000; Messner and Murkovic, 2004).

Table 1. *The limit of detection (LOD), limit of quantification (LOQ), and recovery values of heterocyclic aromatic amines investigated in the present study*

Compound	LOD (ng/g)	LOQ (ng/g)	Recovery (%)
IQx	0.004	0.013	75.65
IQ	0.009	0.029	60.04
MeIQx	0.024	0.081	78.48
MeIQ	0.014	0.047	55.63
7,8-DiMeIQx	0.005	0.018	75.87
4,8-DiMeIQx	0.008	0.025	76.96
PhIP	0.025	0.085	87.16
AαC	0.012	0.039	79.71
MeAαC	0.010	0.035	69.01

3.2. HAA contents in the samples

In the present study, the HAA contents of the samples cooked without and with oven bags belonged to different companies were given in Table 2 by taking the average of two replications of the breast and leg meats (Savaş et al., 2021). IQx, IQ, MeIQ, 4,8-DiMeIQx, AαC, and MeAαC compounds were not determined in any of the samples analyzed in the present study, while MeIQx (up to 39.34 ng/g), 7,8-DiMeIQx (up to 0.74 ng/g), and PhIP (up to 2.60 ng/g) compounds were determined. Each compound was discussed in detail below.

Table 2. *The HAA content of the cooked chicken meats (ng/g)**

Sample	**MeIQx**	**7,8-DiMeIQx**	**PhIP**	**Total HAAs**	**Inhibition (%)**
Control	28.84±14.85	0.37±0.52	2.42±0.26	31.63±15.12	-
A	20.56±14.84	nd	nd	20.56±14.84	35.00
B	21.43±7.07	nd	nd	21.43±7.07	32.25

C	21.69±21.44	nd	0.20±0.28	21.89±21.72	30.79
D	24.00±10.63	nd	nd	24.00±10.63	24.12
E	24.95±11.37	nd	nq	24.95±11.37	21.12

*IQx, IQ, MeIQ, 4,8-DiMeIQx, AαC and MeAαC were not detected, nd: not detected (<LOD), nq: not quantified (LOD<…<LOQ)

3.2.1. The IQx content of the samples

In the present study, IQx compound could not be detected in any of the meat samples analyzed. There are other studies in the literature showing that IQx compound could not be detected in poultry meat cooked by different methods. Indeed, IQx was not detected in chicken meat cooked in microwave for 5-15 min by Chiu et al. (1998), in turkey breast meat and chicken meat fried at 275°C for 30 min by Pais et al. (1999), in chicken meat grilled at 220°C until the internal temperature reach to 82°C by Gasperlin et al. (2009), in chicken and duck meat cooked with different methods (pan-frying without fat or oil, deep-fat frying, barbecue and oven) at 180-200°C for 10-20 min by Liao et al. (2010). On the other hand, IQx was detected as 0.17 ng/g in chicken meat fried at 200°C for 10 min by Chen and Yang (1998). While Oz et al. (2010) could not detect IQx compound in chicken chops cooked in microwave for 3-12 min, IQx was detected up to 0,30 ng/g in chicken chops cooked in oven at 200ºC for 5-20 min, up to 0.29 ng/g in chicken chops cooked on hot plate at 200ºC for 5-20 min, up to 0.33 ng/g in chicken chops fried at 200ºC for 5-20 min and up to 0.49 ng/g in barbecued chicken chops for 3-12 min by the same researchers. Chiu et al. (1998) determined IQx up to 0.51 ng/g in chicken meat fried at 100-200°C for 5-15 min. On the other hand, Oz et al. (2016) determined 0.05 ng/g, 0.07 ng/g and 0.08 ng/g IQx in goose breast meat cooked on hot plate, goose breast meat cooked in microwave and goose leg meat cooked in microwave, respectively.

3.2.2. The IQ content of the samples

In the present study, IQ compound could not be detected in any of the chicken meats analyzed. There are other studies in the literature showing that IQ compound could not be detected in poultry meat cooked by different methods. Indeed, IQ compound was not detected in chicken meats (Knize et al., 1995, 1997a; Skog et al., 1997; Knize et al., 1998; Pais et al., 1999; Busquets et al., 2004; Warzecha et al., 2004; Wong et al., 2005; Gasperlin et al., 2009; Oz et al., 2010, Viegas et al., 2012), duck meat (Wong et al., 2005, Liao et al., 2010) and turkey meat (Pais et al., 1999) cooked by different methods. However, Turesky et al. (2005) determined 0.12 ng/g IQ in barbecued chicken meat for 20 min, while IQ content ranged between 0.10 and 0.51 ng/g in chicken meat fried at 200°C for 5-15 min by Chiu et

al. (1998). Liao et al. (2010) found 1.76 ng/g IQ in chicken meat pan-fried without fat or oil at 180°C for 10 min. On the other hand, Pais and Knize (2000) reported that the amount of IQ in fried chicken meat could be up to 5 ng/g.

3.2.3. The MeIQx content of the samples

One of the most common HAAs found in cooked meats is MeIQx compound (Murray et al., 1993; Knize et al., 1997a; Murkovic et al., 1997; Pais et al., 1999; Warzecha et al., 2004; Turesky et al., 2005; Liao et al., 2010). In the present study, MeIQx compound was detected in all of the cooked meat samples analyzed. 28.84 ng/g MeIQx was detected in the control group meat samples, while the MeIQx content ranged between 21.43 and 24.95 ng/g in the samples cooked with the oven bags. MeIQx was determined as 0.3 ng/g in barbecued chicken meat by Murray et al. (1993), as 0.34 ng/g in chicken meat barbecued for 20 min by Turesky et al. (2005), as 0.36 ng/g in deep-fat fried chicken meat, as 1.26 ng/g in pan-fried chicken meat, 0.19 ng/g in roasted duck meat by Wong et al. (2005), as 1.8 ng/g in chicken meat barbecued for 30 min by Warzecha et al. (2004), as up to 6.1 ng/g in chicken meat grilled for 14-26 min by Knize et al. (1997a). Liao et al. (2010) determined MeIQx content as 1.83 and 3.44 ng/g in chicken and duck meats pan-fried at 180°C for 10 min respectively, as 0.77 and 0.68 ng/g in chicken and duck meats deep-fat fried at 180°C for 10 min respectively, as 1.16 and 2.40 ng/g in chicken and duck meats barbecued at 200°C for 20 min, respectively. There are also studies in the literature showing that higher levels of MeIOx compounds present in cooked poultry. Indeed, Pais and Knize (2000) reported that the amount of MeIQx in fried chicken meat could reach up to 270 ng/g. On the other hand, there are also studies in the literature showing that MeIQx could not be detected in poultry meat. It was reported that MeIQx was not detected in chicken meat cooked in microwave for 5-15 min (Chiu et al., 1998), in chicken meat fried at 175-200°C for 12 min (Busquets et al., 2004) and in chicken and duck meats roasted at 200°C for 20 min (Liao et al., 2010).

3.2.4. The MeIQ content of the samples

In the present study, MeIQ compound could not be detected in any of the chicken meat samples analyzed. There are other studies in the literature showing that MeIQ compound could not be detected in poultry meat cooked by different methods. Indeed, MeIQ was not detected in chicken meat fried at 175-225ºC for 30 min and chicken meat cooked in oven at 150-200ºC for 30 min (Skog et al., 1997), in chicken meat cooked in microwave for 5-15 min (Chiu et al., 1998), in chicken meat fried at 275°C for 30 min (Pais et al., 1999), in chicken meat fried at 175-200°C

for 12 min (Busquets et al., 2004), in chicken meat grilled at 220°C until the internal temperature reached 82°C (Gasperlin et al., 2009), in chicken and duck meats cooked with different methods at 180-200ºC for 10-20 min (Liao et al., 2010) and in turkey meat fried at 275°C for 30 min (Pais et al., 1999). On the other hand, while Oz et al. (2010) did not detect MeIQ compound in chicken chops cooked in microwave for 3-12 min and oven at 200°C for 5-20 min, MeIQ was determined up to 0.43 ng/g in chicken chops grilled at 200°C for 5-20 min, up to 0.96 ng/g in chicken chops fried at 200°C for 5-20 min and up to 1.06 ng/g in barbecued chicken chops for 3-12 min by the same researchers.

3.2.5. The 7,8-DiMeIQx content of the samples

In the present study, 7,8-DiMeIQx compound was only determined in the control group samples. In the literature, 7,8-DiMeIQx compound could not be detected in chicken meat cooked in microwave for 5-15 min (Chiu et al., 1998), in chicken meat fried at 175-200°C for 12 min (Busquets et al., 2004) and in chicken and duck meats cooked with different methods at 180-200ºC for 10-20 min (Liao et al., 2010). On the other hand, 7,8-DiMeIQx was determined as 0.015 ng/g in fried chicken meat by Salmon et al. (2006), as 0.16 ng/g in chicken meat fried at 200°C for 10 min by Chen and Yang (1998), up to 0.87 ng/g in chicken meat fried at 200°C for 15 min by Chiu et al. (1998). On the other hand, while Oz et al. (2010) did not detect 7,8-DiMeIQx compound in chicken chops cooked in microwave for 3-12 min and oven at 200°C for 5-20 min, 7,8-DiMeIQx was determined up to 0.42 ng/g in chicken chops grilled at 200°C for 5-20 min, up to 1.11 ng/g in chicken chops fried at 200°C for 5-20 min and up to 0.78 ng/g in barbecued chicken chops for 3-12 min by the same researchers. On the other hand, Pais and Knize (2000) reported that the amount of 7,8-DiMeIQx in fried chicken meat could be up to 5 ng/g.

3.2.6. The 4,8-DiMeIQx content of the samples

In the present study, 4,8-DiMeIQx compound could not be detected in any of the chicken meat samples analyzed. There are other studies in the literature showing that 4,8-DiMeIQx, one of the most investigated compound, could not be detected in poultry meat cooked by different methods. Indeed, 4,8-DiMeIQx was not detected in chicken meat cooked in microwave for 5-15 min by Chiu et al. (1998) and in chicken and duck meat roasted at 200°C for 20 min by Liao et al. (2010). Solyakov and Skog (2002) reported that 4,8-DiMeIQx was not formed in chicken meat boiled at 100°C for 23 min. On the other hand, 4,8-DiMeIQx was determined up to 0.5 ng/g in chicken meat fried at 175-225°C for 30 min (Skog et al., 1997), as 0.09 ng/g in chicken meat fried at 200°C for 10 min (Chen and Yang, 1998), up to 0.18 ng/g in chicken meat grilled at 220°C until the

internal temperature reached 82 °C (Gasperlin et al., 2009), up to 0.78 ng/g in chicken meat fried at 200°C for 5-15 min (Chiu et al., 1998), as 3.55 ng/g in chicken meat pan-fried at 200 °C for 20 min and as 1.05 ng/g in chicken meat grilled at 180 °C for 5 min (Gibis and Weiss, 2010) and as 2.85 ng/g in chicken meat pan-fried at 180 °C for 24.1 min (Iwasaki et al., 2010). Wong et al. (2005) reported that 0.48 ng/g and 0.23 ng/g 4,8-DiMeIQx were determined in pan-fried chicken meat and deep-fat fried chicken meat, respectively. On the other hand, Pais and Knize (2000) reported that the amount of 4,8-DiMeIQx in fried chicken meat could be up to 4 ng/g.

3.2.7. The PhIP content of the samples

One of the most common HAAs found in cooked meats is reported to be PhIP compound (Pais et al., 1999; Busquets et al., 2004; Warzecha et al., 2004; Turesky et al., 2005; Iwasaki et al., 2010; Liao et al., 2010; Viegas et al., 2012). In the present study, 2.42 ng/g PhIP was determined in the control group samples, while the PhIP content ranged between nd and 0.20 ng/g in the samples cooked with the oven bags belonged to different companies. On the other hand, there are other studies showing that PhIP compound could not be detected in poultry meat cooked by different methods. Indeed, Chiu et al. (1998) reported that PhIP was not detected in chicken meat cooked in microwave for 5-15 min. In addition, PhIP could not be detected in chicken meat (Oz et al., 2010) and goose meat (Oz et al., 2016) cooked by different methods. On the other hand, there are studies in the literature showing that very high levels of PhIP compound were formed in cooked meats. Indeed, PhIP was determined as 18.33 and 21.88 ng/g in chicken and duck meat fried at 180°C for 10 min, respectively, as 37.5 ng/g in chicken meat fried at 275°C for up to 30 min (Pais et al., 1999), as 38.1 ng/g in fried chicken meat (Wakabayashi et al., 1993), up to 46.9 ng/g in chicken meat fried 175-200 °C for up to 12 min (Busquets et al., 2004), up to 270 ng/g in grilled chicken meat (Knize et al., 1997b), up to 315 ng/g in chicken meat grilled for up to 26 min (Knize et al., 1997a). In addition, Pais and Knize (2000) reported that the amount of PhIP in fried chicken meat could be up to 480 ng/g.

3.2.8. The AαC content of the samples

In the present study, AαC compound could not be detected in any of the chicken meat samples analyzed. There are other studies in the literature showing that AαC, one of the few-studied compounds, could not be detected in poultry meat cooked by different methods. Indeed, AαC was not detected in commercial cooked chicken meat samples by Knize et al. (1997a), in chicken meat cooked with different cooking methods such as oven, microwave, hot plate and pan-frying at 200 °C for 3-20 min by Oz et

al. (2010). On the other hand, AαC was determined as 0.2 ng/g in chicken meat grilled at 175-200 °C for 13 min (Busquets et al., 2004), as 0.23 ng/g and 1.26 ng/g in chicken and duck meat pan-fried at 180 °C for 10 min, respectively (Liao et al., 2010), as 1.77 ng/g in chicken meat at 230-300 °C for 30-90 min (Viegas et al., 2012) and as 8.70 ng/g in chicken meat barbecued for 20 min (Turesky et al., 2005). There are also studies in the literature showing that higher levels of AαC present in cooked poultry. Indeed, Pais and Knize (2000) reported that the amount of AαC in fried chicken meat could be up to 100 ng/g.

3.2.9. The MeAαC content of the samples

In the present study, MeAαC compound could not be detected in any of the chicken meat samples analyzed. Similarly, there are other studies in the literature showing that MeAαC, one of the few-studied compounds, could not be detected in poultry meat cooked by different methods. Indeed, MeAαC was not detected in chicken meat fried at 200°C for 10 min by Chen and Yang (1998), in chicken meat fried at 200°C for 5-25 min by Chiu et al. (1998), in chicken and duck meats fried at 275°C for 30 min by Pais et al. (1999) and in chicken meat fried at 175-200°C for 12 min by Busquets et al. (2004). On the other hand, MeAαC was determined up to 0.14 ng/g in chicken meat cooked in microwave for up to 15 min by Chiu et al. (1998), as 0.23 ng/g in chicken meat barbecued for 20 min by Turesky et al. (2005) and up to 2.05 ng/g in chicken meat grilled at 230-300°C for 30-90 min by Viegas et al. (2012).

3.2.10. The total HAA content of the samples

In the present study, the total HAA contents of the chicken meats cooked without and with the oven bags belonged to different companies were also given in Table 2. While 31.63 ng/g total HAA content was calculated in the control group samples, the total HAAs contents in the samples cooked with the oven bag belonged to different companies ranged 20.56 and 24.95 ng/g. As can be seen from the Table, the use of oven bag during the oven cooking of the chicken meats caused a decrease in the total HAA contents of the chicken meats. The use of the oven bag is thought to result in a lower total HAA content due to a more humid cooking environment. Indeed, it is stated in the studies that some kind of HAAs are mostly formed in dry cooking environments (Robbana-Barnat et al., 1996; Oz and Kaya, 2011). In the present study, it was found that the total inhibition rates as a result of oven bag usage ranged between 21.12 and 35.00%. However, these inhibitions were not statistically significant ($P>0.05$).

In the literature, it is stated that oven cooking usually causes low or moderate HAAs formation (Skog et al., 1997; Oz et al., 2016). This could be due to the fact that the heat transfer is carried by the air stream (Solyakov

and Skog, 2002), and the presence of steam, which affects the heat transfer and decreases the surface temperature of the product (Skog et al., 1998). It is stated that during oven cooking, which is a traditional cooking method, there is a decrease in the level of HAA in the meats cooked in the oven due to the fact that the conventional heating inside the oven caused the uniform heat distribution on the product surface and the prevention of overheating (Skog and Jägerstad, 1991; Shabbir et al., 2015).

Oz and Yüzer (2016) reported that total HAA content of turkey breast meat cooked with different cooking methods such as boiling, frying, deep-fat frying, hot plate, microwave and oven ranged between 2.90 and 52.34 ng/g, while total HAA content of turkey leg meat cooked with the same cooking methods ranged between 2.38 and 21.35 ng/g. In addition, 44.58 ng/g and 58.57 ng/g MeIQx was determined in turkey breast and leg meat cooked in oven, respectively. In another study conducted by the same researchers, it was determined that total HAA content of goose breast meat and goose leg meat cooked with different cooking methods (boiling, grilling, pan-frying without fat or oil, pan-frying with oil, deep-fat frying, microwave and oven) was found up to 2.20 ng/g and 2.42 ng/g, respectively (Oz et al., 2015).

Tengilimoğlu-Metin and Kızıl (2017) determined total HAA content as 0.92 ng/g in chicken breast meat cooked at 150 ºC, as 0.52 ng/g in chicken breast meat cooked at 200 ºC and as 83.06 ng/g in chicken breast meat cooked at 250 ºC.

Total HAA content in chicken breast meat was determined as 4 ng/g in samples cooked in oven at 200ºC for 20 min, as 21.30 ng/g in deep-fat fried samples, as 27.4 ng/g in pan-fried samples and as 112 ng/g in barbecued samples by Liao et al. (2010). Oz et al. (2010) found that the highest total HAA content (5.10 ng/g) in chicken leg meat, cooked with hot plate, pan, grill, oven and microwave, was belonged to the samples cooked with microwave.

It is known that a lot of factors such as HAA numbers analyzed, meat and muscle type used as material, product type, dimensions of the product, cooking method, cooking temperature, cooking duration, analysis technique etc. affect the formation of individual HAAs and total HAAs content. In this context, in the present study, the results of HAA number and total HAA content detected in the chicken meats cooked in the oven without and with oven bags belonged to different companies are generally in agreement with the literature data.

The exposure of human beings to HAA is influenced not only by the type of food and cooking method but also by the size of the portion and the frequency of consumption. Studies have shown that the daily intake of

HAA varies from 60 to 1820 ng per person (Chiu et al., 1998; Nowell et al., 2002, Butler et al., 2003) and the maximum uptake is 5000 ng. On the other hand, Skog (2002) estimates that the acceptable daily consumption of HAAs per person is between 0 and 15 μg/day. It is noted that the differences in the amounts arise from differences in dietary habits for the consumers and methods of analysis. In the present study, it is seen that even if 100 g of the control group chicken meat whose total amount of HAA content is the highest (31.63 ng/g), is eaten, the intake amount is below 5 μg.

4. Conclusion

In the present study, of nine different HAAs investigated, only MeIQx (up to 39.34 ng/g), PhIP (up to 2.60 ng/g), and 7,8-DiMeIQx (up to 0.74 ng/g) compounds were determined. The results obtained in the present study showed that the use of oven bag resulted in a lower formation of the carcinogenic and/or mutagenic HAAs in the chicken samples cooked in the oven. Therefore, in terms of the formation of HAAs, it can be suggested to use of oven bag during oven cooking of the chicken meats.

Acknowledgment

This research was supported by Ataturk University Research Center with Project No: FBA-2019-7075. The financial support of Ataturk University is gratefully acknowledged.

REFERENCES

Balogh, Z., Gray, J.I., Gomaa, E.A. & Booren, A.M. (2000). Formation and inhibition of heterocyclic aromatic amines in fried ground beef patties. *Food and Chemical Toxicology, 38 (5),* 395-401.

Butler, L. M., Sinha, R., Millikan, R. C., Martin, C. F., Newman, B., Gammon, M. D., ... & Sandler, R. S. (2003). Heterocyclic amines, meat intake, and association with colon cancer in a population-based study. *American Journal of Epidemiology*, *157*(5), 434-445.

Busquets, R., Bordas, M., Toribio, F., Puignou, L. & Galceran, M.T. (2004). Occurrence of heterocyclic amines in several home-cooked meat dishes of the Spanish diet. *Journal of Chromatography B, 802(1),* 79-86.

Chen, B.H. & Yang, D.J. (1998). An improved analytical method for determination of heterocyclic amines in chicken legs. *Chromatography, 48,* 223–230.

Chiu, C.P., Yang, D.Y. & Chen, B.H. (1998). Formation of heterocyclic amines in cooked chicken legs. *Journal of Food Protection, 61(6),* 712-719.

García-Arias, M.T., Álvarez Pontes, E., García-Linares, M.C., García-Fernández, M.C. & Sánchez-Muniz, F.J. (2003). Cooking–freezing–reheating (CFR) of sardine (Sardina pilchardus) fillets. Effect of different cooking and reheating procedures on the proximate and fatty acid compositions. *Food Chemistry, 83(3),* 349-356.

Gerber, N., Scheeder, M.R.L. & Wenk, C. (2009). The influence of cooking and fat trimming on the actual nutrient intake from meat. *Meat Science, 81(1),* 148-154.

Gibis, M. & Weiss, J. (2010). Inhibitory effect of marinades with hibiscus extract on formation of heterocyclic aromatic amines and sensory quality of fried beef patties. *Meat Science, 85,* 735–742.

International Agency for Research on Cancer (IARC). (1993). Monographs on the evaluation of carcinogenic risks to humans. Some natural occurring substances: Food items and constituents. Heterocyclic amines and mycotoxins. *Vol. 56, pp.* 163-242. Lyon: International Agency for Research on Cancer.

Iwasaki, M., Kataoka, H., Ishihara, J., Takachi, R., Hamada, G.S., Sharma, S., Marchand, L.L. & Tsugane, S. (2010). Heterocyclic amines content of meat and fish cooked by Brazilian methods. *Journal of Food Composition and Analysis, 23,* 61-69.

Jägerstad, M., Laser-Reuterswärd, A., Olsson, R., Grivas, S., Nyhammar, T., Olsson, K. & Dahlqvist, A. (1983). Creatin(ine) and maillard reaction products as precursors of mutagenic compounds: effects of various amino acids. *Food Chemistry, 12,* 255-264.

Jägerstad, M., Skog K., Arvidsson, P. & Solyakov, A. (1998). Chemistry, formation and occurence of genotoxic heterocyclic amines identified in model systems and cooked food. *Zeitschrift für Lebensmittel-Untersuchung und –Forschung A, 207,* 419–427.

Keating, G.A. & Bogen, K.T. (2001). Methods for estimating heterocyclic amine concentrations in cooked meats in the US diet. *Food and Chemical Toxicology, 39(1),* 29-43.

Knize, M.G., Salmon, C.P., Hopmans, E.C. & Felton, J.S. (1997b). Analysis of foods for heterocyclic aromatic amine carcinogens by solid-phase extraction and high-performance liquid chromatography. *Journal of Chromatography A, 763(1-2),* 179-185.

Knize, M.G., Sinha, R., Rothman, N., Brown, E.D., Salmon, C.P., Levander, O.A., Cunningham, P.L. & Felton, J.S. (1995). Heterocyclic amine content in fast-food meat products. *Food and Chemical Toxicology, 33(7),* 545-51.

Knize, M.G., Salmon, C.P., Mehta, S. S. & Felton, J.S. (1997a). Analysis of cooked muscle meats for heterocyclic aromatic amine carcinogens. *Mutation Research, 376,* 129–134.

Knize, M.G., Sinha, R., Brown, E.D., Salmon, C.P., Levander, O.A., Felton, J.S. & Rothman, N. (1998). Heterocyclic amine content in restaurant-cooked hamburgers, steaks, ribs, and chicken. *Journal of Agricultural and Food Chemistry, 46(11),* 4648-4651.

Knasmüller, S., Steinkellner, H., Hirschl, A.M., Rabot, S., Nobis, E.C. & Kassie, F., 2001. Impact of bacteria in dairy products and of the intestinal microflora on the genotoxic and carcinogenic effects of heterocyclic aromatic amines. *Mutation Research, 480–481,* 129–138.

Laser Reuterswärd, A., Skog, K. & Jägerstad, M. (1987a). Effects of creatine and creatinine content on the mutagenic activity of meat extracts, bouillons and gravies from different sources. *Food and Chemical Toxicology, 25 (10),* 747-754.

Laser Reuterswärd, A., Skog, K. & Jägerstad, M. (1987b). Mutagenicity of pan-fried bovine tissues in relation to their content of creatine, creatinine, monosaccharides and free amino acids. *Food and Chemical Toxicology, 25 (10),* 755-762.

Lawrie, R. (1991). Developments in meat science. Applied Sci., London, England.

Liao, G.Z., Wang, G.Y., Xu, X.L. & Zhou, G.H. (2010). Effect of cooking methods on the formation of heterocyclic aromatic amines in chicken and duck breast. *Meat Science, 85,* 149-154.

Messner, C. & Murkovic, M. (2004). Evaluation of a new model system for studying the formation of heterocyclic amines. *Journal of Chromatography B, 802(1),* 19–26.

Murkovic, M., Friedrich M. & Pfannhauser, W. (1997). Heterocyclic aromatic amines in fried poultry meat. *Zeitschrift für Lebensmitteluntersuchung und -Forschung A, 205,* 347-350.

Murkovic, M., Steinberger, D., & Pfannhauser, W. (1998). Antioxidant spices reduce the formation of heterocyclic amines in fried meat. *Zeitschrift für Lebensmitteluntersuchung und -Forschung A, 207 (6),* 477-480.

Murray, S., Lynch, A.M., Knize, M.G. & Gooderham, M.J. (1993). Quantification of the carcinogens 2-amino-3,8-dimethyl- and 2-amino-3,4,8-trimethylimidazo[4,5-f]quinoxaline and 2-amino-1-methyl-6-phenylimidazo[4,5-b]pyridine in food using a combined assay based on gas chromatography-negative ion mass spectrometry. *Journal of Chromatography, 616(2),* 211-219.

Nagao, M., Honda, M., Seino, Y., Yahagi, T. & Sugimura, T. (1977). Mutagenicities of smoke condensates and the charred surface of fish and meat. *Cancer Letters, 2 (4–5),* 221-226.

Nowell, S., Coles, B., Sinha, R., Macleod, S., Luke Ratnasinghe, D. & Stotts, C. (2002). Analysis of total meat intake and exposure to individual heterocyclic amines in a case-control study of colorectal cancer: Contribution of metabolic variation to risk. *Mutation Research,* 506-507(C), 175.

Oz, E. (2021a). The impact of fat content and charcoal types on quality and the development of carcinogenic polycyclic aromatic hydrocarbons and heterocyclic aromatic amines formation of barbecued fish. *International Journal of Food Science & Technology*, *56*(2), 954-964.

Oz, E. (2021b). The presence of polycyclic aromatic hydrocarbons and heterocyclic aromatic amines in barbecued meatballs formulated with different animal fats. *Food Chemistry*, *352*, 129378.

Oz, F., Kaban, G. & Kaya, M. (2010). Effects of cooking methods and levels on formation of heterocyclic aromatic amines in chicken and fish with Oasis extraction method. *LWT-Food Science and Technology*, *43*(9), 1345-1350.

Oz, F. & Kaya, M. (2011). Heterocyclic aromatic amines in meat. *Journal of Food Processing and Preservation, 35,* 739-753.

Oz, F. & Yüzer, M.O. (2016). The effects of cooking on wire and stone barbecue at different cooking levels on the formation of heterocyclic aromatic amines and polycyclic aromatic hydrocarbons in beef steak. *Food Chemistry 203,* 59-66.

Oz, F., Cakmak, I. H., Zikirov, E., Kizil, M., & Turhan, S. (2015). Heterocyclic aromatic amine contents of kavurma commercially cooked in steam and copper cauldron. *Journal of Food Processing and Preservation*, *39*(6), 583-590.

Oz, F., Kızıl, M. & Çelik, T. (2016). Effects of different cooking methods on the formation of heterocyclic aromatic amines in goose meat. *Journal of Food Processing and Preservation*, *40*(5), 1047-1053.

Oz, F. (2019). Yüksek Lisans Ders Notları, Atatürk Üniversitesi; Gıda Mühendisliği Bölümü.

Pais, P., & Knize, M. G. (2000). Chromatographic and related techniques for the determination of aromatic heterocyclic amines in foods. *Journal Chromatography B, 747(1-2),* 139–169.

Pais, P., Salmon, C.P., Knize, M.G. & Felton, J.S. (1999). Formation of mutagenic/carcinogenic heterocyclic amines in dry-heated model systems, meats, and meat drippings. *Journal of Agricultural and Food Chemistry, 47(3),* 1098-1108.

Puignou, L., Casal, J., Santos, F.J. & Galceran, M.T. (1997). Determination of heterocyclic aromatic amines by capillary zone electrophoresis in a meat extract. *J. Chrom. A, 769,* 293–299.

Reistad, R., Rossland, O.J., Latva-Kala, K.J., Rasmussen, T., Vikse, R., Becher, G. & Alexander, J. (1997). Heterocyclic aromatic amines in human urine following a fried meat meal. *Food and Chemical Toxicology, 35(10–11),* 945-955.

Robbana-Barnat, S., Rabache, M., Rialland, E. & Fradin, J. (1996). Heterocyclic amines: occurrence and prevention in cooked food. *Environmental Health Perspectives, 104(3),* 280-288.

Salmon, C.P., Knize, M.G., Felton, J.S., Zhao, B. & Seow, A. (2006). Heterocyclic aromatic amines in domestically prepared chicken and fish from singapore chinese households. *Food and Chemical Toxicology, 44,* 484-492.

Savaş, A., Oz, E., & Oz, F. (2021). Is oven bag really advantageous in terms of heterocyclic aromatic amines and bisphenol-A? Chicken meat perspective. *Food Chemistry, 355,* 129646.

Skog, K. (2002). Problems associated with the determination of heterocyclic amines in cooked foods and human exposure. *Food and Chemical Toxicology, 40(8),* 1197–1203.

Skog, K., Augustsson, K., Steineck, G., Stenberg, M. & Jägerstad, M. (1997). Polar and non-polar heterocyclic amines in cooked fish and meat products and their corresponding pan residues. *Food and Chemical Toxicology, 35,* 555-565.

Skog, K. & Jägerstad, M. (1991). Effects of glucose on the formation of PhIP in A model extract and microwave pre-cooking on the formation of heterocyclic aromatic chicken. *Food Chemistry, 145,* 514-521.

Skog, K., Solyakov, A. & Jägerstad, M. (2000). Effects of heating conditions and additives on the formation of heterocyclic amines with reference to aminocarbolines in a meat juice model system. *Food Chemistry, 68*, 299-308.

Skog, K.I., Johansson, M.A.E. & Jägerstad, M.I. (1998). Carcinogenic heterocyclic amines in model systems and cooked foods: A Review on

formation, occurrence and intake. *Food and Chemical Toxicology, 36(9–10),* 879-896.

Solyakov, A., & Skog, K. (2002). Screening for heterocyclic amines in chicken cooked in varios ways. *Food and Chemical Toxicology, 40,* 1205–1211.

Soyer, A., Kolsarıcı, N. & Candoğan, K. (1998). Tavuk etlerinin bazı kalite özellikleri ve besin ögelerine geleneksel ve mikrodalga ile pişirme yöntemlerinin etkisi. Ankara Üniversitesi, Ziraat Fakültesi, Gıda Mühendisliği Bölümü, Ankara, Türkiye.

Sugimura, T. & Adamson, R. H. (2000). Introduction. Baffins lane, chichester, west sussex, 373, England.

Sugimura, T. (1997). Overview of carcinogenic heterocyclic amines. Mutation Research/Fundamental and Molecular Mechanisms of Mutagenesis, *376(1–2),* 211-219.

Sugimura, T.S. (1995). History, Present and future of heterocyclic amines, cooked food Mutagens. In R.H. Adamson et al. (Eds.) heterocyclic amines in cooked foods: possible human carcinogens (pp. 214-231). Princeton Scientific Publishing Co, Princeton, New Jersey.

Shabbir, M. A., Raza, A., Anjum, F. M., Khan, M. R., & Suleria, H. A. R. (2015). Effect of thermal treatment on meat proteins with special reference to heterocyclic aromatic amines (HAAs). *Critical Reviews in Food Science and Nutrition*, *55*(1), 82-93.

Tengilimoglu-Metin, M. M., Hamzalioglu, A., Gokmen, V., & Kizil, M. (2017). Inhibitory effect of hawthorn extract on heterocyclic aromatic amine formation in beef and chicken breast meat. *Food Research International, 99*, 586–595.

Toribio, F., Moyano, E., Puignou, L. and Galceran, M. T. (2002). Ion-trap tandem mass spectrometry for the determination of heterocyclic amines in food. *Journal of Chromatography A, 948,* 267–281.

Tornberg, E. (2005). Effects of heat on meat proteins – implications on structure and quality of meat products. *Meat Science, 70(3),* 493-508.

Turesky, R.J., Taylor, J., Schnackenberg, L., Freeman, J.P. & Holland, R.D. (2005). Quantitation of carcinogenic heterocyclic aromatic amines and detection of novel heterocyclic aromatic amines in cooked meats and grill scrapings by HPLC/ESI-MS. *Journal of Agricultural and Food Chemistry, 53(8),* 3248-3258.

Viegas O., Novo P. and Pinto O., Ferreira I.M.P.L.V.O. (2012). Effect of charcoal types and grilling conditions on formation of heterocyclic aromatic amines (HAs) and polycyclic aromatic hydrocarbons (PAHs) in grilled muscle foods. *Food and Chemical Toxicology, 50(6),* 2128-2134.

Wakayabashi, K., Ushiyama, H.,,Takahashi, M., Nukaya, H., Kim, S.B.,Hirose, M., Ochiai, M., Sugimura, T. & Nagao, M. (1993). Exposure to heterocyclic amines, *Environmental Health Perspectives*, *99,* 129-133.

Warzecha, L., Janoszka, B., Błaszczyk, U., Stróżyk, M., Bodzek, D. and Dobosz, C., 2004. Determination of heterocyclic aromatic amines (HAs) content in samples of household-prepared meat dishes. *Journal of Chromatography B, 802(1),* 95-106.

Wong, K.-Y., Su, J., Knize, M.G., Koh, W.-P. & Seow, A. (2005). Dietary exposure to heterocyclic amines in a chinese population. *Nutrition and Cancer, 52(2),* 147-155.

Yıldız, N. ve Bircan, H., 1991. Uygulamalı istatistik. *Atatürk Üniversitesi Yayınları,* No: 704-308- 60.

Zorba, A.M. (2009). Tavuk eti ürünlerine (sosis, burger, köfte) uygulanan gama ışınlamanın yağ asitleri kompozisyonu üzerine etkisinin belirlenmesi The effects of gamma irradition on fatty acids composition on chicken meat products (sausage, burger and meatball). Yüksek Lisans Tezi.

Chapter 3

THE UTILIZATION OF DEEP LEARNING BASED IMAGE PROCESSING METHOD IN THE DIAGNOSIS OF ALZHEIMER'S DISEASE

Emrah IRMAK[1]

1 Assist. Prof. Dr. Emrah IRMAK, Alanya Alaaddin Keykubat University, Engineering Faculty, Electrical-Electronics Engineering Department, Alanya/Antalya/Turkey, emrah.irmak@alanya.edu.tr, ORCID ID: 0000-0002-7981-2305

1. INTRODUCTION

1.1. Background

Alzheimer's disease is known as a neurodegenerative brain disease which has gained significant interest especially in recent years. It is also the most common type of dementia which is a broader range of neurodegenerative disease group. The death of human brain cells over time causes memory loss, dementia, and decreased cognitive functions, and this medical abnormality eventually results in Alzheimer's disease. The disease, which manifests itself only with simple forgetfulnesses in the initial phase, may progress as time passes until the patient forgets recent events and is unable to recognize family members and immediate surroundings. In the more advanced stages of the disease, patients have difficulty meeting their basic needs and become in need of care. Social skills, behaviours, and logical thinking are also adversely affected over time. Although the disease mostly affects individuals aged 65 and over, it cannot be considered as an old age disease because younger-onset samples are frequently encountered.

The total number of people suffering from Alzheimer's and other dementias worldwide is approximately 50 million according to the World Dementia Report 2020 announced by the World Health Organization (WHO) [1]. It is also worth noting that this number is increased by 10 million every year. The announced report states that the percentage of dementia patients in the population aged 60 and over is between 5-8%. Alzheimer's Disease Facts and Figures 2020, an annual report released by the Alzheimer's Association, shows that the number of Americans over the age of 65 suffering from Alzheimer's dementia is more than 5 million in 2020 [2]. The same report states that the estimated money spent on Alzheimer's and other dementia diseases is $305 billion while this amount is estimated to increase to $1.1 trillion in 2050.

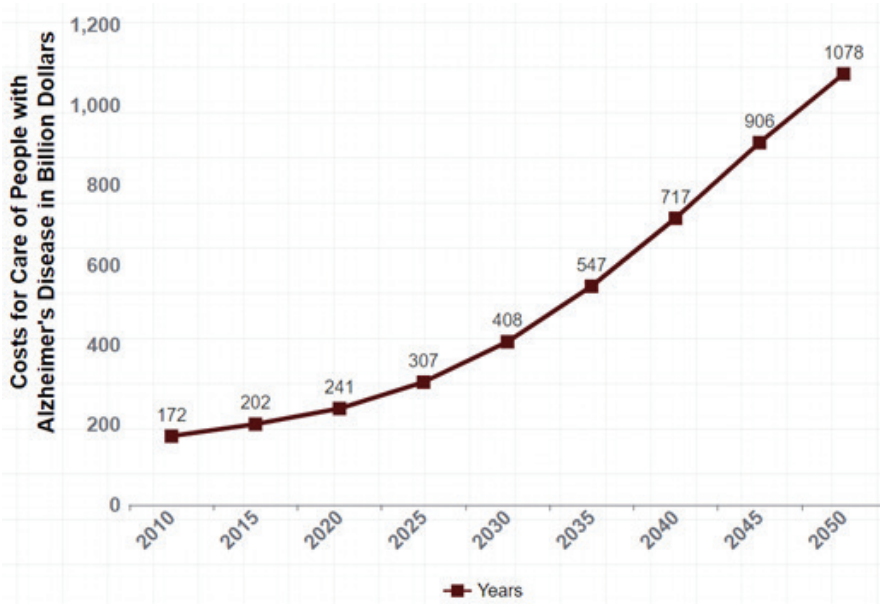

Figure 1. *Costs spent on caring for Alzheimer's patients in billion dollars*

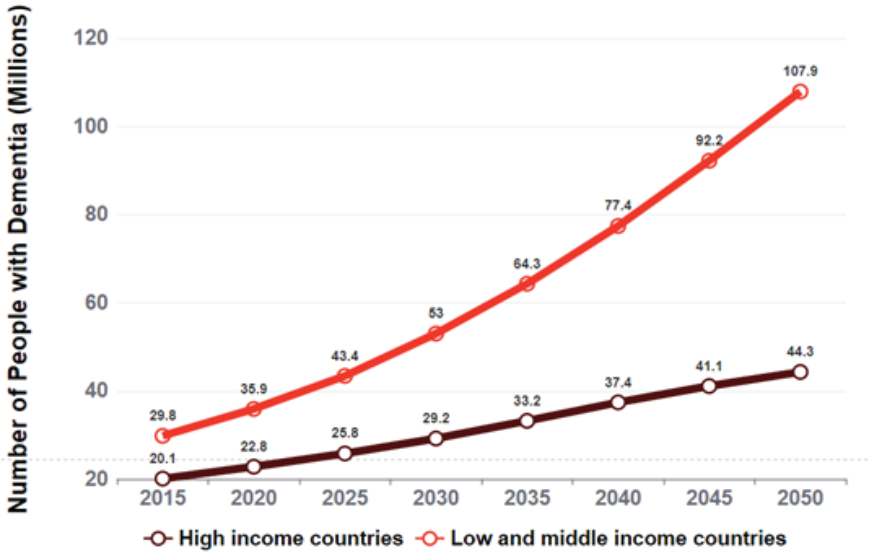

Figure 2. *Number of people with Dementia in High and Low-Middle income countries*

Although Alzheimer's is a disease that has been the subject of scientific research for many years, the cause of the development of the disease has not been determined yet. There is no differential diagnostic test that can give clear information about the diagnosis of Alzheimer's disease. Therefore,

many medical diagnostic tests are evaluated together in the diagnosis of the disease. After the medical history is taken, various scans are performed to measure neurological functions, balance, sensation, behaviour, memory and reflexes. In the brain tissue examinations performed on Alzheimer's patients, beta amyloid plaques seen around the dead brain cells are found. The brain shrinks due to cell loss.

1.2. Role of Deep Learning in Disease Diagnosis

Mankind has thought about reviving and activating inanimate objects for centuries [3]. Although its history dates back to ancient times, the main development in Artificial Intelligence (AI) and Artificial Neural Network (ANN) has occurred in the last sixty years. If Machine Learning (ML) is a sub-branch of Artificial Intelligence (AI), then Deep Learning (DL) can also be considered a sub-branch of ML. The evolution of the subject proceeded as AI > ML > DL [4]. Deep Learning (DL) is a class of Machine Learning (ML) that emerged with the further development of AI [5], [6]. Although the first studies on DL have a long history, one of the main reasons for its successful use in recent years is the availability of sufficient data [7]–[9]. Another reason why DL is more popular nowadays is the availability of computational resources to run larger models today. The use of hidden layers in ANN has increased the memory capacity and processing capacity for computing. The network is deepened by increasing the number of hidden layers, resulting in the need for faster computers with larger memory. Therefore, the Graphical Processing Unit (GPU) is used for general purposes instead of the Central Processing Unit (CPU). The development of big data and GPUs allowed different DL models to be designed. These models are designed to learn from input data without user-specified features [10]. This is achieved by discovering different characteristics of data in different layers. The basic model of these architectures is considered ANN. ANNs are successfully applied to image classification, object identification, image segmentation, and so on. CNNs are the developed and expanded versions of ANNs. The network deepening as a result of increasing the number of hidden layers in ANNs can be defined as CNN. This depth in the CNN was achieved by the use of 2-Dimensional filters. In addition to this difference in depth, CNNs perform learning in a hierarchical structure. Finally, the main difference that CNNs distinguish from ANNs is the DropOut method that CNNs use to prevent memorization during the training of the deepening network structure [11]. This method aims to prevent the memorization by removing some of the nodes of the network nicely in each iteration during the training phase. CNN technique has emerged as the most successful DL method used for the diagnosis of various diseases from medical images in recent years. CNN models are successfully performed to diagnose brain tumor, lung cancer, COVID-19,

malaria etc. using various medical imaging techniques such as MRI, CT, PET, Ultrasound, X-Ray etc [12]–[14].

1.3. Related Work

Diagnosing Alzheimer's disease using radiological imaging and DL is a very popular and hot area of research. Therefore, there are quite a few studies in the literature on this subject and the number of these studies is increasing day by day. For example, Marzban et al. [15] proposed a CNN method to detect the Alzheimer Disease using Magnetic Resonance images and Diffusion Tensor images. They achieved an overall accuracy of 93.5% using ten-fold cross validation scheme. They used 300 scans to train and test the CNN network. In another study which was performed by Sorensen et al. [16], Ensemble Support Vector Machine (SVM) was utilized for dementia classification. They classified input MRI images as Normal (Healthy) Control, mild cognitive impairment (MCI), converting MCI and AD. They performed their method on 240 images and obtained 55.6% and 55.0% classification accuracy using a linear and a radial basis function kernel, respectively. Bidani et al. [17] exploited deep neural networks and transfer learning for dementia detection and and classification. 84 MRI images were used to train and test the DL model. They obtained 68.13% and 81.94% classification accuracy result with transfer learning and deep CNN method, respectively. Another researcher group [18] proposed an ANN technique for dementia diagnosis using multiple modalities of neuroimaging. They used MRI and Positron Emission Tomography (PET) scans of 800 patients. They validated their results using Specificity (SPE), Sensitivity (SEN) and Area Under the Curve (AUC) value performance evaluation metrics. 0.62, 0.97 and 0.85 were found for SPE, SEN and AUC, respectively. Researcher who are interested in more similar literature papers can investigate [19]–[22]. Survey papers by Turner et al. [23] and Pietrzak [24] are also rich reference sources for the researcher who are interested in diagnosis of dementia using DL based methods.

This study presents a DL method which is based on CNN for Alzheimer's disease using publicly available medical dataset. The remainder of this chapter can be organized as follows: Section 2 presents the general purpose CNN structure and CNN model proposed in this study. Section 3 covers the experimental result, discussions and comparison of the proposed method with the state-of-art methods. Finally, Section 4 concludes the chapter.

2. MATERIAL AND METHODS

2.1. Convolutional Neural Network (CNN)

CNN has been inspired by the human visual cortex which is hidden in brain visual structures. Various neurons inside these multiple visual structures react

to different features such as edges, colors and shapes, etc. CNN is composed of artificial neuron structures which serve as basic learner units by extracting characteristic features from the input images. These learnable features in the images are generally primitive components such as edges, colors, circles, squares, etc. and are sometimes complex components such as certain shapes, tumors, lesions, eyes, buildings, etc. As the number of neuron layers increases, the ability of the CNN to extract more features to train by itself that results in self-learning is increased as well. AlexNet (2012), GoogleNet (2014), LeNet (1998), ZFNet (2013), Visual Geometry Group (VGG-2014), ResNet (2015) are the most popular proposed CNN models for image processing purposes. The convolutional layer neurons which are actually convolution filters mathematically convolve with the input data which is generally raw images. Each convolution filters extracts and holds important weights which are actually learnable parameters within the input images after this convolution processes. As the CNN layers deepen, the network tends to learn more features belong to the input images. Although CNNs are composed of several variations, they generally have certain structures. A general purpose CNN architecture is shown in Figure 3. A typical CNN have convolutional and ReLU layers which are generally grouped into single modules. A pooling layer follows each of these modules. Fully connected layers are the last layers of the CNN architectures. CNN are considered as deep learning network because modules are stacked on top of each other which deepen the neural networks. In Figure 3 for example, an MRI image of a patient with suspected illness is directly fed to the CNN. The input image goes through several stacked convolutional and ReLU layers modules until the reach to pooling layers. After that journey, the learned features feed one or more fully connected layers. The predicted class is outputted by the last fully connected layer.

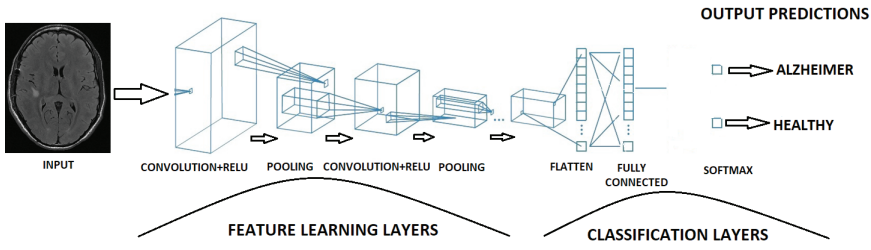

Figure 3. *General purpose CNN structure for Alzheimer detection*

2.2. CNN Structure

2.2.1. Input Layer

First layer of all CNN architecture is input layer in which pre-processing operations such as re-sizing and normalization of the input images are

performed. In performing image processing, a proper image size for input stage should be selected for network depth, hardware calculation cost, and network success.

2.2.2. Convolutional Layer

Convolutional layers are feature extractor layers. A typical convolutional layer includes artificial visual neurons which are weighted filters and are responsible of learning process. These filters perform convolution operation on input images and output feature maps. Figure 4 is a theoretical example of these convolution operations implemented in convolutional layer. Input image is a 5x5x3 in size whereas the convolutional filter is 3x3 for this illustrative example. Now that the input is a 3-dimensional RGB image, the filter must have three channels; each filter corresponds to each color dimension. As can be seen from the figure, each filter applies dot product on a small section of each corresponding image channel, and this operation is carried on until the whole image pixels are gone under dot product with the convolution filter. The dot product results of each filter are summed up to obtain feature map which are known as learnt parameters. Mathematical formulation of convolution operation is shown in Equation 1. A typical CNN model consists of dozens of convolutional layer which includes thousands or even sometimes millions of convolution filter and this explain the learning strategy of these CNN models.

$$x_j^n = f\left(\sum_{i \in F_j} x_j^{n-1} x k_{ij}^n + b_j^n\right) \tag{1}$$

where n is the number of layers in the convolutional layer, b is a bias and:

i = the index of input neuron node

j = the index of output neuron node

f = an activation function

F_j = upper level feature map

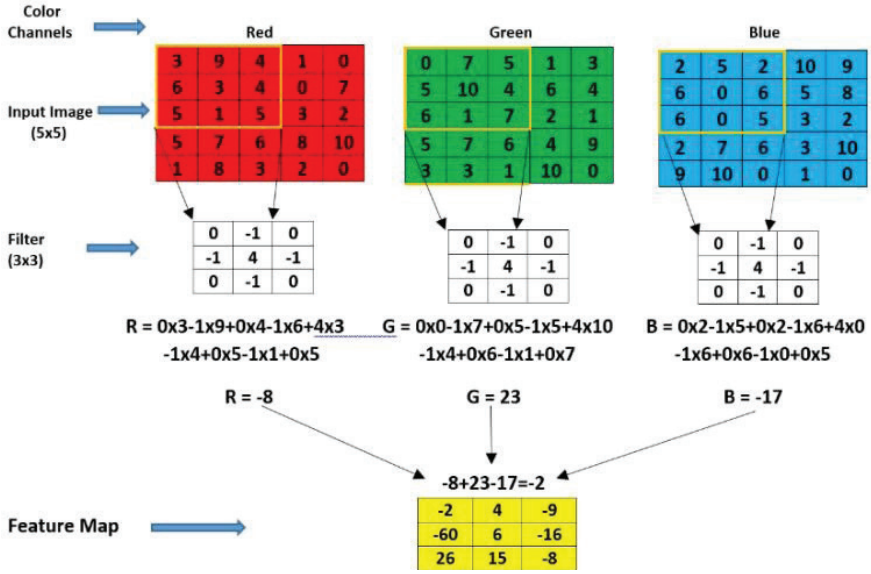

Figure 4. *A 3x3 filter applied on an input image of size 5x5x3 in convolution layer of CNN*

2.2.3. Rectified Linear Units Layer (ReLU)

ReLU is a nonlinear activation function that extracts nonlinear features. Activation functions are important parts of CNNs because they affect the training time of deep neural network. The mathematical form of these activation functions is:

$$f(x) = \begin{cases} 0, & x < 0 \\ x, & x \geq 0 \end{cases} \quad (2)$$

The interpretation of this mathematical statement is that a ReLU operation keeps only the positive values of the activations while converts the negative values to zero. This accelerates the training of the network. Figure 5 is the plot of ReLU function.

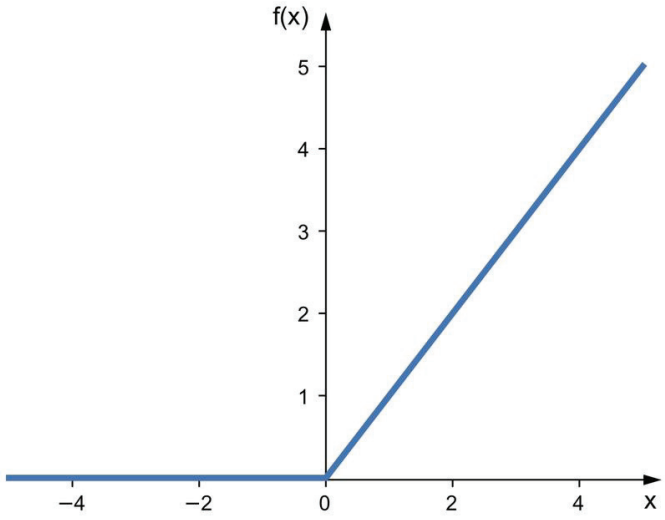

Figure 5. *The plot of ReLU function*

2.2.4. Pooling Layer

Pooling layer down-samples the data dimension of the input feature maps. This operation decreases the network complexity and results in a faster learning. Figure 6 shows a max-pooling process commonly used in CNN models. Figure demonstrates that the 4x4 input data is decreased to 3x3 or 2x2 output data if sliding with stride = 1 or stride = 2 is adopted after the pooling process by using a 2x2 pooling filter.

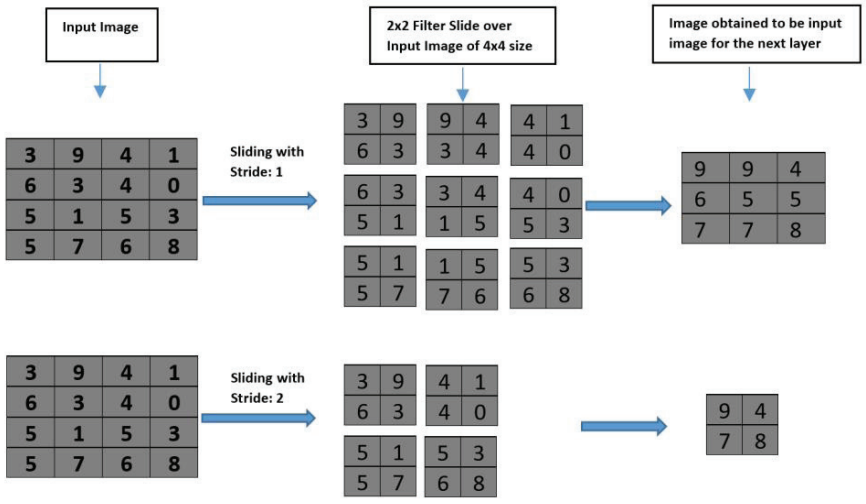

Figure 6. *Implementation of max-pooling with 2x2 filter in 4x4 input image*

2.1.5. Fully Connected Layer

Fully connected layers are responsible for interpretation of feature representations obtained from previous layer. The inputs of these layers are the output maps from the previous pooling layer and these maps are arranged into vectors. The output of last fully connected layer is the learnt feature and is the input to the softmax layer (learning classifier) which gives the predicted classification output. To sum up at this point, CNN learning approach can be considered into two milestones: (a) Network training by feature extracting and (b) classification.

2.1.6. Softmax Layer

Softmax layer provides a decimal probability value for each object class. Softmax layer is a normalized exponential function which is used to bring all the predicted values between 0 and 1 using the Equation 3.

$$y(z)_j = \frac{e^{z_j}}{\sum_{k=1}^{k} e^{z_k}} \quad (3)$$

where y(z) is the probability of any class, j indicates these classes, k is the total number of classes.

3. EXPERIMENTAL RESULTS AND DISCUSSIONS

Dataset for training and test the DL network was obtained from publicly available data source called Alzheimer Disease Neuroimaging Initiative (ADNI) [25]. ADNI is a multi-center long-term initiative established to find solutions for the early diagnosis of Alzheimer's disease and the treatment of Alzheimer's patients. The demographic information of the subjects is listed in Table 1. A total of 670 brain MRI images of 110 healthy subjects and 94 clinically diagnosed with very mild to moderate Alzheimer's disease subjects are used for training and testing the CNN model in this study. These dataset is divided in to training, validation and test data set using 60%-20-%20% scheme. Consequently, 402 images are used for training the network while 134 images are used for validation and 134 images are used for testing. All the images are resized to 227x227.

Table 1. *Alzheimer dataset demographics used in the study*

	Number of Subjects		
Age	Healthy Cases	Alzheimer's Disease Patients	Total Number of Images
60-69	20	10	144
70-79	40	45	256
80-89	30	25	120
Over 90	10	14	150

The experiments of this study are performed on an NVIDIA GeForce GTX-850M platform that has Intel Core i7 5400 GPU, 2.60 GHz, 16.0 GB RAM whereas software platform consists of Windows 10 (64-bit) operating system software platform using MATLAB 2019a version. 17 minutes is elapsed throughout of the training the proposed CNN model.

In this study, a novel CNN model is utilized to detect Alzheimer's disease using Magnetic Resonance Imaging (MRI) images. The proposed CNN model consists of 1 input layer, 3 convolutional layers, 3 ReLU layers, 3 max-pooling layers, 1 dropout layer, 1 softmax layer and 2 fully connected layers. The hyper-parameters tuning used for this experiment are as follows: The Initial Learning Rate is 0.0001, Momentum is 0.9000, L2 regularization is 0.0001, and Mini-batch size is 10. Figure 7 shows the Accuracy plot of the proposed study. As can be seen from the figure, on overall accuracy of 96.33% is achieved after 318 iterations. There 6 epochs and the iteration per each epoch is 53. Figure 8 shows is the Loss plot of the proposed study.

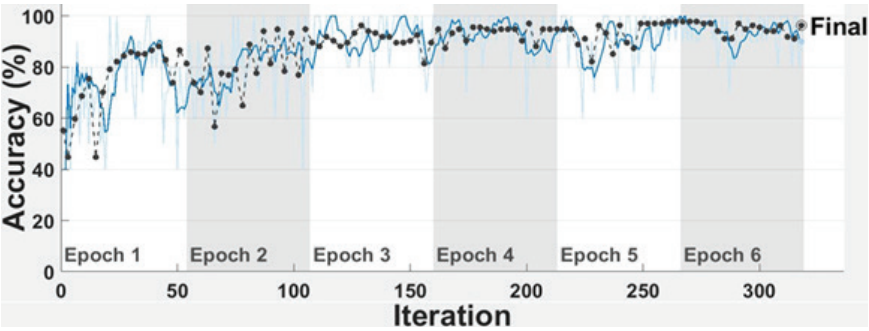

Figure 7. *Accuracy plot*

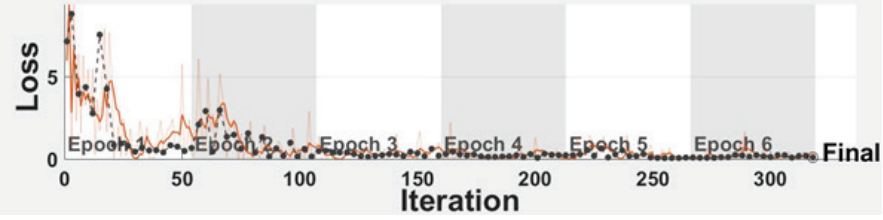

Figure 8. *Loss plot*

In this study, the performance of the proposed CNN method is evaluated using Accuracy, AUC, Sensitivity, Specificity and Precision performance evaluation metrics which are derived from confusion matrix. The corresponding equations are derived from confusion matrix and demonstrated in Equations 4, 5, 6 and 7, respectively. True Positive (TP) stands for correctly classified positive cases whereas True Negative stands

for correctly classified negative cases. False Positive (FP) is for incorrectly classified positive cases and False Negative (FN) is for incorrectly classified negative cases.

$$\text{Accuracy} = \frac{TP+TN}{TP+TN+FP+FN} \quad (4)$$

$$\text{Specificity} = \frac{TN}{TN+FP} \quad (5)$$

$$\text{Sensitivity} = \frac{TP}{TP+FN} \quad (6)$$

$$\text{Precision} = \frac{TP}{TP+FP} \quad (7)$$

Figure 8 is confusion matrix of the classification task. There are a total of 134 MRI test images, of which 74 are Healthy and 60 are Alzheimer's patients. As figure shows, 57 and 72 predictions are correctly classified as Alzheimer and Healthy cases, respectively. On the other hand, 2 Healthy cases are misclassified as Alzheimer cases whereas 3 Alzheimer cases are misclassified as Healthy cases. The overall classification success is 96.33%. Figure 9 is Area Under the Curve (AUC) value of Receiver Operating Characteristics (ROC) Curve. AUC is found to be 0.9801.

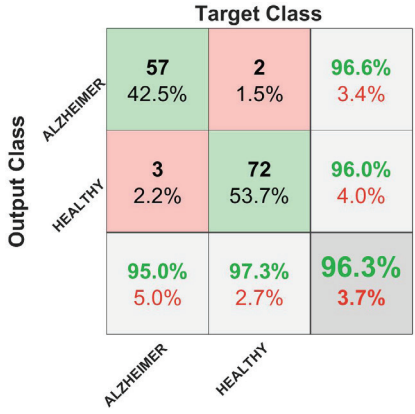

Figure 8. *Confusion matrix*

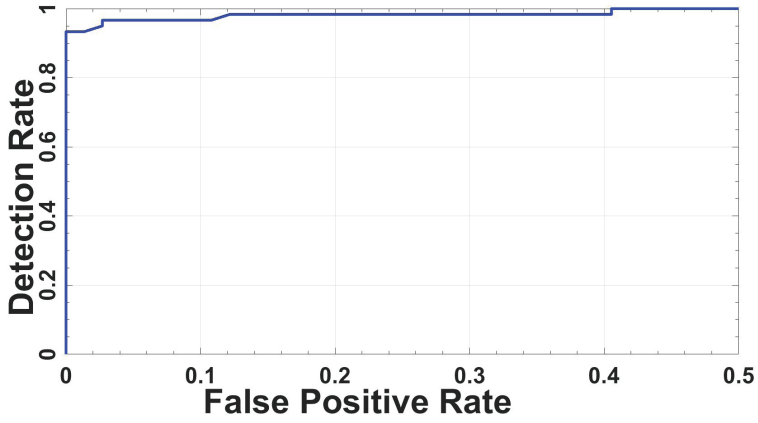

Figure 9. *ROC curve*

In this study, Alzheimer's disease is successfully performed from MRI images using a novel CNN model. The experimental results indicate the success of the proposed method. The results obtained in this study are quite promising when compared with the previous works. For example, Liu et al. [18] used an artificial neural network approach for Alzheimer's disease diagnosis and obtained an AUC value of 0.85. In another DL based study of Alzheimer's disease diagnosis Marzban et al. [15] used the CNN model and obtained an overall classification accuracy of 93.5%. Moreover, Bidani et al. [17] utilized transfer learning approach of pre-trained CNN models to diagnose Alzheimer's disease and achieved an overall accuracy of 81.94%. Sorensen et al. [16] obtained an overall accuracy of 59.1% by using ensemble support vector machine approach to diagnose Alzheimer's disease.

4. CONCLUSION

Alzheimer's disease is a serious health problem that has become very common recently and is expected to increase exponentially in the future. In this study, the diagnosis of Alzheimer's disease is successfully performed using a novel CNN model from publicly available MRI dataset. An overall classification accuracy of 96.33% is achieved and an AUC value of 0.9801 is obtained using the proposed study. This study is thought to be a good reference resource for researchers interested in the diagnosis of Alzheimer's disease with DL.

REFERENCES

[1] World Health Organization (WHO), "World dementia report 2020," 2020. https://www.who.int/health-topics/dementia#tab=tab_1 (accessed Feb. 04, 2020).

[2] The Alzheimer's Association, "2020 Alzheimer's disease facts and figures," 2020. https://www.alz.org/alzheimers-dementia/facts-figures (accessed Feb. 04, 2020).

[3] A. Lindgreen and A. Lindgreen, "Corruption and unethical behavior: report on a set of Danish guidelines," *J. Bus. Ethics*, vol. 51, no. 1, pp. 31–39, 2004, doi: 10.1023/B.

[4] Y. W. T. Geoffrey E. Hinton, Simon Osindero, "A fast learning algorithm for deep belief nets," *Neural Comput.*, vol. 18, no. 7, pp. 1527–1554, 2006.

[5] Y. Bengio, P. Lamblin, D. Popovici, and H. Larochelle, "Greedy layer-wise training of deep networks," *Adv. Neural Inf. Process. Syst.*, no. 1, pp. 153–160, 2007, doi: 10.7551/mitpress/7503.003.0024.

[6] C. Poultney, S. Chopra, Y. L. Cun, and others, "Efficient learning of sparse representations with an energy-based model," *Adv. Neural Inf. Process. Syst.*, pp. 1137–1144, 2006.

[7] Y. Bengio and Y. Lecun, "Scaling Learning Algorithms toward AI," *Large-Scale Kernel Mach.*, no. 1, pp. 1–41, 2019, doi: 10.7551/mitpress/7496.003.0016.

[8] O. Delalleau and Y. Bengio, "Shallow vs. deep sum-product networks," *Adv. Neural Inf. Process. Syst. 24 25th Annu. Conf. Neural Inf. Process. Syst. 2011, NIPS 2011*, pp. 1–9, 2011.

[9] G. F. Montúfar, "Universal approximation depth and errors of narrow belief networks with discrete units," *Neural Comput.*, vol. 26, no. 7, pp. 1386–1407, 2014, doi: 10.1162/NECO_a_00601.

[10] Y. Bengio, A. Courville, and P. Vincent, "Representation learning: A review and new perspectives," *IEEE Trans. Pattern Anal. Mach. Intell.*, vol. 35, no. 8, pp. 1798–1828, 2013, doi: 10.1109/TPAMI.2013.50.

[11] R. S. Nitish Srivastava, Geoffrey E. Hinton, Alex Krizhevsky, Ilya Sutskever, "Dropout: a simple way to prevent neural networks from overfitting," *J. Mach. Learn. Res.*, vol. 15, pp. 1929–1958, 2014.

[12] E. Irmak, "Multi-classification of brain tumor MRI images using deep convolutional neural network with fully optimized framework," *Iran. J. Sci. Technol. - Trans. Electr. Eng.*, vol. 45, no. 3, pp. 1015–1036, 2021, doi: 10.1007/s40998-021-00426-9.

[13] E. Irmak, "COVID-19 disease severity assessment using CNN model," *IET Image Process.*, vol. 15, no. 8, pp. 1814–1824, 2021, doi: 10.1049/ipr2.12153.

[14] E. Irmak, "Implementation of convolutional neural network approach for COVID-19 disease detection," *Physiol. Genomics*, vol. 52, no. 12, pp. 590–601, 2020, doi: 10.1152/physiolgenomics.00084.2020.

[15] E. N. Marzban, A. M. Eldeib, I. A. Yassine, and Y. M. Kadah, "Alzheimer's disease diagnosis from diffusion tensor images using convolutional neural networks," *PLoS One*, vol. 15, no. 3, pp. 1–16, 2020, doi: 10.1371/journal.pone.0230409.

[16] L. Sørensen and M. Nielsen, "Ensemble support vector machine classification of dementia using structural MRI and mini-mental state examination," *J. Neurosci. Methods*, vol. 302, pp. 66–74, 2018, doi: https://doi.org/10.1016/j.jneumeth.2018.01.003.

[17] B. Amen, G. Salah Mohamed, and G. Carlos, "Dementia detection and classification from MRI images using deep neural networks and transfer learning," in *Advances in Computational Intelligence*, A. C. Prof. Ignacio Rojas, Gonzalo Joya, Ed. Springer International Publishing, 2019.

[18] J. Liu, S. Shang, K. Zheng, and J.-R. Wen, "Multi-view ensemble learning for dementia diagnosis from neuroimaging: An artificial neural network approach," *Neurocomputing*, vol. 195, pp. 112–116, 2016, doi: https://doi.org/10.1016/j.neucom.2015.09.119.

[19] M. R. Ahmed, Y. Zhang, Z. Feng, B. Lo, O. T. Inan, and H. Liao, "Neuroimaging and machine learning for dementia diagnosis: Recent advancements and future prospects," *IEEE Rev. Biomed. Eng.*, vol. 12, pp. 19–33, 2019, doi: 10.1109/RBME.2018.2886237.

[20] D. Yim, T. Y. Yeo, and M. H. Park, "Mild cognitive impairment, dementia, and cognitive dysfunction screening using machine learning.," *J. Int. Med. Res.*, vol. 48, no. 7, p. 300060520936881, Jul. 2020, doi: 10.1177/0300060520936881.

[21] S. A. Graham *et al.*, "Artificial intelligence approaches to predicting and detecting cognitive decline in older adults: A conceptual review.," *Psychiatry Res.*, vol. 284, p. 112732, Feb. 2020, doi: 10.1016/j.psychres.2019.112732.

[22] F. Agosta, F. Caso, and M. Filippi, "Dementia and neuroimaging," *J. Neurol.*, vol. 260, no. 2, pp. 685–691, 2013, doi: 10.1007/s00415-012-6778-x.

[23] R. S. Turner, T. Stubbs, D. A. Davies, and B. C. Albensi, "Potential new approaches for diagnosis of Alzheimer's Disease and related dementias.," *Front. Neurol.*, vol. 11, p. 496, 2020, doi: 10.3389/fneur.2020.00496.

[24] K. Pietrzak, K. Czarnecka, E. Mikiciuk-Olasik, and P. Szymanski, "New perspectives of Alzheimer Disease diagnosis - the most popular and future methods," *Med. Chem.*, vol. 14, no. 1, pp. 34–43, 2018, doi: 10.2174/1573406413666171002120847.

[25] "Alzheimer's Disease Neuroimaging Initiative." http://adni.loni.usc.edu/ (accessed Feb. 02, 2021).

Chapter 4

PREEMPTIVE GOAL PROGRAMMING APPROACH FOR ASSEMBLY LINE WORKER ASSIGNMENT AND REBALANCING PROBLEM

Aslıhan KARAŞ[1]
Feriştah ÖZÇELIK[2]

1 Department of Industrial Engineering, Eskişehir Osmangazi University, Eskişehir, Turkey
+90(222)2393750-3615, aslihan.karas@ogu.edu.tr, ORCID: 0000-0002-7317-447X
2 Department of Industrial Engineering, Eskişehir Osmangazi University, Eskişehir, Turkey
+90(222)2393750-3630, fdurmaz@ogu.edu.tr, ORCID: 0000-0003-0329-203X

1. Introduction

Assembly line refers to the manufacturing process where parts move through a transportation system and are assembled at workstations in order. On these lines, operations are performed at each station by following precedence relations of tasks. Large variabilities among workstations in workload bring along efficiency decreases. Therefore, it is critical to keep the assembly lines in balance.

The assembly line balancing (ALB) problem is the assignment of tasks to workstations in a balanced way under certain constraints to optimize the desired efficiency measure. In enterprises working with manual labour, differences in experience and skill cause processing times to vary according to the workers. Regarding this situation, Miralles, García-Sabater, Andrés, and Cardós (2007) proposed the assembly line worker assignment and balancing (ALWAB) problem, in which a group of tasks and a worker are allocated to each workstation concurrently, and worker performances are considered. The ALWAB problem focuses on the line balancing during the initial installation of which assignments cannot be changed.

Falkenauer (2005) argued that the need for rebalancing is more frequent than initial balancing due to some disruptions in production systems. The assembly line rebalancing (ALRB) problem considers the required processing times are independent of the worker executing these tasks.

Karaş and Özçelik (2021) introduced the assembly line worker assignment and rebalancing (ALWARB) problem integrating the ALWAB and ALRB problems with the aim of rebalancing the assembly line when some workstations become unusable with workers who have different performances. They aimed at optimizing the cycle time increase and the workstation assignment changes of tasks following disruptions for rebalancing the line achieving the minimum changes according to the initial case.

In production environments, managers concern with dividing the workload among all workers as equally as possible so as to improve the workload planning and utilize resources rationally. It is also beneficial for decreasing ergonomic risks and preventing fatigues and injuries arising from excessive workload. In spite of the significance of the workload smoothing in assembly lines, studies on this subject are limited.

The studies in the literature on the ALWAB, ALRB, and ALWARB problems are summarized in Table 1. As seen from the table, most researchers have focused on minimizing the cycle time. Although workload smoothing has rarely been studied in ALWAB and ALRB, it has been neglected in the ALWARB literature. To the best of our knowledge, workload smoothing is considered for the first time within the context of the ALWARB problem in the present study.

Table 1
Summary of literature on the ALWAB, ALRB, and ALWARB problems

Study	WA	RB	CS	NW	CT	RT	WS
Miralles et al. (2007)	✓				✓		
Moreira & Costa (2009)	✓				✓		
Chaves, Lorena, & Miralles (2009)	✓				✓		
Blum & Miralles (2011)	✓				✓		
Moreira, Ritt, Costa, & Chaves (2012)	✓				✓		
Araújo, Costa, & Miralles (2012)	✓				✓		
Castellucci & Costa (2012)	✓				✓		
Mutlu, Polat, & Supçiller (2013)	✓				✓		
Vilà & Pereira (2014)	✓				✓		
Borba & Ritt (2014)	✓				✓		
Araújo, Costa, & Miralles (2015)	✓				✓		
Ramezanian & Ezzatpanah (2015)	✓		✓		✓		
Polat, Kalaycı, Mutlu, & Gupta (2016)	✓				✓		
Ritt, Costa, & Miralles (2016)	✓				✓		
Zacharia & Nearchou (2016)	✓				✓		✓
Öksüz, Büyüközkan & Satoğlu (2017)	✓			✓	✓		
Efe, Kremer, & Kurt (2018)	✓			✓			
Akyol & Baykasoğlu (2019)	✓				✓		
Janardhanan, Li &, Nielsen (2019)	✓				✓		
Zhang, Tang, Han, & Li (2019)	✓				✓		
Yılmaz & Erol (2005)		✓	✓				
Gamberini, Grassi, & Rimini (2006)		✓	✓			✓	
Corominas, Pastor, & Plans (2008)		✓		✓			
Gamberini, Gebennini, Grassi, & Regattieri (2009)		✓	✓			✓	
Ağpak (2010)		✓		✓			
Grangeon, Leclaire, & Norre (2011)		✓		✓		✓	✓
Yang, Gao, & Sun (2013)		✓	✓	✓			✓
Çelik, Kara, & Atasagun (2014)		✓	✓				
Makssoud, Battaïa, Dolgui, Mpofu, & Olabanji (2015)		✓		✓		✓	
Sancı & Azizoğlu (2017)		✓			✓	✓	
Li (2017)		✓		✓			
Zhang, Hu, & Wu (2018)		✓	✓		✓		
Belassiria, Mazouzi, ELfezazi, Cherrafi, & ELMaskaoui (2018)		✓		✓	✓		✓
Serin, Mete, & Çelik (2019)		✓	✓				
Zhang, Hu, & Wu (2020)		✓	✓		✓		✓
Karaş & Özçelik (2021)	✓	✓			✓	✓	
This study	✓	✓			✓	✓	✓

WA: Worker assignment, RB: Rebalancing, CS: Cost, NW: The number of workstations, CT: Cycle time, RT: Reassigned tasks, WS: Workload smoothing

This study addresses the ALWARB problem due to the significance of taking into account both rebalancing and worker performance. Considering the importance of workload smoothing in line balancing problems, the objectives are to minimize the cycle time increase, the number of reassigned tasks and smoothness index. Because of the difficulties in expressing the weight of the objectives numerically, a preemptive goal programming (PGP) model was developed in which the objectives are prioritized with their importance. An artificial bee colony (ABC) algorithm, which takes into consideration the priorities among the objectives, was developed to solve large-sized problems.

In the second and third sections, the proposed PGP model and ABC algorithm are explained in detail, respectively. The results obtained with the developed methods are given in the fourth section. The study is concluded and recommendations for future studies are presented in the last section.

2. Proposed PGP Model

Goal programming allows more than one objective to be considered concurrently and is divided into two as weighted and preemptive. In weighted goal programming, weight values are given in direct proportion to the importance levels of the objectives. However, it may not always be possible to determine these values precisely. In such cases, the preemptive goal programming method can be used, in which the objectives are prioritized with their relative significance to each other. This study presents a preemptive goal programming approach in which the order of priority among objectives was determined as cycle time increase-the number of reassigned tasks-workload smoothness.

In the initial case, tasks are considered to be performed on a single model assembly line where a certain number of workers and workstations sequenced in series. It is assumed that some workstations are permanently or prolonged shut down after some failures. For the line to continue to operate, each task in the disrupted stations must be assigned to an open station. There are more workers than the number of open stations as the workers in the closed stations get idle. The processing time of tasks varies regarding the workers and some workers are not capable of executing some tasks.

One worker works at each workstation and each task must be assigned to only one workstation where precedence relations are provided and of which the worker can perform it. The ALWARB problem deals with both worker and task assignments to the open stations simultaneously. Making these assignments with the minimum cycle time increase is the primary objective. Moving tasks between stations may bring about an additional cost since it requires the transfer or purchase of the resources needed for the relevant task. Thereby, minimization of the number of reassigned tasks received the second priority. Workload smoothness has the third priority as it is generally desired to distribute the total load to the stations as equally as possible.

The PGP model of the discussed problem was developed based on the ALWAB model presented by Miralles et al. (2007). The proposed PGP model is shown below.

Indices

i, j: task ($i, j = 1,2,\ldots,N$)
s: workstation ($s = 1,2,\ldots,S$)
w: worker ($w = 1,2,\ldots,W$)

Sets and parameters

F: the set of disrupted workstations
P_j: the set of immediate predecessors of task j
CT_0: initial cycle time
t_{iw}: processing time of task i for worker w
$a_{is} = 1$, if task i is performed in workstation s in the initial case; 0, otherwise
$G1$: goal value for cycle time; $G1 = CT_0$
$G2$: goal value for the number of reassigned tasks; $G2 = \sum_i \sum_{s \in F} a_{is}$
$G3$: goal value for workload smoothness; $G3 = 0$

Decision variables

x_{isw} = 1, if task i is performed by worker w in workstation s after rebalancing; 0, otherwise
y_{sw} = 1, if worker w is working in workstation s after rebalancing; 0, otherwise
CT: cycle time of the rebalanced line
$d_1^+, d_1^-, d_2^+, d_2^-, d_3^+, d_3^-$: deviation variables

$$\sum_{s}\sum_{w} x_{isw} = 1 \quad \forall i \tag{1}$$

$$\sum_{s} y_{sw} \leq 1 \quad \forall w \tag{2}$$

$$\sum_{w} y_{sw} \leq 1 \quad \forall s \tag{3}$$

$$\sum_{s}\sum_{w} s.x_{isw} \leq \sum_{s}\sum_{w} s.x_{jsw} \quad \forall i,j/\ i \in P_j \tag{4}$$

$$\sum_{i} t_{iw}.x_{isw} \leq CT \quad \forall s,w \tag{5}$$

$$\sum_{i} x_{isw} \leq M.y_{sw} \quad \forall s,w \tag{6}$$

$$\sum_{i}\sum_{w} x_{isw} = 0 \quad \forall s \in F \tag{7}$$

$$CT + d_1^- - d_1^+ = G1 \tag{8}$$

$$\sum_{i}\sum_{s\,|\,a_{is}=0}(\sum_{w} x_{isw} - a_{is}) + d_2^- - d_2^+ = G2 \tag{9}$$

$$\sum_{s\notin F}(CT - \sum_{i}\sum_{w} t_{iw}.x_{isw}) + d_3^- - d_3^+ = G3 \tag{10}$$

$$x_{isw}, y_{sw}, q_{is} \in [0,1] \qquad \forall i,s,w \tag{11}$$

$$CT, d_1^+, d_1^-, d_2^+, d_2^-, d_3^+, d_3^- \geq 0 \tag{12}$$

subject to

$$lexmin\ \{d_1^+, d_2^+, d_3^+\} \tag{13}$$

Constraint (1) controls that each task is performed in one workstation by one worker. Constraint (2) guarantees that a worker can work in at most one workstation. Constraint (3) ensures that at most one worker is assigned to each workstation. Constraint (4) fulfils the precedence relationships for tasks. Constraints (5) and (6) express that worker w in station s is able to perform multiple tasks within cycle time, where M is a sufficiently large number ($\sum_i \sum_w t_{iw} < M$). Constraint (7) implies that any task cannot be allocated to disrupted stations. Constraints (8), (9), and (10) calculate the deviation of cycle time, reassigned number of tasks, and smoothness index from specified goal values, respectively, where$\sum_{s\notin F}(CT - \sum_i \sum_w t_{iw} * x_{isw})$ is the smoothness index. Constraints (11) and (12) are the sign constraints of decision variables. The objective function (13) of the proposed PGP model is minimizing the sum of the positive deviations of the considered objectives from their goal values.

3. Proposed ABC Algorithm

ABC algorithm is a meta-heuristic approach proposed by Karaboğa (2005) inspiring by the foraging behaviour of bee swarms. There are three types of bees in this algorithm: employed, onlooker, and scout. Each solution is represented by a food source, and the quality of a food source shows the success of that solution. In the swarm, there is an employed bee responsible for each food source. They gather information about the quality of the sources and transmit it to the onlooker bees. Onlookers benefit from higher quality resources based on this information. Food sources that cannot be further developed and thus depleted are abandoned. The employed bee of each abandoned source turns into a scout and seeks a random new food source instead. After the new source is found, the scout bee becomes an employed bee again (Karaboğa & Akay 2011; Szeto, Wu, & Ho 2011).

The algorithm starts with the derivation of the initial solutions. Then, neighbour food sources are found during the employed and onlooker bee stages. In the algorithm, the maximum number of trials that can be done consecutively to improve each source is the value of the limit parameter. The sources that exceed limit value are abandoned and new sources are found instead in the scout bee stage. After an iteration, the same steps are repeated from the employed bee stage. As the termination condition, the maximum iteration failure parameter is used. If the best solution accomplished in an iteration is not better than the best solution achieved in all iterations, the iteration failure numerator is incremented by one unit, or else the numerator is set to zero. When the maximum iteration failure value is surpassed, the algorithm is terminated. The pseudocode of the developed ABC algorithm is presented in Figure 1.

```
Initialize parameters
Scout bees find food sources randomly
While iteration failure numerator ≤ Maximum number of iteration failure
    Employed bee stage
    Onlooker bee stage
    Scout bee stage
End While
```

Figure 1. Pseudocode of the proposed ABC algorithm

In the proposed algorithm, solutions are represented by a vector consisting of two segments of which lengths are equivalent to the number

of tasks and workers, respectively. Vector elements are integers, and these present the station to which the respective task/worker is allocated. An example solution vector with eight tasks, three workstations, and three workers is given in Figure 2.

1	1	2	1	2	2	3	3	2	1	3
T-1	T-2	T-3	T-4	T-5	T-6	T-7	T-8	W-1	W-2	W-3

Figure 2. Solution vector

Since disrupted stations cannot be assigned tasks after some stations are closed, only the IDs of open workstations can be placed in the solution vector. Tasks and workers of the disrupted stations get idle. In the new line balance, an idle worker may be assigned to an open workstation, and a different worker may get idle. Each task should be executed in one workstation, including those currently at disrupted stations.

3.1. Derivation of initial solutions

The algorithm begins by generating initial feasible solutions. Three different approaches are applied in this stage. In the first approach, task and worker assignments to open workstations of the current assembly line are handled. Then, only the tasks of disrupted stations are distributed to open stations, taking into account the precedence relations and task-worker compatibility.

Assume the workstation assignments of tasks and workers, precedence relations among tasks, and processing times of tasks for each worker are given in Figure 2, Figure 3 and Table 2, respectively. 'Inf' denotes the cases workers cannot perform the tasks. In case of workstation 2 is disrupted and worker W-1 gets idle, tasks T-3, T-5 and T-6 should be reassigned for the assembly line to continue to operate. If the algorithm selects the first approach for deriving an initial solution, task and worker assignments in open stations are maintained. The algorithm determines a random sequence among the disrupted tasks and assigns each of them an open workstation ensuring the constraints following this sequence. Considering the algorithm generates the sequence T5-T3-T6, the first reassigned task is T5. Since T5 has no predecessor, this task can be allocated to both workstation 1 and workstation 3 for the precedence relations constraint. However, worker W-3 in workstation 3 does not have the ability to compute task T-5. Hence, T-5 can only be reassigned to workstation 1 for the task-worker

capabilities constraint. After T-5 is transferred to workstation 1, the algorithm passes to task T-3. This task should not be processed before T-1 and after T-6 owing to precedence relations (Figure 3). As T-6 is also disrupted and comes after the T-3 in the reassigning sequence, the algorithm takes into account the precedence relations only for between T-1 and T-5. Thus, it is possible to move T-5 to both workstation 1 and workstation 3. T-3 cannot be operated by worker W-2 in workstation 1 and it is reassigned to workstation 3. While task T-6 can be handled by both workers, it must not assign to workstation 1 due to the precedence relation with T-3. When T-6 is allocated to workstation 3, all constraints are provided, and an initial solution is generated (Figure 4). The 'X' in the second part of the vector indicates that the worker of workstation 2 gets idle.

Table 2
Processing times of tasks for each worker (Akyol & Baykasoğlu, 2019)

Tasks	W-1	W-2	W-3
1	8	6	10
2	Inf	20	22
3	10	Inf	30
4	Inf	20	25
5	8	6	Inf
6	22	32	42
7	25	20	30
8	30	25	15

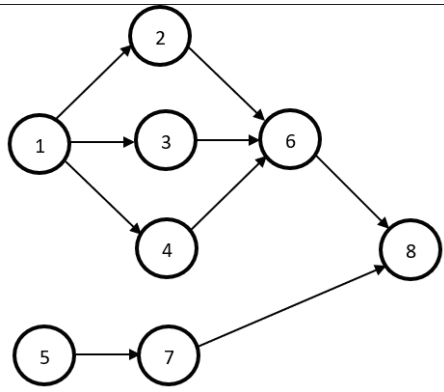

Figure 3. Precedence graph for the example problem (Akyol & Baykasoglu, 2019)

1	1	3	1	1	3	3	3	X	1	3

Figure 4. An initial solution

As regards the second approach, only task-to-workstation assignments of the current line are preserved. Each task at disrupted stations is assigned to an open station ensuring precedence relations. Worker assignments are then made. To obtain a feasible solution, each worker is assigned to an open station where he can do all the tasks.

In the third approach, initial solutions are generated independently of the current assignments. Not only the tasks in the disrupted workstations but all tasks are assigned to open workstations providing precedence relations. Then, a worker is allocated per workstation, considering the ability of the workers to perform the tasks.

In each approach, a feasible initial solution is attained when each task is allocated to an open workstation and task-worker compatibilities are achieved. The approach to be used for generating each solution is chosen randomly. Once a feasible solution is found, the same steps are repeated to derive the next solution. This stage is completed by obtaining the predetermined number of initial solutions.

3.2. Employed bee stage

In this stage, a feasible neighbour solution is obtained for each current solution in the population. In this study, as neighbour solution search structure; moving a task from one station to another (TASK-INSERT), exchanging workstations of two tasks (TASK-SWAP), and exchanging workstations of two workers (WORKER-SWAP) are used. The neighbourhood structure to find a neighbour for each solution is selected randomly. In finding neighbour solutions, precedence relations and task-worker compatibilities are always provided. No task can be assigned to closed stations, but an idle worker may be replaced with a different worker at an open station.

If the neighbour is better than the current solution, it replaces the current one. In this algorithm, unlike the classical ABC algorithm, worse neighbour solutions to a certain extent than the existing solution are also accepted. If the neighbour solution meets the acceptance criteria, the solution failure numerator of this solution is set to zero. Elsewise, this current solution is maintained, and this numerator is incremented by one unit. This stage ends after repeating the same steps for all solutions in the population. For the initial solution given in Figure 4, neighbour solutions found by using the neighbourhood operators are depicted in Figure 5.

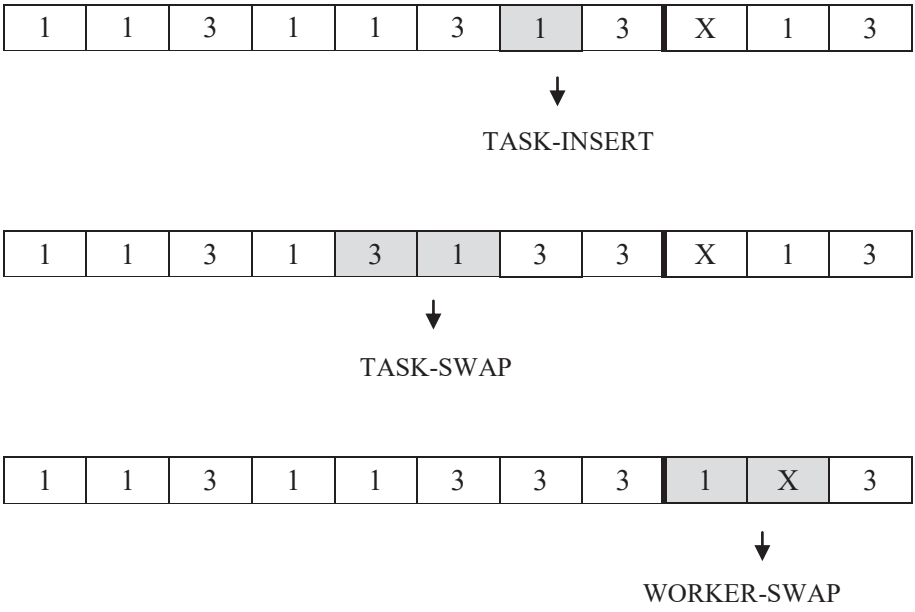

Figure 5. Neighbour solution

3.3. Onlooker bee stage

In this stage, the same neighbourhood structures and acceptance criteria as the employed bee stage are adopted. However, neighbour solutions are found for solutions determined by binary tournament selection instead of all solutions. The solution failure numerators of accepted neighbour solutions are set to zero. If a neighbour solution is rejected, the current one is preserved, and the failure numerator of the respective solution is incremented by one unit. The same steps are repeated for the number of food sources.

3.4. Scout bee stage

In the scout bee stage of the classical ABC algorithm, solutions of which the solution failure numerator exceeds limit value are abandoned and random solutions are generated in place of abandoned ones. In the proposed algorithm, a new solution can be found either selecting one of the strategies randomly in the initial solution derivation stage or from a neighbourhood of the best solution in the population using one of the neighbourhood structures in the employed bee and onlooker bee stages randomly with a certain probability to achieve better

solutions faster. Unlike the classical ABC algorithm, the solution with the minimum objective function value in the population is not abandoned to continue the possibility of finding better solutions even if its limit is surpassed, and the solution failure numerator is set to zero. After the scout bee stage, an iteration is complete.

While the most successful solution attained in the relevant iteration is called the local best solution, the most successful solution achieved during all the iterations is the global best solution. At the end of each iteration, the local and global best solutions are compared. If the global best solution cannot be developed in that iteration, the iteration failure numerator is incremented by one unit, or else the numerator is set to zero. The algorithm terminates when the numerator value surpasses the maximum iteration failure value. If the predetermined value has not been exceeded yet, the next iteration starts from the employed bee stage.

3.5. Evaluating Solutions

In this study, the objectives are handled by prioritizing them concerning their importance compared to each other. Whereas the primary objective is cycle time increase, the secondary and tertiary objectives are the number of reassigned tasks and workload smoothness, respectively. In the proposed algorithm, this priority order is taken into account when determining which solution is better than the other. For this purpose, the approach suggested by Baykasoğlu (2005) is used to evaluate the solutions. Two solutions are first evaluated concerning cycle time and the solution with the smaller cycle time is decided to be better. If the cycle times are equal, it is determined that the solution that has the lower number of reassigned tasks is more successful, considering the secondary objective. If two solutions are equal for the first two objectives, the solution with the smaller smoothness index is better.

4. Results and Discussion

The developed PGP model and ABC algorithm were tested using a computer having Intel Core i5 1.80GHz processor and 8 GB RAM. The performances of the proposed approaches were evaluated on the ALWAB problem benchmark instances presented by Chaves, Insa, and Lorena (2007). These problems consist of 4 families: Roszieg, Heskia, Tonge and, Wee-Mag. There are 8 groups in each problem family and each group contains 10 test problems. By taking the first problems of all groups of problem families, results were obtained on a total of 32 instances.

Since the current line design must be known to solve the ALWARB problem, the assignments before disruption obtained by solving the ALWAB-II problem in Karaş and Özçelik's (2021) study were used for the selected instances. Subsequently, the same workstations were closed for the same test problems as this study.

The PGP model was coded with the GAMS program and CPLEX was used as the solver. The goal values for cycle time, reassigned tasks, and smoothness index are the cycle time of the current assembly line, the number of tasks in the disrupted stations, and zero, respectively. The model was given 3600 seconds time limit for each objective.

The ABC algorithm was coded in MATLAB 2020a programming language. 20 runs were made to solve each instance. The solution population size is 50 and the maximum iteration failure value is 2000. The limit value is taken as 50. In place of abandoned solutions, a random solution is generated with 20% probability, or a neighbour of the local best solution is found with 80% probability in the scout stage.

4.1. Obtained results

The results attained by the proposed approaches for the selected benchmark problems are given in Table 3. From the fifth to seventh columns; the problem name (P), the number of tasks (N), the number of workers (H), the disrupted workstations (F), and goal values ($G1$, $G2$, and $G3$) are presented, respectively. In the next columns; the cycle time (CT) after rebalancing, the number of reassigned tasks (T), and the smoothness index (SI) values achieved by both solution approaches are included. In the columns for the ABC algorithm, the values of the most successful solution among all the runs for the relevant test problem are shown. In the last two columns, there are solution times in seconds.

Table 3
The results obtained by the proposed methods

				Goal values	($CT;T;SI$)		CPU	
P	N	H	F	($G1;G2;G3$)	PGP	ABC	PGP	ABC
R1	25	4	2	(20;7;0)	(28;9;3)	(28;9;3)	0.50	0.11
R11	25	4	2	(30;3;0)	(35;3;17)	(35;3;7)	0.37	0.05
R21	25	4	4	(28;7;0)	(39;12;1)	(39;12;1)	0.39	0.03
R31	25	4	1	(31;5;0)	(41;13;1)	(41;13;1)	0.45	0.12
R41	25	6	4	(10;7;0)	(11;11;2)	(11;11;2)	2.17	0.12
R51	25	6	3	(11;6;0)	(12;11;7)	(12;11;7)	1.67	0.21
R61	25	6	6	(16;4;0)	(19;8;1)	(19;8;1)	2.33	0.20

R71	25	6	5	(15;5;0)	(18;10;1)	(18;10;1)	1.92	0.10
H1	28	4	2	(94;6;0)	(152;21;1)	(152;21;1)	0.74	0.36
H11	28	4	2	(169;7;0)	(244;21;6)	(244;21;6)	0.58	0.24
H21	28	4	3	(216;8;0)	(270;20;4)	(270;20;4)	0.44	0.52
H31	28	4	3	(204;6;0)	(278;11;1)	(278;11;1)	0.67	0.32
H41	28	7	5	(35;5;0)	(37;8;3)	(37;8;3)	1.09	0.13
H51	28	7	4	(51;3;0)	(53;9;20)	(53;9;20)	5.00	19.43
H61	28	7	3	(66;2;0)	(77;9;14)	(77;9;14)	2.67	1.87
H71	28	7	1	(91;2;0)	(91;7;22)	(91;7;22)	1.86	2.18
T1	70	10	2, 8	(87;12;0)	(110;40;8)	(110;40;8)	9535.08	4.40
T11	70	10	6, 10	(112;13;0)	(142;15;101)	(142;15;101)	515.13	2.55
T21	70	10	6, 8	(158;10;0)	(214;34;45)	(214;34;45)	4587.72	31.29
T31	70	10	3, 5	(171;9;0)	(212;43;29)	(212;43;29)	7940.88	34.56
T41	70	17	2, 6, 15	(31;10;0)	(43;16;81)	(36;34;18)	8160.81	53.56
T51	70	17	5, 9, 16	(40;15;0)	(55;-;-)	(43;44;17)	-	49.58
T61	70	17	2, 5 ,12	(71;12;0)	(100;-;-)	(76;45;81)	-	72.93
T71	70	17	11, 12, 14	(57;16;0)	(103;-;-)	(67;42;78)	-	43.91
W1	75	11	5, 8	(27;15;0)	(34;-;-)	(34;32;4)	-	12.08
W11	75	11	6, 7	(30;17;0)	(38;-;-)	(38;36;1)	-	96.37
W21	75	11	8, 9	(48;13;0)	(70;-;-)	(67;35;11)	-	16.34
W31	75	11	4, 10	(50;10;0)	(69;18;35)	(64;38;9)	7577.31	37.53
W41	75	19	9, 12, 16	(11;11;0)	(14;-;-)	(12;26;10)	-	38.09
W51	75	19	12, 14, 15	(14;8;0)	(19;-;-)	(15;42;17)	-	48.42
W61	75	19	3, 16, 17	(19;12;0)	(23;-;-)	(22;35;24)	-	83.90
W71	75	19	6, 11, 19	(21;10;0)	(27;15;49)	(22;25;11)	8244.47	43.14

According to the results, both methods achieved the same solution values in small-sized problems. As the problem size grew, the algorithm surpassed the model for solution quality and time. The PGP model was able to solve 7 of the 16 large-sized instances. In the remaining 11 large-sized problems, the model could acquire feasible solutions only for the first objective. The ABC algorithm reached more successful or the same solution values in all these problems in a very short time.

4.2. Effect of the Goal Values

To see the effect of the goal values on the results, the instances were solved with the proposed approaches by firstly relaxing the only $G1$, then $G1$ and $G2$ together. Relaxed goal values are taken as the maximum value obtained for the relevant goals in cases where a solution is found in

accordance with the results in Table 1 for each problem. Positive deviations (d_1^+, d_2^+ and d_3^+) achieved only when $G1$ is relaxed are given in Table 4, and those attained when $G1$ and $G2$ are relaxed together are given in Table 5.

Table 4
Results obtained when $G1$ is relaxed

	Goal values	$(d_1^+; d_2^+; d_3^+)$		CPU	
P	$(G1; G2; G3)$	PGP	ABC	PGP	ABC
R1	(28;7;0)	(0;2;3)	(0;2;3)	0.19	0.08
R11	(35;3;0)	(0;0;17)	(0;0;17)	0.34	0.04
R21	(39;7;0)	(0;5;1)	(0;5;1)	0.30	0.04
R31	(41;5;0)	(0;8;1)	(0;8;1)	0.34	0.12
R41	(11;7;0)	(0;4;2)	(0;4;2)	1.95	0.12
R51	(12;6;0)	(0;5;7)	(0;5;7)	1.47	0.28
R61	(19;4;0)	(0;4;1)	(0;4;1)	1.84	0.30
R71	(18;5;0)	(0;5;1)	(0;5;1)	1.56	0.16
H1	(152;6;0)	(0;15;1)	(0;15;1)	0.80	0.64
H11	(244;7;0)	(0;14;6)	(0;14;6)	0.37	0.43
H21	(270;8;0)	(0;12;4)	(0;12;4)	0.34	0.73
H31	(278;6;0)	(0;5;1)	(0;5;1)	0.61	0.47
H41	(37;5;0)	(0;3;3)	(0;3;3)	1.11	0.17
H51	(53;3;0)	(0;6;20)	(0;6;20)	2.06	8.41
H61	(77;2;0)	(0;7;14)	(0;7;14)	2.06	6.15
H71	(91;2;0)	(0;5;22)	(0;5;22)	1.11	2.40
T1	(110;12;0)	(0;28;8)	(0;28;8)	9422.66	46.75
T11	(142;13;0)	(0;2;101)	(0;2;101)	354.44	2.83
T21	(214;10;0)	(0;24;45)	(0;24;45)	3599.69	24.79
T31	(212;9;0)	(0;34;29)	(0;34;29)	6109.27	22.11
T41	(43;10;0)	(3;1;121)	(0;9;74)	4118.94	96.44
T51	(55;15;0)	(1;-;-)	(0;14;75)	-	31.31
T61	(100;12;0)	(0;-;-)	(0;18;254)	-	112.25
T71	(103;16;0)	(14;4;-)	(0;13;208)	-	52.96
W1	(34;15;0)	(0;-;-)	(0;17;4)	-	26.51
W11	(38;17;0)	(0;-;-)	(0;19;1)	-	31.20
W21	(70;13;0)	(0;-;-)	(0;18;10)	-	35.72
W31	(69;10;0)	(0;8;35)	(0;9;20)	4942.50	73.75
W41	(14;11;0)	(1;6;27)	(0;12;14)	10800.00	29.14
W51	(19;8;0)	(0;-;-)	(0;15;28)	-	47.03
W61	(23;12;0)	(4;-;-)	(0;15;31)	-	66.05
W71	(27;10;0)	(7;2;105)	(0;10;41)	4681.72	28.92

The ABC algorithm and PGP model succeeded in providing goal values for the cycle time in all small-sized instances when $G1$ is relaxed. Both solution methods found the same deviation values for the second and third goals in these problems. While the algorithm reached solutions

that do not cause any positive deviation from the first goal value in all 16 large-sized problems, the model did in 11 of them. Except for the W31 instance, the algorithm achieved results equal to or better than the proposed model in much shorter times.

Table 5
Results obtained when $G1$ and $G2$ are relaxed

	Goal values	$(d_1^+; d_2^+; d_3^+)$		CPU	
P	$(G1; G2; G3)$	PGP	ABC	PGP	ABC
R1	(28;9;0)	(0;0;3)	(0;0;3)	0.13	0.10
R11	(35;3;0)	(0;0;17)	(0;0;17)	0.11	0.05
R21	(39;12;0)	(0;0;1)	(0;0;1)	0.28	0.04
R31	(41;13;0)	(0;0;1)	(0;0;1)	0.38	0.11
R41	(11;11;0)	(0;0;2)	(0;0;2)	2.09	0.07
R51	(12;11;0)	(0;0;7)	(0;0;7)	1.50	0.25
R61	(19;8;0)	(0;0;1)	(0;0;1)	1.66	0.22
R71	(18;10;0)	(0;0;1)	(0;0;1)	1.77	0.13
H1	(152;21;0)	(0;0;1)	(0;0;1)	0.98	0.43
H11	(244;21;0)	(0;0;6)	(0;0;6)	0.31	0.35
H21	(270;20;0)	(0;0;4)	(0;0;4)	0.42	0.37
H31	(278;11;0)	(0;0;1)	(0;0;1)	0.61	0.20
H41	(37;8;0)	(0;0;3)	(0;0;3)	1.06	0.18
H51	(53;9;0)	(0;0;20)	(0;0;20)	2.00	29.79
H61	(77;9;0)	(0;0;14)	(0;0;14)	2.02	3.49
H71	(91;7;0)	(0;0;22)	(0;0;22)	1.38	1.25
T1	(110;40;0)	(0;0;8)	(0;0;8)	7843.2	42.82
T11	(142;15;0)	(0;0;101)	(0;0;101)	347.52	3.61
T21	(214;34;0)	(0;0;45)	(0;0;45)	3096.3	40.25
T31	(212;43;0)	(0;0;29)	(0;0;29)	4914.00	37.50
T41	43;34;0	(3;-;-)	(0;0;9)	-	80.36
T51	55;44;0	(3;0;-)	(0;0;12)	-	54.8
T61	100;45;0	(0;0;-)	(0;0;17)	-	60.61
T71	103;42;0	(14;0;51)	(0;0;43)	7308.89	76.81
W1	34;32;0	(0;0;4)	(0;0;4)	8581.97	46.02
W11	38;36;0	(0;18;0)	(0;0;0)	8013.72	40.58
W21	70;35;0	(0;3;-)	(0;0;7)	-	36.58
W31	69;30;0	(0;1;6)	(0;0;8)	8374.3	42.08
W41	14;26;0	(1;0;-)	(0;0;9)	-	24.99
W51	19;42;0	(0;1;-)	(0;0;2)	-	168.56
W61	23;35;0	(4;-;-)	(0;0;19)	-	104.4
W71	27;25;0	(1;-;-)	(0;0;12)	-	71.18

Whereas both approaches reached the same positive deviation values in small-sized benchmark problems, the ABC algorithm achieved more successful or the same results in pretty short times for large-sized instances in the case of relaxed $G1$ and $G2$.

As can be seen from Tables 4 and 5, although the goal values were relaxed, the model could not obtain a solution for all objectives in a significant part of large-sized problems. The ABC algorithm for the ALWARB problem, where the solution may be impossible or costly according to solution time, is superior.

5. Conclusion

Assembly lines, which are one of the main components of mass production systems, must be in balance to use limited resources efficiently. However, in real production environments, there are circumstances where these lines are out of balance due to various reasons such as workstation failures. If some stations are disrupted, the line needs to be rebalanced so that production can continue. Since the main purpose of balancing assembly lines is to distribute the total workload to the workstations as evenly as possible, the performance of workers should also be taken into account. In this study, to find a trade-off among cycle time, the number of reassigned tasks, and workload smoothness, the multi-objective ALWARB problem was addressed. To tackle this problem, an ABC algorithm was developed as well as a PGP model and these approaches were compared using the benchmark instances. The computational results demonstrated that the proposed ABC algorithm provides a significant advantage, especially in large-sized problems. In future studies, U-type or two-sided lines, and stochastic processing times can be handled. Moreover, the ALWARB problem could be considered by determining different priorities among the considered objectives.

References

Ağpak, K. (2010). An approach to find task sequence for re-balancing of assembly lines. *Assembly Automation*, *30*(4), 378–387. doi:10.1108/01445151011075834

Akyol, S. D., & Baykasoğlu, A. (2019). A multiple-rule based constructive randomized search algorithm for solving assembly line worker assignment and balancing problem. *Journal of Intelligent Manufacturing*, *30*(2), 557–573. doi:10.1007/s10845-016-1262-6

Araújo, F. F. B., Costa, A. M., & Miralles, C. (2012). Two extensions for the ALWABP: Parallel stations and collaborative approach. *International Journal of Production Economics*, *140*(1), 483–495. doi:10.1016/j.ijpe.2012.06.032

Araújo, F. F. B., Costa, A. M., & Miralles, C. (2015). Balancing parallel assembly lines with disabled workers. *European Journal of Industrial Engineering*, *9*(3), 344–365. doi:10.1504/EJIE.2015.069343

Baykasoğlu, A. (2005). Preemptive goal programming using simulated annealing. *Engineering Optimization,* 37(1):49–63. doi:10.1080/0305215042000268606

Belassiria, I., Mazouzi, M., ELfezazi, S., Cherrafi, A., & ELMaskaoui, Z. (2018). An integrated model for assembly line re-balancing problem. *International Journal of Production Research*, *56*(16), 5324–5344. doi:10.1080/00207543.2018.1467061

Blum, C., & Miralles, C. (2011). On solving the assembly line worker assignment and balancing problem via beam search. *Computers and Operations Research*, *38*(1), 328–339. doi:10.1016/j.cor.2010.05.008

Borba, L., & Ritt, M. (2014). A heuristic and a branch-and-bound algorithm for the assembly line worker assignment and balancing problem. *Computers and Operations Research*, *45*, 87–96. doi:10.1016/j.cor.2013.12.002

Castellucci, P. B., & Costa, A. M. (2015). A new look at the bowl phenomenon. *Pesquisa Operacional*, *35*(1), 57–72. doi:10.1590/0101-7438.2015.035.01.0057

Chaves, A. A., Insa, C. M., & Lorena, L. A. N. (2007). Clustering search approach for the assembly line worker assignment and balancing problem. *37th International Conference on Computers and Industrial Engineering*, *2*, 1151–1160.

Chaves, A. A., Lorena, L. A. N., & Miralles, C. (2009). Hybrid metaheuristic for the assembly line worker assignment and balancing problem. *Lecture Notes in Computer Science (Including Subseries Lecture Notes in Artificial Intelligence and Lecture Notes in Bioinformatics)*, *5818 LNCS*, 1–14. doi:10.1007/978-3-642-04918-7_1

Corominas, A., Pastor, R., & Plans, J. (2008). Balancing assembly line with skilled and unskilled workers. *Omega*, 36(6):1126-1132. doi:10.1016/j.omega.2006.03.003

Çelik, E., Kara, Y., & Atasagun, Y. (2014). A new approach for rebalancing of U-lines with stochastic task times using ant colony optimisation algorithm. *International Journal of Production Research*, *52*(24), 7262–7275. doi:10.1080/00207543.2014.917768

Efe, B., Kremer, G. E. O., & Kurt, M. (2018). Age and gender-based workload constraint for assembly line worker assignment and balancing problem in a textile firm. *International Journal of Industrial Engineering : Theory Applications and Practice*, *25*(1), 1–17.

Falkenauer, E. (2005). Line balancing in the real world. *Proceedings of the International Conference on Product Lifecycle Management PLM*, *5*, 360–370. Retrieved from http://www.optimaldesign.com/Download/OptiLine/FalkenauerPLM05.pdf

Gamberini, R., Gebennini, E., Grassi, A., & Regattieri, A. (2009). A multiple single-pass heuristic algorithm solving the stochastic assembly line rebalancing problem. *International Journal of Production Research*, *47*(8), 2141–2164. doi:10.1080/00207540802176046

Gamberini, R., Grassi, A., & Rimini, B. (2006). A new multi-objective heuristic algorithm for solving the stochastic assembly line re-balancing problem. *International Journal of Production Economics*, *102*(2), 226–243. doi:10.1016/j.ijpe.2005.02.013

Grangeon, N., Leclaire, P., & Norre, S. (2011). Heuristics for the re-balancing of a vehicle assembly line. *International Journal of Production Research*, *49*(22), 6609–6628. doi:10.1080/00207543.2010.539025

Janardhanan, M. N., Li, Z., & Nielsen, P. (2019). Model and migrating birds optimization algorithm for two-sided assembly line worker assignment and balancing problem. *Soft Computing*, *23*(21), 11263–11276. doi:10.1007/s00500-018-03684-8

Karaboğa D (2005) An idea based on honey bee swarm for numerical optimization. Technical Report TR06, Erciyes University.

Karaboğa, D., & Akay, B. (2011). A modified Artificial Bee Colony (ABC) algorithm for constrained optimization problems. *Applied Soft Computing Journal*, *11*(3), 3021–3031. doi:10.1016/j.asoc.2010.12.001

Karaş, A., & Özçelik, F. (2021). Assembly Line Worker Assignment and Rebalancing Problem: A Mathematical Model and An Artificial Bee Colony Algorithm. *Computers Industrial Engineering*, 156:1-16. doi:10.1016/j.cie.2021.107195

Li, Y. (2017). The type-II assembly line rebalancing problem considering stochastic task learning. *International Journal of Production Research*, *55*(24), 7334-7355. doi:10.1080/00207543.2017.1346316

Makssoud, F., Battaïa, O., Dolgui, A., Mpofu, K., & Olabanji, O. (2015). Re-balancing problem for assembly lines: New mathematical model and exact solution method. *Assembly Automation*, *35*(1), 16–21. doi:10.1108/AA-07-2014-061

Miralles, C., García-Sabater, J. P., Andrés, C., & Cardós, M. (2007). Advantages of assembly lines in Sheltered Work Centres for Disabled. A case study. *International Journal of Production Economics*, *110*(1–2), 187–197. doi:10.1016/j.ijpe.2007.02.023

Moreira, M. C. O., & Costa, A. M. (2009). A minimalist yet efficient tabu search algorithm for balancing assembly lines with disabled workers. *Anais Do XLI Simpósio Brasileiro de Pesquisa Operacional*, 660–671.

Moreira, M. C. O., & Costa, A. M. (2013). Hybrid heuristics for planning job rotation schedules in assembly lines with heterogeneous workers.

International Journal of Production Economics, *141*(2), 552–560. doi:10.1016/j.ijpe.2012.09.011

Moreira, M. C. O., Ritt, M., Costa, A. M., & Chaves, A. A. (2012). Simple heuristics for the assembly line worker assignment and balancing problem. *Journal of Heuristics*, *18*(3), 505–524. doi:10.1007/s10732-012-9195-5

Mutlu, Ö., Polat, O., & Supçiller, A. A. (2013). An iterative genetic algorithm for the assembly line worker assignment and balancing problem of type-II. *Computers and Operations Research*, *40*(1), 418–426. doi:10.1016/j.cor.2012.07.010

Öksüz, M. K., Büyüközkan, K., & Satoğlu, Ş. I. (2017). U-shaped assembly line worker assignment and balancing problem: A mathematical model and two meta-heuristics. *Computers and Industrial Engineering*, *112*, 246–263. doi:10.1016/j.cie.2017.08.030

Polat, O., Kalaycı, C. B., Mutlu, Ö., & Gupta, S. M. (2016). A two-phase variable neighbourhood search algorithm for assembly line worker assignment and balancing problem type-II: An industrial case study. *International Journal of Production Research*, *54*(3), 722–741. doi:10.1080/00207543.2015.1055344

Ramezanian, R., & Ezzatpanah, A. (2015). Modeling and solving multi-objective mixed-model assembly line balancing and worker assignment problem. *Computers and Industrial Engineering*, *87*, 74–80. doi:10.1016/j.cie.2015.04.017

Ritt, M., Costa, A. M., & Miralles, C. (2016). The assembly line worker assignment and balancing problem with stochastic worker availability. *International Journal of Production Research*, *54*(3), 907–922. doi:10.1080/00207543.2015.1108534

Sancı, E., & Azizoğlu, M. (2017). Rebalancing the assembly lines: exact solution approaches. *International Journal of Production Research*, *55*(20), 5991–6010. doi:10.1080/00207543.2017.1319583

Serin, F., Mete, S., & Çelik, E. (2019). An efficient algorithm for U-type assembly line re-balancing problem with stochastic task times. *Assembly Automation*, *39*(4), 581–595. doi:10.1108/AA-07-2018-106

Szeto, W. Y., Wu, Y., & Ho, S. C. (2011). An artificial bee colony algorithm for the capacitated vehicle routing problem. *European Journal of Operational Research*, *215*(1), 126–135. doi:10.1016/j.ejor.2011.06.006

Vilà, M., & Pereira, J. (2014). A branch-and-bound algorithm for assembly line worker assignment and balancing problems. *Computers and Operations Research*, *44*, 105–114. doi:10.1016/j.cor.2013.10.016

Yang, C., Gao, J., & Sun, L. (2013). A multi-objective genetic algorithm for mixed-model assembly line rebalancing. *Computers and Industrial Engineering*, *65*(1), 109–116. doi:10.1016/j.cie.2011.11.033

Yılmaz, E., & Erol, R. (2005). Montaj HatlarininDeğişen Koşullar AltindaYenidenDengelenmesi. *Çukurova Üniversitesi Mühendislik Mimarlık Fakültesi Dergisi*, *20*(1), 213–228.

Zacharia, P. T., & Nearchou, A. C. (2016). A population-based algorithm for the bi-objective assembly line worker assignment and balancing problem. *Engineering Applications of Artificial Intelligence*, *49*, 1–9. doi:10.1016/j.engappai.2015.11.007

Zhang, Y., Hu, X., & Wu, C. (2018). A modified multi-objective genetic algorithm for two-sided assembly line re-balancing problem of a shovel loader. *International Journal of Production Research*, *56*(9), 3043–3063. doi:10.1080/00207543.2017.1402136

Zhang, Y., Hu, X., & Wu, C. (2020) Improved imperialist competitive algorithms for rebalancing multi-objective two-sided assembly lines with space and resource constraints. *International Journal of Production Research*, 58(12):3589–3617. doi:10.1080/00207543.2019.1633023

Zhang, Z., Tang, Q., Han, D., & Li, Z. (2019). Enhanced migrating birds optimization algorithm for U-shaped assembly line balancing problems with workers assignment. *Neural Computing and Applications*, *31*(11), 7501–7515. doi:10.1007/s00521-018-3596-9

Chapter 5

COMPARISON OF DIFFERENT FINITE ELEMENT TYPES IN CURVED PLATE STRUCTURES

Can GÖNENLI[1]

1 Dr. Can Gonenli, Machine Drawing and Construction Department, Ege Vocational School, Ege University, Izmir, Turkey, can.gonenli@ege.edu.tr, ORCID ID: 0000-0001-9163-1569

1. INTRODUCTION

In engineering structures, the importance of curved plates is as much as flat plates. These plates are subjected to different dynamic loads in engineering structures, such as aircraft bodies, ship decks, car bodywork, etc. Accordingly, it is necessary to create strong numerical model of curved plates with different methods in the modeling stage before production to predict their dynamic characteristics. In this study, two different finite element types are compared, which are rectangular shell element and cylindrical shell element. These curved plates are examined under different boundary conditions in MATLAB. The first ten natural frequencies are taken into consideration when comparing the natural frequencies of the curved plates. The obtained results are also compared and interpreted with the ANSYS. Based on the obtained results, the mathematical model approach for two types of finite element types can be used in curved plate modeling. This study showed that the rectangular shell element gives reliable results as good as the cylindrical shell element even though the element stiffness and mass matrix includes a smaller number of elements.

Curved plates are used in many applications, and it is important and necessary to determine their static and dynamic characteristics for different engineering areas. Curved plates are commonly using in engineering structures in terms of aesthetics and design. Thin shells as structural elements are the most predominantly used in engineering, particularly in civil, mechanical, architectural, aeronautical, and marine engineering. Knowledge of the free vibration characteristics of the thin circular cylindrical shells is important both for understanding the fundamental shell behavior and for designing shell structures for industrial applications (Olson and Lindberg, 1968). Therefore, the natural frequency values of the curved plates should be known at the design stage. In many types of research, different mathematical models for plates are modeled and investigated under different load conditions. Senjanovic et al. (2015) studied a simple analytical procedure for estimation of natural frequencies of free thin rectangular plates based on Rayleigh's quotient. Based on their detailed FEM analysis, some additional natural modes were recognized, which are defined as the sum and difference of the cross products of beam modes. These natural mode shapes of beam form a complete natural frequency spectrum of a free rectangular plate as a novelty. In their paper, the application of the developed procedure was illustrated in the case of a free thin square and rectangular plate. Dey et al. (2016) investigated a composite rectangular plate that was modeled according to the Mindlin-Reissner plates theory using classical plates theory and high-order differential equations. In their paper, triangular finite elements are used as mesh elements. Nasirmensh and Mohammadi

(2017) investigated the vibrational behavior of cracked FGM shells. In their study, multiple examples are introduced and analyzed and the effects of various parameters such as the length and angle of the crack and different distribution patterns of material stiffness and density across the thickness of the shell are extensively studied. Danzi et al. (2017) presented the equivalent plate model of curvilinear stiffened panels. Rawat et al. (2016) investigated the thin circular cylindrical shell that can vibrate in different modes. Li et al. (2016) studied analytic free vibration solutions of free rectangular thin plates with or without an elastic foundation were obtained by using an up-to-date Hamiltonian system-based symplectic superposition method because such boundary value problems are known to be very difficult and they were generally solved by the approximate/numerical methods. In their paper, the advantage of this method is that the solution procedure was conducted in the symplectic space, where the symplectic eigen expansion is valid and the predetermination of the solution form is avoided. This significantly extends the approach to the analytic solutions of similar problems. Li et al. (2017), examined accurate analytic solutions for free vibration of rectangular thick plates with an edge-free were obtained. The Hamiltonian system-based governing equation was first constructed. In their paper, the eigenvalue problems of two fundamental vibration problems were formed for a thick plate with an edge-free and the others clamped and by symplectic expansion, the fundamental solutions were obtained. Kumar et al. (2017) studied linear and nonlinear vibration analyses of shear deformable thin and thick arbitrary straight-sided quadrilateral plates using smoothed finite element technique. In their study, the Mindlin-Reissner plates were discretized with quadrilateral background cells, then membrane and bending stiffness matrices of background quadrilateral cells are evaluated using the edge-based smoothed finite element method. Spagnoli et al. (2019) presented an experimental test under fixed loading on the geometrically nonlinear bending behavior of plates. The study shows the critical plate displacement almost independent on the plate size, but linearly depends on the plate thickness. Eisenberger & Deutsch (2019) suggested a novel high-efficiency numerical results that covers all the potential combinations for thin rectangular plate that solve the partial differential equations of motion. Their study also gives examples of their new solution and compared with other approximate solutions.

In this study, rectangular shell element (RSE) and cylindrical shell element (CSE) are employed for creating the curved structure. RSE is a combination of two different theories, including the out-of-plane and in-plane vibration theories, and this finite element type has six generalized coordinates. When RSE is a planar finite element type, CSE is a curved finite element type and has seven generalized coordinates. These theories

are coded with the MATLAB. In order to validate the approaches, the flat and curved geometries are also modeled in ANSYS to validate the results.

2. MATHEMATICAL MODEL

The curved geometry is created with the help of the large deflection equation, which is given in equation (1). The large deflection equation is taken into account for only its geometrical structure, without pre-stress effect to perform a realistic model, and the created structure consists of elements with different radii. The deflection equation works on the principle of applying a distributed force on the free end of a plate, which is fixed on the opposite side. Considering the assembly styles in engineering structures, two different boundary conditions are investigated which are two opposite sides fixed and four sides fixed. RSE includes six generalized coordinates when CSE includes seven generalized coordinates. Using a different approach to modeling the curved structure, the theory of rectangular plate is formed as a combination of two different theories. On the other hand, the CSE is used as a combination of different radii and it is also used for modeling a curved form. The curved form of the plate is shown in Figure 1.

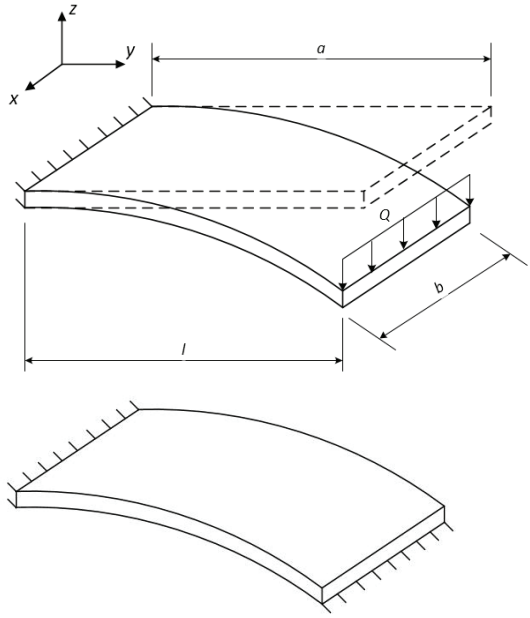

(a) **(b)**

Figure 1. The curved form of the thin plate. (a) Distributed load applied to flat plate, (b) The curved plate with two opposite sides are fixed

Q represents uniformly distributed load in Figure 1. It is necessary to find deflection points to create curved model. Ozturk (2011) used beam deflection equation in his study. Deflection points of the plate can be found for desired mesh size with the help of the force value and the beam deflection equation. This equation can be used for modeling plates because thin plates deforme under load just like beams (Jairazhboy et al., 2012).

$$\begin{aligned} z(x) = {} & \frac{P}{2EI}\left(-\frac{x^3}{3} + lx^2\right) \\ & + \frac{1}{2}\left(\frac{P}{2EI}\right)^3\left(-\frac{x^7}{7} + lx^6 - \frac{12}{5}l^2x^5 + 2l^3x^4\right) \\ & + \frac{3}{8}\left(\frac{P}{2EI}\right)^5\left(-\frac{x^{11}}{11} + lx^{10} - \frac{40}{9}l^2x^9 + 10l^3x^8\right. \\ & \left. - \frac{80}{7}l^4x^7 + \frac{16}{3}l^5x^6\right) + \cdots \end{aligned} \tag{1}$$

E represents young modulus, P represents force, I represents the moment of inertia for the beam and l represents exact length of the beam after the force are applied. P is obtained from equation (2).

$$P = Q\ b \tag{2}$$

The equation of the exact length of the beam is given with equation (3).

$$a = \int_0^l \sqrt{1 + \left(\frac{\mathrm{dz}}{\mathrm{dx}}\right)^2}\ \mathrm{dx} \tag{3}$$

2.1. Cylindrical Shell Element (CSE)

The curved model is formed by joining the plates in different radii of curvature tangentially. The representative curved model with CSE form is given in Figure 2.

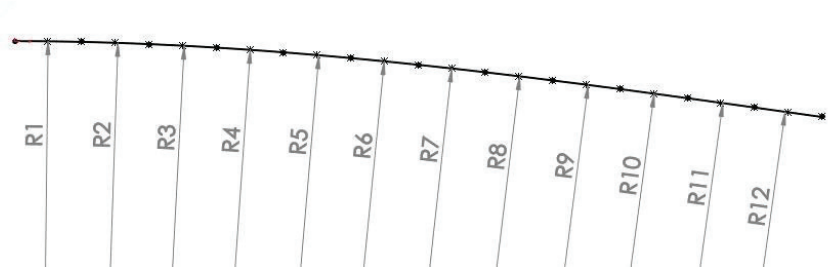

Figure 2. Representative curved model with cylindrical shell element

The cylindrical shell element which is used for modeling each curve part is shown in Figure 3 (Rawat et al., 2016).

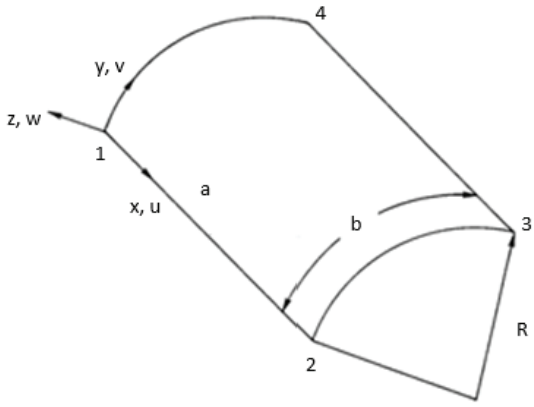

Figure 3. Cylindrical shell element

For using the CSE, stiffness and mass matrices have to be calculated to obtain natural frequencies. This calculation is done by through the strain energy of an isotropic thin cylindrical shell element**.**

$$U = \int_0^b \int_0^a \int_{-h/2}^{h/2} \left[\frac{E}{2(1-v^2)} \varepsilon_x^2 + \varepsilon_y^2 + 2v\varepsilon_x\varepsilon_y + \frac{1-v}{2}\varepsilon_{xy}^2 \right] dzdxdy \quad (4)$$

where h is thickness of the plate, E is young modulus and v is Poisson's ratio. The strain displacement relations are given by equation (5).

$$\varepsilon_x = \frac{\partial u}{\partial x} - z\frac{\partial^2 w}{\partial x^2}$$
$$\varepsilon_y = \frac{\partial v}{\partial y} + \frac{w}{R} - z\left(\frac{\partial^2 w}{\partial y^2} - \frac{1}{R}\frac{\partial v}{\partial y}\right) \quad (5)$$
$$\varepsilon_{xy} = \frac{\partial v}{\partial x} + \frac{\partial u}{\partial y} - 2z\left(\frac{\partial^2 w}{\partial x \partial y} - \frac{1}{R}\frac{\partial v}{\partial x}\right)$$

According to equation 5, the CSE requires special displacement functions in order to ensure all six degree of freedoms. The displacement functions are given by equation (6) to satisfy strain-displacement relations.

$$\begin{aligned} w(x,y) &= a_1 + a_2 x + a_3 y + a_4 xy + a_5 x^2 \\ &\quad + a_6 y^2 + a_7 x^2 y + a_8 x y^2 + a_g x^3 \\ &\quad + a_{10} y^3 + a_{11} x^3 y + a_{12} x y^3 \end{aligned} \quad (6)$$
$$\begin{aligned} u(x,y) &= a_{13} + a_{14} x + a_{15} y + a_{16} xy + a_{17} y^2 \\ &\quad + a_{18} x y^2 + a_{19} y^3 + a_{20} x y^3 \end{aligned}$$
$$\begin{aligned} v(x,y) &= a_{21} + a_{22} x + a_{23} y + a_{24} xy + a_{25} y^2 \\ &\quad + a_{26} x y^2 + a_{27} y^3 + a_{28} x y^3 \end{aligned}$$

The resulting strain energy expression is a quadratic function of the 28 corner displacements for each element, and it is given in equation (7). The stiffness matrix K can be calculated next.

$$U = \frac{1}{2} W^T K W \quad (7)$$

The kinetic energy for the cylindrical element at any instant of time with neglecting rotary inertia is given in equation (8).

$$T = \frac{1}{2}\int_0^b \int_0^a \int_{-h/2}^{h/2} \left(\rho\left(\frac{\partial u}{\partial t}\right)^2 + \left(\frac{\partial v}{\partial t}\right)^2 + \left(\frac{\partial w}{\partial t}\right)^2\right) \mathrm{dzdxdy} \quad (8)$$

The mass matrix M can be calculated as follows.

$$T = \frac{1}{2} W^T M W \tag{9}$$

Natural frequencies can be obtained with using stiffness and mass matrices through equation (10), because λ includes natural frequency parameter w^2.

$$K - \lambda M = 0 \tag{10}$$

2.2. Rectangular Shell Element (RSE)

In order to create the curved pattern with using RSE, the flat plate is rotated at appropriate angles respect to y axis. The representative model form is given in Figure 4.

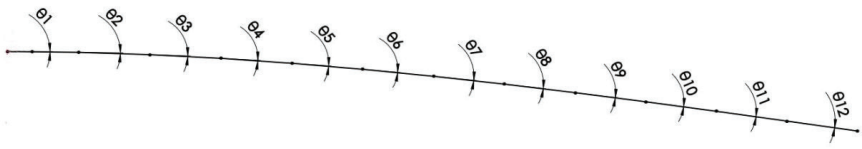

Figure 4. Representative curved model with rectangular shell element

The RSE have to has six degrees of freedom to create the pattern. Thin rectangular plate model is given in Figure 5 (Petyt, 2010).

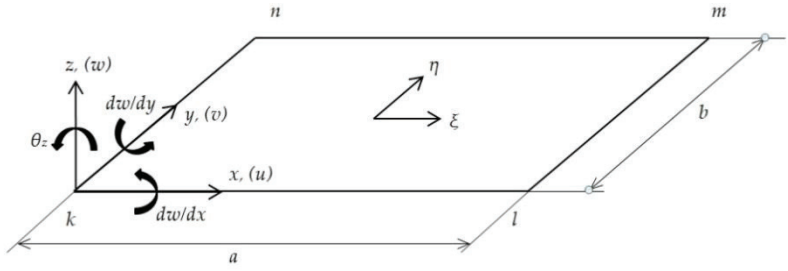

Figure 5. Thin rectangular shell element for bending

This model has twelve degrees of freedom corresponding to the three generalized coordinates (*w*, *dw/dy* and *dw/dx*) at each corner. The displacement function is given in equation (11) (Sudhir, 2012).

$$w(x,y) = a_1 + a_2x + a_3y + a_4x^2 + a_5xy + a_6y^2 + a_7x^3 + a_8x^2y + a_9xy^2 + a_{10}y^3 + a_{11}x^3y + a_{12}xy^3 \quad (11)$$

The displacement matrix is given in equation (12).

$$\{d_k, d_l, d_m, d_n\}^T = [A]^e x[\alpha] \quad (12)$$

Strain matrix for bending plate element is given in equation (13).

$$\{\varepsilon\}^e = \left\{-\frac{\partial^2 w}{\partial x^2}, -\frac{\partial^2 w}{\partial y^2}, -2\frac{\partial^2 w}{\partial x \partial y}\right\} \quad (13)$$

The strain matrix can be written in the form that is given in equation (14).

$$[\varepsilon]^e = [H]x[\alpha] \quad (14)$$

The strain displacement matrix which is given in equation (15) can be obtained through equation (12) and (14).

$$[B] = [H]x[A]^{-1} \quad (15)$$

The element stiffness matrix is calculated and is given in equation (16).

$$[K]^e = \int_A \int [B]^T[D][B]\mathrm{dxdy} \quad (16)$$

D represents the material matrix. For an isotropic composite thin plate, the material matrix is given in equation (17).

$$[D] = \frac{Eh^3}{12(1-\nu^2)}\begin{bmatrix} 1 & \nu & 0 \\ \nu & 1 & 0 \\ 0 & 0 & \frac{1-\nu}{2} \end{bmatrix} \quad (17)$$

E represents Young modulus, *h* represents thickness of the plate and *v* represents Poisson's ratio. The mass matrix is also calculated with interpolation matrix which is given in equation (18).

$$[w] = [1 \quad x \quad y \quad x^2 \quad xy \quad y^2 \quad x^3 \quad x^2y \quad xy^2 \quad y^3 \quad x^3y \quad xy^3] \quad (18)$$

The element mass matrix is given in equation (19).

$$[M]^e = \rho h \int_A \int [w]^T [w] \mathrm{dxdy} \quad (19)$$

For modeling curved model with using three degrees of freedom thin plate, it is necessary to add longitidunal effects to model. Stiffness and mass matrices of in-plane vibration which includes *u*, *v* and θ_z (8x8) are added to out-of plane vibration stiffness and mass matrices which includes *w*, θ_y and θ_x (12x12). The shape function of in-plate theory is given in equation (20) (Chandrupatra & Belegundu, 2012).

$$N_i = \frac{1}{4}(1 + \xi\xi_i)(1 + \eta\eta_i) \quad (20)$$

where ξ_i and η_i are the coordinates of node *i*, represents *k*, *l*, *m*, and *n* in Figure-5. The displacement vector *u* can be obtained with help of the displacement components (q) through the equation (21).

$$u = Nq \quad (21)$$

The strain-displacement relation matrix is ε consists ε_x, ε_y and Υ_{xy} and these relations can be found through the displacement vector. The strain-displacement matrix can be written in the form of equation (22).

$$\varepsilon = Bq \quad (22)$$

The stiffness matrix of in-plane vibrations can be calculated and given in equation (23), where *D* is a material matrix.

$$[K]^e = h \int_A \int [B]^T [D][B] \ \det \mathrm{J} \, \mathrm{dxdy} \quad (23)$$

The mass matrix can be also found with shape functions. The element mass matrix is shown in equation (24).

$$[M]^e = \rho h \int_A \int [N]^T [N] \mathrm{dxdy} \quad (24)$$

The element stiffness and the mass matrices are obtained with merging the out-of-plane and in-plane matrices. Equation (25) shows the relation:

$$[Bending]_{12\times12} + [Longitudinal]_{8\times8} = \begin{bmatrix} 12\times12 & 0 \\ 0 & 8\times8 \end{bmatrix}_{20\times20} \tag{25}$$

This model have six degrees of freedom, but the stiffness and mass matrices have (20x20) size matrices. Although these matrices carry the effect of θ_z, last value has to be added formally into matrices for drilling effect. This relation is given in equation (26).

$$\begin{bmatrix} 12\times12 & 0 \\ 0 & 8\times8 \end{bmatrix}_{20\times20} + \theta_z = \begin{bmatrix} 12\times12 & 0 & 0 \\ 0 & 8\times8 & 0 \\ 0 & 0 & 4\times4 \end{bmatrix}_{24\times24} \tag{26}$$

The value of θ_z is 1/1000 of the minimum value in (20x20) stiffness and mass matrices (Niyogi et al., 1999). The rotation angles have to be found to create curved pattern. These rotation angles are found with taking first derivative of equation (1) respect to x. The transformation matrix is given in Table 1, and this relation is obtained with rotating the coordinate system respect to y axis is shown in Figure 6.

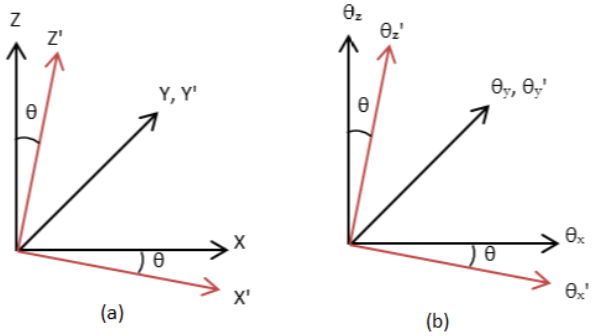

Figure 6. Rotation of the coordinate system. (a) The rotation of the translation in three perpendicular axes, (b) The rotation of the rotation in three perpendicular axes.

Table 1. Transformation matrix.

θ_x	θ_y	w	u	v	θ_z	
cos(θ)	0	0	0	0	sin(θ)	θ_x
0	1	0	0	0	0	θ_y
0	0	cos(θ)	-sin(θ)	0	0	w
0	0	sin(θ)	cos(θ)	0	0	u
0	0	0	0	1	0	v
-sin(θ)	0	0	0	0	cos(θ)	θ_z

Stiffness and mass matrices can be obtained through transformation matrix is given in equation (27).

$$K_r = T^T \times K_e \times T$$
$$M_r = T^T \times M_e \times T \tag{27}$$

where K_e and M_e represent element stiffness and mass matrices. Then rotated element matrices K_r and M_r can be obtained with using transformation matrices. The curved model, which is formed by two different finite element types, is also modeled in the same form in ANSYS with using SHELL181 element type. The ANSYS model of the curved plate is shown in Figure-7.

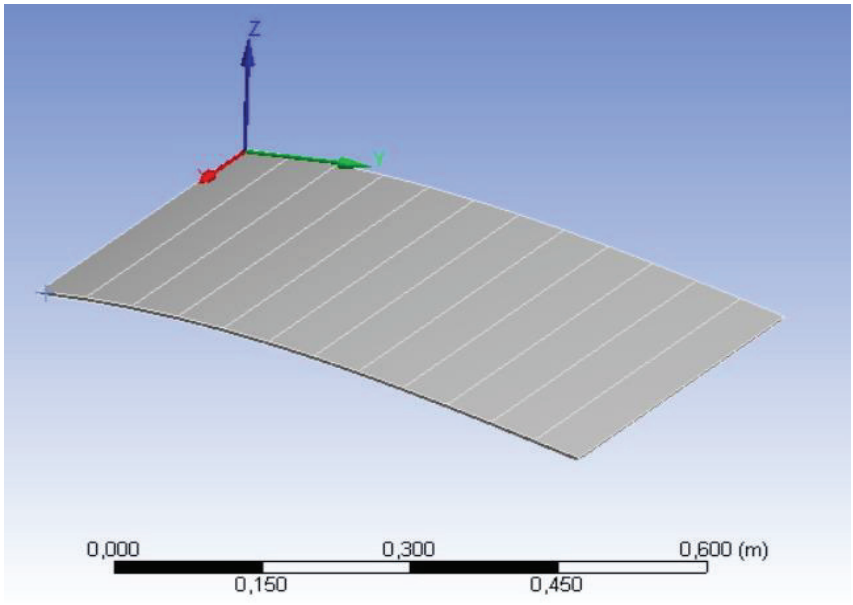

Figure 7. ANSYS model for curved thin plate.

3. RESULTS

In order to compare two different finite element types for both flat and curved structures with ANSYS, 600x600x5 mm dimensions are chosen for numerical example. The material properties are given in Table-2.

Table 2. Material properties and plate sizes.

Symbol	Name	Quantity, Order
E	Elasticity modulus	200 GPa
ρ	Mass density	7900 kg/m^3
v	Poisson ratio	0.30
a	Length of the plate	0.6 m
b	Width of the plate	0.6 m
h	Thickness of the plate element	5 mm
...	Mesh density 1	6 x 6
...	Mesh density 2	12 x 12

The natural frequency values are given as non-dimensional natural frequency, λ.

$$\lambda = \omega\sqrt{\frac{\rho A a^4}{EI}} \tag{28}$$

where ω is natural frequency, A is cross section area of the plate, I is area moment of inertia. The first ten non-dimensional natural frequency parameters are shown in Table-3, with error rates (ER) for 6x6 and 12x12 mesh densities on the two-side-fixed flat plate. The error rates of both CSE and RSE results are calculated with reference to ANSYS model. Although the results for the flat plate model are very close, RSE gives slightly better results for both 6x6 and 12x12 mesh density. When using 12x12 mesh density, the biggest error rate seen for both CSE and RSE occurred at the ninth natural frequency, with a value of approximately 1.5%.

Table 3. Non-dimensional natural frequencies of flat plate for two-side-fixed boundary condition.

Freq	ANSYS	CSE	ER	RSE	ER	CSE	ER	RSE	ER
		6x6 Mesh				12x12 Mesh			
1	3.70	3.72	0.46 %	3.72	0.45 %	3.70	0.08 %	3.70	0.08 %

			0.07		0.07		0.05		0.05
2	4.40	4.41	%	4.41	%	4.41	%	4.41	%
			1.66		1.57		0.40		0.38
3	7.26	7.14	%	7.15	%	7.24	%	7.24	%
		10.3	0.71	10.3	0.71	10.2	0.08	10.2	0.07
4	10.23	0	%	0	%	3	%	3	%
		11.2	0.00	11.2	0.05	11.2	0.00	11.2	0.00
5	11.22	2	%	1	%	2	%	2	%
		13.0	2.37	13.0	2.07	13.2	0.74	13.2	0.71
6	13.31	0	%	4	%	2	%	2	%
		14.2	2.75	14.2	2.76	14.5	0.76	14.5	0.75
7	14.61	1	%	1	%	0	%	0	%
		19.7	1.89	19.8	1.42	20.1	0.02	20.1	0.02
8	20.12	4	%	4	%	2	%	2	%
		20.3	2.13	20.3	2.13	20.4	1.52	20.4	1.47
9	20.74	0	%	0	%	3	%	4	%
		21.2	0.05	21.1	0.20	21.1	0.08	21.1	0.09
10	21.21	0	%	7	%	9	%	9	%

Table-4 gives the first ten non-dimensional natural frequency parameters for ANSYS, CSE, and RSE on the four-side-fixed flat plate. The error rates show that the RSE has better results in both 6x6 and 12x12 mesh densities. Besides, higher mesh density is a better for four-side-fixed boundary condition. For the four-side-fixed boundary condition, error rates of up to 7% can be seen at higher natural frequencies at low mesh density. In 12x12 mesh density, there is no error rate greater than 1% in the first three natural frequencies, while the largest error rate remains around 2%.

Table 4. Non-dimensional natural frequencies of flat plate for four-side-fixed boundary condition.

Freq	ANSYS	CSE	ER	RSE	ER	CSE	ER	RSE	ER
		6x6 Mesh				12x12 Mesh			
			2.48		2.23		0.69		0.67
1	6.00	5.86	%	5.87	%	5.96	%	5.96	%
		11.8	3.02	11.9	2.75	12.1	0.99	12.1	0.97
2	12.26	9	%	2	%	4	%	4	%
		11.8	3.02	11.9	2.43	12.1	0.99	12.1	0.95
3	12.26	9	%	6	%	4	%	4	%
		16.9	6.45	17.1	5.24	17.6	2.08	17.7	1.97
4	18.06	0	%	1	%	8	%	0	%
		21.4	2.58	21.5	2.28	21.7	1.18	21.7	1.13
5	22.02	5	%	2	%	6	%	7	%
		21.6	2.21	21.7	1.65	21.8	1.10	21.8	1.06
6	22.13	4	%	6	%	8	%	9	%
7	27.56	25.6	7.12	25.8	6.15	26.8	2.65	26.8	2.52

		0	%	7	%	3	%	7	%
		25.6	7.12	26.2	4.85	26.8	2.65	26.8	2.44
8	27.56	0	%	3	%	3	%	9	%
		33.1	6.19	34.2	3.15	34.8	1.29	34.8	1.27
9	35.34	5	%	2	%	8	%	9	%
		34.8	1.32	34.8	1.51	34.8	1.29	34.9	1.20
10	35.34	7	%	0	%	8	%	1	%

The curved geometry is created by the force, which brings the one-side-fixed plate's free end to deflect 1/5 of the plate length. As mentioned before, this method is used only for the geometric features in order to establish a more realistic model, without pre-stress effects. Table 5 gives the first ten non-dimensional natural frequency parameters of the curved plate structure for RSE, CSE, and ANSYS, with two-side-fixed boundary condition. It is seen that the error rates according to ANSYS are generally closer to zero. Although the error rates for both 6x6 and 12x12 mesh densities are good for both finite element types, it is seen that the RSE is slightly better. In 12x12 mesh density, neither CSE nor RSE has an error rate exceeding 1%.

Table 5. Non-dimensional natural frequencies of curved plate for two-side-fixed boundary condition.

Freq	ANSYS	CSE	ER	RSE	ER	CSE	ER	RSE	ER
		6x6 Mesh				12x12 Mesh			
			2.61		0.76		0.69		0.14
1	9.19	9.43	%	9.26	%	9.25	%	9.20	%
		11.2	2.19	11.0	0.42	11.1	0.85	11.0	0.30
2	11.02	6	%	6	%	1	%	5	%
		15.1	0.28	14.9	0.97	15.1	0.26	15.1	0.02
3	15.13	7	%	8	%	7	%	3	%
		16.7	2.32	16.5	0.80	16.5	0.69	16.4	0.16
4	16.40	8	%	3	%	1	%	2	%
		17.5	1.68	17.2	0.26	17.3	0.64	17.2	0.24
5	17.24	3	%	8	%	5	%	8	%
		20.2	0.86	19.8	2.50	20.3	0.22	20.2	0.55
6	20.40	2	%	9	%	5	%	8	%
		21.3	0.53	21.0	1.98	21.4	0.07	21.4	0.22
7	21.48	7	%	6	%	7	%	4	%
		23.8	2.18	23.4	0.49	23.5	0.70	23.3	0.16
8	23.35	5	%	6	%	1	%	8	%
		24.9	1.72	24.4	0.44	24.7	0.66	24.5	0.19
9	24.54	7	%	4	%	0	%	9	%
		27.1	1.44	26.5	3.47	27.3	0.47	27.2	0.76
10	27.50	0	%	5	%	7	%	9	%

Table 6 gives the results of the first ten non-dimensional natural frequency parameters of the curved plate structure for four-side-fixed boundary condition. It is seen that both finite element types give very good results, especially for 12x12 mesh density. However, CSE performs slightly better than RSE in four-side-fixed boundary condition and the maximum error rate does not exceed around 2%.

Table 6. Non-dimensional natural frequencies of curved plate for four-side-fixed boundary condition.

Freq	ANSYS	CSE	ER	RSE	ER	CSE	ER	RSE	ER
		6x6 Mesh				12x12 Mesh			
1	12.62	12.58	0.33 %	12.42	1.59 %	12.61	0.08 %	12.55	0.54 %
2	18.57	18.17	2.16 %	17.85	3.89 %	18.45	0.66 %	18.33	1.32 %
3	18.82	18.77	0.25 %	18.52	1.55 %	18.78	0.19 %	18.70	0.62 %
4	24.56	23.88	2.78 %	23.48	4.37 %	24.31	1.00 %	24.18	1.56 %
5	25.77	25.77	0.01 %	25.28	1.92 %	25.75	0.11 %	25.59	0.70 %
6	27.23	26.60	2.30 %	26.23	3.66 %	26.95	1.03 %	26.75	1.74 %
7	31.26	30.39	2.79 %	29.76	4.81 %	30.88	1.21 %	30.69	1.82 %
8	33.29	31.98	3.93 %	31.40	5.67 %	32.77	1.57 %	32.50	2.38 %
9	36.17	36.09	0.23 %	35.76	1.13 %	35.90	0.76 %	35.85	0.88 %
10	39.29	37.92	3.48 %	37.65	4.17 %	38.78	1.31 %	38.51	1.98 %

4. CONCLUSIONS

In the scope of the study, the results of two different finite element types and ANSYS are compared for both flat and curved geometry. The rectangular shell element (RSE) is a planar finite element type and has six generalized coordinates. The cylindrical shell element (CSE) is a curved finite element and has seven generalized coordinates. and The curved geometry is created by utilizing the large deflection equation. Two different boundary conditions which are two-side-fixed and four-side-fixed are examined for both flat and curved structure models. According to the generalized results:

- It can be concluded that the error rates for both finite element types are quite low in higher mesh densities.

- While acceptable results can be obtained at low mesh density for two-side-fixed boundary condition, higher mesh density is required for four-side-fixed boundary condition.
- Both RSE and CSE give reliable results for the two-side-fixed flat plate structure. However, by comparison, the RSE gives slightly better results.
- Error rates increase at low mesh density for the four-side-fixed flat plate structure. However, the error rates are low with high mesh density.
- For the two-side-fixed curved plate structure, error rates are quite low at both low and high mesh density. As in the flat plate structure, the RSE gives slightly better results.
- For the four-side-fixed curved plate structure, the low-density mesh affects the error rates badly, especially at higher frequencies. Nonetheless, both finite element types give very good results at high mesh density.
- CSE gives lower error rates than RSE for four-side-fixed boundary condition.
- For all geometry and boundary conditions under examination, the RSE model provides reliable results, although it contains fewer generalized coordinates.
- Both finite element types are suitable for flat and curved plate structures. However, RSE has a great advantage due to its lower stiffness and mass matrix sizes compared to CSE.

5. REFERENCES

Chandrupatla, T.R., & Belegundu, A.D. 2002. *Introduction to Finite Elements in Engineering*. New Jersey: Prentice Hall.

Danzi, F., Cestino, E., Frulla, G., & Gilbert, J. (2017). Equivalent plate model of curvilinear stiffened panels. In: *Proceedings of the 7th International Conference on Mechanics and Materials in Design, Albufeira, Portugal,* 11-15 June, 2017.

Dey, P., Haldar, S., Sengupta, D., & Sheikh, A. (2016). An efficient plate element for the vibration of composite plates. *Applied Mathematical Modelling, 40*(9-10), 5589-5604. doi:10.1016/j.apm.2016.01.021

Eisenberger, M., & Deutsch, A. (2019). Solution of thin rectangular plate vibrations for all combinations of boundary conditions. *Journal of Sound and Vibration, 452*, 1-12.

Jairazbhoy, V. A., Petukhov, P., & Qu, J. (2012). Large deflection of thin plates in convex or Concave Cylindrical Bending. *Journal of Engineering Mechanics, 138*(2), 230-234.

Kumar, A., Singha, M., & Tiwari, V. (2017). Nonlinear bending and vibration analyses of quadrilateral composite plates. *Thin-Walled Structures, 113*, 170-180. doi:10.1016/j.tws.2017.01.011

Li, R., Wang, B., Li, G., & Tian, B. (2016). Hamiltonian system-based analytic modeling of the free rectangular Thin PLATES' free vibration. *Applied Mathematical Modelling, 40*(2), 984-992.

Li, R., Wang, P., Xue, R., & Guo, X. (2017). New analytic solutions for free vibration of rectangular thick plates with an edge free. *International Journal of Mechanical Sciences, 131-132*, 179-190.

Nasirmanesh, A., & Mohammadi, S. (2017). An extended finite element framework for vibration analysis of Cracked FGM shells. *Composite Structures, 180*, 298-315.

Guha Niyogi, A., Laha, M., & Sinha, P. (1999). Finite element vibration analysis of laminated composite folded plate structures. *Shock and Vibration, 6*(5-6), 273-283.

Olson, M.D., & Lindberg, G.M. (1968). Vibration Analysis of Cantilevered Curved Plates Using a New Cylindrical Shell Finite Element. In: *Proceedings of the Conference on Matrix Methods in Structural Mechanics*; *Ohio, USA*.

Ozturk, H. (2011). In-plane free vibration of a pre-stressed curved beam obtained from a large deflected cantilever beam. *Finite Elements in Analysis and Design, 47*(3), 229-236.

Petyt, M. 2010. *Introduction to finite element vibration analysis*. New York: Cambridge University Press.

Rawat, A., Matsagar, V., & Nagpal, A. K. (2016). Finite element analysis of thin circular cylindrical shells. *Proceedings of the Indian National Science Academy, 82*(2), 349-355.

Senjanović, I., Tomić, M., Vladimir, N., & Hadžić, N. (2015). An approximate analytical procedure for natural vibration analysis of free rectangular plates. *Thin-Walled Structures, 95*, 101-114.

Spagnoli, A., Brighenti, R., Biancospino, M., Rossi, M., & Roncella, R. (2019). Geometrically non-linear bending of plates: Implications in curved building façades. *Construction and Building Materials, 214*, 698-708. doi:10.1016/j.conbuildmat.2019.04.175

Sudhir, N. (2012). Plate Bending Analysis Using Finite Element Method. Retrieved January, 2020, from http://ethesis.nitrkl.ac.in/3303/1/108ME015.pdf

Chapter 6

ANALYSIS OF WASTE IN A SMALL-SCALED MANUFACTURING FACILITY AND THE PROCESS IMPROVEMENT STUDIES

Büşra BAKDAAL[1],
Serap AKCAN[2]

1 Industrial Engineer, Sakarya 1. Organized Industial Zone, Sakarya, Turkey. bakdaalbusra@gmail.com, ORCID: 0000-0002-3936-2928
2 Associate Professor Dr., Tarsus University, Faculty of Engineering, Industrial Engineering Department, Tarsus, Turkey. serapakcan@tarsus.edu.tr, ORCID: 0000-0003-2621-9142

1. INTRODUCTION

Efficient and effective new generation production strategies have come to the forefront today as they intend to meet customer demands and preferences in the shortest time. Lean production is the most important and successful production method (Kara, 2004). Simplicity is a way of thought that involves continuous improvement, prevention of waste and adaptation to change. In general, it means the prevention of any waste.

In the literature, it is possible to come across studies using lean production techniques in different fields. Lasa et al. (2009) analyzed the causes for the limited adoption of lean manufacturing concepts in proposals for the redesign and improvement of productive systems in serial production companies. Tanco et al. (2013) applied the lean tools to nougat fabrication. Results showed that the inventory of nougat bars in the flow pack could fall from 10.4 to 0.25 days on average. Forno et al. (2014) presented a study about the problems and challenges found in the literature from the past 15 years about application of lean tools. Vargas and et al. (2018) used PDCA (plan-do-check-act) cycle in order to decrease the failures occurred during the welding operation in the production business. Kumar and et al. (2018) presented the achievements of the business through Kaizen and the value stream mapping technique in the business production the automotive parts. Shou et al. (2019) developed a system to classify value added and non-value added activities for lean applications in turnaround maintenance projects. Jimenez et al. (2019) presented an expansion of the lean 5S methodology to 6S. Iranmanesh et al. (2019) examined the effect of lean manufacturing practices on firms' environmental performance by considering lean culture as a moderator. For this aim a survey is used to 187 manufacturing firms in Malaysia. Kumar et al. (2019) implemented the lean tools in the garment industry. According to the results, the production cycle time is reduced 34% and the inventory time is reduced 14%. Çayır and Akcan (2020) aimed to determine and eliminate the bottlenecks occurred in the packing, planning and quality control departments of a firm which carries on its business in the textile sector. They presented the process improvement studies made through Kaizen technique.

The purpose of this research is to minimize waste and costs and maximize efficiency and profitability by using lean production techniques in a small-scaled plant which performs contract production to companies offering safety and security products. For that purpose, current situation analysis was performed to identify the waste in production stage and process improvement studies were applied to minimize waste. (This research was supported by the TUBITAK 2209-B Projects Fund, under project number 1139B411802366).

2. VALUE AND WASTE

2.1. Value

Value is the worth of a product determined by the customer by nature, which is reflected on sales price and market demand. The value of a typical product is created by the producer with the combination of actions. Some of these actions create the value perceived by the customer whereas some others are only necessary because of the current structure of the design and production process. The goal of lean thought is to protect and augment the actions in the first group and to destroy those in the second group (Lean concepts dictionary, 2016: 22).

2.2. Waste

Lean philosophy aims to reduce over-capacity and stock, remove out actions not adding value to the system and to minimize waste. In lean production, anything worthless or non-functional for the end-user is a waste, thus, lean production cannot be performed by preventing waste in production process only. Table 1 presents the waste that needs to be prevented when implementing lean systems. In lean systems, the system should be eliminated from the above-mentioned types of waste in order to ensure seamless flow of materials.

Table 1. *Eight Types of Waste (David McBride, "The Seven Manufacturing Wastes," August 29, 2003)*

WASTE	DESCRIPTION
Over-production	Producing a product before the need comes out, making it difficult to find the errors and creating over-stock
Over-processing	Doing more process than adequate
Transporting	Excessive movement of the product between the processes
Defects	Quality errors
Unnecessary motion	Works that involve too many actions
Waiting	Waste of time endured when the product is not being processed
Inventory	Conceals the problems in the field of production, extends streaming time, is a waste of place. Buffer stock is the direct result of over-processing and waiting.
Underutilization of Employees	Not making the best use of the knowledge and creativity of the employee

3. CASE STUDY

This study aims to assess the potential solutions against the production delays and buffer stock increases experienced in a plant performing contract production. For that purpose, we studied all the processes involved in the production line and tried to explain the study system as the first step.

3.1. About the Manufacturing Facility

The plant was founded in 1996 to offer contract production activities to leading safety and security product companies in Turkey. Panel, PVC door handles, door locks, support sheets and joints are produced in the plant. There are 4 white-collar and 20 blue-collar personnel working in the plant. The plant mainly supplies its raw materials and semi products domestically. The plant is a small-scaled private company that could be defined as a SME.

3.2. Product Family Selection

Waste and interruptions experienced in casting and decoupage departments cause bottlenecks in other production stages and have negative impact on timely delivery of purchase orders. Considering the system as a whole, there are 3 different types of products that undergo through these stages. When the demands for the types of products were reviewed, it was decided to apply the lean techniques for Corpo Staffa product with a monthly demand of 40000 pcs. Corpo Staffa is a part of the fittings that are used to ease the opening of doors in emergency situations such as fire and earthquakes. Images of the product are given in Figure 1 and Figure 2. The product has a complicated appearance due to its geometric structure, which makes its production rather difficult. Complexity of the production process encourages large companies to resort to contract production.

Figure 1. *Corpo Staffa Right-Bottom View*

Figure 2. *Corpo Staffa Upper View*

3.3. Description of the Process

Upon entering into the plant, the raw materials undergo a conformity check and then, they are stocked besides the machine they are to be processed with. The process stream of a raw material until the obtainment of the final product is given in Figure 3:

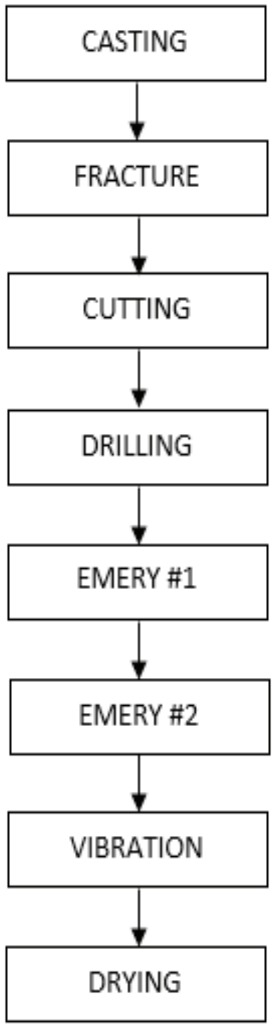

Figure 3. *Production Stream*

Casting: 300-ton aluminum injection machine is used in casting. For pressing, aluminum melted at 700°C furnace is casted into the tank of the machine by the operator with the help of a ladle. Operator gets the pressed product out of the mold and cleans the surface of the mold before going on with a new pressing process. 4 pieces of products are obtained at the end of each pressing process. The products are checked with gauges to prevent that any defective product progresses to the next process. The

pieces getting out of the injection machine are deposited on the palette and kept waiting to move on to the next process. As the work requires qualified labor force, operators working at the cast house have received a special training. Two operators work on the machines in shifts. These operators change shifts every half an hour. The operator who is in idle state keeps working wherever needed.

Fracture: The pieces coming out of the injection machine are sorted out through the runners. The pieces sorted out are deposited on top of each other and kept waiting to move on to the next process.

Cutting: Air pockets of the pieces sorted through the runners are cut.

Drilling: Desktop driller is used to clean the burrs found at the holes on the pieces.

Emery #1: Excessive fractions arising from the cutting process are eliminated with rough emery. However; as these products have rather narrow tolerance values, they are subjected to fine emery if they are not well cleaned in this process.

Emery #2: Pieces for which Emery#1 has been insufficient, undergo the same process.

Vibration: Upon the completion of the emery process, the products are subjected to vibration process to clean the grease residues sprayed to prevent the material from adhering onto the mold surface during casting and to clean the emery dust.

Drying: The pieces are subjected to drying process to prevent any oxidation that could be formed on the surface of the wet material following the vibration process, and they are made ready for shipping.

3.4. Wastes in Production Process

Current situation is reviewed to determine the wastes causing problems in the plant (Table 2).

Table 2. *Wastes in Corpo Staffa Production Process*

WASTE	DESCRIPTION
Over-processing	Currently, the pieces getting out of the cast machine are broken manually and ejected from the runners. This process leads to an over-processing in the further steps of the stream.

Transport	Currently, the pieces getting out of the emery process are transported to 7 m away for vibration and drying. As there is a disconnection between the production processes and the distances are not well measured, the need for such transport rises.
Defects	Currently, operators check the drilling process by hands and eyes. Therefore, some holes are missed out and the process is not completed in an appropriate manner.
Unnecessary motion	As the layout of the plant is not arranged in a manner that will ensure continuous streaming, unnecessary movements of employees emerge.
Waiting	Considering that qualified labor force is required in production, reduction of the performance of the employees due to fatigue or other similar reasons, leads to delays and waiting periods. Long vibration work times lead to delays in forwarding.
Inventory	When the pieces getting out of the casting process are ejected from the runners, they are deposited between the fracture and cutting processes. Thus, a buffer stock appears between the fracture and cutting processes, leading to waste of space. Long streaming times leads to inventory, which covers up the problems in the production area, indeed.

4. RESULTS

In this research, values throughout the production stream were identified and studies were carried out to prevent and eliminate waste. Besides, current situation analysis was performed to suggest a future system to enhance system performance. The majority of the suggested systems were implemented, and some others were subjected to an evaluation process. Estimated effects of the suggested system are described below.

RECCOMENDATIONS;

I. Making New investment

Fracture and cutting processes required too much labor force and were time-consuming, leading to delays and waiting periods. If machine power, instead of labor force, is used in the processes, time will be saved, and better-quality outputs will be achieved. Therefore, investment was made on relevant machine (trim press injection machine). Trim press enables

that, the pieces getting out of the injection machine are ejected from the runners and air pockets formed in molds. In future situation, fracture and cutting processes are individually carried out in a shorter time and under more favorable conditions. The benefits of trim press are given in Table 3.

Table 3. *The Benefits of the Investment*

	Current situation	***Future situation***
Daily production amount	1250	1800
Description	Injection machine was running at low speed to prevent accumulation in production. Thanks to the injection machine working at speed conforming to Takt time and trim press, daily purchase orders were made ready.	
Labor force	3 operators	1 operator
Description	A total of 3 operators were working in fracture and cutting processes, trim press helped transfer of such labor force to other positions requiring labor force.	
Failure rate	0.08	0.024
Description	Failure rate was reduced 70%.	
Processing time	37 seconds	15 seconds
Description	The process for each product lasted for 37 seconds previously, trim press enabled that 4 products were processed in 15 seconds. Thus, yield was received throughout the process and system efficiency was boosted.	

II. Kaizen

Kaizen-1: The molds used in injection machines change from one product to another. In production culture, these molds should be located close to the machines where change will occur and should be easily accessible. There are three different injection machines used in the plant. In front of these machines, there are shelves for the molds. The shelves narrow the space, the molds cannot be found when needed and the molds are at a distance from the machines, which all have a negative impact on production stream. Due to these negative impacts, production halts and other lines keep waiting. Consequently, it was decided to rearrange the mold shelves.

The production engineer and operator performed a teamwork for the mold shelves to determine the best location. It was decided that shelves would be mounted by walls in order to enlarge space and each shelf would be numbered to arrange the molds on the shelves in an orderly manner (Figure 4). In this way, the molds needed will be easily found and the replacement process will start immediately.

Before Kaizen	*After Kaizen*
The shelves molds are kept waiting	The new shelves for the orderly arrangement of molds
	

Figure 4. *Process improvement studies concerning mold shelves*

Thanks to the studies carried out, product replacement times which previously lasted for 75 minutes, were reduced to 45 minutes.

Kaizen-2: Pieces getting out of the injection machine are carried manually and taken to the fracture area. The products getting out of this process are ejected from the runners. The pieces ejected are then deposited on top of each other and kept waiting to move on to the next step. This process carried out in the fracture area causes impact and scratches on products and leads to buffer stock deposition arising from transports.

Before Kaizen	*After Kaizen*
The space where the products are deposited and kept waiting	Rubber container to be used for transport and for the waiting period

Figure 5. *Semi-Product Stock Containers*

In order to correct the current situation, the purchase department was contacted and they were asked to provide rubber containers where the products could wait without being exposed to any impact and thus, would be protected against any defect (Figure 5). A pallet truck was purchased to carry the containers to save labor force. Besides, the complexity of the process and waiting periods were eliminated.

Minimum 30% and maximum 75% improvement was achieved during Kaizen studies, leading to savings in movements and time and elimination of the system from waste and failures. The arrangements needed for the improvements were systematized and lean production practices were used. Product quality was increased, and monetary gains were achieved as a result.

III. Andon System

Vibration machine allows the processing of 120 products in 30 min. Products getting out of the vibration machine are subjected to drying process against the risk of oxidation that could emerge in 15 min. The operator of this process deals with other works in the meantime and cannot perform loading-unloading timely when the process is completed, which causes delays.

Andon is a Japanese word meaning ‘lamp’. It is an audio and/or light warning system that informs the relevant person about any problem occurring in any station in the mounting line or in the production unit. The system drives production and is used in vibration and drying machines in order to ensure sustainability of production. Currently, 850 items of products get ready for forwarding daily. A daily capacity of 1900 items is achieved with the use of the Andon system.

5. CONCLUSIONS

This project explains the available outputs of an ongoing study. Significant acquisitions were achieved with the improvements made. Acquisitions such as cost and time savings, faster and failure-free works all helped application of greater improvements. The values on the stream were determined and Kaizen studies were performed to prevent and eliminate the wastes in production. In the study intended for mold shelves, 40% improvement was achieved in mold replacement times. The plant achieved a gain of 9408 TRY with the help of the Kaizen study performed to prevent impacts. Besides, current situation analysis was performed to suggest a future system to enhance system performance. The majority of the suggested systems were implemented, and some others were subjected to an evaluation process. In future researches, value stream can be analyzed not only for the production process but for the whole system.

6. REFERENCES

Çayır, E., Akcan S. 2020. "The Process Improvement Studies to Increase the Productivity in a Printed Fabric Production Facility*". 4th International Symposium on Multidisciplinary Studies and Innovative Technologies*. **Doi**:https://dx.doi.org/ 10.1109/ISMSIT50672.2020.9254379

Forno et al. 2014. "Value Stream Mapping: a study about the problems and challenges found in the literature from the past 15 years about application of Lean tools". *The International Journal of Advanced Manufacturing Technology* 72: 779–790. Doi: https://doi.org/10.1007/s00170-014-5712-z

Iranmanesh, M. et al. 2019. "Impact of Lean Manufacturing Practices on Firms' Sustainable Performance: Lean Culture as a Moderator". *Sustainability* 11: 1112. Doi: https://doi.org/10.3390/su11041112

Jimenez, M. et al. 2019. "Extension of the Lean 5S Methodology to 6S with an Additional Layer to Ensure Occupational Safety and Health Levels". *Sustainability* 11: 3827. Doi: https://doi.org/ 10.3390/su11143827

Kara, Y.2004. U-tipi montaj hattı dengeleme problemleri için yeni modeller ve otomotiv yan sanayinde bir uygulama. Doktora tezi, Selçuk Üniversitesi, Konya.

Kumar S., Dhingra A.K., Singh B. 2018. "Process improvement through Lean-Kaizen using value stream map: a case study in India". *The International* Journal of Advanced Manufacturing Technology 96:2687–2698. Doi: https://doi.org/10.1007/s00170-018-1684-8

Kumar D.V, Mohan G.M., Mohanasundaram K.M. 2019. "Lean Tool Implementation in the Garment Industry". FIBRES & TEXTILES in Eastern Europe 27, 2(134): 19-23. Doi: https://doi.org/10.5604/01.3001.0012.9982

Lasa I. S., Castro R. and Laburu C. O. 2009. "Extent of the use of Lean concepts proposed for a value stream mapping application". *Production Planning and Control* 20 (1): 82-98. Doi: https://doi.org/10.1080/09537280802685322

Lean concepts dictionary, Optimist Press, 2016.

McBride D, The Seven Manufacturing Wastes, August 29, 2003. http://www.emsstrategies.com

Shou W., Wang J., Wu P and Wang X. 2019. "Value adding and non-value adding activities in turnaround maintenance process: classification, validation, and benefits". *Production Planning and Control* Doi: https://doi.org/10.1080/09537287.2019.1629038

Tanco et al. 2013. "Applying lean techniques to nougat fabrication: a seasonal case study". *The International Journal of Advanced Manufacturing Technology* 68: 1639–1654. Doi: https://doi.org/10.1007/s00170-013-4960-7

Vargas A.R. et al. 2018. "Applying the Plan-Do-Check-Act (PDCA) Cycle to Reduce the Defects in the Manufacturing Industry: A Case Study". *Appl. Sci*. 8: 2181. Doi: https://doi.org/ 10.3390/app8112181

Chapter 7

IMPACT OF VIRTUAL INERTIA AND DEMAND RESPONSE CONTROLS ON STABILITY DELAY MARGINS IN LOAD FREQUENCY CONTROL SYSTEM

Ausnain NAVEED[1]
Ömer AYDIN[2]
Şahin SÖNMEZ[3]
Saffet AYASUN[4]

1 Dr., University of Azad Jammu & Kashmir, Faculty of Engineering, Department of Electrical Engineering, Muzaffarabad, Pakistan. husnain.naveed@gmail.com, Orcid: 0000-0002-4603-9942.
2 Ph.D., Gazi University, Faculty of Engineering, Department of Electrical and Electronics Engineering, Ankara, Turkey. omeraydin89@gazi.edu.tr, Orcid: 0000-0002-4603-9942.
3 Assoc. Prof. Dr., Malatya Turgut Özal University, Yeşilyurt Vocational School, Electronics and Automation, Malatya, Turkey. sahin.sonmez@ozal.edu.tr, Orcid: 0000-0002-0057-2522. (*Corresponding author)
4 Prof. Dr., Gazi University, Faculty of Engineering, Department of Electrical and Electronics Engineering, Ankara, Turkey. saffetayasun@gazi.edu.tr, Orcid: 0000-0002-6785-3775.

INTRODUCTION

This paper investigates the effect of virtual inertia (VI) and demand response (DR) control on stability margins of Load Frequency Control (LFC) systems having communication time delays. The function of LFC system is to regulate the frequency around the nominal value and to maintain scheduled power exchanges of the tie-line connecting control areas. The frequency regulation is achieved by adjusting power outputs of conventional thermal or hydro power plants (Kundur, 1994). It is expected that renewable energy (RE) sources including photovoltaic (PV) and wind power systems will have significant share of power generation in the smart power grid prospect (Bevrani et al., 2010; "U.S. Department of Energy Smart Grid", 2020). Because of this penetration, the frequency regulation is becoming a difficult task as conventional LFC systems get more complex with regard to frequency regulation. Additionally, highly variable generation of RE sources is inadequate to regulate the system frequency. The massive integration of the RE sources based generation leads to some stability issues introducing lack of inertia and insufficient damping properties (Kerdphol et al., 2019). Large synchronous generators owing to rotational mass and damper windings could keep grid stability during any disturbances (Krismanto et al., 2018; Ulbig et al., 2014). However, the high level penetration of power electronic devices connected to non-synchronous generators causes significant reduction in system's inertia that plays an important role on frequency stability, dynamic performance and reliability (Tamrakar et al., 2017). Furthermore, abrupt power fluctuations because of intermittent nature of RESs deteriorate dynamic performance of the modern power systems (Bevrani, 2014). The research present in the literature proposes short-term energy storage systems (ESSs) that could behave like classic synchronous generator and virtually provide the required inertia to the system (Chen et al., 2011; Driesen and Visscher, 2008; Dreidy et al., 2017). The strategy known as virtual synchronous generator (VSG) consists of ESS, power electronic devices and virtual inertia control mechanism mimics inertia response and damping properties of a classic synchronous generator (Chen et al., 2011; Driesen and Visscher, 2008; Karapanos et al., 2011). The control strategy is effectively implemented for HVDC interconnected systems (Rakhshani et al. 2016; Rakhshani et al. 2017), improvement of frequency stabilization in a two-area power system (Kerdphol et al., 2018) and emulating the inertia power by utilizing different control methods (Ali et al., 2019).

On the other hand, the shortcomings of RE sources including high costs, low efficiency, and intermittent nature of their power generations encourage to utilize dynamic demand response (DR) for frequency regulation, which may also provide ancillary services (Bao et al., 2017;

Beil et al., 2016; Wang et al., 2017). The DR control not only contributes in load reduction but also improves grid's stability during peak demand times. Moreover, with the implementation of the DR control the power grid having less operational costs becomes more flexible, reliable and efficient (Pourmousavi and Nehrir, 2014; Singh et al., 2017).

In LFC control system, various control actions for all ESSs and other units are typically performed by primary and secondary control loops. Primary control, which locally activates units such as ESSs, is initial control action. Secondary control based on load frequency control (LFC) mechanism is employed to keep the system frequency in a nominal fixed value after load disturbance events. With the increasing integration of VI and DR control, inevitable time delays in the open or dedicated communication network have become a notable concern in frequency regulation since time delays cause the poorer controller performance and negatively influence the frequency dynamic and stability (Jiang et al., 2012; Naveed et al., 2019; Saeed et al., 2018; Singh et al., 2016; Sönmez et al., 2016). To serve the purpose, the secondary control is coordinated by a central controller introducing complex communication networks. The task of the central controller is to send/receive the control information to/from local controllers. The controller then decides and performs essential control actions for regulating the system voltage and frequency (Saeed et al., 2018). Therefore, communication delays could not be neglected and could be considered in the controller design.

The frequency control issue and its complexity have become a big concern because of the negative effects of communication delays on system stability, uncertainties in RESs, and low inertia. Therefore, computation of communication time delays that guarantees the stability of the time-delayed LFC system including VI and DR loop is required. In this work, a direct method (Walton and Marshall, 1987) used in frequency-domain is employed to eliminate the exponential expressions from the characteristic equation having transcendental terms and thereby to calculate the stability delay margins of single-area LFC-VI-DR system. This method has already been effectively utilized in analyzing the delay-dependent stability of conventional LFC system (Sönmez et al., 2016) with no VI and DR loops involved. Therefore, the main contributions of this work are briefly summarized in the following:

1) The first main contribution of the study is the investigation of the individual and combined effect of VI and DR on the stability delay margins of a LFC system. The proposed method provides an opportunity to analyze the delay-dependency of system when VI and DR loops are integrated into the conventional LFC system. Results indicate that stability

delay margins show different trends for different power sharing schemes between the conventional LFC and/or VI, DR.

2) The second main contribution is to verification of theoretical delay margins by time-domain simulations and quasi-polynomial mapping-based root finder (QPmR) algorithm, which computes the quasi-polynomials spectrum (zeros) over a large region of the complex plane (Simulink, 2019; Vyhlídal and Zitek, 2009). Effectiveness of the algorithm has been demonstrated by many research studies (Kammer and Olgaç, 2016; Vyhlídal et al., 2014).

2. SYSTEM DESCRIPTION

2.1. Virtual Inertia Control Concept for Conventional LFC

VSG imitates behavior of a real synchronous generator by controlling the inverter via virtual inertia control. To compensate the frequency fluctuation of system, ESSs should absorb the excess power like a load or inject the power like a generator from/into the LFC within very short-time. Because the rotor of a synchronous generator has rotational speed and damper windings, stored kinetic energy in mechanical part of a synchronous generator could be expressed as follows (Kundur, 1994):

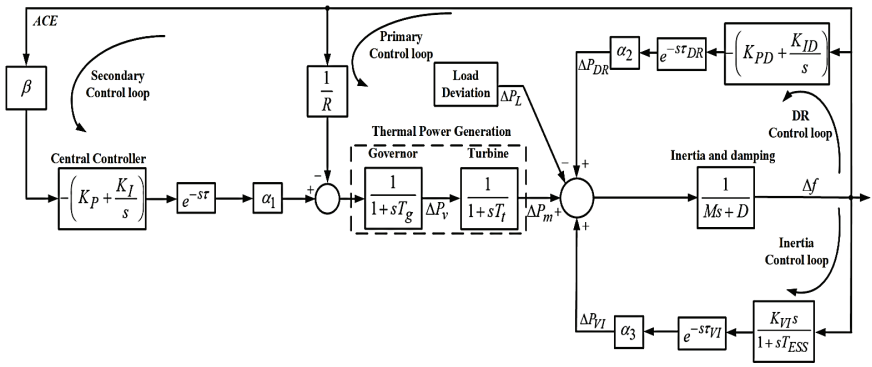

Figure 1. *The dynamical model of LFC system including VI and DR control loops.*

$$W_k = \frac{1}{2} K \omega^2 \tag{1}$$

where, W_k, ω and K are stored kinetic energy of the rotor, rotor speed (rad/s) and inertia moment of system (kgm^2), respectively. By taking first order derivative of (1), we could obtain a relationship between

mechanical power (P_m) and electrical power (P_e) described as follow (Kundur, 1994):

$$T_m - T_e = \frac{P_m}{\omega} - \frac{P_e}{\omega} = K\frac{d\omega}{dt} \tag{2}$$

where, T_m and T_e are mechanical and electrical torques, respectively. Substituting $H = W_k / S$ known as system inertia constant (H) and apparent power (S) into (2), the rate of change of frequency (RoCoF) of a power system is computed to determine the required system inertia and initial inertia power (Ali et al., 2019; Kundur, 1994). The resulting equation describes the emulation of a VSG output power (Ali et al., 2019):

$$P_{VSG} = P_m - P_e = K_{VI}\frac{d\omega}{dt} \tag{3}$$

where, K_{VI} is inertia constant of VSG and equal to $\left(2HS/\omega_0\right)$ in per-unit. Also, P_{VSG} indicates that power will be absorbed and injected by VSG according to initial RoCoF sign (Karapanos et al., 2011). Considering the damper winding of a synchronous generator, equation (3) can be transformed into the swing equation of a synchronous generator that enables us to investigate the impact of inertia and damping on frequency deviation during the mismatch between load demand and generation.

2.2. Dynamic modeling of a time-delayed LFC including VI and DR loops

Figure 1 presents the dynamic model of single-area LFC system including VI and DR loops. In the system model, $\Delta P_m, \Delta f, \Delta P_v, \Delta P_L$ and ACE are the mechanical output of generator, deviation in the frequency, the valve position, load disturbance and area control error, respectively. Also, T_g, T_t, M, D, R and β represent time constant of the governor and turbine, the inertia constant, damping coefficient, speed drop of the control area and frequency bias factor, respectively. Whereas, K_{PD} and K_{ID} are the local controller gains of DR control loop. Furthermore, α_1, α_2 and α_3 are the power sharing factors of conventional generator, demand response and virtual inertia, respectively. It should be noted that the sum of all these power sharing factors is equal to 1.

The three different controls levels for regulating the frequency are

primary, virtual inertia and/or DR and secondary control. Primary control is first control action considering droop control activity of prime mover. The primary control loop locally controls governor and synchronous generator inertia of small-scale thermal power plant for frequency regulation. Secondly, inertia control as a supplementary control is applied to provide inertia kinetic energy according to initial sign of df/dt by imitating the action of prime mover or the DR loop comes into action as directed by the central controller. Finally, the load frequency control (LFC) mechanism is being used to zero the steady state error and enhance the frequency stability. Additionally, in this control level, low-bandwidth communication networks transmit the output commands to both VI and DR loops considering ACE control signal to restore the system frequency. To serve the purposes, a proportional-integral (PI) type central controller is used in the LFC that is given as follows:

$$G_C(s) = K_P + \frac{K_I}{s} \tag{5}$$

where, K_P and K_I are the gains of the central PI controller. Virtual inertia control that uses the derivative control technique based RoCoF is responsible for contribution of virtually inertia to regulate the frequency fluctuations. First-order transfer function of VSG is given in the following (Saeed et al., 2018)

$$G_{VI}(s) = \frac{K_{VI}s}{1 + sT_{ESS}} \tag{6}$$

In the VI control loop, K_{VI} and T_{ESS} represent virtual inertia constant and time constant of inverter based ESS, respectively. In Figure 1, τ represents total communication time delays for receiving/transmitting the data between the LFC controller and the conventional generator. Moreover, τ_{DR} and τ_{VI} denote communication time delays in the DR and VI control loops, respectively. The delay terms are modeled as exponential transfer functions of $e^{-s\tau}$, $e^{-s\tau_{DR}}$ and $e^{-s\tau_{VI}}$, respectively. It must be stated here that a first-order Padé approximation is used to model the delays $e^{-s\tau_{DR}}$ and $e^{-s\tau_{VI}}$ in the DR and VI control loops since communication time delays observed in DR and VI control loops are much smaller than one observed in the secondary control loop (Saeed et al., 2018). These approximations are given as follows:

$$e^{-s\tau_{DR}} = \frac{1-0.5\tau_{DR}s}{1+0.5\tau_{DR}s},\ e^{-s\tau_{VI}} = \frac{1-0.5\tau_{VI}s}{1+0.5\tau_{VI}s} \tag{7}$$

In order to compute the stability delay margins of the time-delayed LFC including VI and DR loops, the characteristic equation of the LFC-VI-DR system is obtained as follows:

$$\begin{aligned} &\Delta(s,\tau) = s\left[P(s)+Q(s)e^{-s\tau}\right] = 0 \\ &\Delta(s,\tau) = s\Delta'(s,\tau) = 0 \end{aligned} \tag{8}$$

where $\Delta'(s,\tau) = P(s)+Q(s)e^{-s\tau} = 0$, $P(s)$ and $Q(s)$ are polynomials of s and given as follows:

$$\begin{aligned} P(s) &= p_7s^7 + p_6s^6 + p_5s^5 + p_4s^4 + p_3s^3 + p_2s^2 + p_1s + p_0 \\ Q(s) &= q_4s^4 + q_3s^3 + q_2s^2 + q_1s + q_0 \end{aligned} \tag{9}$$

where *p* and *q* coefficients depending on parameters of LFC-VI-DR system are given in Appendix.

It should be noted that the characteristic equation of (8) has a simple root at the origin, $s = 0$, which is independent from the time delay τ. Therefore, it is sufficient to investigate the delay-dependent stability of $\Delta'(s,\tau) = 0$ (Walton and Marshall, 1987).

3. COMPUTATION OF STABILITY DELAY MARGINS BY DIRECT METHOD

The aim of studying the time-delayed system stability is to determine the delay-dependent or delay-independent stability of the system. For the former type, the system remains stable for $\tau < \tau^*$ where τ and τ^* represent delay and stability delay margin. However, the system becomes unstable when the delay exceeds the margin $\tau > \tau^*$. Whereas, in the latter case, the system remains stable for all finite values of time delays. The delay margin is the basic requirement for stability assessment of LFC-VI-DR systems and it should always be more than the total time delays observed system. In order to assess the stability of the single-area LFC-VI-DR system shown in Figure 1, it is necessary to have the information of delay margins for a wide range of LFC-VI-DR system and controller parameters.

The necessary condition for the single-area LFC-VI-DR system to be asymptotically stable is that all the roots of (8) must be situated in the left half of the s-plane. In consideration of the single delay, the delay margin computation can be done by finding values of τ^* for which (8) has roots (if any) on the $j\omega$-axis. Here, $\Delta'(s,\tau)=0$ is clearly an implicit function of s and τ that may or may not cross the $j\omega$- axis. To simplify the task, it is assumed that $\Delta'(s,0)=0$ has all the roots situated in the left half plane, that is, system with no delay is already stable. It is to be noted that (8) has an exponential term $e^{-s\tau}$ resulting in infinitely many finite roots. This makes the computation of the roots and delay margin a challenging issue. However, determination of these infinite numbers of roots is not necessary for delay-dependent stability assessment of the LFC-VI-DR system. The roots located on the $j\omega$-axis and the corresponding delay value are required to be determined. If, for some finite value of τ, the characteristic polynomial of $\Delta'(s,\tau)=0$ has a root on the imaginary axis at $s=j\omega_c$, the equation of $\Delta'(-s,\tau)=0$ will also have the same root on the imaginary axis for the same value of τ and ω_c due to the complex conjugate symmetry of complex roots. That means $s=j\omega_c$ will be a common root of the following two equations;

$$\Delta'(j\omega_c,\tau)=P(j\omega_c)+Q(j\omega_c)e^{-j\omega_c\tau}=0$$
$$\Delta'(-j\omega_c,\tau)=P(-j\omega_c)+Q(-j\omega_c)e^{j\omega_c\tau}=0 \quad (10)$$

By eliminating the exponential term between two equations in (10), the following augmented polynomial is obtained:

$$W(\omega_c^2)=P(j\omega_c)P(-j\omega_c)-Q(j\omega_c)Q(-j\omega_c)=0 \quad (11)$$

After substituting the polynomials of $P(j\omega_c)$, $P(-j\omega_c)$, $Q(j\omega_c)$ and $Q(-j\omega_c)$ presented in (9) into (11), the augmented polynomial of $W(\omega_c{}^2)$ can be represented as

$$W(\omega_c^2)=t_{14}\omega_c^{14}+t_{12}\omega_c^{12}+t_{10}\omega_c^{10}+t_8\omega_c^8+t_6\omega_c^6+t_4\omega_c^4+t_2\omega_c^2+t_0=0 \quad (12)$$

where

$t_{14} = p_7^2;\ t_{12} = (-2p_5p_7 + p_6^2); t_{10} = 2(p_3p_7 - p_4p_6) + p_5^2;$

$t_8 = 2(-p_1p_7 + p_2p_6 - p_3p_5) + p_4^2 - q_4^2;\ t_6 = 2(-p_0p_6 + p_1p_5 - p_2p_4 + q_2q_4) + p_3^2 - q_3^2;$

$t_4 = 2(p_0p_4 - p_1p_3 - q_0q_4 + q_1q_3) + p_2^2 - q_2^2;\ t_2 = 2(-p_0p_2 + q_0q_2) + p_1^2 - q_1^2;\ t_0 = p_0^2 - q_0^2;$

It is to be observed that the characteristic equation of (8) having exponential terms is now converted into a polynomial of (12) having no transcendental terms. More importantly, the real positive roots of (12) exactly coincide with the imaginary roots $s = \pm j\omega_c$ of (8). Now, the roots of the new polynomial of (12) can be easily computed using any standard method. Following situations may occur depending upon the roots of the new polynomial:

i) The system is stable for all finite delays $\tau \geq 0$ indicating that the system is delay-independent stable. This happens when the polynomial of (12) does not have any positive real roots inferring that (8) also does not have any roots on the $j\omega$-axis.

ii) The system is delay-dependent stable in interval of $[0, \tau_c]$ where τ^* is the stability delay margin. This happens when the polynomial of (12) has at least one positive real root inferring that (8) has at least one complex roots pair on the $j\omega$-axis.

The corresponding value of τ^* for a real positive root ω_c is simply obtained by using (8) as (Sönmez et al., 2016; Walton and Marshall, 1987):

$$\tau^* = \frac{1}{\omega_c}\mathrm{Tan}^{-1}\left(\frac{a_{11}\omega_c^{11} + a_9\omega_c^9 + a_7\omega_c^7 + a_5\omega_c^5 + a_3\omega_c^3 + a_1\omega_c}{a_{10}\omega_c^{10} + a_8\omega_c^8 + a_6\omega_c^6 + a_4\omega_c^4 + a_2\omega_c^2 + a_0}\right) \quad (13)$$

where

$a_{11} = -p_7q_4;\ a_{10} = p_6q_4 - p_7q_3;\ a_9 = p_5q_4 - p_6q_3 + p_7q_2;$

$a_8 = p_5q_3 - p_4q_4 - p_6q_2 + p_7q_1;\ a_7 = p_4q_3 - p_3q_4 - p_5q_2 + p_6q_1 - p_7q_0;$

$a_6 = p_2q_4 - p_3q_3 + p_4q_2 - p_5q_1 + p_6q_0;\ a_5 = p_1q_4 - p_2q_3 + p_3q_2 - p_4q_1 + p_5q_0;$

$a_4 = p_1q_3 - p_0q_4 - p_2q_2 + p_3q_1 - p_4q_0;\ a_3 = p_0q_3 - p_1q_2 + p_2q_1 - p_3q_0;$

$a_2 = p_0q_2 - p_1q_1 + p_2q_0;\ a_1 = p_1q_0 - p_0q_1;\ a_0 = -p_0q_0;$

4. RESULTS

In the section, the individual and combined impact of VI and DR parameters on the stability delay margin is broadly investigated. Then, the accuracy of stability delay margins is verified by QPmR algorithm and time-domain simulations. The parameters of the LFC-VI-DR system are given as (Kerdphol et al., 2018).

$$M = 0.166;\ D = 0.015;\ R = 3;\ \beta = 0.3483;\ \ T_g = 0.08;$$
$$T_t = 0.4;\ \ K_{VI} = 1;\ \ T_{ESS} = 10;\ K_{PD} = 0.1;\ K_{ID} = 0.1;$$

In the computation of delay margins, gains of PI controller in the DR control loop is fixed and stability delay margins are determined for a wide range of PI controller gains in the secondary control loop and power sharing factors. Table 1 shows stability delay margins for the classic LFC system not including VI or DR control loops $(\alpha_1 = 1,\ \alpha_2 = \alpha_3 = 0)$. This scheme corresponds to the case where all required control effort for frequency regulation is provided by the conventional generator. For fixed K_P gains, it can be observed that the stability delay margin τ decreases with the increase in K_I gain values. However, for K_I values fixed, delay margins first increase and then starts to decrease with an increase in K_P gain values. Table 2 presents stability delay margins for $\alpha_1 = 0.8,\ \alpha_2 = 0.2,$ and $\alpha_3 = 0.$ In this case, the conventional generator provides 80% of the total control effort while the DR control not having communication time delay $(\tau_{DR} = 0\ s)$ provides 20% of the total control effort. Table 2 clearly shows that the inclusion of DR has improved the stability of the system as delay margin values are greater than that of presented in Table 1 for all controller gains. Table 3 gives stability delay margins when only a VI control loop with a 20% participation factor and not including time delay $(\tau_{VI} = 0\ s)$ is integrated to the LFC system $(\alpha_1 = 0.8, \alpha_2 = 0, \alpha_2 = 0.2)$. Delay margins in Table 3 verify that the integration of VI control loop into the LFC system has improved the stability of the system as delay margins are relatively greater when compared with the classic LFC system given in Table 1. Moreover, when delay margins in Table 2 and 3 are compared, it is observed that the integration of the DR control loop results in larger delay margins than those of VI control loop case.

Furthermore, the impact of time delays in the DR and VI control loops are investigated. Table 4 gives stability delay margins for $\tau_{DR} = 0.2\ s$ and participation factors of $(\alpha_1 = 0.8,\ \alpha_2 = 0.2,\ \alpha_3 = 0)$. When compared with Table 2, it observed that the delay margins decrease yet the system stability is better than that of classic LFC system shown in Table 1. Also, Table 5 shows stability delay margins for the time delay of $\tau_{VI} = 0.2\ s$ in the VI control loop and participation factors of $(\alpha_1 = 0.8,\ \alpha_2 = 0,\ \alpha_3 = 0.2)$. When compared with Table 3 where the delay τ_{VI} was neglected, it is observed that delay margins are slightly bigger.

Finally, Table 6 presents delay margins to study the collaborative effect of VI and DR control loops both including time delays, τ_{VI} and τ_{DR}, respectively. Time delays in VI and DR control loops are selected as $\tau_{VI} = \tau_{DR} = 0.2\ s$ and participation ratios are $(\alpha_1 = 0.8, \alpha_2 = 0.1, \alpha_3 = 0.1)$. It is to be noticed that the stability delay margins are greater than the values presented in Table 1. This is a clear indication that the DR and VI loops improve the stability of the LFC system.

Stability delay margins computed theoretically need to be verified. For that purpose, QPmR algorithm and time-domain simulations are used. The PI controller gains are chosen as $K_P = 0.2,\ K_I = 0.4$ and the power sharing factors are selected as $\alpha_1 = 0.8,\ \alpha_2 = 0.1$ and $\alpha_3 = 0.1$. It is clear from Table 6 that the stability delay margin is calculated as $\tau^* = 5.3247 s$ for this case. Figure 2 shows dominant roots distribution of (8) and frequency response of the LFC-VI-DR system for stable, marginally stable and unstable cases. Figure 2(a) shows that for $\tau = 4.8\ s$ all the roots are located in left half of the s-plane and the frequency response has decaying oscillations, which indicates that the LFC-VI-DR system is stable. Figure 2(b) shows that the system is marginally stable for the computed stability delay margin $\tau^* = 5.3247\ s$ as a pair of complex conjugate roots of (8) is now positioned on the $j\omega -$ axis. Hence, showing an undamped frequency response. Whereas, for $\tau = 5.8\ s$, the system becomes unstable due to a pair of complex roots located in the right half of s -plane and the frequency response has increasing oscillations as depicted by Figure 2(c). Moreover, it is also imperative to study the individual impact of virtual inertia on stability delay margins by considering the variations in the participation

factor of virtual inertia α_3 while neglecting the demand response, $\alpha_2 = 0$. Figure 3 presents the variation of the stability delay margin with respect to the participation ratio α_3 of the VI control loop for $(K_P = 0.2,\ K_I = 0.4)$, a time delay of $\tau_{VI} = 0.2\ s$ on the VI control loop and three different values of VI constant, $K_{VI} = 0.6,\ 1.0$ and 1.6. It is clear from Figure 3 that the increase in power share of VI control loop improves the stability of the system for all K_{VI} constants. Moreover, Figure 3 clearly illustrates that the delay margin increases as K_{VI} for any given participation factor of the VI control loop. Similarly, the individual impact of demand response loop by considering the variations in participation factor of demand response α_2 on the stability delay margins when $\alpha_3 = 0,\ (K_P = 0.2,\ K_I = 0.4)$ and $\tau_{DR} = 0.2\ s.$ is shown in Figure 4. It should be observed that with an increase in the power share of demand response the stability delay margin values increase.

Table 1 Stability delay margins for $\alpha_1 = 1,\ \alpha_2 = \alpha_3 = 0$

$\tau^*(s)$	K_I				
K_P	**0.2**	**0.4**	**0.6**	**0.8**	**1.0**
0.0	7.3216	3.3525	1.9944	1.2815	0.8211
0.05	7.5614	3.4722	2.0739	1.3407	0.8680
0.1	7.7800	3.5808	2.1453	1.3931	0.9085
0.2	8.1470	3.7613	2.2616	1.4750	0.9676
0.4	8.5399	3.9415	2.3596	1.5181	0.9677
0.6	8.2840	3.7613	2.1574	1.2329	0.7086
1.0	0.5214	0.4738	0.4230	0.3722	0.3234

Table 2 *Stability delay margins for* $\alpha_1 = 0.8,\ \alpha_2 = 0.2,\ \alpha_3 = 0$ *and* $\tau_{DR} = 0\ s$

$\tau^*(s)$	K_I				
K_P	**0.2**	**0.4**	**0.6**	**0.8**	**1.0**
0.0	13.1933	5.3297	3.1684	2.1367	1.5187
0.05	13.4316	5.4498	3.2486	2.1968	1.5666
0.1	13.6461	5.5601	3.3224	2.2520	1.6104
0.2	14.0004	5.7492	3.4496	2.3466	1.6844
0.4	14.3823	5.9865	3.6110	2.4630	1.7692
0.6	14.2504	5.9936	3.6162	2.4526	1.7379
1.0	11.6017	4.8162	2.6506	1.0145	0.7059

Table 3 *Stability delay margins for* $\alpha_1 = 0.8,\ \alpha_2 = 0,\ \alpha_3 = 0.2$ *and* $\tau_{VI} = 0\ s$

$\tau^*(s)$	K_I				
K_P	**0.2**	**0.4**	**0.6**	**0.8**	1.0
0.0	9.5330	4.5639	2.8501	1.9668	1.4167
0.05	9.7756	4.6851	2.9308	2.0272	1.4648
0.1	10.0029	4.7984	3.0060	2.0832	1.5092
0.2	10.4082	4.9997	3.1388	2.1811	1.5856
0.4	10.9914	5.2856	3.3224	2.3110	1.6805
0.6	11.1931	5.3737	3.3653	2.3245	1.6686
1.0	9.6530	4.4720	2.5564	1.2167	0.7590

Table 4 *Stability delay margins for* $\alpha_1 = 0.8,\ \alpha_2 = 0.2,\ \alpha_3 = 0$ *and* $\tau_{DR} = 0.2\ s$

$\tau^*(s)$	K_I				
K_P	**0.2**	**0.4**	**0.6**	0.8	1.0

0.0	13.0602	5.2764	3.1358	2.1128	1.4984
0.05	13.2984	5.3965	3.2160	2.1728	1.5463
0.1	13.5125	5.5066	3.2897	2.2279	1.5899
0.2	13.8651	5.6950	3.4163	2.3219	1.6632
0.4	14.2395	5.9287	3.5749	2.4354	1.7445
0.6	14.0919	5.9277	3.5734	2.4178	1.7033
1.0	11.3426	4.6834	2.4976	0.7954	0.6210

Table 5 *Stability delay margins for* $\alpha_1 = 0.8,\ \alpha_2 = 0,\ \alpha_3 = 0.2$ *and* $\tau_{VI} = 0.2\ s$

$\tau^*(s)$	K_I				
K_P	**0.2**	**0.4**	0.6	0.8	1.0
0.0	9.5481	4.5783	2.8636	1.9794	1.4284
0.05	9.7907	4.6995	2.9443	2.0398	1.4766
0.1	10.0181	4.8129	3.0195	2.0958	1.5209
0.2	10.4235	5.0143	3.1522	2.1937	1.5973
0.4	11.0074	5.3004	3.3360	2.3236	1.6918
0.6	11.2104	5.3891	3.3791	2.3369	1.6787
1.0	9.6787	4.4907	2.5671	1.0918	0.7111

Table 6 *Stability delay margins for* $\alpha_1 = 0.8,\ \alpha_2 = 0.1,\ \alpha_3 = 0.1,\ \tau_{DR} = 0.2\ s$ *and* $\tau_{VI} = 0.2\ s$

$\tau^*(s)$	K_I				
K_P	**0.2**	**0.4**	**0.6**	**0.8**	**1.0**
0.0	10.9843	4.8971	2.9916	2.0429	1.4619
0.05	11.2249	5.0178	3.0721	2.1031	1.5099
0.1	11.4462	5.1296	3.1465	2.1587	1.5539
0.2	11.8277	5.3247	3.2763	2.2547	1.6288
0.4	12.3160	5.5856	3.4478	2.3765	1.7168
0.6	12.3590	5.6310	3.4690	2.3747	1.6901
1.0	10.2794	4.5653	2.5317	0.9010	0.6624

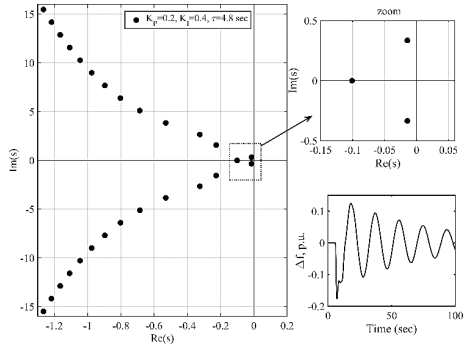

(a)

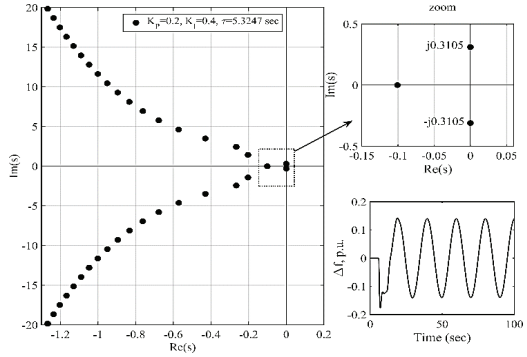

(b)

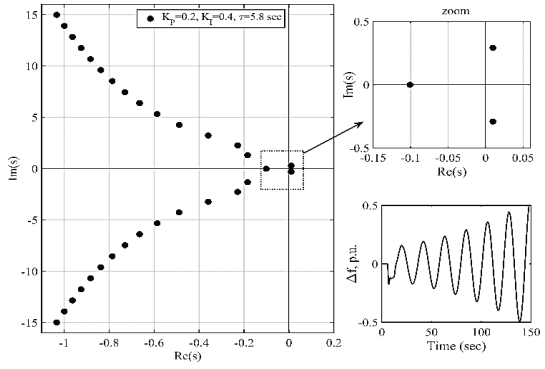

(c)

Figure 2. *Dominant roots distribution of the LFC-VI-DR system for* $\alpha_1 = 0.8,$ $\alpha_2 = 0.1,\ \alpha_3 = 0.1,\quad \tau_{DR} = 0.2\ s$ *and* $\tau_{VI} = 0.2\ s$ *.* **(a)** *Stable Case,* **(b)** *Marginally Stable Case* **(c)** *Unstable Case.*

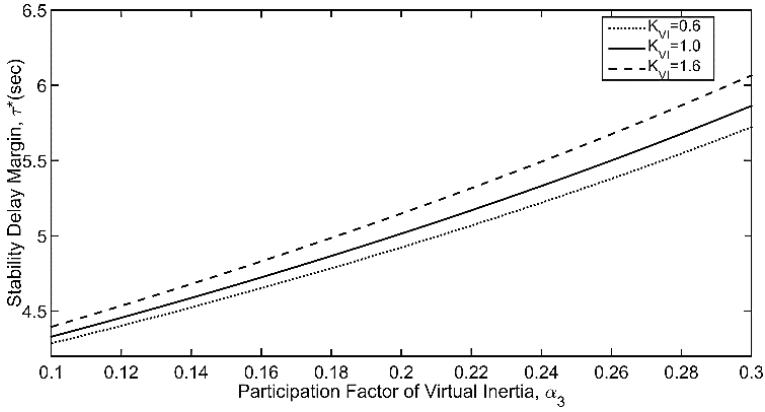

Figure 3. *Variation of stability delay margins against the participation factors of virtual inertia.*

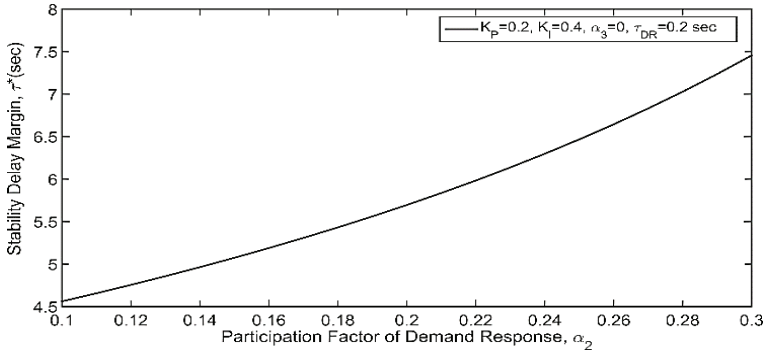

Figure 4. *Variation of stability delay margins against the participation factors of demand response.*

5. CONCLUSION

This paper has investigated the impact of VI and DR control loops on stability delay margins of a single-area LFC system with communication time delay. A frequency-domain exact method has been utilized to determine stability delay margins for different power sharing schemes between conventional generator and/or DR, VI control loops. The individual and combined effects of virtual inertia and demand response control loop on the stability delay margins in LFC system have been completely analyzed. It is observed that the LFC system with a VI or DR control loops has larger stability delay margins when compared with the one not including VI or DR control loops. It is also observed that stability delays slightly get smaller with an inclusion of time delay in the DR control loop when compared with the results where the time delay in the DR control loop

is neglected. On the other hand, stability delay margins slightly become larger with an inclusion of time delay in the VI control loop when compared with the results where the time delay in the VI control loop is not considered. Nonetheless, stability delay margins increased when both DR and VI control loops including time delays are taken into account. The results indicate that VI and DR control loops should be integrated into LFC systems in order to achieve a better frequency regulation in the presence of inevitable communication delays.

Future studies will encompass the following two significant issues: 1) Investigation of the impact of both VI and DR control loops on stability regions in the parameter space of PI controller gains in multi-area LFC systems. 2) The uncertainties in parameters of the LFC system along wıth the communication delays will be taken into consideration. Also, robust stability regions will be computed using the complex Kharitinov's theorem that will guarantee the stability for all admissible uncertainties.

REFERENCES

Ali, H., Magdy, G., Li, B., Shabib, G., Elbaset, A. A., Xu, D. and Mitani, Y. (2019). A New Frequency Control Strategy in an Islanded Microgrid Using Virtual Inertia Control-Based Coefficient Diagram Method. *IEEE Access*, *7*, 16979–16990.

Bao, Y.Q., Li, Y., Wang, B., Hu, M. and Chen, P. (2017). Demand response for frequency control of multi-area power system. *Journal of Modern Power Systems and Clean Energy*, *5*(1), 20–29.

Beil, I., Hiskens, I. and Backhaus, S. (2016). Frequency Regulation from Commercial Building HVAC Demand Response. *Proceedings of the IEEE*, *104*(4), 745–757.

Bevrani, H. (2014). *Robust Power System Frequency Control*. Springer Publishing.

Bevrani, H., Ghosh, A. and Ledwich, G. (2010). Renewable energy sources and frequency regulation: survey and new perspectives. *IET Renewable Power Generation*, *4*(5), 438.

Bukhari, S., Hazazi, K., Haider, Z., Haider, R. and Kim, C. H. (2018). Frequency Response Analysis of a Single-Area Power System with a Modified LFC Model Considering Demand Response and Virtual Inertia. *Energies*, *11*(4), 787.

Chen, Y., Hesse, R., Turschner, D., Beck, H.P. (2011) 'Improving the grid power quality using virtual synchronous machines', *IEEE International Power Engineering, Energy and Electrical Drives (POWERENG)*, Torremolinos, Spain, pp. 1–6.

Dreidy, M., Mokhlis, H. and Mekhilef, S. (2017). Inertia response and frequency control techniques for renewable energy sources: A review. *Renewable and Sustainable Energy Reviews*, *69*, 144–155.

Driesen, J. and Visscher, K. (2008). Virtual synchronous generators. *IEEE Power Energy Society General Meeting, Pittsburgh, USA*, pp. 1-3.

Grid Modernization and the Smart Grid. (2020, March 10). Energy.Gov. https://www.energy.gov/oe/technology-development/smart-grid

Jiang, L., Yao, W., Wu, Q.H., Wen, J.Y. and Cheng, S.J. (2012). Delay-Dependent Stability for Load Frequency Control with Constant and Time-Varying Delays. *IEEE Transactions on Power Systems*, *27*(2), 932–941.

Kammer, A.S. and Olgac, N. (2016). Delayed-feedback vibration absorbers to enhance energy harvesting. *Journal of Sound and Vibration*, *363*, 54–67.

Karapanos, V., Haan, D. and Zwetsloot, K. (2011). Real time simulation of a power system with VSG hardware in the loop. *37th Annual Conference of the IEEE Industrial Electronics Society (IECON)*, Melbourne, Australia, pp. 3748–3754.

Kerdphol, T., Rahman, F. and Mitani, Y. (2018). Virtual Inertia Control Application to Enhance Frequency Stability of Interconnected Power Systems with High Renewable Energy Penetration. *Energies*, *11*(4), 981.

Kerdphol, T., Rahman, F.S., Watanabe, M., Mitani, Y., Turschner, D. and Beck, H.P. (2019). Enhanced Virtual Inertia Control Based on Derivative Technique to Emulate Simultaneous Inertia and Damping Properties for Microgrid Frequency Regulation. *IEEE Access*, *7*, 14422–14433.

Krismanto, A.U., Mithulananthan, N. and Krause, O. (2018). Stability of Renewable Energy based Microgrid in Autonomous Operation. *Sustainable Energy, Grids and Networks*, *13*, 134–147.

Kundur, P. (1994). *Power System Stability and Control* (1st ed.). McGraw-Hill Education.

Naveed, A., Sönmez, A. and Ayasun, S. (2021). Impact of load sharing schemes on the stability delay margins computed by Rekasius substitution method in load frequency control system with electric vehicles aggregator. *International Transactions on Electrical Energy Systems*, *31*(5).

Pourmousavi, S.A. and Nehrir, M.H. (2014). Introducing Dynamic Demand Response in the LFC Model. *IEEE Transactions on Power Systems*, *29*(4), 1562–1572.

Rakhshani, E., Remon, D., Cantarellas, A.M., Garcia, J.M. and Rodriguez, P. (2017). Virtual Synchronous Power Strategy for Multiple HVDC Interconnections of Multi-Area AGC Power Systems. *IEEE Transactions on Power Systems*, *32*(3), 1665–1677.

Rakhshani, E., Remon, D., Mir Cantarellas, A. and Rodriguez, P. (2016). Analysis of derivative control based virtual inertia in multi-area high-voltage direct current interconnected power systems. *IET Generation, Transmission & Distribution*, *10*(6), 1458–1469.

Simulink. (2019). *Simulation and model-based design*. Natick, MA, USA, MathWorks.

Singh, V.P., Kishor, N. and Samuel, P. (2016). Communication time delay estimation for load frequency control in two-area power system. *Ad Hoc Networks*, *41*, 69–85.

Singh, V.P., Samuel, P. and Kishor, N. (2016). Impact of demand response for frequency regulation in two-area thermal power system. *International Transactions on Electrical Energy Systems*, *27*(2), e2246.

Sönmez, S., Ayasun, S. and Nwankpa, C.O. (2016). An Exact Method for Computing Delay Margin for Stability of Load Frequency Control Systems With Constant Communication Delays. *IEEE Transactions on Power Systems*, *31*(1), 370–377.

Tamrakar, U., Shrestha, D., Maharjan, M., Bhattarai, B., Hansen, T. and Tonkoski, R. (2017). Virtual Inertia: Current Trends and Future Directions. *Applied Sciences*, *7*(7), 654.

Ulbig, A., Borsche, T.S. and Andersson, G. (2014). Impact of Low Rotational Inertia on Power System Stability and Operation. *IFAC Proceedings Volumes*, *47*(3), 7290–7297.

Vyhlídal, T., Olgac, N. and Kučera, V. (2014). Delayed resonator with acceleration feedback – Complete stability analysis by spectral methods and vibration absorber design. *Journal of Sound and Vibration*, *333*(25), 6781–6795.

Vyhlidal, T. and Zitek, P. (2009). Mapping Based Algorithm for Large-Scale Computation of Quasi-Polynomial Zeros. *IEEE Transactions on Automatic Control*, *54*(1), 171–177.

Walton, K. and Marshall, J. (1987). Direct method for TDS stability analysis. *IEE Proceedings D Control Theory and Applications*, *134*(2), 101.

Wang, J., Zhong, H., Ma, Z., Xia, Q. and Kang, C. (2017). Review and prospect of integrated demand response in the multi-energy system. *Applied Energy*, *202*, 772–782.

APPENDICES

Coefficients of $P(s)$ and $Q(s)$ polynomials of (8) are :

$$p_7 = MRT_{ESS}\tau_{DR}\tau_{VI}T_gT_t;$$

$$p_6 = MRT_{ESS}(2\tau_{DR}T_gT_t + \tau_{DR}\tau_{VI}T_g + \tau_{DR}\tau_{VI}T_t + 2\tau_{VI}T_gT_t) + R\tau_{DR}\tau_{VI}T_gT_t(M + DT_{ESS} - K_{VI}\alpha_3 - K_{PD}T_{ESS}\alpha_3);$$

$$p_5 = MRT_{ESS}(2\tau_{DR}T_g + 2\tau_{DR}T_t + \tau_{DR}\tau_{VI} + 4T_gT_t + 2\tau_{VI}T_g + 2\tau_{VI}T_t) + MRT_{DR}(2T_gT_t + \tau_{VI}T_g + \tau_{VI}T_t) + 2RT_gT_t(M\tau_{VI} + DT_{ESS}\tau_{DR}) + DR\tau_{VI}(T_{ESS}\tau_{DR}T_g + T_{ESS}\tau_{DR}T_t + 2T_{ESS}T_gT_t + \tau_{DR}T_gT_t) + K_{VI}R\alpha_3(2\tau_{DR}T_gT_t - \tau_{DR}\tau_{VI}T_g - \tau_{DR}\tau_{VI}T_t - 2\tau_{VI}T_gT_t) - K_{PD}RT_{ESS}\alpha_2(2\tau_{DR}T_gT_t - \tau_{DR}\tau_{VI}T_g - \tau_{DR}\tau_{VI}T_t + 2\tau_{VI}T_gT_t) - R\tau_{DR}\tau_{VI}T_gT_t\alpha_2(K_{PD} - K_{ID}T_{ESS});$$

$$p_4 = T_{ESS}\tau_{DR}\tau_{VI} + MRT_{ESS}(2\tau_{DR} + 4T_g + 4T_t + 2\tau_{VI}) + MR\tau_{DR}(2T_g + 2T_t + \tau_{VI}) + MR(4T_gT_t + 2\tau_{VI}T_g + 2\tau_{VI}T_t) + K_{VI}R\tau_{DR}\alpha_3(2T_g + 2T_t - \tau_{VI}) + K_{VI}R\alpha_3(4T_gT_t - 2\tau_{VI}T_g - 2\tau_{VI}T_t) + DRT_{ESS}\tau_{DR}(2T_g + 2T_t + \tau_{VI}) + DRT_{ESS}(4T_gT_t + 2\tau_{VI}T_g + 2\tau_{VI}T_t) + DR(2\tau_{DR}T_gT_t + \tau_{DR}\tau_{VI}T_g + \tau_{DR}\tau_{VI}T_t + 2\tau_{VI}T_gT_t) - K_{PD}RT_{ESS}\tau_{DR}\alpha_2(2T_g - 2T_t - \tau_{VI}) + K_{PD}RT_{ESS}\alpha_2(4T_gT_t + 2\tau_{VI}T_g + 2\tau_{VI}T_t) - K_{PD}R\alpha_2(2\tau_{DR}T_gT_t - \tau_{DR}\tau_{VI}T_g - \tau_{DR}\tau_{VI}T_t + 2\tau_{VI}T_gT_t) - K_{ID}RT_{ESS}\tau_{DR}\alpha_2(2T_gT_t - \tau_{VI}T_g - \tau_{VI}T_t) + K_{ID}R\tau_{VI}T_gT_t\alpha_2(2T_{ESS} - \tau_{DR});$$

$$p_3 = 2T_{ESS}(\tau_{DR} + \tau_{VI}) + \tau_{DR}\tau_{VI} + MR(4T_{ESS} + 2\tau_{DR} + 4T_g + 4T_t + 2\tau_{VI}) + DRT_{ESS}(2\tau_{DR} + 4T_g + 4T_t + 2\tau_{VI}) + DR\tau_{DR}(2T_g + 2T_t + \tau_{VI}) + DR(4T_gT_t + 2\tau_{VI}T_g + 2\tau_{VI}T_t) + K_{VI}R\alpha_3(2\tau_{DR} + 4T_g + 4T_t - 2\tau_{VI}) - K_{PD}RT_{ESS}\alpha_2(2\tau_{DR} + 4T_g + 4T_t + 2\tau_{VI}) + (2T_g - 2T_t - \tau_{VI})(-K_{PD}R\tau_{DR}\alpha_2 - K_{ID}RT_{ESS}\tau_{DR}\alpha_2) + K_{PD}R\alpha_2(4T_gT_t + 2\tau_{VI}T_g + 2\tau_{VI}T_t) + K_{ID}RT_{ESS}\alpha_2(4T_gT_t + 2\tau_{VI}T_g + 2\tau_{VI}T_t) - K_{ID}R\alpha_2(2\tau_{DR}T_gT_t - \tau_{DR}\tau_{VI}T_g - \tau_{DR}\tau_{VI}T_t + 2\tau_{VI}T_gT_t);$$

$$p_2 = 4T_{ESS} + 2\tau_{DR} + 2\tau_{VI} + 4MR + DR(4T_{ESS} + 2\tau_{DR} + 4T_g + 4T_t + 2\tau_{VI}) + 4K_{VI}R\alpha_3 + K_{PD}R\alpha_2(4T_{ESS} - 2\tau_{DR} + 4T_g + 4T_t + 2\tau_{VI}) - K_{ID}RT_{ESS}\alpha_2(2\tau_{DR} + 4T_g + 4T_t + 2\tau_{VI}) - K_{ID}R\tau_{DR}\alpha_2(2T_g - 2T_t - \tau_{VI}) + K_{ID}R\alpha_2(4T_gT_t + 2T_g\tau_{VI} + 2T_t\tau_{VI});$$

$$p_1 = 4R(D + K_{PD}\alpha_2 + K_{ID}T_{ESS}\alpha_2) - K_{ID}R\alpha_2(2\tau_{DR} + 4T_g + 4T_t + 2\tau_{VI}) + 4;$$

$$p_0 = 4K_{ID}R\alpha_2;$$

$$q_4 = \beta K_PRT_{ESS}\tau_{DR}\tau_{VI}\alpha_1;$$

$$q_3 = \beta R\alpha_1(2K_PT_{ESS}\tau_{DR} + 2K_PT_{ESS}\tau_{VI} + K_P\tau_{DR}\tau_{VI} + K_IT_{ESS}\tau_{DR}\tau_{VI});$$

$$q_2 = \beta R\alpha_1(4K_PT_{ESS} + 2K_P\tau_{DR} + 2K_P\tau_{VI} + 2K_IT_{ESS}\tau_{DR} + 2K_IT_{ESS}\tau_{VI} + \beta K_I\tau_{DR}\tau_{VI});$$

$$q_1 = \beta R\alpha_1(4K_P + 4K_IT_{ESS} + 2K_I\tau_{DR} + 2K_I\tau_{VI});$$

$$q_0 = 4\beta K_IR\alpha_1;$$

Chapter 8

AIRFOIL GEOMETRY BASED HARMONIC RESPONSE ANALYSIS OF AIRCRAFT WINGS

Oguzhan DAS[1]

1 Dr. Oguzhan Das, Dokuz Eylül University, Bergama Vocational School, Department of Motor Vehicles and Transportation Technologies, https://orcid.org/0000-0001-7623-9278

Introduction

Aerospace structures are one of the most complex engineering products of which each part should be designed and tested meticulously. Among these structures, wings are essential to provide lift for an aircraft. Wings are designed considering many planforms (e.g., delta, rectangular, swept, and tapered) and airfoils. Besides, a wing may comprise various systems such as ailerons, flaps, and spoilers to modify the operating characteristics of the aircraft by affecting its geometrical properties. These structures may face excessive vibrations during a flight, which may result in failure or additional operational challenges. Therefore, it is essential to examine the vibrational behavior of aircraft wings. There are numerous studies that cover harmonic response analysis and various researches about aircraft wing structures. Some of these studies are briefly presented as follows. Kıral (2009) examined the dynamic response of laminated composite beams subjected to harmonic loading. For this purpose, the Finite Element Method is employed to obtain the structural stiffness and the Newmark method is used for examining the dynamic response of the structure. Abdulameer and Wasmi (2015) performed a vibrational control analysis of aircraft wings. They used piezoelectric sensors and actuators which are embedded in the aircraft wing. Zhang et al. (2018) conducted a harmonic response analysis for coupled plate structures. For this purpose, they employed the dynamic stiffness method considering both in-plane and out-of-plane vibrations. Eguea et al. (2018) employed the genetic algorithm to optimize the camber section of the winglet. They considered four flight phases called light cruise, mid-cruise, heavycruise, and climb. Hoseini and Hodges (2018) presented a flutter suppression control system for damaged HALE aircraft wings. Instead of modeling the entire structure, they modeled a small region, which is close to the boundary. Santos et al. (2018) examined the effect of design parameters on the mass of a variable-span morphing wing. For this purpose, they employed Finite Element Analysis and Optimization techniques. E et al. (2019) investigated the harmonic response of a large dish solar power generation system. They used computer fluid dynamics (CFD) and the Finite Element Method to develop the dish concentrator. Benaouali and Kachel (2019) developed a multidisciplinary design optimization for an aircraft wing. For this purpose, they employed commercial software called Siemens NX, ICEM CFD, ANSYS, MSC. Nastran, and MSC. Patran. Eken (2019) performed a free vibration analysis for composite aircraft wings. For this purpose, the aircraft wings with NACA airfoil sections are modeled as thin-walled beams. Tuken (2019) investigated the dynamic response of a three-story shear frame under harmonic loading. The responses are obtained for the end of the

foundation and the soil using ABAQUS software. Arachchige et al. (2020) investigated the bird strikes on the leading edge of the sandwich composite aircraft wings. For this purpose, Finite Element Analysis is conducted to analyze the effect of skin thickness, layups, and impact velocities. Evran et al. (2020) performed a numerical free vibration analysis for aircraft wings having different NACA airfoils and wing lengths. They considered Taguchi L9 orthogonal array with two control factors comprising three levels to obtain the frequencies. Agrawal et al. (2020) employed the Finite Element Method to evaluate the characteristics of the aircraft wings having different materials.

Airfoils are one of the key parameters in designing aircraft wings since their geometry affects the four aerodynamic forces (lift, weight, thrust, and drag) considerably. On the other hand, it is also essential to understand the effects of airfoil geometry on the vibrational behavior of an aircraft wing since it may face inertial forces that may lead the structure to fail. In this study, the effects of the airfoil geometry on the harmonic response of an aircraft wing have been measured. For this purpose, NACA 0015, NACA 2415, NACA 4415, and NACA 6412 airfoils have been considered. An aircraft wing of a mid-size business jet (Eguea et al., 2018) has been modeled via SolidWorks 2019. The Finite Element Harmonic Response Analyses have been conducted via ANSYS Workbench 18.2 – Mode Superposition Method considering 1kN sinusoidial load applied to the planform of the wing. For each airfoil geometry, variations of the first three natural frequencies, phase angle, maximum stress, maximum displacement values have been examined.

Methodology

The harmonic response analyses of the aircraft wing shown in Figure 1, have been performed by using the Finite Element Method considering the aircraft wing as a three-dimensional plate structure. The effects of the airfoil geometry have been examined considering four NACA airfoils as seen in Figure 2.

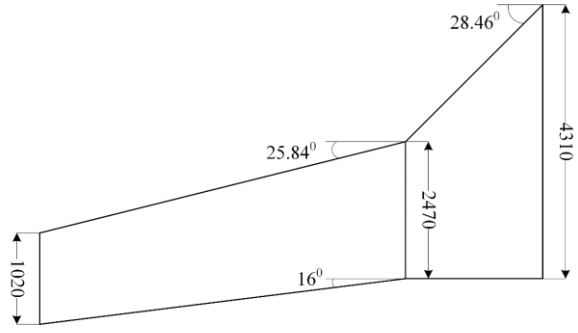

Figure 1. The aircraft wing dimensions of a mid-size business jet

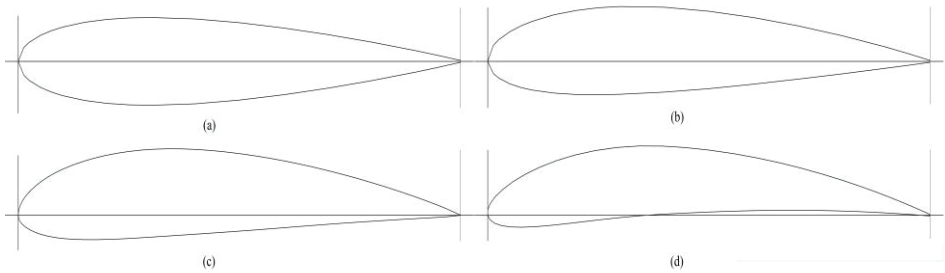

Figure 2. NACA four digits airfoils (a) 0015, (b) 2415, (c) 4415, and (d) 6412

The harmonic response of the structure has been obtained by considering the equation of motion, which is

$$\boldsymbol{M}\{\ddot{u}\} + \boldsymbol{C}\{\dot{u}\} + \boldsymbol{K}\{u\} = \{P\} \tag{1}$$

where **M**, **C**, and **K** represent the mass, damping, and stiffness matrices. The generalized displacement vector {u} comprises in-plane and out-of-plane displacement components (Petyt, 2010). The evaluation of the mass, damping, and stiffness matrices can be found in detail in various textbooks (Petyt, 2010).

The harmonic load {P}can be denoted considering the complex notation as

$$P = P_{max} e^{j\psi} e^{j\lambda t} \tag{2}$$

where λ is the excitation frequency and ψ is the phase angle of the applied harmonic load. Therefore, the response of the structure to the harmonic load is

$$q = q_{max} e^{j\tau} e^{j\lambda t} \tag{3}$$

where τ is the response's phase angle. The solution of the equation of motion considering the harmonic loading can be written as

$$(-\lambda^2 \boldsymbol{M} + j\lambda \boldsymbol{C} + \boldsymbol{K})\{q\} = \{F\} \tag{4}$$

As seen from Equations (2) and (3), the frequencies of both the harmonic load and the response of the system are the same while the phase angle values could be different. Such a difference may occur due to the damping characteristics of the structure (Ansys Training Manual, 2005).

Considering the solution of the equation of motion given in Equation (4), the airfoil geometry-based harmonic response analysis of the aircraft wings has been conducted via ANSYS Workbench 18.2. For this purpose, the computer-aided model of the aircraft wings with four different airfoil geometry has been build in SolidWorks 2019 as seen in Figure 3. Afterward, these models have been imported to ANSYS Workbench 18.2 as Parasolid models.

Figure 3. The solid model of the considered aircraft wing

To perform the harmonic response analysis, the aircraft wings have been meshed by considering a total of 26010 SOLID186 elements with 108 mm mesh size. Since the aircraft wings are cantilevered structures, fixed from one end boundary condition has been considered as seen in Figure 4(a). Before performing the harmonic response analysis, it is required to performed the free vibration analysis of the aircraft structure to understand the critical frequencies and to evaluate the frequency range in which the maximum response occurs. For this purpose, the first three natural frequencies are considered. Following the modal analysis, the harmonic response analysis has been performed by applying 1kN distributed harmonic load to the planform of the aircraft wing as seen in Figure 4(b).

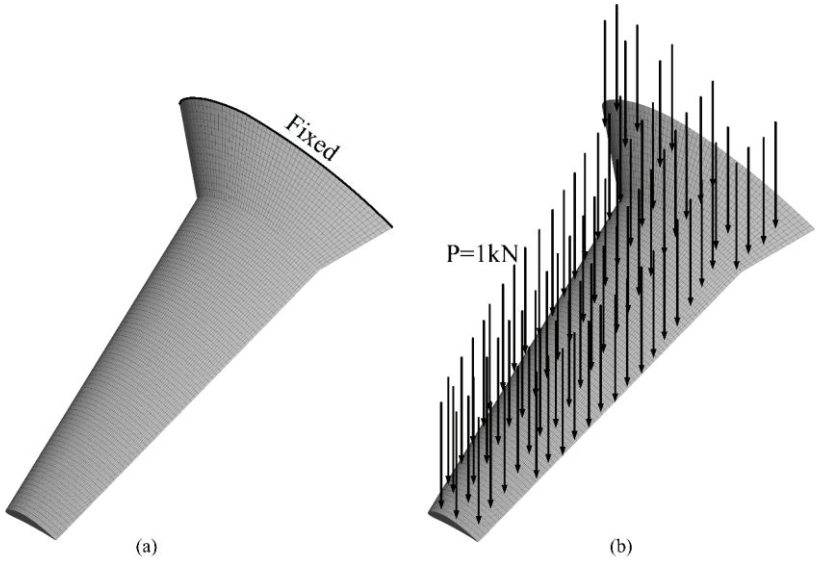

Figure 4. Meshed aircraft wing (a) under fixed boundary conditions (b) subjected to the distributed load

The frequency range has been determined by employing the rules of thumbs which implies the frequency range should be 1.5 times bigger than the frequency of interest. Therefore, the frequency range has been considered as 1.5 times bigger than the third natural frequency. The solution of the harmonic response analysis has been evaluated by employing the Model Superposition Method in which the damping matrix is not calculated. Instead, the damping ratio, which is the ratio between the actual and critical damping has been taken as ξ=0.02 (Kıral, 2009). Frequency responses have been evaluated by considering the maximum displacement and maximum stress parameters. Similarly, the phase angles of the responses have been obtained by considering the same parameters and the critical frequencies in which the maximum displacement and stress occurs. Likewise, the maximum stress and maximum displacement values have been evaluated by considering the critical phase angle and the critical excitation frequency.

Results

The harmonic response analyses results have been evaluated for each airfoil geometry by taking the first natural frequencies, frequency responses, phase angles, maximum stress, and maximum displacement values into account. As the material, Grade 2024-T4 aluminum has been considered. Table 1 gives the properties of the considered material.

Table 1. Material properties of Grade 2024-T4 aluminum

Property	Symbol	Value
Modulus of Elasticity	E	73.1 GPa
Shear Modulus	G	28 GPa
Density	ρ	2780 kg/m^3
Poisson Ratio	υ	0.33

Four-digit NACA airfoils have been specified by the maximum camber as a percentage of the chord (C), the position of the maximum camber multiplied by 10 as a percentage of the chord (P), and the maximum thickness as a percentage of the chord (YY). Therefore the four-digit has been constituted as CPYY. Considering NACA 2415 airfoil, the maximum camber is 2% of the chord length, the location of the maximum camber is 40% of the chord length, and the maximum thickness is 15% of the chord length. If the first two digits are equal to zero then the airfoil has no camber. The results have been interpreted by considering the variation of the parameters above and the geometric specifications of four different airfoils.

Table 2 presents the first three natural frequencies of the considered aircraft wing structure under fixed boundary conditions.

Table 2. Meshed aircraft wing (a) under fixed boundary conditions (b) subjected to the distributed load

Frequency (Hz)	NACA 0015	NACA 2415	NACA 4415	NACA 6412
1st	4.979	5.037	5.163	4.456
2nd	18.386	18.602	19.041	16.387
3rd	30.287	30.338	30.388	30.221

It is seen from Table 2 that the highest frequencies have been evaluated for NACA 2415, while the lowest ones have been obtained for NACA 6412. Therefore, it can be interpreted that the thickness of the airfoil has the most impact on the natural frequency values since the maximum thickness of NACA 6412 is the smallest one (12% of the chord length) when compared with other airfoils. On the other hand, although other airfoils' maximum thickness values as the percentage of the chord length are equal, the natural frequency values have slightly increased as the airfoil becomes highly cambered. However, it has been concluded that the maximum thickness has affected the natural frequencies more when compared with that of the maximum camber. Among the frequency modes, the second natural frequency (second bending mode) has been the most affected one by the airfoil geometry.

Figure 5 shows the frequency response of the aircraft wing having NACA 0015 airfoil under 1kN distributed harmonic load.

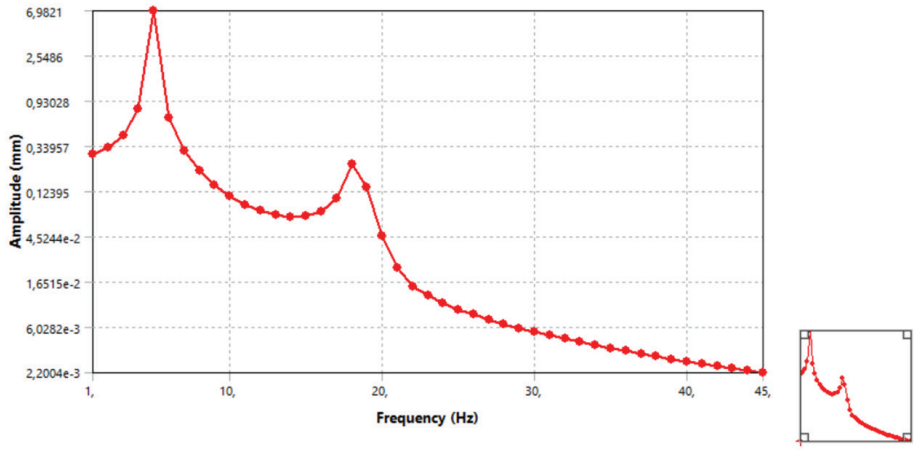

Figure 5. Frequency – displacement response of the aircraft wing having NACA 0015 airfoil

It is seen from Figure 5 that the maximum displacement occurred at approximately the first natural frequency. Although another displacement peak has been observed around the second natural frequency, the displacement value at this region is not higher than those of the first peak displacement value.

Figure 6 shows the phase shift of the aircraft wing with NACA 0015 airfoil geometry.

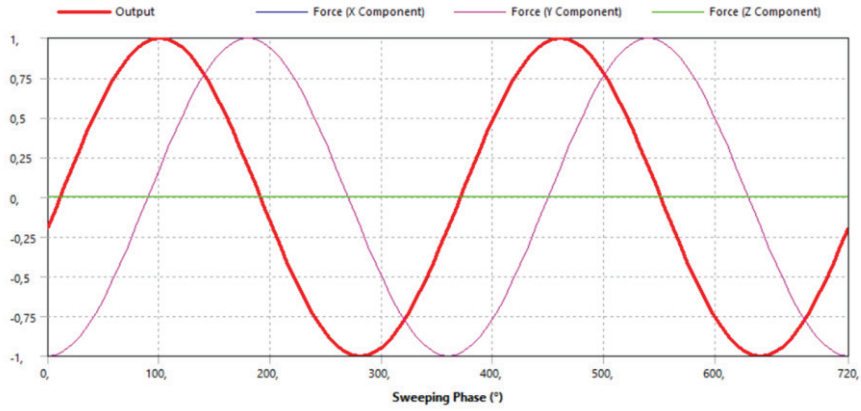

Figure 6. The phase angle of the aircraft wing with NACA 0015 airfoil

As seen from Figure 6, there is a phase shift between the harmonic force and the response of the aircraft wing structure with NACA 0015 airfoil due to the damping ratio of ξ=0.02. The highest response has been obtained for the sweeping phase angle of 100.8^0. Considering critical

frequency and sweeping phase angle, the maximum stress and displacement values have been evaluated.

Figure 7 shows the maximum stress and displacement of the aircraft wing having NACA 0015 airfoil considering the critical sweeping phase angle and frequency.

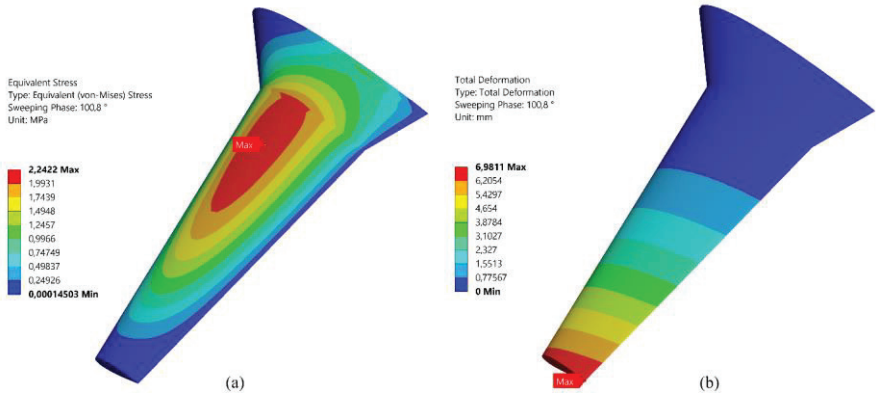

Figure 7. The maximum (a) stress and (b) displacement of the aircraft wing with NACA 0015 airfoil

It is seen from Figure 7 that the maximum stress is 2.2422 MPa and the maximum displacement is 6.9811 mm. The maximum stress occurs in the near-mid region of the structure, while the maximum displacement is located at the tip of the wing where the thickness of the structure is minimum.

Figure 8 shows the frequency response of the aircraft wing with NACA 2415 airfoil geometry.

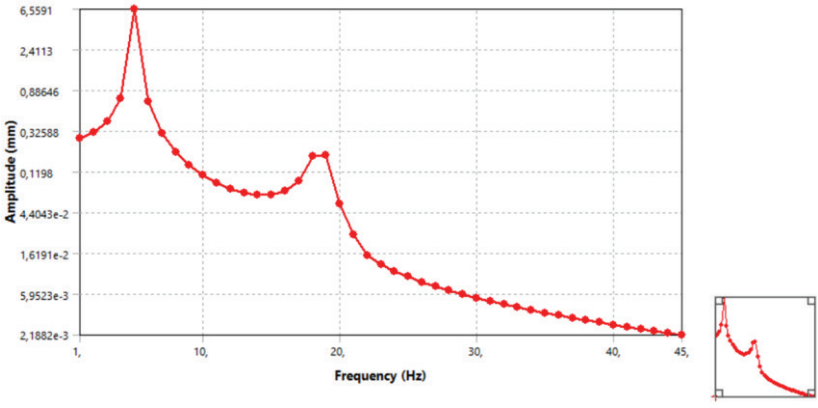

Figure 8. Frequency – displacement response of the aircraft wing having NACA 2415 airfoil

It is seen from Figure 8 that the maximum displacement occurred at nearly the first natural frequency. Similar to the frequency response of NACA 0015, another displacement peak has been observed around the second natural frequency. However, the displacement value at this region is not higher than those of the first peak displacement value.

Figure 9 shows the phase shift of the aircraft wing with NACA 2415 airfoil geometry.

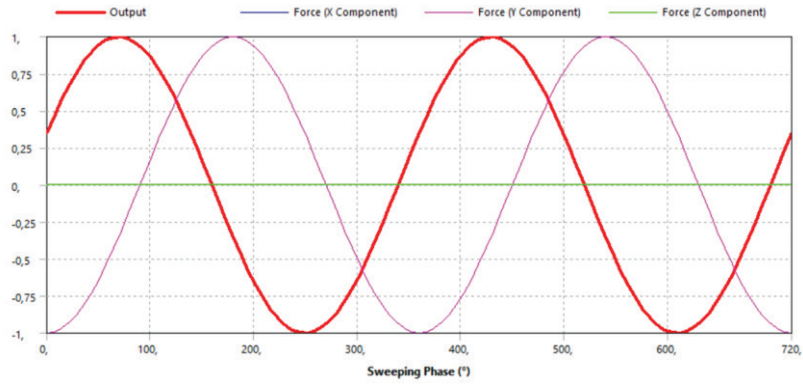

Figure 9. The phase angle of the aircraft wing having NACA 2415

As seen from Figure 9, a phase shift occurs between the applied harmonic load and the response. The highest response has been obtained for the sweeping phase angle of 72^0. The maximum stress and displacement values have been obtained for the first natural frequency and phase angle.

Figure 10 shows the maximum stress and displacement of the aircraft wing having NACA 2415 airfoil considering the critical sweeping phase angle and frequency.

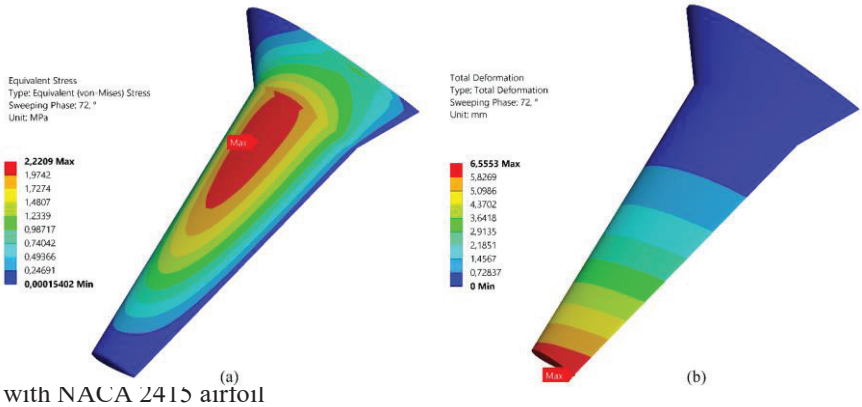

(a) (b)

with NACA 2415 airfoil

It is seen from Figure 10 that the maximum stress is 2.2209 MPa and the maximum displacement is 6.5553 mm. The maximum stress occurs in the near-mid region of the structure, while the maximum displacement is located at the tip of the wing where the thickness of the structure is minimum. Comparing with NACA 0015 airfoil, the maximum stress and displacement of the aircraft wing having NACA 2415 airfoil have slightly decreased. However, the locations where the maximum stress and displacement occur for both NACA 2415 and NACA 0015 airfoils have not changed.

Figure 11 shows the frequency response of the aircraft wing with NACA 4415 airfoil geometry.

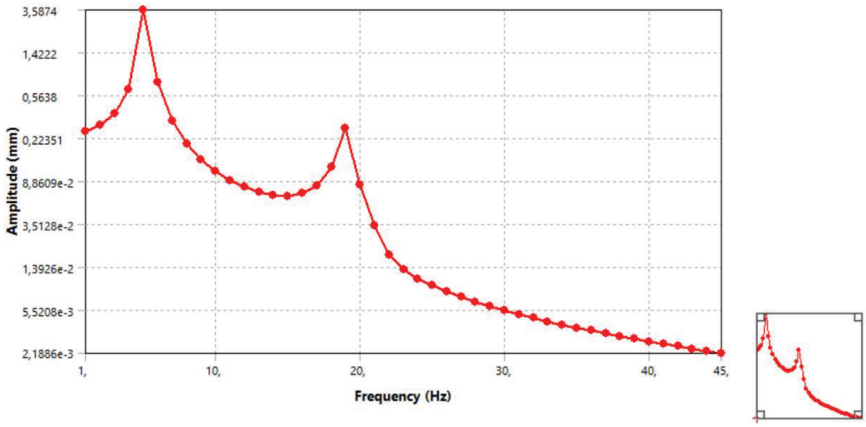

Figure 11. Frequency – displacement response of the aircraft wing with NACA 4415 airfoil

It is seen from Figure 11 that the maximum displacement occurred at nearly the first natural frequency. Comparing with NACA 0015 and NACA 2415, a second displacement peak has occurred nearby the second natural frequency. Similar to the displacement response characteristics of NACA 0015 and NACA 2415, the second displacement peak is smaller than the first one.

Figure 12 shows the phase shift of the aircraft wing with NACA 4415 airfoil geometry.

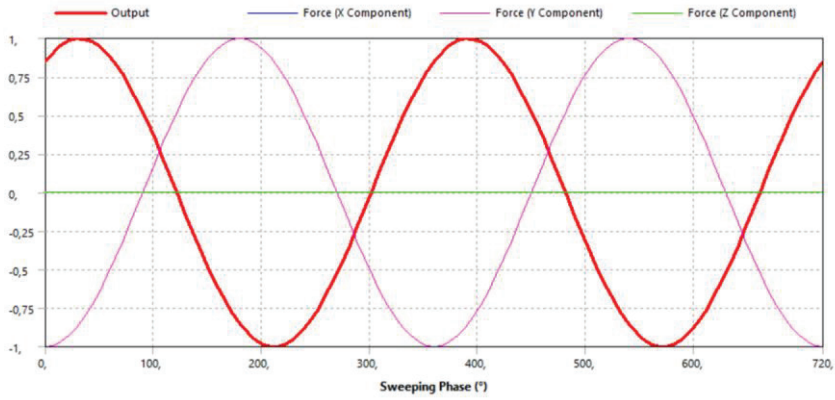

Figure 12. The phase angle of the aircraft wing having NACA 4415

It is seen from Figure 9 that a phase shift has occurred just like it has appeared for NACA 0015 and NACA 2415. The highest response has been evaluated for the sweeping phase angle of 28^0. The maximum stress and displacement values have been calculated for the critical frequency and this phase angle.

Figure 13 shows the maximum stress and displacement of the aircraft wing with NACA 4415 airfoil occurred for the critical sweeping phase angle and frequency.

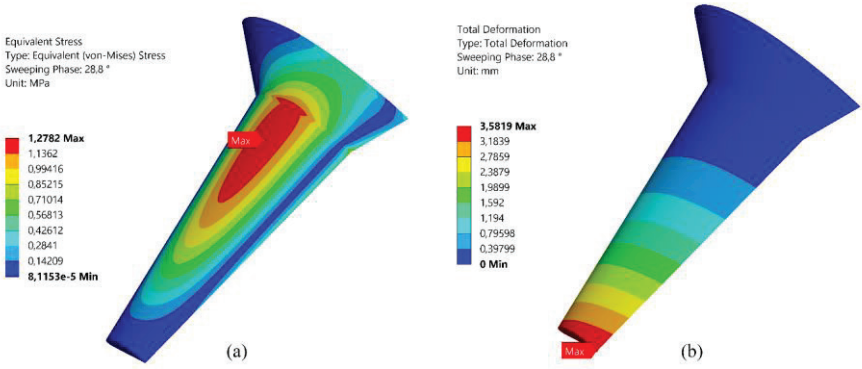

Figure 13. The maximum (a) stress and (b) displacement of the aircraft wing with NACA 4415 airfoil

It is seen from Figure 13 that the maximum stress is 1.2782 MPa and the maximum displacement is 3.5819 mm. Comparing with NACA 0015 and NACA 2415 airfoil, the maximum stress and displacement of the aircraft wing having NACA 4415 airfoil have decreased. Considering the only difference between NACA 2415 and NACA 4415 is the camber, changing the camber only by 2% significantly affects the maximum stress

and displacement values. The locations where the maximum stress and displacement occur have not changed.

Figure 14 shows the frequency response of the aircraft wing having NACA 6412 airfoil under 1kN harmonic loading.

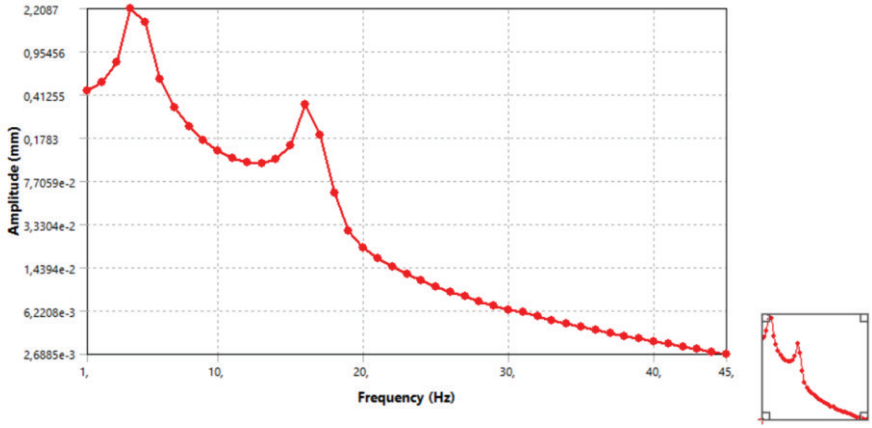

Figure 14. Frequency – displacement response of the aircraft wing with NACA 6412 airfoil

As seen from Figure 14, similar to all other airfoils, the maximum displacement occurred at nearly the first natural frequency. Likewise, another displacement peak has occurred nearby the second natural frequency.

Figure 15 shows the sweeping phase angle of the aircraft wing with NACA 6412 airfoil.

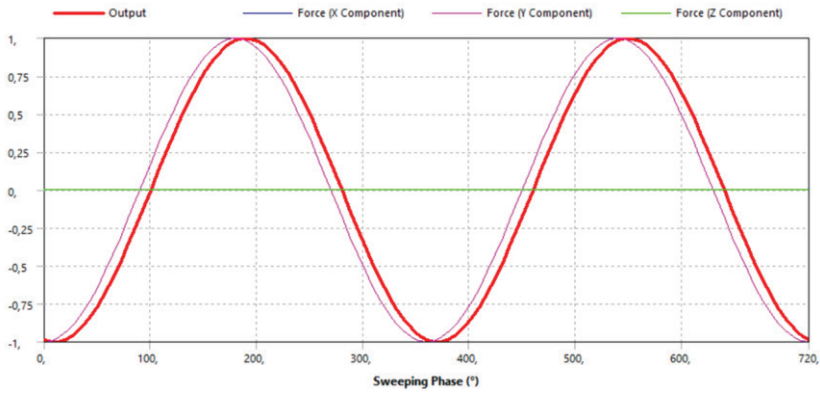

Figure 15. The phase angle of the aircraft wing having NACA 6412 airfoil

As seen from Figure 15 that a phase shift has occurred just like it has appeared for other NACA airfoils. The highest response has been evaluated for the sweeping phase angle of 7.2^0. The maximum stress and displacement values have been evaluated for the fundamental frequency and phase angle.

Figure 16 shows the maximum stress and displacement of the aircraft wing with NACA 6412 airfoil occurred for the first natural frequency and the critical sweeping phase angle.

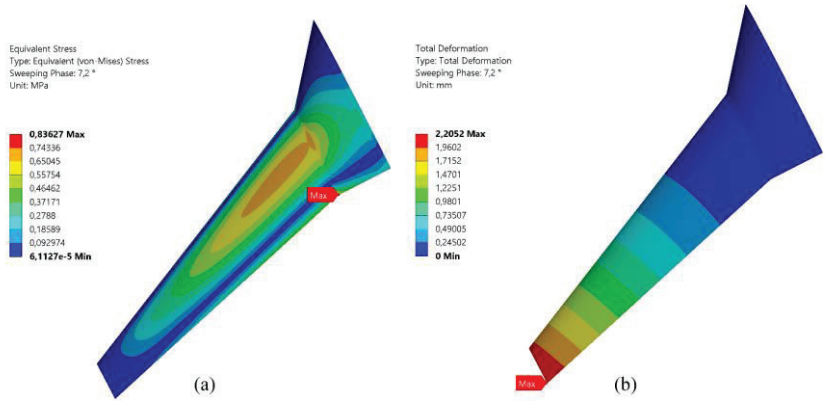

Figure 16. The maximum (a) stress and (b) displacement of the aircraft wing with NACA 6412 airfoil

It is seen from Figure 16 that the maximum stress is 0.83627 MPa, while the maximum displacement is 2.2052 mm. Comparing with other NACA airfoils, both maximum stress and displacement values have been decreased. Apart from other airfoils, the maximum stress occurred in the region where the taper angle becomes 16^0. On the other hand, the high-stress region of NACA 6412 is similar to those of other airfoil profiles. The maximum displacement occurs at the same region as those of other NACA airfoils.

Considering the frequency response of all airfoils, it is seen that no matter which airfoil is considered, the maximum displacement occurs at the frequency value close to the fundamental frequency. All wings have a secondary displacement peak that takes place around the second natural frequency. However, this secondary displacement peak is smaller than the first one regardless of the airfoil geometry. Therefore, it can be concluded that the response pattern is not affected by the maximum camber, maximum camber position, and maximum thickness values. These values only affect the magnitude of the wing's harmonic response.

According to the results, it can be concluded that the maximum camber affects the phase angle significantly. As the maximum camber increases the sweeping phase angle decreases. It can be also concluded that the

maximum thickness has an impact on the phase angle. However, to measure the level of such an impact, the same analyses can be performed by considering NACA airfoils, which have different maximum thickness values and the same maximum camber and maximum camber position. The effect of the maximum camber position can be measured by employing a similar procedure.

The maximum stress and displacement values are mostly depended on the maximum camber of the airfoil. As the maximum camber increases the maximum stress and displacement values decrease. Although the maximum thickness of the NACA 6412 is smaller than other airfoils, the increment in the maximum camber resulted in a decrement of both maximum stress and displacement values.

Conclusions

In this study, the effects of the airfoil geometry on the harmonic response of an aircraft wing structure have been investigated. For this purpose, four different airfoils namely, NACA 0015, NACA 2415, NACA 4415, and NACA 6412 have been taken into account. The harmonic response analysis results have been interpreted considering the frequency response, phase angle, maximum stress, and maximum displacement parameters. According to the results given above, the following conclusions have been drawn.

- The frequency response pattern is the same for all airfoils, while the magnitude of the peak response varies for each airfoil.
- The phase angle is mostly dependent on the maximum camber value since as the maximum camber value increases the phase angle decreases and the response becomes closer to be in phase with the force.
- The maximum stress value decreases as the maximum camber value increases. Besides, it can be concluded that the maximum camber value has a higher impact on the maximum stress than the maximum thickness value since the maximum stress of NACA 6412 is smaller than other thicker airfoils. The maximum stress location has been also affected by the maximum camber value as the location of the maximum stress occurs at the near-mid of the aircraft wing to the position for NACA 0015, NACA 2415, and NACA 4415 while it occurs at the edge of the wing where the taper angle becomes 16^0.
- The maximum displacement value decreases as the maximum camber value increases. The location of the maximum displacement occurs at the tip of the wing regardless of the airfoil geometry. The maximum displacement value of the wing having

NACA 6412 airfoil is the smallest displacement when compared with that of other wings having different airfoils. This indicates that the maximum camber has a higher impact on the maximum displacement value than that of the maximum thickness value.

References

Abdulameer, H. A., & Wasmi, H. R. (2015). Vibration Control Analysis of Aircraft Wing by Using Smart Material. *Innovative Systems Design and Engineering, 6*(8).

ANSYS ®. (2005). Training Manual. Available from: http://www-eng.lbl.gov/~als/FEA/ANSYS_V9_INFO/Workbench_Simulation_9.0_Intro_3rd_Edition/ppt/AWS90_Ch10_Harmonic.ppt

Agrawal, P., Dhatrak, P., & Choudhary, P. (2021). Comparative study on vibration characteristics of aircraft wings using finite element method. *Materials Today: Proceedings, 46*, 176-183. doi:10.1016/j.matpr.2020.07.229

Arachchige, B., Ghasemnejad, H., & Yasaee, M. (2020). Effect of bird-strike on sandwich composite aircraft wing leading edge. *Advances in Engineering Software, 148*, 102839. doi:10.1016/j.advengsoft.2020.102839

Benaouali, A., & Kachel, S. (2019). Multidisciplinary design optimization of aircraft wing using commercial software integration. *Aerospace Science and Technology, 92*, 766-776. doi:10.1016/j.ast.2019.06.040

E, J., Liu, G., Liu, T., Zhang, Z., Zuo, H., Hu, W., & Wei, K. (2019). Harmonic response analysis of a large dish solar thermal power generation system with wind-induced vibration. *Solar Energy, 181*, 116-129. doi:10.1016/j.solener.2019.01.089

Eguea, J. P., Catalano, F. M., Abdalla, A. M., De Santana, L. D., Venner, C. H., & Fontes Silva, A. L. (2018). Study on a camber adaptive winglet. *2018 Applied Aerodynamics Conference*. doi:10.2514/6.2018-3960

Eken, S. (2019). Free vibration analysis of composite aircraft WINGS modeled as thin-walled beams with NACA airfoil sections. *Thin-Walled Structures, 139*, 362-371. doi:10.1016/j.tws.2019.01.042

Evran, S., Kurt, M., & Kurt, A. (2020). Evaluation of cross-section and wing length in Free vibration analysis of aircraft wings. *Journal of Aviation*. doi:10.30518/jav.778273

Hoseini, H., & Hodges, D. H. (2018). Flutter suppression for finite element modeling of damaged hale aircraft wings. *2018 AIAA/ASCE/AHS/ASC Structures, Structural Dynamics, and Materials Conference*. doi:10.2514/6.2018-1205

Kıral, Z. (2009). Numerical investigation of the dynamic response of symmetric Laminated Composite beams to Harmonıc Excıtatıons. *Advanced Composites Letters, 18*(5), 096369350901800. doi:10.1177/096369350901800503

Petyt, M. (2015). *Introduction to finite element vibration analysis*. New York: Cambridge University Press.

Ramesha, C. M., Abhijith, K. G., Singh, A., Raj, A., & Naik, C. S. (2015). Modal Analysis and Harmonic Response Analysis of a Crankshaft. *International Journal of Emerging Technology and Advanced Engineering, 5*(6).

Santos, P. D., Sousa, D. B., Gamboa, P. V., & Zhao, Y. (2018). Effect of design parameters on the mass of a variable-span morphing wing based on finite element structural analysis and optimization. *Aerospace Science and Technology*, 80, 587-603. doi:10.1016/j.ast.2018.07.033

Tüken, A. (2019). Harmonik yüklemeye Maruz Kalan 3-Katlı Kayma Çerçevesının Dinamik Tepki Analizi: Analitik Bır Yaklaşım. *Uludağ University Journal of The Faculty of Engineering, 24*(2), 725-734. doi:10.17482/uumfd.449686

Zhang, C., Jin, G., Ye, T., & Zhang, Y. (2018). Harmonic response analysis of coupled plate structures using the dynamic stiffness method. *Thin-Walled Structures*, *127*, 402-415. doi:10.1016/j.tws.2018.02.014

Chapter 9

HEXACOPTER UNMANNED AERIAL VEHICLE DYNAMIC MODELLING AND COMPOSITE ANTI-DISTURBANCE CONTROL

Hasan BAŞAK
Emre KEMER

INTRODUCTION

Unmanned Aerial Vehicles (UAVs) have been significantly developing for wide applications such as cargo transportation, photography, agriculture, search and rescue, surveillance in the complex environment. As a result, dynamic modelling and controlling of UAVs have become a challenging problem to researchers [1], [2]. Among the UAVs, multirotors such as quadrotor and hexacopter have become popular platforms in the literature. In flight operation, environmental conditions such as gust or external disturbances will affect stability of UAV systems [3]. In order to achieve control objectives considering weather conditions, some control algorithms are proposed in the literature. Different control algorithms can be proposed with disturbance observers for different control objectives. Authors in [4] designed a nonlinear observer in order to estimate disturbances. Angular tracking of a quadrotor is achieved using the information of the disturbance estimator. Also, the disturbance is estimated by an observer in [5] to improve the disturbance rejection of UAV systems. A controller and a disturbance observer are developed in [6] to reduce the effect of a partially known disturbance and to reject the wind disturbance. A composite disturbance rejection algorithm is developed by authors in [7] which consists of a disturbance estimator and a sliding mode controller. Quadrotor tracks the given trajectories in the presence of different type of disturbances. Slow disturbance variations are estimated by the observer and the influence of fast time-varying disturbance is rejected by the sliding mode control. For hexacopter UAVs, a robust and adaptive backstepping controller is proposed in [8] to enhance the robustness capacity of the hexacopter UAV in the presence of the disturbances. The information of parameter uncertainties and external perturbations are obtained using an extended state observer. In [9], anti-disturbance controller is designed for a hexacopter UAV. A single external disturbance is estimated by an equivalent disturbance estimator with a low pass filter. The anti-disturbance controller enables the hexacopter UAV tracks the given attitude trajectory. In [10], a neural network based PID controller is designed for the hexacopter under the model uncertainties. Also, a model predictive controller in [11] and PID control in [12] are designed for the hexacopter UAV that tracks the desired trajectory. On the other hand, motor faults in hexacopter UAV are taken into consideration in [13] where the observer estimates states of the UAV for detection and isolation of motor faults.

Especially, developing controllers for hexacopter UAVs under the time-varying multiple disturbances is a challenging task. A classical control method may be developed to cope with the effects of

disturbances. The fact is that a feedback closed-loop controller is preferred for the disturbance rejection. Nevertheless, control systems requirements such as disturbance attenuation, robustness, stability, performance and tracking often conflict each other. Hence, the traditional feedback strategy has many design constraints. For example, well known ones are disturbance rejection versus tracking and robustness versus performance [14]. In this study, a robust controller and a disturbance observer are integrated to obtain a composite anti-disturbance controller which addresses aforementioned constraints. The proposed composite controller enables the hexacopter UAV performs its duties in the presence of the external multiple disturbances.

DYNAMIC MODEL OF HEXACOPTER UAV

This section describes a hexacopter UAV dynamics. Let us assume that hexacopter body and propellers are rigid; the six motors are symmetrically located at the end of arms; the motors dynamics are fast so they are neglectable. Motors generate the required forces $(F_1, F_2, F_3, F_4, F_5, F_6)$ as illustrated in Figure 1. Motors 1, 3 and 5 make rotations counterclockwise while motors 2, 4 and 6 make rotations clockwise. The vehicle achieves the altitude position by increasing/deceasing the six motors with the equal quantity. Rising the speed of motors 4 and 5 and reducing speed of motors 1 and 2 at the same time results in forward motion. Rising the speed of motors (1, 5, and 6) and reducing the speed of motors (2, 3, and 4) achieves the leftward motion. Similarly, rightward and backward movements are obtained. Yaw orientation is obtained by regulating the speed of motors (1, 3, and 5) and motors (2, 4, and 6). To give the mathematical model of the hexacopter, the inertial frame $\{I\}$ $(X_I\ Y_I\ Z_I)$ and body fixed frame $\{B\}$ $(X_B Y_B Z_B)$ are defined as illustrated in Figure 1. The position vector of the hexacopter mass center expressed in the inertial frame, $\xi = (x_I\ y_I\ z_I)^T$. Angles of the body fixed frame referring the inertial frame is expressed as $\eta = (\Phi\ \theta\ \psi)^T$ where these angles are restricted as roll angle (Φ) by$|\Phi| < 90^{\circ}$; pitch angles (θ) by $|\theta| < 90^{\circ}$; yaw angle (ψ) by $|\psi| < 180^{\circ}$. Body-fixed angular velocity vector about the body $(X_B Y_B Z_B)$ axes, respectively is $\omega = (p\ q\ r)^T$

Transforming body-fixed frame coordinates to inertial frame coordinates is obtained with the following R_f rotation matrix:

$$R_f = \begin{vmatrix} C\theta C\psi & S\Phi S\theta C\psi - C\Phi S\psi & C\Phi S\theta C\psi + S\Phi S\psi \\ C\theta S\psi & S\Phi S\theta S\psi + C\Phi C\psi & c\Phi s\theta s\psi - S\Phi C\psi \\ -S\theta & S\Phi C\theta & C\Phi C\theta \end{vmatrix} \quad (1)$$

where $C(.) = cos(.)$ and $S(.) = sin(.)$. The rotational kinematics is obtained as $\dot{\eta} = W_{\eta}^{-1}\,\omega$. The inverse rotation matrix is here

$$W_{\eta}^{-1}=\begin{vmatrix}1 & \sin\Phi\tan\theta & \cos\Phi\tan\theta\\ 0 & \cos\Phi & -\sin\Phi\\ 0 & \sec\theta\sin\Phi & \cos\Phi\sec\theta\end{vmatrix} \tag{2}$$

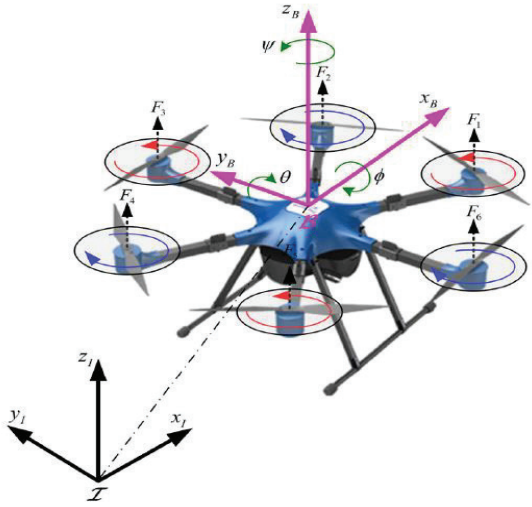

Figure 1. Diagram of hexacopter UAV model [8].

Using the Newton-Euler approach, the rotational motion of the quadrotor referring to the body frame and the translational dynamics in the presence of external forces applied to the mass center referring inertial frame is given as [8],[9],[12]:

$$\dot{\xi} = \mathrm{v} \tag{3}$$

$$\mathrm{m}\dot{\mathrm{v}} = -\mathrm{mge_z} + \mathrm{R_f T_f} \tag{4}$$

$$\dot{\eta} = \mathrm{W_{\eta}^{-1}}\omega \tag{5}$$

$$\mathrm{J}\dot{\omega} = -\omega \times \mathrm{J}\omega + \tau_{\mathrm{f}} \tag{6}$$

where v is linear velocity of the hexacopter expressed in the inertial frame, $e_z = (0,0,1)^T$ represents a vector along the z-axis, the inertia matrix is diagonal as J =diag(I_{xx}, I_{yy}, I_{zz}) due to symmetrical design.

$T_f = (0,0,u_1)^T$ and $\tau_f = (u_2,u_3,u_4)^T$ are force and torques in the {B} - frame and here

$$u_1 = F_1 + F_2 + F_3 + F_4 + F_5 + F_6 \tag{7}$$

$$u_2 = -\frac{1}{2}F_1 l + \frac{1}{2}F_2 l + F_3 l + \frac{1}{2}F_4 l - \frac{1}{2}F_5 l - F_6 l \tag{8}$$

$$u_3 = -\frac{\sqrt{3}}{2}F_1 l - \frac{\sqrt{3}}{2}F_2 l + \frac{\sqrt{3}}{2}F_4 l + \frac{\sqrt{3}}{2}F_5 l \tag{9}$$

$$u_4 = \frac{d}{b}(-F_1 + F_2 - F_3 + F_4 - F_5 + F_6) \tag{10}$$

where $i.$ motor produces the thrust force, $F_i = b\Omega_i^2$; b is the thrust coefficient of the propeller; d is the drug coefficient of the propeller; Ω_i denotes rotational speed of $i.$ motor. The nonlinear equation set of the hexacopter UAV model is

$$\ddot{x}_I = (\cos\phi\sin\theta\cos\psi + \sin\phi\sin\psi)\frac{1}{m}u_1 \tag{11}$$

$$\ddot{y}_I = (\cos\phi\sin\theta\sin\psi - \sin\phi\cos\psi)\ \frac{1}{m}u_1 \tag{12}$$

$$\ddot{z}_I = -g + \cos\phi\cos\theta\frac{1}{m}u_1 \tag{13}$$

$$\dot{\phi} = p + q\sin\phi\tan\theta + r\cos\phi\tan\theta \tag{14}$$

$$\dot{\theta} = q\cos\phi - r\sin\phi \tag{15}$$

$$\dot{\psi} = q\frac{\sin\phi}{\cos\theta} + r\frac{\cos\phi}{\cos\theta} \tag{16}$$

$$\dot{p} = qr\left(\frac{I_{yy} - I_{zz}}{I_{xx}}\right) + \frac{1}{I_{xx}}u_2 \tag{17}$$

$$\dot{q} = pr\left(\frac{I_{zz} - I_{xx}}{I_{yy}}\right) + \frac{1}{I_{yy}}u_3 \tag{18}$$

$$\dot{r} = qp\left(\frac{I_{xx} - I_{yy}}{I_{zz}}\right) + \frac{1}{I_{zz}}u_4 \tag{19}$$

Non-linear dynamics of the vehicle is given in form of state-space representation as:

$$\begin{aligned} \dot{x}(t) &= f(x(t), u(t)) \\ y(t) &= h(x(t)) \end{aligned} \tag{20}$$

in which $x(t)$ and $u(t)$ are the state and input variables respectively.

$$x = [x_1\ x_2\ x_3\ \dots\ x_{12}]^T = [\ x_I\ y_I\ z_I\ \dot{x}_I\ \dot{y}_I\ \dot{z}_I\ \phi\ \theta\ \psi\ p\ q\ r\ ]^T \tag{21}$$

$$u = [u_1\ u_2\ u_3\ u_4]^T \tag{22}$$

To design attitude control system, the rotational system dynamics (Eqs.14-19) are linearized at hover for which the input $u_{eq} = [u_2\ u_3\ u_4] = [0\ 0\ 0]$. The dynamics of the linearized model about $x_{eq} = [\ \phi\ \theta\ \psi\ p\ q\ r] = [\ 0\ 0\ 0\ 0\ 0\ 0]$ and u_{eq} is

$$\begin{aligned} \dot{x} &= Ax + Bu \\ y &= Cx = [\phi\ \theta\ \psi] \end{aligned} \tag{23}$$

where matrices A and B are computed as follows:

$$A = \frac{\partial f}{\partial x} = \begin{bmatrix} \frac{\partial f_1}{\partial x_1}|_{x_e,u_e} & \cdots & \frac{\partial f_1}{\partial x_n}|_{x_e,u_e} \\ \vdots & \ddots & \vdots \\ \frac{\partial f_n}{\partial x_1}|_{x_e,u_e} & \cdots & \frac{\partial f_n}{\partial x_n}|_{x_e,u_e} \end{bmatrix},$$

$$B = \frac{\partial f}{\partial u} = \begin{bmatrix} \frac{\partial f_1}{\partial u_1}|_{x_e,u_e} & \cdots & \frac{\partial f_1}{\partial u_m}|_{x_e,u_e} \\ \vdots & \ddots & \vdots \\ \frac{\partial f_n}{\partial u_1}|_{x_e,u_e} & \cdots & \frac{\partial f_n}{\partial u_m}|_{x_e,u_e} \end{bmatrix} \tag{24}$$

Augmenting model of (23) with integrators so that we can get zero steady state errors of attitude tracking that results in the following model:

$$\begin{vmatrix} \dot{x}(t) \\ \dot{e}(t)_y \end{vmatrix} = \begin{vmatrix} A & 0 \\ -C & 0 \end{vmatrix} \begin{vmatrix} x(t) \\ e_{y(t)} \end{vmatrix} + \begin{vmatrix} B \\ 0 \end{vmatrix} u(t) \tag{25}$$

where $x = [\ \phi\ \ \theta\ \psi\ \ p\ q\ r]^T$ is the state vector, $e_y = [e_\phi\ e_\theta\ e_\psi]^T$ is the error vector and $u = [\ u_2\ \ u_3\ \ u_4]^T$ is the input vector. Matrices $A_{aug} = \begin{vmatrix} A & 0 \\ -C & 0 \end{vmatrix}$ and $B_{aug} = \begin{vmatrix} B \\ 0 \end{vmatrix}$ are computed by using physical parameters of the hexacopter UAV (Table 1).

Table 1. The hexacopter UAV parameters [3]

Parameters	Descriptions	Values	Units
m	Mass	1.535	kg
g	Gravity acceleration	9.8	$\mathrm{m/s^2}$
l	Length of arms	0.275	m
I_{xx}	Moment of inertia around x-axis	0.0411	$\mathrm{kg.m^2}$
I_{yy}	Moment of inertia around y-axis	0,04178	$\mathrm{kg.m^2}$
I_{zz}	Moment of inertia around z-axis	0.0599	$\mathrm{kg.m^2}$
d/b	Ratio between thrust and drag coefficients	0.1	-

COMPOSITE ANTI –DISTURBANCE CONTROL

Preliminary

This section gives results from robust control theory to be used in the following section. Consider the following LTI system:

$$\begin{aligned} \dot{\mathrm{x}}(\mathrm{t}) &= \mathrm{A_{aug}x(t)} + \mathrm{Ew(t)} \\ \mathrm{z(t)} &= \mathrm{C_z x(t)} \end{aligned} \tag{26}$$

in which the all-system matrices (A_{aug}, C_z) are compatible dimensions. $x(t) \in \mathbb{R}^n$ represents the state vector of the system, $w(t) \in L_2[0, +\infty)$ represents the external disturbance vector, $z(t)$ is the controlled output vector. For the given scalar $\gamma > 0$, the H_∞ problem is stated as

$$\mathrm{J(w)} \coloneqq \sup{}_{\mathrm{w}\in\mathrm{L_2}} \int_0^\infty (\mathrm{z^T z} - \gamma^2 \mathrm{w^T w})\mathrm{dt} \tag{27}$$

Lemma 1: (Bounded Real Lemma [1]) If a symmetric positive definite matrix $P \in \mathbb{R}^{nxn} > 0$ satifies the following inequality:

$$\begin{vmatrix} {A_{aug}}^T P + P A_{aug} & PE & C_z \\ E^T P & -\gamma^2 I & 0 \\ {C_z}^T & 0 & -I \end{vmatrix} < 0 \tag{28}$$

then $J(w) < 0$ for all nonzero external disturbance, $w(t) \in L_2[0, +\infty)$.

Composite Anti-disturbance Control Design

Let a LTI system be given in state space realization under the external disturbances by

$$\dot{x}(t) = A_{aug}x(t) + B_{aug}\big(u(t) + d_1(t)\big) + Ed_2(t) \tag{29}$$

Assuming that $\mathrm{d_2(t)} \in \mathbb{R}^{\mathrm{l}}$ is an external disturbance that belongs to $\mathrm{L_2}\,[0, +\infty)$. The disturbance $\mathrm{d_1}\,(\mathrm{t}) \in \mathbb{R}^{\mathrm{m}}$ is given by [16]:

$$\begin{aligned} \dot{\omega}\,(\mathrm{t}) &= \mathrm{W}\omega(\mathrm{t}) + \mathrm{Hd_3(t)} \\ \mathrm{d_1}\,(\mathrm{t}) &= \mathrm{V}\omega(\mathrm{t}) \end{aligned} \tag{30}$$

where $\omega(\mathrm{t})$ is the state of the exogenous system and $\mathrm{d_3(t)} \in \mathbb{R}^{\mathrm{r}}$, $(\mathrm{d_3(t)} \in \mathrm{L_2}\,[0, +\infty))$ is the additional disturbance due to uncertainties in the modelled disturbance. The harmonic perturbation is denoted by $d_1\,(t)$ which is common in practice. $W(t) = \begin{bmatrix} 0 & c \\ -c & 0 \end{bmatrix}, c > 0$ is selected and c represents the frequency of $d_1\,(t)$. Note that Eq. (30) denotes harmonic perturbation with unknown phase and amplitude.

Here the disturbance observer is structured as:

$$\dot{\mathrm{v}}(\mathrm{t}) = \big(\mathrm{W} + \mathrm{LB_{aug}V}\big)(\mathrm{v(t)} - \mathrm{Lx(t)}) + \mathrm{L}(\mathrm{A_{aug}x(t)} + \mathrm{B_{aug}u(t)})$$

$$\dot{\hat{\omega}}(\mathrm{t}) = \mathrm{v(t)} - \mathrm{Lx(t)} \tag{31}$$

$$\hat{\mathrm{d}}_1\,(\mathrm{t}) = \mathrm{V}\,\hat{\omega}(\mathrm{t})$$

where $\mathrm{L} \in \mathbb{R}^{\mathrm{r\times n}}$ is the gain of the disturbance observer. We assume that all states of system are measurable. In anti-disturbance control scheme, the controller is structured as following form:

$$\mathrm{u(t)} = \mathrm{Kx(t)} - \hat{\mathrm{d}}_1\,(\mathrm{t}) \tag{32}$$

In which $\hat{\mathrm{d}}_1\,(\mathrm{t})$ estimates the external disturbance $\mathrm{d_1(t)}$.

The estimated disturbance error is

$$e_{\omega}(t) = \omega(t) - \hat{\omega}(t) \tag{33}$$

Eqs. (30) and (31) are (33) combined as follows:

$$\dot{e_{\omega}}(t) = (W + LB_{aug}\,V)\,e_{\omega}(t) + \mathrm{L}Ed_2(t) + \mathrm{H}d_3(t) \tag{34}$$

and resulting controlled output is

$$\mathrm{z(t)} = \mathrm{C_1x(t)} + \mathrm{C_2e_{\omega}(t)} \tag{35}$$

Eqs. (34) and (35) are augmented with (29) that leads to

$$\begin{aligned}\dot{\bar{x}}(t) &= \tilde{A}\bar{x}(t) + \tilde{B}_w d(t)\\ z(t) &= \tilde{C}\bar{x}(t)\end{aligned} \tag{36}$$

where $\bar{x}(t) = [x'(t)\ \ e'(t)]^T$, $d(t) = [d'_2(t)\ \ d'_3(t)]^T$,

$\tilde{A} = \begin{bmatrix} A_{aug} + B_{aug}K & B_{aug}V \\ 0 & W + LB_{aug}V \end{bmatrix}$, $\tilde{E} = \begin{vmatrix} E & 0 \\ LE & H \end{vmatrix}$,

and $\tilde{C} = [C_1\ \ C_2]$.

Theorem 1: For the system (29) with the disturbance (30), there exist a disturbance observer in (31) and the controller law in (32) so that the augmented system in (36) is robust stable and assures the H_∞ performance $\int_0^\infty (z^T z - \gamma^2 w^T w)dt < 0$, if and only if there exits constant $\gamma > 0$, positive definite matrices X and P_2, matrix Y_2 satisfying the inequalities

$$\begin{vmatrix} \Pi_{11} & B_{aug}V & E & 0 & XC_1{}^T \\ V^T B^T & \Pi_{22} & Y_2 E & P_2 H & C_2^T \\ E^T & E^T Y_2{}^T & -\gamma^2 I & 0 & 0 \\ 0 & H^T P_2{}^T & 0 & -\gamma^2 I & 0 \\ C_1 X^T & C_2 & 0 & 0 & -I \end{vmatrix} < 0 \tag{37}$$

where $\Pi_{11} = XA_{aug}{}^T + A_{aug}X^T + Y_1{}^T B_{aug}{}^T + B_{aug}Y_1$ and $\Pi_{22} = P_2 W + W^T P_2{}^T + Y_2 B_{aug}V + V^T B_{aug}{}^T Y_2{}^T$ also, the gains of the disturbance observer and the controller in the form of (31) and (32) are given by $K = Y_1 X^{-1}$ and $L = P_2{}^{-1} Y_2$ respectively.

Proof: Assume that the inequality in Eq. (37) hold. First using the matrices of augmented system in (36) Lemma 1 is rewritten as

$$\begin{vmatrix} \tilde{\mathrm{A}}^{\mathrm{T}}\mathrm{P} + \mathrm{P}\tilde{\mathrm{A}} & \mathrm{P}\tilde{\mathrm{E}} & \tilde{\mathrm{C}} \\ \tilde{\mathrm{E}}^{\mathrm{T}}\mathrm{P} & -\gamma^2\mathrm{I} & 0 \\ \tilde{\mathrm{C}}^{\mathrm{T}} & 0 & -\mathrm{I} \end{vmatrix} < 0 \tag{38}$$

where

$$P = \begin{vmatrix} P_1 & 0 \\ 0 & P_2 \end{vmatrix} \tag{39}$$

$$P\tilde{A} = \begin{vmatrix} P_1 A + P_1 B_{aug} K & P_1 B_{aug} V \\ 0 & P_2 W + P_2 L B_{aug} V \end{vmatrix}, \tag{40}$$

$$\tilde{E}^T P = \begin{vmatrix} E^T P_1 & E^T L P_2 \\ 0 & H^T P_2 \end{vmatrix} \tag{41}$$

$$\tilde{\mathrm{C}} = [\mathrm{C}_1 \ \mathrm{C}_2] \tag{42}$$

Performing a congruence transformation to the inequality in Eq. (38) by diag $(P_1{}^{-1}, I, I, I, I)$ and denoting $\mathrm{X} = P_1{}^{-1}$, we obtain the following result

$$\begin{vmatrix} \Pi_{11} & B_{aug}V & E & 0 & XC_1{}^T \\ V^TB^T & \Pi_{22} & Y_2E & P_2H & C_2^T \\ E^T & E^TY_2{}^T & -\gamma^2 I & 0 & 0 \\ 0 & H^TP_2{}^T & 0 & -\gamma^2 I & 0 \\ C_1X^T & C_2 & 0 & 0 & -I \end{vmatrix} < 0 \tag{43}$$

with $Y_2 = P_2L$ and $Y_1 = KX$. This gives the linear matrix inequality condition in Eq. (37).

SIMULATION RESULTS AND DISCUSSIONS

In this section, we shall give the simulation results to demonstrate the efficiency of the developed composite anti-disturbance control algorithm. This scheme is implemented in MATLAB/Simulink and applied to hexacopter UAV that tracks the desired attitude in the presence of multiple disturbances. Matrices of the disturbance $d_1(t)$ are selected as follows:

$$W = \begin{bmatrix} 0 & 0.5 \\ -0.5 & 0 \end{bmatrix}, H = \begin{bmatrix} 0.2 \\ 0.2 \end{bmatrix} \text{ and } V = \begin{bmatrix} 0.5 & 0.1 \\ 2 & 0 \\ 0 & 1 \end{bmatrix}. \tag{44}$$

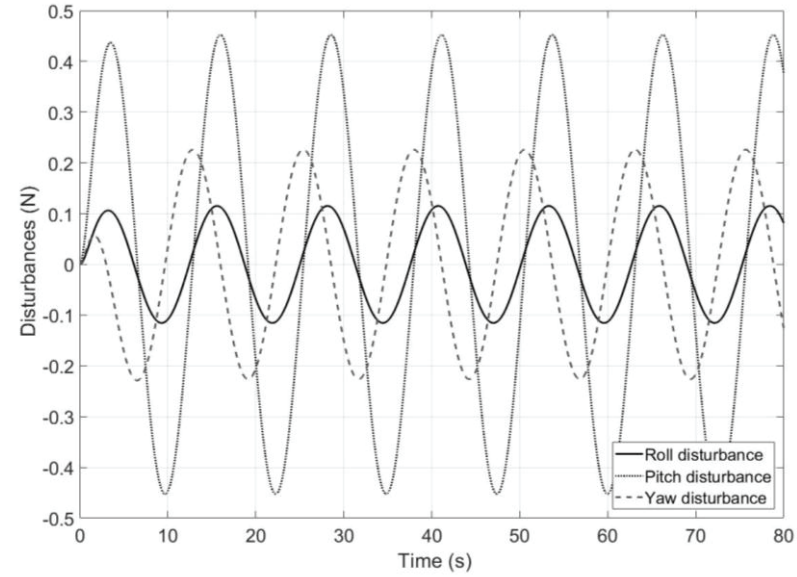

Figure 2. Disturbance torques in roll, pitch and yaw angles.

The disturbance $d_1(t)$ is builded as given in Eq. (30). Disturbance forces influences the hexacopter UAV along the inertial axes and these multiple disturbances are illustrated in Figure 2.

To compare results, the gains of PID controllers are selected using MATLAB/PID Tuner toolbox with the best robustness and tracking performance. Obtained PID (K_p, K_I, K_D) gains and N filter coefficient are given in Table 2.

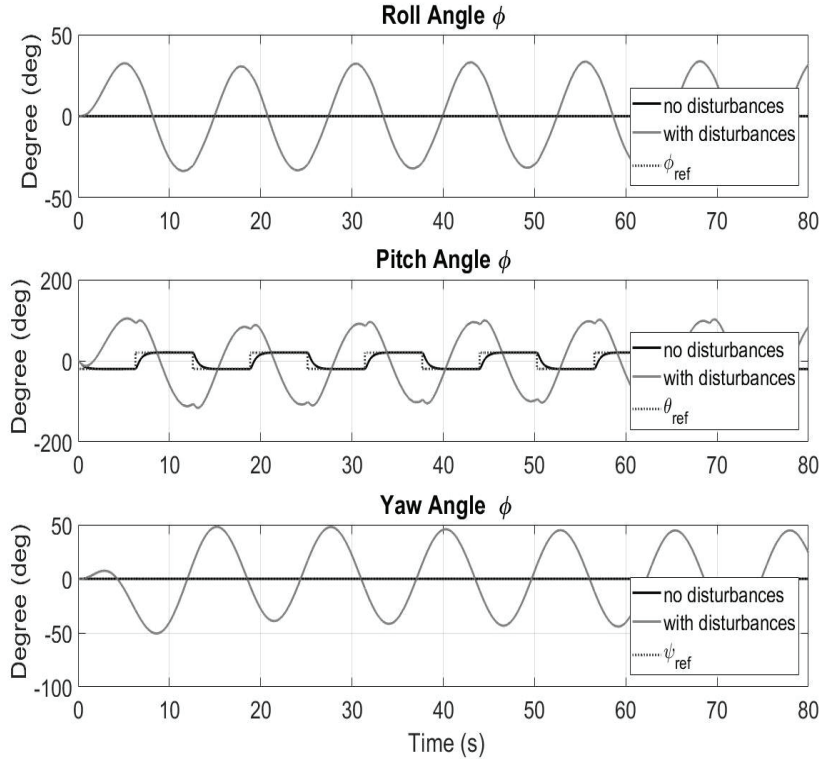

Figure 3. Attitude tracking performance with the PID controller.

Table 2. Tuning parameters of attitude PID controllers.

Controllers	K_p	K_I	K_D	N
PID1	0.098	0.006	0.39	1091
PID2	0.109	0.006	0.41	1142
PID3	0.143	0.007	0.57	1091

The performance of resulting PID controllers are shown in Figure 3. As it can be seen from figure, the classical PID controllers can stabilize the hexacopter UAV while there does not exist disturbances on the hexacopter UAV system. The reference tracking performance of PID controllers is good. However, PID controllers cannot track the desired signals under the multiple disturbances in the roll, pitch and yaw channels. Large oscillations are observed in the response of the PID controller when disturbances are injected into roll, pitch and yaw torque

channels in simulation. Multiple disturbances are perturbing the hexacopter UAV significantly.

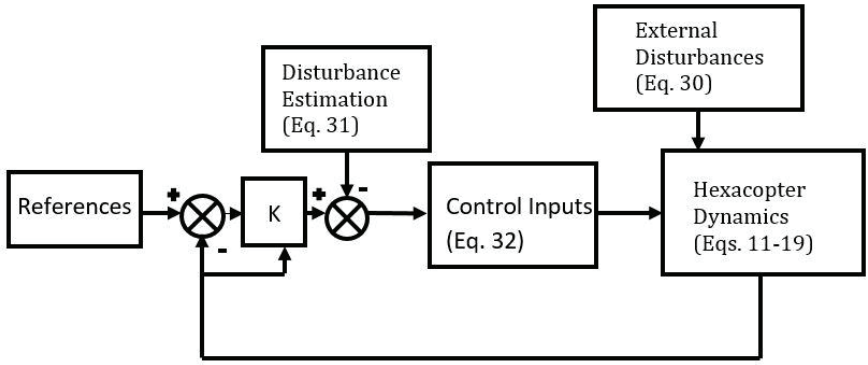

Figure 4. Control structure of the developed composite anti-disturbance control

Now, the composite anti-disturbance controller is developed as given in Figure 4 which consists of a disturbance observer and a state feedback controller. LMI condition of Theorem 1 is solved with MATLAB LMI toolbox. The gain of the robust controller and the gain of the observer are given in Table 3.

Table 3. Gains of the robust controller and the disturbance observer.

$$K = 10^4 \begin{vmatrix} -9 & -9 & -9 & -0.01 & -0.01 & -0.01 & 112 & 112 & 112 \\ -16 & -16 & -16 & -0.01 & -0.01 & -0.01 & 207 & 207 & 207 \\ -45 & -45 & -45 & -0.03 & -0.04 & -0.04 & 559 & 559 & 559 \end{vmatrix}$$

$$L = \begin{vmatrix} 12 & 162 & -15 & -785 & 61 & 464 & 217 & -146 & -81 \\ 12 & 163 & -15 & -786 & 61 & 464 & 217 & -146 & -81 \end{vmatrix}$$

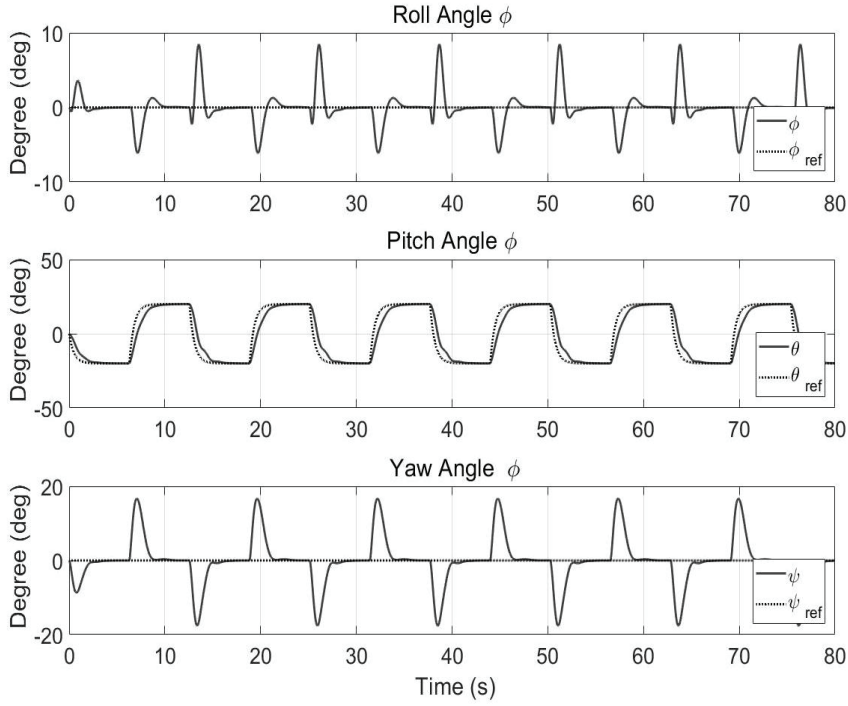

Figure 5. Results of the attitude tracking with multiple disturbances.

To evaluate the performance of the proposed control approach, the nonlinear dynamics (Eqs.11-19) of the hexacopter UAV and the gains computed in Table 3 is simulated. Figure 5 shows that closed-loop response of the hexacopter UAV with the developed composite anti-disturbance controller. As can be seen from Figure 5, the developed control structure has accomplished a good tracking performance in the presence of multiple disturbance.

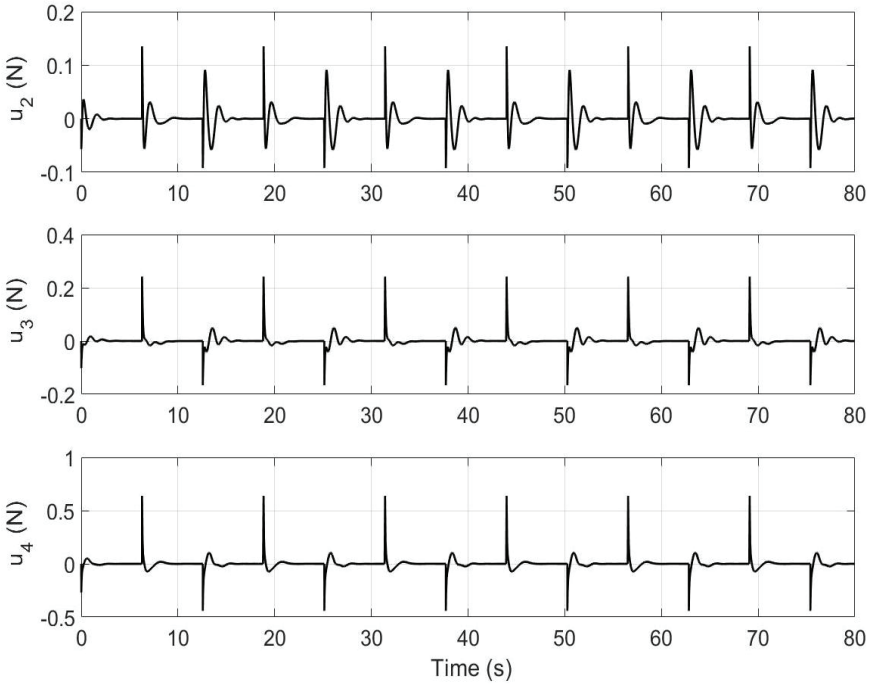

Figure 6. Control inputs with the proposed composite anti-disturbance controller.

Figure 6 shows control inputs while the hexacopter is tracking the reference profile in the presence of multiple disturbances with the proposed composite anti-disturbance controller. Errors of disturbance estimations are shown in Figure 7. From Figure 7, it can be seen that disturbance estimation errors are nearly zero. The developed control structure provides robust tracking under the reference trajectory variation and the effect of multiple disturbance torques. Overall, the performance of the developed controller is well.

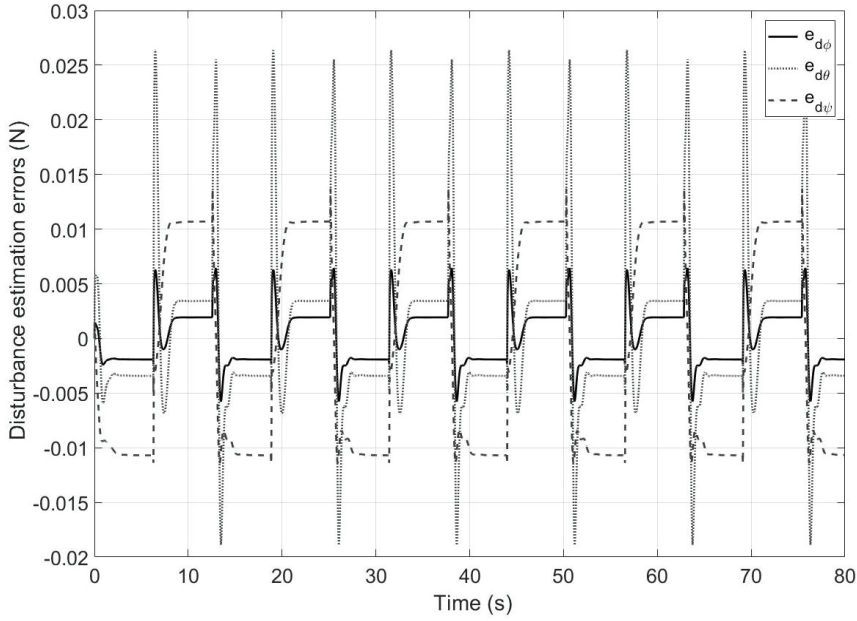

Figure 7. Estimation errors of disturbances affecting the hexacopter UAV.

CONCLUSIONS

In this study, dynamic model of a hexacopter UAV is given by using Newton Euler approach. The hexacopter model is simulated in MATLAB/Simulink in order to apply and drive a control algorithm. A composite anti-disturbance control algorithm is developed which is consists of a disturbance observer and a robust state feedback controller. Simulations have been carried out so as to compare the disturbance rejection capacity of the developed control algorithm with respect to a classical PID control technique. The classical PID controller exhibits bad disturbance rejection properties. Simulation results have also demonstrated the effectives of the developed composite anti-disturbance control approach in the presence of external multiple disturbances. The developed control approach has a high capability of the disturbance attenuation against multiple disturbances.

ACKNOWLEDGEMENT

This study was supported by Artvin Çoruh University Scientific Research Unit (BAP, Turkey) Project No: 2019.F13.02.01.

REFERENCES

1. G. Antonelli, E. Cataldi, F. Arrichiello, P. R. Giordano, S. Chiaverini, A. Franchi "Adaptive trajectory tracking for quadrotor MAVS in presence of parameter uncertainties and external disturbances", IEEE Transactions on Control Systems Technology 26(1): 248–254, 2018.
2. X. Liang, Y. Fang, N. Sun, and H. Lin, "Nonlinear hierarchical control for unmanned quadrotor transportation systems", IEEE Transactions on Industrial Electronics, 65(4), 3395-3405, 2017.
3. D. Shi, W. Zhong and C. Wusheng, "Anti-disturbance trajectory tracking of quadrotor vehicles via generalized extended state observer", Journal of Vibration and Control 26(13-14),1173-1186, 2020.
4. Y. Yuan, L. Cheng, Z. Wang and C. Sun, "Position tracking and attitude control for quadrotors via active disturbance rejection control method", Science China Information Sciences, 62(1), 1-10, 2019.
5. A. Castillo, R. Sanz, P. Garcia, W. Qiu, H. Wang and C. Xu, "Disturbance observer-based quadrotor attitude tracking control for aggressive maneuvers", Control Engineering Practice, 82, 14-23, 2019.
6. K. Guo, J. Jia, X. Yu, L. Guo and L. Xie, "Multiple observers based anti-disturbance control for a quadrotor UAV against payload and wind disturbances", Control Engineering Practice, 102, 104560, 2020.
7. A. Aboudonia, R. Rashad, & A. El-Badawy "Composite hierarchical anti-disturbance control of a quadrotor UAV in the presence of matched and mismatched disturbances", Journal of Intelligent & Robotic Systems, 90(1), 201-216, 2018.
8. J. Zhang, D. Gu, C. Deng, and B. Wen, "Robust and Adaptive Backstepping Control for Hexacopter UAVs", IEEE Access, 7, 163502-163514, 2019.
9. H. Başak, E. Kemer, "Hekzakopter insansız hava aracı için eşdeğer bozucu etki tahmini kullanılarak bozucu etki önleyici denetleyici tasarımı", Niğde Ömer Halisdemir Üniversitesi Mühendislik Bilimleri Dergisi, vol. 10, no. 2, pp. 535-544, 2021.
10. C. Rosales, C. M. Soria, F. G. Rossomando, "Identification and adaptive PID Control of a hexacopter UAV based on neural networks", International Journal of Adaptive Control and Signal Processing, 33(1), 74-9, 2019.
11. J. A. Ligthart, P. Poksawat, L. Wang, H. Nijmeijer, "Experimentally validated model predictive controller for a hexacopter", IFAC-PapersOnLine, 50(1), pp. 4076–4081, Toulouse, France, 2017.
12. A. Alaimo, V. Artale, C. L. R. Milazzo, A. Ricciardello, "PID controller applied to hexacopter flight. Journal of Intelligent & Robotic Systems", 73(1-4), 261-270, 2014.
13. A. Freddi, S. Longhi, A. Monteriù, M. Prist, "Actuator fault detection and isolation system for an hexacopter", IEEE/ASME 10th International Conference on Mechatronic and Embedded Systems and Applications (MESA) (pp. 1-6), Senigallia, Italy, 2014.

14. W.H. Chen, J. Yang, L. Guo, S. Li, “Disturbance-observer-based control and related methods—An overview”, IEEE Transactions on Industrial Electronics, 63.2, 1083-1095, 2016.
15. S. Boyd, L. EI Ghaoui, E. Feron, V. Balakrishnan, “Linear Matrix Inequalities in System and Control Theory”, vol. 15 of SIAM Studies in Applied Mathematics, SIAM, Philadelphia, Pa, USA, 1994.
16. X. Wei, L. Guo. “Composite disturbance-observer-based control and H∞ control for complex continuous models”, International Journal of Robust and Nonlinear Control: IFAC-Affiliated Journal, 20(1), 106-118, 2010.

Chapter 10

FOOD SMART PACKAGING AND MICROBIOLOGICAL PERSPECTIVE

Özlem ERTEKİN[1]
Yeliz İPEK[2]

1 Dr. Öğr. Üyesi Özlem Ertekin, Department of Nutrition and Dietetics, Faculty of Health Sciences, Munzur University, 62000, Tunceli, Turkey. Corresponding Author, E-mail: oertekin@munzur.edu.tr, ORCID: 0000-0002-2548-2478
2 Dr. Öğr. Üyesi Yeliz İpek, Department of Chemistry and Chemical Process Technologies, Vocational School of Tunceli, Munzur University, 62000, Tunceli, Turkey. E-mail: yelizipek@munzur.edu.tr,ORCID: 0000-0002-9390-9875

Introduction

Packaging ensures safe delivery of food to the consumer without spoiling, protects the product, increases its durability, and provides convenience in terms of storage (Üçüncü, 2007). Food packaging is used to protect food against environmental conditions. The concepts of active and smart packaging technologies developing in food packaging systems offer innovations and solutions to many problems. Some of these innovations are extending the shelf life of foods, protecting the quality of products, ensuring safe transportation and distribution of food products, development of sustainable-environmentally friendly packaging with high thermal stability and high mechanical strength (Han et al., 2018).

Packaging in the food industry is defined as a tool that preserves the quality of the food and ensures that the food is delivered to the consumer reliably, without spoiling, at the least cost (Üçüncü, 2007; Cutter, 2006).

Food deteriorates when exposed to an environment that is not suitable for maintaining its stability during distribution and storage. The main causes of deterioration are foodborne pathogens and microorganisms that grow on the food surface, such as *Escherichia coli* and *Listeria monocytogenes* (Farah et al., 2016; Murariu and Dubois, 2016). Some conventional food protection methods are freezing, cooling, drying, fermentation, application of additives and thermal treatment (Saini et al., 2016). Active packaging or smart packaging, which is a relatively new concept, is also among the applications introduced (Raquez et al., 2013).

Food packaging is necessary to ensure the quality and safety of food against contamination and environmental factors. In addition, extending the shelf life of foods and minimizing food losses are important in this context (Robertson, 2012; Carocho et al., 2015; Narayanan et al., 2017). Although many factors such as oxidation and microbial spoilage cause food spoilage; the situations encountered during production, transportation, storage and marketing processes can also directly affect food quality, consumer health, and the industrial economy (Fern´andez–Pan et al., 2014; Sanches–Silva et al., 2014; Zhao et al., 2016). In this case, packaging acts as a physical barrier, protects food from external factors, increases food quality and safety, and makes an economic contribution by extending the shelf life of food (Gupta and Dudeja, 2017).

Recently, food packaging trends have emerged. Changes in consumer demand, industrial production trends, controlled product quality, retailing practices, and customer lifestyles have led to these trends. Innovative packaging techniques improve food safety and quality, extend the shelf life of foods and reduce the impact of the environment (Dainelli et al., 2008).

Plastics, one of the most used materials in food packaging, are mostly produced from petroleum–derived materials and these materials are known to cause environmental pollution (Davis and Song, 2006). For this reason, biodegradable materials have started to be used today. Biodegradation is the breakdown of plastics by microorganisms such as yeast and bacteria (Restrepo-Flórez et al., 2014). Among the biodegradable food packaging materials such as starch, polyhydroxyalkonates, polylactic acid, cellulose derivatives, poly-β-hydroxy butyrate, polyvinylalcohol and chitosan etc. are most popular (Kılınç et al., 2017). For example, chitosan is one of the biodegradable materials that has been used recently. However, chitosan has also antibacterial properties, especially against gram–positive bacteria (Yıldız and Yangılar, 2016).

In recent years, consumers' interest in minimally processed, quality and safe foods has increased. Therefore, new technologies such as smart packaging, active packaging, antimicrobial packaging, edible film packaging have been developed (Budak Bağdatlı and Kayaardı, 2010).

Considering the innovations in food packaging, technologies such as active and smart packaging technologies are mainly used. Active packaging refers to the inclusion of the active ingredient in the packaging to preserve product quality and shelf life. Intelligent systems, on the other hand, can monitor the condition of packaged food during transportation and storage to give information about the food quality. These packaging technologies can also work synergistically (Drago et al., 2020).

1. Smart Packaging

These are the packaging systems which present situation about the packaged food quality after a transportation and storage process. Sensors and indicators are used in most smart packaging systems (Kerry et al., 2006). Generally used sensors are gas sensors, fluorescent-based oxygen sensors, biosensors, while indicators are freshness indicators, time-temperature indicators.

Time-temperature indicators placed outside the package can be called external indicators, while indicators such as oxygen, carbon dioxide, microbial growth and pathogen indicators placed inside the package can be called internal indicators (Ahvenainen, 2003). Intelligent packaging systems are used as an indicator of inside and outside the packaging, especially during distribution and storage, to protect the quality characteristics of food and to ensure food safety.

1.1. Indicators

1.1.1. Time–temperature indicators

Time-temperature indicators are important in monitoring the shelf life of perishable food products. Temperature monitoring and control is very important as it will cause food waste throughout the supply chain (Dutra Resem Brizio, 2016). Food freshness indicators are based on the principle of detecting differences such as metabolites, microorganisms or pH changes that occur as a result of food deterioration. Temperature–time indicators record temperature rises that occur during storage or transportation of the food product, indicating that the food has been exposed to unsuitable temperatures. Wang et al. (2015), classified the time-temperature indicators as;

- Chemical time temperature indicator;

Polymerization-based, photochromic-based, redox reaction-based, diffusion-based, nanoparticle-based and electronic time temperature indicators,

- Enzymatic time temperature indicator;

Acid–base reaction-based, redox reaction-based, yeast-based and lactobacillus-based time temperature indicators,

- Other new systems of time temperature indicator;

Photonic lattice change and thermochromic polymer/dye blends based time temperature indicators.

Some commercial time temperature indicators' trade names are Cook-Chex (Pymah Corp.), Timestrip (Timestrip Plc), Colour-Therm (Colour-Therm company), MonitorMark (3M, Minnesota), Onvu (Ciba Specialty Chemical and FreshPoint), Fresh-Check (Temptime Corp.), Thermax (Thermographic Measurements Ltd.) and CheckPoint (Vitsab) (Fuertes et al., 2016). The time temperature indicator can be placed on the products one by one, or it can be placed in cardboard box or containers depending on the transport vehicle.

1.1.2. Freshness indicators

This indicators are smart devices that monitor food quality during storage and transportation. Freshness indicators follow the alterations in the concentration of metabolic molecules such as sugar, ethyl alcohol, carbon dioxide, biogenic amines, organic acids, which are the indicators of microbial growth during the spoilage of food (Poyatos-Racionero et al., 2018).

Freshness indicators give information about the freshness of the food. According to Smolander (2003), the indicators can be grouped as follows;

- Indicators sensitive to pH change,
- Indicators sensitive to volatile nitrogen compounds,
- Hydrogen sulfide sensitive indicators,
- Indicators sensitive to various microbial metabolites.

Freshness indicators generally function as a result of discoloration in the presence of metabolites of microorganisms in contaminated food (Figure 1).

Figure 1. *An indicator sensitive to pH change.*

Fresh Tag (COX Technologies), SensorQ (DSM NV and Food Quality Sensor) and RipeSense (RipSense and ort Research) are commercial freshness indicators (Fuertes et al., 2016).

1.1.3. Gas indicators

The gas composition in the headspace of the package often varies depending on the nature of the food, the nature of the package, or environmental conditions (Yezza, 2008; Kerry et al., 2006). Gas indicators are systems that show the presence or absence of some gases used in modified atmosphere packaging. These indicators basically provide information about packaging integrity and leaks. Gas indicators are generally usefull to trace oxygen and carbon dioxide density (Meng et al., 2014). Oxygen causes microbial and biochemical degradation in food, and therefore to reduce its effect it is replaced with gas such as nitrogen. On the other hand using an oxygen scavenger in packaging is also possible (Vu and Won, 2013). When proteins are broken down by microorganisms, the volatile amines utrescine, cadaverine, and histamine are released. The gas indicator mounted on/into the food package interacts with these volatile amines and indicates that the food is spoiled.

However, according to Ahvenainen and Hurme (1997), gas indicators particularly oxygen/carbon dioxide indicators can also show misleading results. For example, when deformation occurs in a food package, oxygen will enter the package and microorganisms will produce carbon dioxide as a result of contamination. This will increase the carbon dioxide level and the gas indicator will show the carbon dioxide level high even though the food is contaminated.

1.2. Sensors

Sensor is an apparatus that responds to the changes of a chemical, biological or physical feature (Ghaani et al., 2016). Although sensors designed for smart food packaging utilization are grouped into two main categories as chemical sensors and biosensors, edible sensors are also used for food safety systems. Most sensors are basically composed of two units; the receptor and the transducer. The receptors convert the physical and chemical information they receive from the source into energy suitable for transducer measurement (Kokangül and Fenercioğlu, 2012).

1.2.1. Biosensors

Biosensors are analytical devices/tools that determine and visually reveal the substance to be analyzed with the help of biochemical reactions. These smart tools consist of a bioreceptor that recognizes the target substance or analyte and a converter that converts biochemical signals into a measurable electrical signal.

Bioreceptors are usually organic materials such as DNA, RNA, enzymes, antibodies, antigens, microbes, and hormones (Vanderroost et al., 2014; Siracusa and Lotti, 2019). The transducer, on the other hand, can be electrochemical, optical, colorimetric, etc. system depending on the variable being measured. In electrochemical biosensors, microorganisms in the structure of the food and metabolites resulting from deterioration are detected by an electrode. Food contamination caused by pathogenic bacteria is a serious problem. *E. coli*, *S. typhimurium*, *S. aureus*, *B. cereus*, Streptococci, etc. lead various ailments (Mishra et al., 2018). In optical-based biosensors, in a pathogenic bacteria contaminated food, the bacterial toxin binds to antibodies that is immobilized on a thin flexible film. Then, a noticable change in the color of the thin flexible polyethylene film biosensor occurs (Ghaani et al., 2016; Müller and Schmid, 2019). Toxin biosensors that are highly selective are specific for the toxin of a single microorganism. The biosensor used for food safety must be extremely sensitive and fully in contact with food (Kocaman and Sarımehmetoğlu, 2010).

Biosensors must be sensitive, selective, have a low detection limit, and have a wide operating range. Because pathogenic microorganisms are dangerous, although they are usually present in very low concentrations in or on the surface of foods.

1.2.2. Edible sensors

They are sensors used to detect food spoilage, made with only natural and biodegradable materials in the field of smart food packaging (Drago et al., 2020). Edible food films such as wax coatings, chocolate and candy coatings, and capsules have been used for years (Ayrancı and Tunç, 2003). Modern edible protective films:

- Should have good sensory properties, be transparent, tasteless and odorless (Vargas et al., 2008),
- Should have superior barrier and mechanical efficiency,
- Should have sufficient biochemical, physico-chemical and microbial stability,
- Should be non-toxic, reliable in terms of health,
- Should not pollute the environment and be easily produced at low cost (Debeaufort et al., 1998).

Considering the environmental damage of packaging materials, the trend towards edible packaging is increasing. Thus food contamination indicators are dopped into the edible films to achieve edible sensors. Dipping, spraying, dripping, pouring and foaming techniques are used in edible coating application (Işık et al., 2013).

1.3. Active Packaging

It is classified as a subclass of smart packaging. The development of active packaging has led to many improvements: delaying oxidation, controlling bacterial growth and moisture migration, absorbing odors (Hu et al., 2016; Youssef et al., 2016).

The purpose of active packaging is to increase the quality and safety of food using natural methods. In active packaging technology, the most appropriate approach is applied considering the food, packaging material and environmental atmosphere (Sivertsvik et al., 2002). The active packaging process includes one or more of the stages such as oxygen scavengers, carbon dioxide regulators, humidity regulators, antioxidant use, and antimicrobial packaging (Vermeiren et al., 1999).

With smart and active packaging technologies, in the process from production to consumption of food, food quality is kept under control to protect consumer health and prevent economic losses.

1.3.1. Antimicrobial food packaging

Antimicrobial packaging is a type of active packaging. It is an effective method especially in extending the shelf life of meat and meat products and increasing their safety in food products. The use of antimicrobial agents controls the microbial population and provides high product safety and quality by targeting specific microorganisms. Antimicrobial materials can be classified as films, edible films, and synthetic polymers (Vermeiren et al., 1999).

The shelf life of food is greatly affected by the presence of microorganisms. When food is exposed to the environment, contamination can occur at any stage of the supply chain. One of the main causes of spoilage is microbial growth, which results in discoloration, development of aroma defect, textural changes and loss of nutritional value. Therefore, it reduces the shelf life of foods and increases the risk of foodborne illness (Biji et al., 2015; Malhotra et al., 2015). Among the technologies developed to prevent this problem, antimicrobial packaging can be an effective method. Inhibition of microorganism growth is possible with active antimicrobial packaging technology. To protect product safety and quality, antimicrobial food packaging systems inhibit or retard the growth of microorganisms (Appendini and Hotchkiss, 2002; Lopez et al., 2005). Antibacterial packaging can be a tool to increase food safety, extend food shelf life and reduce economic losses. When the substances in active packaging are released in a controlled manner, the development of harmful microorganisms is prevented for a long time and a significant increase in the shelf life of foods is observed (Wyrwa and Barska, 2017).

Methods such as moisture absorbers, CO_2 diffusers and antioxidant packaging all have antimicrobial effects. They provide food quality and safety by slowing down the growth of microorganisms (Han, 2000).

Generally, the following substances have antimicrobial properties;

Protectors

Chlorine dioxide and sulfur dioxide are the volatile agents of the package with antimicrobial effect (Özdemir and Floros, 2004; Sung et al., 2013). Nguyen Van Long et al. (2016) reported the antifungal effect of potassium sorbate that is used in food packaging films.

Inorganic nanoparticles

Inorganic nanoparticles consisting of metal ions such as silver, copper, gold, platinum, etc., and metal oxides such as TiO_2, ZnO, MgO and CuO are active packaging films obtained by incorporating such materials into adsorbent pads or polymers (Drago et al., 2020).

Ethanol

Drago et al. (2020) stated in their study that ethanol is an antimicrobial agent which can inhibit yeast and bacterial growth.

Carbon dioxide

Carbon dioxide has an antimicrobial impact on different microorganisms and is used to lengthen food shelf life (López-Rubio et al., 2004).

Natural active packaging agents

Today, the use of natural materials for the production of active/smart food package is in demand for sustainable environmental and human health. Organic agents are thought to be safer than synthetic agents by consumers. For this reason, studies are carried out on the use of various natural compounds in active packaging (Drago et al., 2020).

Bacteriocins

Bacteriocins are peptides that produced by bacteria such as pediocins, nisins, enterocins, and sacacins. Bacteriocins are of great interest to the food industry due to their antimicrobial effects (Bagde and Nadanathangam, 2019). Bacteriocins are mainly produced by lactic acid bacteria. Bacteriocins found in many fermented foods are natural compounds. They can inhibit many of the pathogenic microorganisms (Santos et al., 2018).

Antibacterial agents

Organic-based antibacterial agents include linoleic acid, propionic acid, formic acid, sorbic acid, lactic acid, acetic acid, etc. (Attilio and Gatti, 2016). Along with these, there are also plant extracts with antibacterial properties such as eucalyptus oil and olive oil (Galet et al., 2016). These substances create a barrier in the package by restricting microbial growth (Quintavalla and Vicini, 2002). There are also inorganic antibacterial agents based on silver (Ag), gold (Au), and titanium (Ti). Nanoparticle complexes (Au/TiO_2, $Ag/N\text{-}TiO_2$, etc.) also prevent microbial activities (Peter et al., 2016).

In a study, carboxymethyl cellulose (CMC) nanocomposite films doped with metallic nanoparticles such as silver (Ag), zinc oxide (ZnO) and copper oxide (CuO) were used. Films containing nanoparticles showed antibacterial properties against the growth of *S. aureus* and *E. coli*, thus revealing the fact that nanobiocomposite films can be used as active packaging films (Ebrahimi et al., 2019).

In a study, the antibacterial property of CuNPs-C-PLA nanocomposite material was studied and its effect on *Pseudomonas auroginosa*, one of the Gram-negative bacteria, was examined. As a result, it has been determined

that this nanocomposite material has good potential for food packaging applications (Longano et al., 2012).

A new approach has been proposed in another study. According to this study, Shemesh et al. (2014) developed antimicrobial active films based on low density polyethylene (LDPE), organo-modified montmorillonite and carvacrol. LDPE/clay/carvacrol films had superior and long-term antimicrobial activity towards Listeria and *E. coli.* The films also showed high antifungal activity towards the plant pathogenic fungus *Alternaria alternata*.

Segura Gonzalez et al. (2018) prepared Polylactic acid (PLA) based polymer composite materials filled with titanium dioxide (TiO_2) nanoparticles. According to this study, the effect of TiO_2 antibacterial agent against *E. coli* (DH5α) strain was investigated and it was stated that studies in this area should be continued.

The antimicrobial properties of food packaging material is based on antimicrobial activities of packaging dopant materials. There are two types of antimicrobial agents as natural and synthetic antibacterial agents. Robertson et al. (2005) developed antimicrobial agents from natural sources in their study. Natural antimicrobial agents are thought to be relatively safer and easy to achieve.

2. Conclusions

Packaging of food is a critical point for food protection from microbial contamination. Therefore, both safe and low cost packaging techniques must be developed. Since non-degradable food packaging will lead pollution of environment, biodegradable packaging materials are more suitable for a sustainable life cycle. These packages are environmentally friendly as well as renewable.

Natural antibacterial agents have low toxicity but high production cost, which causes them to be used in a narrower area. Smart technology applications should also be added to antimicrobial materials. In this way, it is necessary to make packaging production economical and widespread. The smart packaging systems, which have not yet found a wide application area in our country and in the world, will become more widespread for food safety and traceability in the future.

3. References

Ahvenainen, R. (2003). Active and Intelligent Packaging. In Novel Food Packaging Techniques. Woodhead Publishing Limited Cambridge, England p.5-21.

Ahvenainen, R., Hurme, E. (1997). Active and Smart Packaging for Meeting Consumer Demands for Quality and Safety. In Food Additive Contaminants, vol. 14, 1997, no. 6/7, p. 753–763.

Appendini, P., Hotchkiss, J.H. (2002). Review of Antimicrobial Food Packaging. Innovative Food Science & Emerging Technologies, 3, 113-126. http://dx.doi.org/10.1016/S1466-8564(02)00012-7

Attilio, L., Gatti M. (2016). Film-forming composition for disinfection and preservation of foodstuffs. EP3072401A1

Ayrancı, E., Tunc, S. (2003). A method for the measurement of the oxygen permeability and the development of edible films to reduce the rate of oxidative reactions in fresh foods. Food Chemistry, 80:423-431.

Bagde, P., Nadanathangam, V. (2019). Improving the stability of bacteriocin extracted from *Enterococcus faecium* by immobilization onto cellulose nanocrystals. Carbohydr. Polym., 209, 172–180.

Biji, K. B., Ravishankar, C. N., Mohan, C. O., Srinivasa Gopal, T. K. (2015). Smart packaging systems for food applications: a review. Journal of Food Science and Technology, 52, 6125–6135.

Budak Bağdatlı, A., Kayaardı, S. (2010) . Et ve Et Ürünlerinde Kullanılan Paketleme Yöntemleri. Akademik Gıda, 8 (2) 24-30.

Carocho, M., Morales, P., Ferreira, I. C. F. R. (2015). Natural food additives: Quo vadis?. Trends in Food Science & Technology, 45, 284–295.

Cutter, C.N. (2006). Opportunities for bio-based packaging technologies to improve the quality and safety of fresh and further processed muscle foods. Meat Science, 74: 131-142.

Dainelli, D., Gontard, N., Spyropoulos, D., Zondervan-van den Beuken, E.,Tobback, P. (2008). Active and intelligent food packaging: Legal aspects and safety concerns. Trends in Food Science & Technology, 19(Suppl 1):S103–S112.

Davis, G., Song, J.H., 2006. Biodegradable packaging based on raw materials from crops and their impact on waste management. Industrial Crops and Products, 23(2): 147-161.

Debeaufort, F., Quezada-Gallo ,J.A., Voilley, A. (1998). Edible Films and Coatings: Tomorrow's Packaging's: A Review. Critical Reviews in Food Science and Nutrition, 38, 299–313.

Drago, E.,Campardelli, R., Pettinato , M., Perego, P. (2020). Innovations in Smart Packaging Concepts for Food: An Extensive Review. Foods, 9, 1628; doi:10.3390/foods9111628.

Dutra Resem Brizio, A.P. (2016). Use of indicators in intelligent food packaging. Ref. Modul. Food Sci., 1–5.

Ebrahimi, Y., Peighambardoust, S.J., Peighambardoust, S.H., Karkaj, S.Z. (2019). Development of Antibacterial Carboxymethyl Cellulose-Based Nanobiocomposite Films Containing Various Metallic Nanoparticles for Food Packaging Applications. Journal of Food Science, 84(9).

Farah, S., Anderson, D.G., Langer, R. (2016). Physical and mechanical properties of PLA, and their functions in widespread applications—A comprehensive review. Adv. Drug Deliv. Rev., 107, 367–392.

Fern´andez-Pan, I., Carri´on-Granda, X., Mat´e, J. I. (2014). Antimicrobial efficiency of edible coatings on the preservation of chicken breast fillets. Food Control, 36, 69–75.

Fuertes, G., Soto, I., Carrasco, R., Vargas, M., Sabattin, J., Lagos, C. (2016). Intelligent Packaging Systems: Sensors and Nanosensors to Monitor Food Quality and Safety. J. Sensors, 4046061:1-4046061:8.

Galet, D.A.G., Prats, G.L., Monedero, P.F.M., Saldaña, J.M.B., Calvo, V.M.T., Lara, L.M.I. (2016). Antimicrobial compositions for food packaging consisting of salicylaldehyde and carvacrol, thymol or their mixture. US20160325911A1

Ghaani, M., Cozzolino, C.A., Castelli, G., Farris, S. (2016). An overview of the intelligent packaging technologies in the food sector. Trends Food Sci. Technol., 51, 1–11.

Gupta, R. K., Dudeja, P. (2017). Chapter 46 Food packaging. In: Food Safety in the 21st Century. p 547–53.

Han, J. H. (2000). Antimicrobial food packaging. Food Technology, 54, 56–65.

Han, J.W., Ruiz-Garcia, L., Qian, J.P., Yang, X.T. (2018). Food packaging: A comprehensive review and future trends. Compr. Rev. Food Sci. Food Saf., 17, 860–877.

Hu, D.,Wang, H.,Wang, L. (2016). Physical properties and antibacterial activity of quaternized chitosan/carboxymethyl cellulose blend films. LWT-Food Science and Technology, 65, 398–405. https://doi.org/10.1016/j.lwt.2015.08.033

Işık, H., Dağhan,Ş., Gökmen, S. (2013). Gıda Endüstrisinde Kullanılan Yenilebilir Kaplamalar Üzerine Bir Araştırma, Gıda Teknolojileri Elektronik Dergisi, Cilt: 8, No: 1, (26–35).

Kerry, J.P., O'Grady, M.N., Hogan, S.A. (2006). Past, current and potential utilisation of active and intelligent packaging systems for meat and musclebased products: a review. Meat Science, 74: 113-130.

Kılınç, M., Tomar, O., Çağlar, A. (2017). Biyobozunur Gıda Ambalaj Malzemeleri. AKÜ FEMÜBİD 17 035404 (988-996) DOİ: 10.5578/fmbd.66307.

Kocaman, N., Sarımehmetoğlu, B. (2010). Gıdalarda Akıllı Ambalaj Kullanımı. Vet Hekim Der Derg 81(2): 67–72.

Kokangül, G., Fenercioğlu, H. (2012). Gıda Endüstrisinde Akıllı Ambalaj Kullanımı, Electronic Journal of Food Technologies, 7(2), 31–43.

Longano , D., Ditaranto, N., Cioffi, N., Di Niso, F., Sibillano, T., Ancona, A., Conte, A., Del Nobile, M. A., Sabbatini, L., Torsi, L. (2012). Analytical characterization of laser-generated copper nanoparticles for antibacterial composite food packaging. Anal Bioanal Chem, 403:1179–1186 DOI 10.1007/s00216-011-5689-5

López-Rubio, A., Almenar, E., Hernandez-Muñoz, P., Lagarón, J.M., Catalá, R., Gavara, R. (2004). Overview of active polymer-based packaging technologies for food applications. Food Rev. Int., 20, 357–387.

Lopez, P., Sanchez, C., Batlle, R., Nerin, C., J. (2005). Agric., Solid- and vapor-phase antimicrobial activities of six essential oils: susceptibility of selected foodborne bacterial and fungal strains. Food Chem. 53 (17), 6939-46

Malhotra, B., Keshwani, A., Kharkwal, H. (2015). Antimicrobial food packaging: Potential and pitfalls. Frontiers in Microbiology. 6, 611.https://doi.org/10.3389/fmicb.2015.00611.

Meng, X., Kim, S., Puligundla, P., Ko, S. (2014). Carbon dioxide and oxygen gas sensors-possible application for monitoring quality, freshness, and safety of agricultural and food products with emphasis on importance of analytical signals and their transformation. J. Korean Soc. Appl. Biol. Chem., 57, 723–733.

Mishra, G.K., Barfidokht, A., Tehrani, F., Mishra, R.K. (2018). Food safety analysis using electrochemical biosensors. Foods, 7.

Murariu, M., Dubois, P. (2016). PLA composites: From production to properties. Adv. Drug Deliv. Rev., 107,17–46.

Müller, P., Schmid, M. (2019). Intelligent packaging in the food sector: A brief overview. Foods, 8.

Narayanan, M., Loganathan, S., Valapa, R. B., Thomas, S.,Varghese, T. O. (2017). Uv protective poly(lactic acid)/rosin films for sustainable packaging. International Journal of Biological Macromolecules, 99, 37–45.

Nguyen Van Long, N., Joly, C., Dantigny, P. (2016). Active packaging with antifungal activities. Int. J. Food Microbiol., 220, 73–90.

Özdemir, M., Floros, J.D. (2004). Active food packaging technologies. Crit. Rev. Food Sci. Nutr, 44, 185–193.

Peter, A., Nicula, C., Mihaly, C.A., Mihaly, C.L., Danciu, V., Baia, G.L., Kovacs, G., Ciric, A., Begea, M., Craciun, L. (2016). Process for obtaining nanocomposite food packages. EP3078275A1

Poyatos-Racionero, E., Ros-Lis, J.V., Vivancos, J.L., Martìnez-Mànez, R. (2018). Recent advances on intelligent packaging as tools to reduce food waste. J. Clean. Prod., 172, 3398–3409.

Quintavalla, S., Vicini, L. (2002). Antimicrobial food packaging in meat industry. Meat Sci; 62(3): 373-380.

Raquez, J.M., Habibi, Y., Murariu, M., Dubois, P. (2013). Polylactide (PLA)-based nanocomposites. Prog. Polym. Sci., 38, 1504–1542.

Restrepo-Flórez, J.M., Bassi, A., Thompson, M. R. (2014). Microbial degradation and deterioration of polyethylene–A review. International Biodeterioration & Biodegradation, 88: 83-90.

Robertson, G. L. (2012). Food packaging: Principles and practice (3rd ed.). Carocho, M., Morales, P., & Ferreira, I. C. F. R. (2015). Natural food additives: Quo vadis?. Trends in Food Science & Technology, 45, 284–295.

Robertson, J.M.C., Robertson, P.K.J., Lawton, L.A. (2005). A comparison of the effectiveness of TiO_2 photocatalysis and UVA photolysis for the destruction of three pathogenic micro-organisms. J. Photochem. Photobiol. A Chem., 175, 51–56.

Saini, P., Arora, M., Kumar, M.N.V.R. (2016). Poly(lactic acid) blends in biomedical applications. Adv. Drug Deliv. Rev., 107, 47–59.

Sanches-Silva, A., Costa, D., Albuquerque, T. G., Buonocore, G. G., Ramos, F., Castilho, M. C., Machado, A.V., Costa, H. S. (2014). Trends in the use of natural antioxidants in active food packaging: A review. Food Additives and Contaminants, 31, 374–395.

Santos, J.C.P., Sousa, R.C.S., Otoni, C.G., Moraes, A.R.F., Souza, V.G.L., Medeiros, E.A.A., Espitia, P.J.P., Pires, A.C.S., Coimbra, J.S.R., Soares, N.F.F. (2018). Nisin and other antimicrobial peptides: Production, mechanisms of action, and application in active food packaging. Innov. Food Sci. Emerg. Technol., 48, 179–194.

Segura González, E. A., Olmos, D., Lorente,M.A., Vélaz, I., González-Benito, J. (2018). Preparation and Characterization of Polymer Composite Materials Based on PLA/TiO_2 for Antibacterial Packaging. Polymers, 10 (12), 1365; doi:10.3390/polym10121365

Shemesh, R., Krepker, M., Goldman, D., Danin-Poleg, Y.,Kashi,Y.,Nitzan, N., Vaxman, A. ,Segal, E. (2014). Antibacterial and antifungal LDPE films for active packaging.wileyonlinelibrary DOI: 10.1002/pat.3434.

Siracusa, V., Lotti, N. (2019). Intelligent packaging to improve shelf life. Food Qual. Shelf Life 2019, 261–279.

Sivertsvik, M., Rosnes J.T., Bergslien, H. (2002). Modified Atmosphere Packaging. In: Minimal Processing Technologies In The Food Industry.

Ohlsson, T., Bengtsson, N. (Edit.) Woodhead Publishing Limited and CRC Press Boca Raton, Boston, NewYork Washington, DC. p.61-85.

Smolander, M. (2003).The use of freshness indicators in packaging, In Novel food packaging Techniques, R Ahvenainen (eds), Woodhead Publishing Limited, pp. 127–143, Cambridge.

Sung, S.Y., Sin, L.T., Tee, T.T., Bee, S.T., Rahmat, A.R., Rahman, W.A.W.A., Tan, A.C., Vikhraman, M. (2013). Antimicrobial agents for food packaging applications. Trends Food Sci. Technol. 33, 110–123.

Üçüncü, M. (2007). Gıdaların Ambalajlanması. Ege Üniversitesi Basımevi, İzmir,733-787p.

Vanderroost, M., Ragaert, P., Devlieghere, F. De Meulenaer, B. (2014). Intelligent food packaging: The next generation. Trends Food Sci. Technol., 39, 47–62.

Vargas, M., Pastor, C., Chiralt, A., Mc Clements, D.J., Gonzalez-Martinez, C. (2008). Recent Advances in Edible Coatings for Fresh and Minimally Processed Fruits. Critical Reviews in Food Science and Nutrition, 48, 496-511.

Vermeiren, L., Devlieghere, F., Beest, V. M., Kruijf, N. D., & Debevere, J. (1999). Developments in the active packaging of foods. Trends in Food Science & Technology, 10, 77–86.

Vu, C.H.T., Won, K. (2013). Novel water-resistant UV-activated oxygen indicator for intelligent food packaging. Food Chem., 140, 52–56.

Yezza, I.A. (2008). Active/Intelligent Packaging: Concept, Applications and Innovations, 2008 Technical Symposium, New Packaging Technologies to Improve and Maintain Food Safety, September 18–19, Toronto.

Yıldız, P.O., Yangılar, F. (2016). Gıda endüstrisinde kitosanın kullanımı/The use of chitosan in food industry. Erciyes Üniversitesi Fen Bilimleri Enstitüsü Dergisi, 30(3): 198-206.

Youssef, A. M., El-Sayed, S. M., El-Sayed, H. S., Salama, H. H., Dufresne, A. (2016). Enhancement of Egyptian soft white cheese shelf life using a novel chitosan/carboxymethyl cellulose/zinc oxide bionanocomposite film. Carbohydrate Polymers, 151, 9–19. https://doi.org/10.1016/j.carbpol.2016.05.023

Wang, S., Liu, X., Yang, M., Zhang, Y., Xiang, K., Tang, R. (2015). Review of Time Temperature Indicators as Quality Monitors in Food Packaging. Packaging Technology and Science, 28, 839–867.

Wyrwa, J., Barska, A. (2017). Innovations in the food packaging market: Active packaging. Eur. Food Res. Technol., 243, 1681–1692.

Zhao, C. J., Han, J. W., Yang, X. T., Qian, J. P., Fan, B. L. (2016). A review of computational fluid dynamics for forced-air cooling process. Applied Energy, 168,314-331.

Chapter 11

SIMULATION - APPLICATIONS IN APPAREL INDUSTRY

Mahmut KAYAR[1]

1 Assoc. Prof. Dr. Mahmut KAYAR, Marmara University, Faculty of Technology, Department of Textile Engineering, Göztepe Campus, Istanbul / Turkey mkayar@marmara.edu.tr

INTRODUCTION

Today, increasing customer demands, frequently changing technology and increasingly fierce global competition force companies to find out how they can produce their products or services faster, more effectively, with higher quality and at less cost. In order to ensure customer satisfaction, which has become increasingly important in the last 40 years, it is necessary to keep the quality and diversity high, while keeping the price of the product or service sold at lower levels than the prices of competing companies. While they have similar resources with the competitors in the market in terms of basic input, technology and workforce, it is important how they are produced rather than what is produced in order to provide price, quality and diversity advantages against them. It is not possible for companies that offer prices, diversity and quality below customer expectations to survive commercially without customer-oriented production [1].

The way to solve all these problems is to make quick and onsite changes in the system. In order to find the causes of the problems in the system and to eliminate them, it is necessary to examine and understand what kind of relationship there is between all the elements (which seems to be independent from each other but actually works as a whole) in the system, what parameters the system is sensitive and how the system reacts to certain changes.

Engineers and managers who know the system well and know the working logic based on their experience can answer this to some extent. However, it is almost impossible to find someone who knows the whole system well, especially in systems that are physically large, technologically complex, have a large number of operations and a wide variety of product groups. It is even more difficult to combine the experiences of people who know the parts of the system, to comment on the whole system based on this, to make changes or try alternatives. Moreover, the risk of such a method is too great. Changes made based on experience may not have the expected positive effect on the system. In such a case, if the change required a financial investment, it is impossible to go back [2].

Despite partial applications, it is not possible to directly implement a complex system without an evaluation phase. If a company approves the implementation of a particular system, for example; fast underground system, etc. It is quite risky to configure it immediately without evaluating its feasibility and estimating the system in a real-world environment [3].

Not all of the problems in the system may require any investment. Problems arising from the design and operating logic of the system can adversely affect the overall performance of the system. Buying expensive and fast machines, increasing the workforce, increasing the number of

shifts may provide some improvement. However, if the return on these investments is less than or equal to the cost, making similar changes will not provide a radical solution to the problem. However, in similar situations, there is a completely risk-free method that can show the result of the change to be made before the investment is made, and perhaps find ways to solve the problem without investing; ***simulation*** [2].

1. HISTORY OF SIMULATION

In the last half of our century, the science of modelling and simulation, from education to entertainment, from user education to transportation and animation, has advanced very rapidly. In the last 60 years, as the capabilities and scope of simulation languages and package programs have increased, the ways and uses of simulation have increased. In the late 1950s and 1960s, simulation was a very expensive and specialized tool, often used by companies that required large capital investments. These companies had established working groups of people with PhDs to develop large and complex simulation models with programming languages such as Fortran. The developed models were then run in large central processing units. The cost of these machines could reach up to a thousand dollars an hour. Today, even a personal computer that anyone can own is much more powerful and much faster than these machines.

The use of simulation as we know it today began at the end of 1979. The cost of computers has decreased considerably and is much faster, and the value of simulation has begun to be discovered in many areas. At the same time, simulation has become a standardized part of industrial engineering and operations research at universities. The rapid progress of simulation in the industry has forced universities to teach simulation more extensively. At the same time, with the growing demand, the number of researchers and students working on this subject has increased considerably. Recently, it has been observed that simulation is used as an important tool in modern management science. At the end of the

1980s, with the increase in the capacities of personal computers, the use of simulation has become well established in the business world. Although simulation is still used in the analysis of systems that have failed or need to be developed, many institutions now require simulation before the planned system is installed. In fact, in many cases, it is too late to change the design of the system once the simulation is resorted to. However, the system administrator and the system designer can still be given a chance to direct the system in the remaining operations. By the late 1980s, many large firms recognized the value of simulation, and many of them did simulations as a requirement before approving large capital investments. However, simulation was not very common in these years and

was used by very few serious companies.

By the early 1990s, the simulation had begun to mature. Many organizations have adopted simulation tools and have started using simulation in the very early stages of their projects where it can be most effective. A very good animation ability, ease of use, improvement in the capacity of computers, easy compatibility with other package programs and the development of simulators have made simulation a standard tool for many companies. The way the simulation is implemented can vary; Simulation programs used in the design phase of the systems can be used in different areas of the system with any changes, thus a living simulation can be used [1-4].

2. HISTORICAL DEVELOPMENT OF SIMULATION

The history of the simulation comes from the Chinese War Games called "WEICH", that is, 5000 years ago and continues until the 1780s, until the Prussians used these games on the trains of their armies. Since then, heads of all military forces have used wargames to test military strategies under simulated environmental conditions [5].

Having one of the largest armies in the world, the Roman Empire trained both groups of soldiers on how to fight in an unfamiliar terrain by dividing their armies into two different colours as blue-red and creating the conditions of war. Leonardo Da Vinci (1452-1519), one of the important artists of the Renaissance, tested the designs of his projects and inventions using models. He created the first schematic representations of how machines work and how to assemble their parts. In 1780, Scottish John Clerk developed a method using model ships to tactically strengthen the British army's naval forces. Prussia, which was at its strongest in the 18th and 19th centuries, trained its soldiers with 1824 exercises in order to make its army professional. In 1883, W. R. Livermore carried out the first exercise in the American army. After the first unsuccessful application, Livermore's model was adopted in 1887 and the exercises continued to be used in the training of the American army from the 20th century [6]. One of the most important events in this period until the 1945s, which we can call the pre-computer period, is Buffon's needle experiment in 1777. Buffon tried to estimate the number of pi by randomly throwing needles on a plane marked with parallel lines with equal intervals [7]. During World War II, a new technique, the Monte Carlo Simulation Technique, was developed by the great mathematician Jhon Van Neumann (from military and operational games). While working with neutrons at the Los Alamos Scientific Laboratory as a quantification technique, Van Neumann Simulation was used to solve physics problems that were complex and expensive to analyse manually or with physical models. The random nature of neutrons

suggested the use of the roulette wheel to deal with probabilities. Because of the game structure, Van Neumann called the change of laws the Monte Carlo Model. With the advent and unified use of business computers in the 1950s, simulation developed as a management tool. Specialized computer languages were developed in the 1960s to handle large-scale problems more effectively. In the 1980s, simulation programs were developed to deal with sequencing situations from queued inventions. They have different names such as XCELL, SLAM, WITNESS, MAP/1 [5].

3. DEFINITION OF SIMULATION AND RELATED CONCEPTS

In the most general terms, simulation; is the shaping of reality in a computer environment by minimizing it. It is possible to encounter many more scientific and more descriptive definitions of simulation. It is possible to list a few of them as follows.

The observation of a feature or behaviour related to an event, process or system on the model is called simulation. “Simulation”; is a word meaning imitation [8]. Shannon defined simulation as “a method of designing a computerized system model and conducting experiments with this model to understand system behaviour or evaluate different strategies for managing the system” [9]. Simulation is the whole of efforts to visualize the event in a computer environment and to establish control over the event in order to examine and explain the structure and behaviour of complex real-life systems in logical and mathematical relations within an extended time period. In other words, it is a good tool that will form the basis for managers’ decisions so that they can see alternatives better [10]. “Simulation is a modelling technique that enables the behaviour of the real system to be followed in a computer model under different conditions by projecting the cause-effect relationships of a theoretical or real physical system onto a computer model” [2]. “Simulation is the process of designing the model of the real system and conducting experiments in order to understand the behaviour of the system or evaluate different strategies for the purpose of operating the system with this model” [5]. Simulation is an inevitable solution tool in solving many real problems. It is used to analyse and explain the behaviour of the system by asking “what if” questions about the real system [11].

Instead of leaving business decisions to chance, simulation provides the opportunity to test the consequences of the decisions made. In this respect, it is quite advantageous compared to the classical trial and error methods, which can be time-consuming, expensive and sometimes negative [12].

Examination of systems that cannot be experimentally examined on real dimensions on models to be established is called simulation [13].

As can be understood from the above definitions, modelling with simulation;

(1) describe the behaviour of the system,

(2) theorizing or hypothesizing,

(3) is a “trial and practice” methodology, in which the established theory is used to predict the behaviour of the actual system. [14].

Accordingly, the purposes of establishing a simulation model and analysing different systems can be listed as follows [12]:

- Detailed examination of the operation of the system
- Developing work and resource policies to increase system performance,
- Testing of new concepts and working systems without the need for real implementation,
- It allows having knowledge without making changes to the real system and without causing errors.

The simulation technique is more than a theory, it is a methodology used in solving problems. The approach of the simulation technique to the problems varies according to the structure of the system and the model to be established depending on this structure [10].

It is possible to make many definitions similar to the definitions above. More importantly, it is to open the words "system" and "model" in the definitions a little more and to make the definitions more understandable. In this section, while explaining what simulation is, system and model concepts will also be discussed in order to better understand this.

3.1. System

A new approach has emerged as a result of searches in various disciplines due to reasons such as excessive consensus in the sciences, the concept of efficiency gaining importance, automation, and the problems of automation becoming multidimensional and complex. This approach is also called the systems approach or the operations research approach. In this context, one of the most used words today is the word "system" [10].

The basic element in any simulation study is the "system" idea [9]. System; It is the whole of elements such as humans and machines that come together to reach a result and interact with each other. In fact, in practice, the meaning of the word system can be defined in different ways depending on the purpose of the study [4]. In the context of simulation work, the term system is generally defined as the collection of objects that

interact with each other in a well-defined set of [9].

Below are the different system definitions.

"A system is a collection of entities or elements that takes certain inputs and processes them appropriately and aims to maximize a function that shows the relationship between certain outputs." "A system is a collection of elements that have certain inputs and process them and output them" [15]. The system is defined by researchers as "a whole, consisting of multiple components, physical or conceptual, interrelated to achieve one or more purposes or results" [10].

A general definition for the system has also been made by the International Systems Engineering Council (INCOSE). Accordingly, the system is the aggregation of different entities to produce results that they could not achieve alone. These assets can be people, hardware, software, facilities, policies, documents, or anything necessary to produce quality, features, attributes, functions, behaviour or performance [16].

Generally, systems are shown schematically as follows.

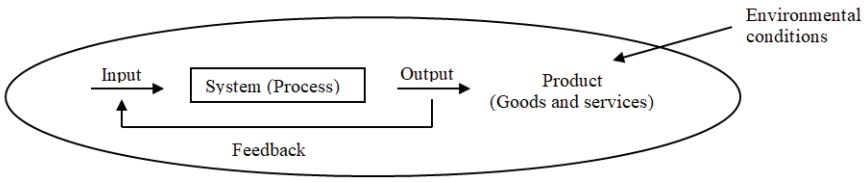

Figure 1. *Schematic representation of the system [1].*

Systems are very complex in terms of both the relations between their units (items) and their relations with the environment. In general, systems can be examined in two different groups as discrete and continuous. In discrete systems, state variables change abruptly at certain time intervals. In fact, it cannot be said with certainty that a system is discrete or continuous, and some systems can even be classified as both discrete and continuous [4].

It is possible to classify systems from different perspectives.

- Natural and artificial systems,
- Continuous (with regular changes, not splashy),
- Adaptive and non-adaptive,
- Stable (not overly affected by changes in external factors) and unstable (small changes in inputs versus large variations in outputs),
- Deterministic (cause-effect relationships are exact) and stochastic

(cause-effect relationships contain randomness) systems.

- Dynamic (the probability of transition from one state to another in system states changes over time) and static (permanent) systems [15].

Systems are studied in order to understand the relationships between the different components that make up them or to understand what their behaviour and performance will be in case of new situations [4].

The purpose of examining a system can be learning the behaviour of the system, controlling the system, renewing or preserve the system. In some cases, it may be required to extract information about what the outputs will be depending on the system for known inputs, or about the system itself (system parameters) by observing (knowing) the inputs and outputs. In some cases, the aim may be to provide controllable input to the system in order to get the desired output [15].

The main purpose of this approach; is the determination of the system and the problems in the system, and then, starting from the definition of the system, the problem in the system is handled as a whole and the possible solution options are developed. A technique that is effectively used in determining these solution options is the simulation technique [10].

Systems are subjected to experiments to understand the relationships between their components or to observe how they behave under certain conditions. It is possible to divide the experiments into two groups as indirect experiments on a real system and indirect experiments on a model of the system. Figure 2 shows the paths that can be followed in experiments on a system [17].

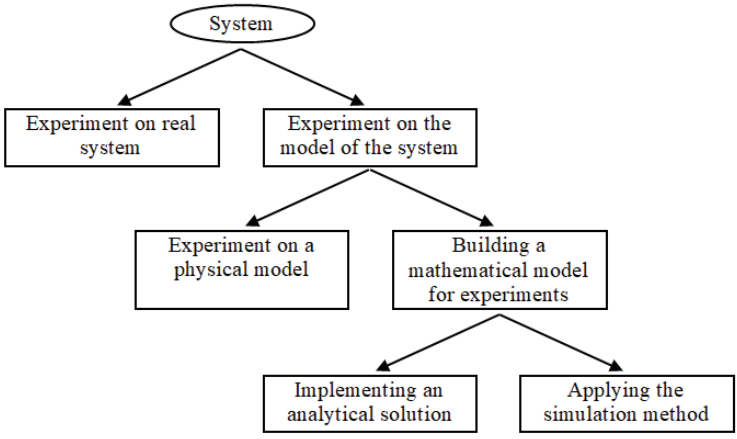

Figure 2. *Ways of working on the system*

The path that can be followed while working on a system depends on the questions to be answered by the system and the available facilities and tools. Comparisons of the alternatives at each level of the pathways shown in Figure 2 are given below in items [17].

- Comparing experimenting on a real system versus experimenting on a model of the system: Experimenting on a real system is most convenient if possible and if it is cost-effective. Because in this way, no one has any doubt about the accuracy of the work done. However, it is often not possible to do such a study, as it will be very costly or have a damaging effect on the system. For example, trying to determine how many employees are needed by playing with the number of customer service personnel in a bank will cause customers to wait, and customers will not be very satisfied with such a situation. At the same time, the system being studied may not exist, and we may wonder what the consequences of the different configuration alternatives of this system will be. In such a case, creating a model is a must. For example, the most natural way to learn the effect of a nuclear bomb on the atmosphere is to create a model.
- Comparing the physical model with the mathematical model: When it comes to models, most people think of physical models such as ship models floating in pools, automobile models whose aerodynamic structures are tested in air tunnels. But most models are modelled mathematically. In mathematical models, logical and quantitative relationships between system components are expressed in mathematical language. For example, the path taken by a car traveling at a constant speed on a road is established as a mathematical model based on the relationship between speed and time (distance = speed x time).
- Comparison of analytical solution and simulation method: Naturally, a model is created to answer a set of questions. Therefore, as soon as we create a mathematical model, we should look at whether we will use the model to answer these questions. If the model is simple enough, the relationships and quantities in the model make the analytical solution possible. For example, as in the (distance = speed * time) model, the answer to the question of how far is the distance is found by operating the product of speed and time. However, it is obvious that this model is a very simple and analytical solution is possible even with only pen and paper. However, many real-life systems are very complex, so useful models of these systems are also complex and analytical solutions are hardly possible. As a result, these models are handled with

the simulation method. The simulation method is the imitation of the quantitative relations between the components of the system in the computer environment. However, an analytical solution of a model should always be preferred to the simulation of the analytical solution if it is possible and has an acceptable solution time. Therefore, simulation is considered a last resort. However, most mathematical models are studied using the simulation method, and for this reason, these models are called simulation models.

As stated earlier, the supply chain is a dynamic system consisting of components with conflicting objectives. At the same time, the structure of the supply chain differs from industry to industry and from company to company. Therefore, it is necessary to use mathematical modelling approaches to examine the behaviour of the supply chain system under different conditions and to produce optimum solutions [17].

3.1.1. Simulation Study on Systems

Any system can be simulated under different conditions. According to the characteristics of these conditions, a simulation study can be done in Deterministic and Stochastic Systems.

1 a. Simulation Study in Deterministic Systems

Often when the system is very complex and continuous, the values of other variables of the system can be calculated for different conditions when the value of one of the variables is known to recognize the system.

When there are discontinuous and independent equations describing the system, we can simulate using one of the well-known optimization methods to find the best solution and solutions.

Simulation is perhaps not the best solution in the system. This way gives confidence when all possible values are found. Simulation is the predictive solution that provides benefits.

The decision-maker operates the trial solutions and observes the resulting values. It does this until it finds the predictive value.

1.b. Simulation Study in Stochastic Systems

Simulation in management science often deals with the use of stochastic models that model reality. In a simulation model, the outputs cannot be predicted with certainty from the inputs, but the results may depend on several probability distributions. The coin flip is a process just like this one. Although money is a fair coin, we cannot predict in advance that the result will be 50% coin flips.

The models we will deal with will be finite models, that is, they will consist of a finite number of outcomes and values. Simulation models can also be continuous. In these, the values are not limited by the boundaries of probability distributions. We can distinguish between these two models with the example of two separate jars filled with 6 different coloured marbles and many peas. If a marble is drawn from a jar full of marbles, one of 6 colours will appear, this is a limited model. However, if pea is pulled from a jar full of peas and its weight is weighed precisely, it is obvious that we will see peas of different weights. [1,5].

3.2. Model

The simulation of a system is the imitation of the operation of the system over time. The tool for this is the "model". In other words; “Simulation of a system is the process of building a model that can represent a system. This model allows performing operations that are too expensive or impossible to perform on the system it represents. Properties and reactions related to the behaviour of the real system or its subsystems are predicted” [13].

A model is a simplified description of any system, state, or process, often expressed in mathematical terms, to facilitate calculations and predictions [18].

With another definition, the model; is a simplified representation of a system at a particular point in time or in a designed space to facilitate understanding of the real system [19]. According to Banks et al., the model is the description and abstraction of systems [6]. Shannon defines the model as a certain representation of a group of objects or ideas by entities other than itself [20]. Sanchez, on the other hand, defined the model as a system that we use as a replica of another system [21].

A model is an abstract representation of a real event that exists outside of our thought process. Models are an intermediate stage of the abstraction process that creates a more intelligible picture of the complex real-world situation [22].

In an effort to understand and explain what is going on in the universe, human beings establish various models about the events and processes they are interested in, and by working on these models, they try to know what kind of situations may arise in the future. A model is the expression of the structure and functioning of a system in the real world, depending on the concepts and laws of the related field of science (physics, chemistry, biology, geology, astronomy, economics, sociology, ...). A model is a representation of a phenomenon in the real world. Because the real world is very complex, the models simplified the phenomena and systems they want to describe and consider them under certain assumptions. Models are

not reality themselves, and however complex they may seem, they are an understatement of reality. In short, what is called a model is a product of the model builder's "understanding" of reality, and every model building process is an abstraction process [8].

The purpose of the model; It helps us to explain, understand or improve the system. Simulation is one of the modelling types. Modelling is nothing new. Some functions of the models are listed below;

1. to help thinking,

2. to assist communication,

3. to serve education,

4. to help estimate,

5. to assisting trials [14].

Models are classified in different ways;

- *Verbal models: Words are the most common form of expression of any thought, written or spoken. However, it is not a valid way to describe the load distribution in a section of a certain column of a building in words.*
- *Schematic models: They are forms of expression such as drawings, pictures, flow charts, organizational charts, and graphics.*
- *Scale models: Expression of creating a physical similarity with a certain scale.*
- *Mathematical models:*

1. Stochastic (with random variables) and deterministic (without random variables) mathematical models

2. Linear and non-linear models

3. Continuous (differential equation,...) and discrete (difference equation,...) models.

Mathematical models are the models with the most expressive power and the most valid ones. Depending on the model builder’s perspective on the real-world phenomenon, different situations may be involved in modelling [8]. In the mathematical model of a particular system, the input is the numerical values obtained as a result of the measurements [15]. The creation of the mathematical model is one of the simulation stages. If the mathematical model is not complex, a multivariate and analytical solution is possible, the analytical solution of the model should be preferred to the simulation technique [4].

A model is deterministic if it does not contain probabilistic (stochastic) components. When the input elements and the effects of the components of the model are known, it can be found out what the result will be with some complicated calculations. However, since there is at least one random input component in many systems, they are called stochastic models and the simulation technique can be used. Many queuing and inventory systems can be examined in this context [4].

3.2.1. Modelling

Models are tools used to analyse systems. A model can be used to analyse an existing system or to describe and describe a system that is being created. Modelling; is an approach used to describe the systems studied, to create an idealized example of a real system, and to explain the basic relationships in systems [23].

Modelling is the basis for studying the behaviour of large and complex systems. The model is the description of the real system, but also the abstraction of the system. By abstraction, the model deals with the part of the purpose that is intended to be achieved. The boundaries and details of the model should be determined in accordance with the determined purpose [11].

Modelling is an essential part of any scientific activity. Many scientific disciplines have views on certain types of modelling. There is a growing interest in scientific modelling, particularly in philosophy of science, systems theory, and information visualization systems. The scientific model seeks a logical and objective representation of experimental objects, phenomena, and physical processes. Although all models are a simplified representation of reality and inherently flawed, they are very useful.

Modelling is the process of creating abstract, conceptual, graphical or mathematical models. A model can be defined as a simplified representation of a system at a certain point in time or in a designed space to facilitate understanding of the real system [19].

According to another definition, modelling is the creation of a simplified version of a complex system to make predictions about system performance measures. This simplified form is called a model [24].

Simulation is the process of designing a real system model and experimenting with this model in order to understand the system or evaluate different strategies for the operation of the system. Therefore, model building and analytical use of the model constitute the simulation process [14].

Before modelling a system, it is necessary to decide whether the

planned changes can be tested directly on the real system. If it can be tried, the application on the real system will give the safest and safest result [4].

Every model-building process (modelling) is an abstraction process. The process of abstraction is the transfer of images of the phenomena of the world, purified from details to human thought. In order to establish and select the model, it is necessary to know the basic features of the phenomenon or system in question, the internal relations between its units and the relations with the environment. The success of the model, its practical and scientific usefulness depend on the degree of accuracy in abstracting the essence of the phenomenon or system, and on how fundamental the features (characteristics) are considered [15].

In modelling the supply chain, it is possible to divide the modelling approaches into four depending on the purpose of the study and the nature of the data used. These approaches are:

1. Deterministic Analytical Models: In these models, system state variables are known.

2. Stochastic Analytical Models: In these models, at least one system state variable is expressed with a probability distribution.

3. Economic Models.

4. Simulation Models [25].

4. SIMULATION MODELS

The mathematical modelling of a system in a special way is called simulation modelling [26]. Models developed for the simulation of systems are classified in different ways according to the structure of the model and the characteristics of the variables they use. All these classifications are used only to express models developed for these real systems, not real systems. In other words, a system can be modelled using different types of simulations. The important thing here is to determine the most suitable simulation model type for the characteristics of the system [17].

It has been stated before that if a mathematical model is handled using the simulation method, this model is called a simulation model. It is useful to examine simulation models in three different dimensions [17].

- Static and Dynamic Simulation Models: Static simulation models are simulation models that reflect the state of the system at a certain moment or that time does not have a role. For example, Monte Carlo models are static simulation models. On the other hand, dynamic simulation models are simulation models in which time-varying systems are modelled. An example of this is simulation models of conveyor systems.

- Deterministic and Stochastic Simulation Models: If a simulation model does not contain any probabilistic components, it is called deterministic. However, in general, simulation models have at least one probabilistic input, and such models are called stochastic simulation models. Most queue and stock simulations are stochastic. Since the outputs of stochastic models will also be probabilistic, the outputs are an estimate of the characteristics. This is the most important disadvantage of simulation.
- Continuous and Discrete Simulation Models: Before talking about continuous and discrete simulation models, it is necessary to explain what a continuous and discrete system is. The set of variables that define a system at a certain time according to the purpose of the study is called the system state and these variables are called state variables. If the state of a system changes suddenly along the time axis, such systems are called discrete systems. On the other hand, if the state of the system changes continuously depending on time, such systems are called continuous systems. The definition of continuous and discrete simulation models is exactly like this. However, the use of continuous or discrete simulation models in a study depends on the purpose of the study. For example, in a traffic-flow simulation, if the movement and characteristics of each vehicle are important, a discrete simulation model is used. However, if the sum of the vehicles is evaluated at once, a continuous simulation model is created by defining the traffic flow with differential equations.

Figure 3 shows the steps for creating the simulation model [27].

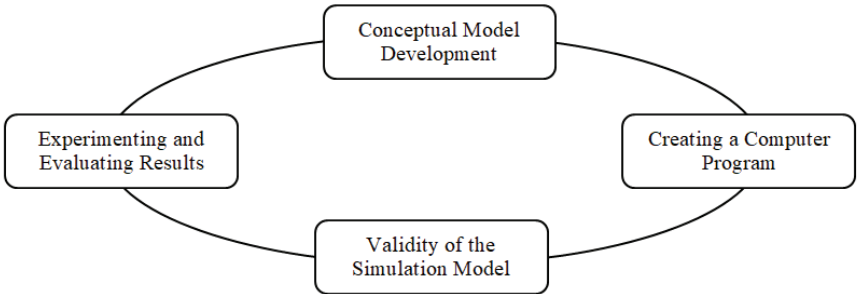

Figure 3. *Steps to create a simulation model*

Conceptual model: It is the explanation of the simulation model that is planned to be developed.

Creation of the computer program: It is the creation of the designed conceptual model on the computer [28].

Validity of the system: The results of the simulation model created for a specified target are compatible with the results of the real system.

Experimenting and evaluating the results: It is the execution of experiments on the model established and proven to solve a problem or achieve a goal and evaluate the results [27].

4.1. Simulation Model Properties

The characteristics of a good simulation model are:

1. Simulation is about the operations of the system.

2. Simulation is about solving real-world problems.

3. The simulation is done for the benefit of the services that are under the control of the system and related to the behaviour of the system.

If these are briefly explained; The systems of interest are goal- or goal-oriented. This necessitates that we should be closely concerned with the goals and objectives of a system while trying to build a model. In order to establish the appropriate model, the objectives of the system and the model must be constantly kept in mind. It should be ensured that the result obtained with the simulation reflects the real situation in real terms. Any model should be examined from the extreme values of its parameters and variables. If meaningless conclusions are drawn, it is imperative to suspect and revise the model. Finally, an important point is not to forget the users of the derived information. A model that is not used or not usable by the decision-maker cannot be defended in any way.

For a model to achieve its purpose and to be a good model, it must contain two important features: realism and simplicity. That is, a good approach that shows all the important features of the real system on the one hand, and on the other hand, must be understandable and solvable. But unfortunately, they can't be close to the truth.

After these explanations, what is expected from a good simulation model can be listed as follows:

- It should be easily understood by the user.
- It should be purpose and/or target oriented.
- It should be strong enough not to give meaningless results. It should be easy to control and operate by the user.

- It must be complete.
- It should be easily adjustable for model change and updating.
- It should be evolutionary, that is, it should start out simple and get progressively more complex [13].

4.2. Structure of the Simulation Model

Almost all simulation models consist of the following elements:

- Components: These are the parts that make up the system when they are put together. Their combined performance gives the output of the system. For example, components in an urban system, education system, health system, etc. can be counted as.
- They are the properties of the system. They take different values in different conditions and in different system states. Variables can be classified into four opposing categories:

1. Independent and dependent
2. Auditable and non-auditable
3. Intrinsic and extrinsic
4. Input and output

- Parameters: These are the quantities that the simulator can give arbitrary values. They cannot be changed during a harness. They remain constant For example, in an equation like Y=3X, 3 parameters. Y and X are variables.
- Relationships: Relationships are the connections between the components, variables, and parameters of the system. They monitor changes in the state of the system. Relationships show how the values of different variables in the system are related to each other and the values of the parameters of the system. Relationships that may exist in the system can be classified as follows:

1. Structural relationship
2. Functional relationship
3. Sequential
4. Spatial
5. Temporal
6. Cause-effect
7. The relationship of conservation of energy

8. Logical relationship
9. Mathematical relation

- Assumptions: These are the assumptions that abstract the model from the real situation. With the assumptions made on the assumptions, the degree of abstraction of the model will also change.
- Constraints: Limitations on the values of variables and how resources are allocated. These constraints may be in the nature of the system as well as set by the designer. It is possible to manipulate, tighten and loosen the constraints set by the designer.
- Criteria: The criteria function is a state of the system's goals or objectives and how they will be evaluated. The criterion can be defined as the standard of judgment. Accordingly, the criterion function gains importance in two aspects. First, it has a great influence on the design and operation of the model. Second, misidentifying the criterion will give the wrong result [13].

5. ADVANTAGES AND DISADVANTAGES OF USING SIMULATION TECHNIQUE

5.1. Advantages of Simulation

When the simulation is used to make improvement studies on an existing system, scenario analyses can be performed on the model without making any changes to the existing system. Imaginary objects and resources in the simulation model both provide greater flexibility in evaluating the results of changes to the system and are less costly than real investments. In the design of a new system, tests of the system can only be made on a model to be created for the system, because a real system does not yet exist. Simulation significantly reduces the time spent on fault finding and "fine-tuning" of the system required during the installation phase of the system.

Computer simulation is a rapidly popular tool in system design and analysis. Simulation helps engineers and planners make timely and intelligent decisions regarding system design and operation. Simulation alone cannot solve problems but clearly defines the problem. Evaluates alternative solutions numerically. Before installing a new system or testing business policies, it helps us to foresee many pitfalls that may be encountered when the system is first started by modelling the system on the computer. In order to obtain a good product during the commissioning phase, the studies that take months or even years are compressed into days or even hours with simulation.

Simulation is a modelling technique that enables the monitoring of real system behaviours in a computer model under different conditions by transferring cause-effect relationships in the system to the computer. The simulation process also produces a statistical summary of all movements in the model. The results after running the simulation give measurable values for system performance. From this point of view, a simulation is an evaluation tool [2].

Along with the above, the advantages of simulation can be summarized as follows:

1. It allows controlled experimentation. A simulation experiment can be performed multiple times with varying input parameters to test the behaviour of the system under varying states and conditions.

2. Allows time comparisons. With ultra-fast computers, system administration is simulated in minutes.

3. Allows precise analysis by managing input variables.

4. It does not change the normal state of the actual system. This is a huge advantage because many administrators may be reluctant to try experimental strategies on an online system.

5. It is an effective educational tool [9].

6. Simulation methods are suitable when the system data is not detailed.

7. Data for later analysis on the simulation model is often obtained more cheaply than in real life.

8. Simulation provides the ability to study and experiment with complex internal interactions in a system.

9. The detailed observation of the simulated system (which is one of the necessary processes while simulating the system) can provide a better understanding, eliminate the previously unseen deficiencies, and establish a more effective physical and operational system.

10. Simulation can be used to experiment with new situations for which we have little or no data about how the system will behave under different conditions.

11. The simulation can be used to verify the accuracy of analytical solutions.

12. With simulation, the real time of dynamical systems can be studied in a narrowed or expanded time.

13. Simulation forces analysts to think more broadly [14].

14. Simulation allows a system to run over a long period of time and to examine the results.

15. Simulation can be used to predict and evaluate the performance of an existing system under anticipated operating conditions.

16. Simulation can be used to select alternative policies for a system or alternatively to evaluate proposed system designs. In simulation, it is possible to establish control over the experimental conditions to a greater extent than with the system itself [4].

17. The data required for simulation is often obtained very easily.

18. We can examine the behaviour of the system under changing conditions and new situations [5]

19. By using the animation features of the simulation, it is possible to see the activities from various angles, zooming in and out as much as desired, or in three dimensions. It also plays an important role in the detection of errors in the simulation model [11].

20. Simulation makes it possible to hide secondary effects such as faults and minor deviations that are inevitable in the measurement of system performance. Being able to exclude such effects from the system when desired provides a better understanding of these effects [29].

5.2. Disadvantages of Simulation

The development of successful simulation models is expensive, time-consuming and requires skill. If the established model is not solved correctly, it may produce wrong results. Building a simulation model is noted by many authors as an art. In general, model building is an art rather than a science [14].

One of the obstacles that prevent the simulation from being a well-used and universally accepted tool is the long model development time, and the other is the modelling capability required to develop a successful simulation. The pace of change and development of simulation has gained great momentum in recent years and it will continue to progress rapidly in the coming years.

Simulation models are often expensive and modelling a system is time-consuming. It also requires the use of specialized personnel.

The production of many numbers as a result of the simulation work and the persuasive effect created by the realistic animation generally tend to create a great deal of confidence in the results of the work. If the model is not a suitable representation of the studied system, however impressive the simulation results may seem, it will provide little useful information

about the real system [4].

Along with the above, the disadvantages of simulation can be summarized as follows:

1. Considerable time evolution can be encountered. Most simulation models are quite large and take time like other large program projects.

2. Hidden critical predictions may distract the model from reality. Ideally, this event occurs during the validation phase of the simulation process.

3. Model parameters can be difficult to actuate. Collection, analysis and interpretation can require a lot of time [9].

4. A simulation model can be expensive in terms of manpower and computer time. In general, there is a need to write a separate program for each system. Simulation languages have eliminated these drawbacks to some extent [9, 14].

5. Running an installed simulation program on the computer may take a lot of time. This has a high cost.

6. After the researchers learn the simulation technique, they tend to use it in more appropriate situations than analytical methods [14].

7. Modeling with simulation requires more expertise than writing a computer program or using a software package. Conceptual modelling, statistics, accuracy and validity, project management and working with people, etc. You must have many skills.

8. Inexperienced model builders focus too much on simulation software and technology, add too much detail to the model, and spend too much time in model development, causing the project's goals and timeline to be forgotten [1].

6. USAGE AREAS OF SIMULATION

The ability of the simulation to collect a large number of variables with a large number of features in a single model makes it an indispensable tool for the design of today's complex systems. The possible combinations, permutations, and consequent performance evaluations of workpieces, tools, pallets, transport vehicles, transport routes, processes, etc., in a production system are virtually endless. The computer system has become a necessity for designing practical systems. Planning customer flow for service systems, personnel management, resource management and simulating information flow is as important as production systems [2].

The simulation was first used as a planning tool in new production projects or extensive renovation projects. Recently, however, some

organizations simulation has been used for the purpose of optimizing operations in use. Simulation applications are on the way to become an integral part of the daily operations of factories and their application area is expanding [13]. Computer simulation is accepted as an alternative to traditional design and testing methods in the scientific field, electronics, education and business environments. The decrease in the price of simulation programs and the increase in their capabilities have made simulation a suitable tool for many private sector enterprises and public enterprises. Balancing assembly lines, designing processes in terms of time, deploying and dispatching fire brigades to different locations, design of distribution systems, personnel recruitment systems, design of traffic lights, etc. Simulation is used in production management issues such as [13].

Simulation is a technique that can be applied in many branches of science and there are many publications on this subject. For example, management, economics, marketing, education, politics, social sciences, behavioural sciences, transportation, workforce, urbanism, global systems, etc. application areas can be shown [14]. Examples of areas where simulation can be applied are design and analysis of production systems, evaluation of computer software and hardware requirements, evaluation of new military weapon systems, determination of order policies of inventory systems, design of communication systems and their message protocols, operation and design of transportation services, hospital or restaurant. determination of the designs of service organizations, such as the analysis of economic and monetary systems, etc. [4].

When used primarily as a design tool, whether designing a new system or improving an existing system, simulation can be used in the following areas:

- Selection of Methods: Will all activities take place on a workstation or will they be divided into specific operations?
- Technology Selection: What are the implications of choosing automation over manual processing?
- Optimization: What is the optimum number of resources to achieve the best performance objectives?
- Capacity Analysis: What is the output capacity of the system?
- Control System Decisions: Which work should be assigned to which resource [2].

Simulation can be applied to many aspects of production systems, but it stands out in two areas in particular;

1. At workplaces: Simulating shipping rules and evaluating the impact of different rules on the workplace's ability to use machines and meet distribution deadlines.

2. On production lines: Examining to what extent the loss of interstage intermediate stocks in the output of the line can be reduced due to malfunctions in the workstations [18].

If we look at the general application areas related to production, we can briefly summarize these areas as follows; capacity analysis and planning, equipment and personnel planning, resource needs analysis and planning, bottleneck and throttling analysis, production planning, schedule optimization, inventory method, logistics planning, layout optimization, arrangement of maintenance and protection, detailed and complex resource modelling, delivery performance analysis, engineer and technician on-the-job and process training, new operator training [2]

Non-production application areas of simulation can also be summarized as follows; bank, post offices, computer systems, medicine, education, electronic etc. [13]

The following are examples of many problems that can be addressed with a simulation study in terms of system design and management.

System Design Decisions:

- What number and type of machines or work centres should be used?
- What number and type of auxiliary equipment and operators are needed?
- How many tools and moulds are needed?
- What is the current system throughput rate?
- What number and size of material handling systems should be used?
- What is the optimum number and size of warehouse buffer zones?
- What is the best layout of business centres?
- Which is the most effective control logic?
- What is the optimum loading amount?
- What are the effective usage percentages of available resources?
- What is the effect on a whole production of a different process or method?
- How balanced is the workflow?

- What are the bottleneck operations and resources?
- What is the effect of machine failures on production? (reliability analysis)
- What is the effect of machine setup times on production?
- What is the effect of general and local storage systems on the system?
- What effect does the speed of conveyor belts or vehicles have on the flow of parts?
- How many maintenance staff do we need?
- What effect does automation of an operation have on the system? [2]

System Management Decisions

- What is the number of shifts required to meet production needs?
- What is the optimum production lot size?
- What is the optimum scheduling rule required to meet production?
- What is the best timing for preventive maintenance?
- What are the best priority criteria to use to select a job?
- What is the best way to distribute resources among specific jobs?
- What is the total time that jobs spend in the system?
- What is the effect of different product combinations on production?
- How much of a production plan can be met?
- What impact might a particular inventory policy have on production? [2]

7. SIMULATION PROCESS

Any simulation study can consist of several different main stages. Some simulation studies may not consist of all of these stages and may not occur in the order that will be expressed here [30]. The simulation modelling process has many stages such as defining the project and determining the objectives, collecting data and establishing the conceptual model, displaying the model in the digital environment, performing experiments with the model, and documenting the project. This process is a process in which the steps tend to be repeated continuously by selecting different scenarios and performing experiments after the steps such as designing

a model, defining a scenario, performing an experiment, analysing the results. The simulation modelling process is information and data-intensive process [31]. The flow steps of the simulation study are shown in Figure 4 [7].

8. USING SIMULATION IN THE APPAREL INDUSTRY

Simulation, which has a wide range of uses and is one of the scientific decision-making tools, has different application areas in the ready-made clothing industry. For example, the capacity estimation to be made during the establishment of a new enterprise, feasibility studies and how the enterprise to be established will react to changes in demand can be easily measured using simulation technique. Firms interested in the establishment of production facilities frequently use this approach [1].

The simulation will facilitate the use of new methods and technologies in the ready-made clothing industry, and will greatly benefit the establishment of today's rising values of cost, speed, quality and unconditional customer satisfaction philosophies in businesses.

What these applications will bring to the ready-made clothing industry can be easily and cheaply understood with the simulation technique. In addition, this method will make it easier for the manager to make decisions on many issues. Simulation can be used in many subjects, from buying a new machine to investigating and eliminating the causes of decreases in performance criteria [13].

In parallel with the explanations above, when the studies on the use of simulation in ready-made clothing are examined, it is seen that these studies are mostly carried out on assembly line balancing [32-46]. The studies carried out other than the assembly line balancing studies can be listed as follows; 3D virtual garment fit simulation [47-49], 3D virtual garment simulation [50-53], Spatial visualization in clothing design [54], Pattern preparing with 3D simulation [55], 3D visualization [56], Custom garment design and simulation, [57-60], Simulation in Online Clothing Shopping and Virtual Experiment in Consumer Preferences [61], Modeling and simulation techniques for garments [62],Garment supply chain simulation studies [63-66].

Figure 4. *Simulation flow steps.*

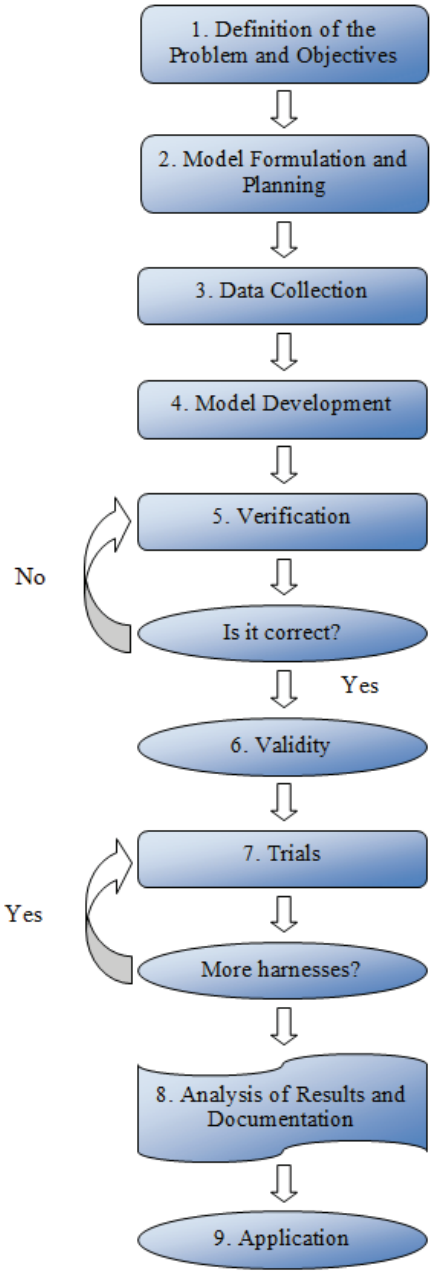

Note: *This book chapter was produced from* ***Mahmut KAYAR****'s* ***Master's thesis*** *titled "****Comparison of Different Production Technologies' Productivity in Jean Trousers Sewing by Simulation Technique****", which he prepared in the Marmara University Institute of Pure and Applied Science, Textile Education Program in 2003.*

REFERENCES

1. Kayar, M.: "Kot Pantolon Dikiminde Farklı Üretim Teknolojileri Verimliliğinin Simülasyon Yöntemiyle Karşılaştırılması", MSc Thesis, Marmara University Institute of Pure and Applied Sciences, Istanbul (2003).
2. www.uytes.com.tr (Accessed: February 2003).
3. Colella, A.M., O'Sullivan, M.J., Carlino, D.J.: "System Simulation", Massachusetts, D. C. Heath, pp. 1-10, (1974).
4. Kuş, P.: "Sistem Simülasyonu ve Uygulamaları", Bilim Dergisi, Kara Harp Okulu Yayınları, 2, pp. 53 – 57, (2000).
5. www.bilgibirikimi.tripod.com/simulasyon.htm (Accessed: May 2003).
6. Sokolowski J., Banks, C.: "Principles of Modeling and Simulation: A Multidisciplinary Approach". John Wiley & Sons, Inc, New Jersey, (2009).
7. Yılmaz, A.: "Esnekliği Sağlamak Amacıyla Üretim Süreçlerinin Simülasyon Yöntemi İle Yeniden Düzenlenmesi", PhD Thesis, Marmara University Institute of Pure and Applied Sciences, Istanbul (2013).
8. Özbek, L.: "Yeniden Pi", Pivolka 2(5), pp. 8-11, (2003).
9. Graybeal, W.J., Pooch U.W.: "Simulation: Principles and Methods", Winthrop Publishers Inc., Massachusetts, pp. 1-11, (1980).
10. Öztürk, L.: "Simülasyon Tekniğinin İncelenmesi ve Bir Monte Carlo Çalışması", MSc Thesis, Marmara University Institute of Social Sciences, Istanbul, pp. 4-19, (1997).
11. Banks, J.: "Handbook of Simulation: Principles, Methodology,Advances, Applications and Practice", John Wiley & Sons, Inc., Canada, (1998).
12. Chung, C.A.: "Simulation Modeling Handbook", 1st Edition, CRC Pres., USA, (2004).
13. Kıpır, Ş., Candan, C.: "Simülasyon: Tekstil Sektörüne Yönelik Bir Uygulama", Journal of Tekstil & Teknik, pp. 193 – 200, (2001).
14. Halaç, O.: "İşletmelerde Simülasyon Teknikleri" , Alfa Press, İstanbul, 3, pp. 1 – 8, (1998).
15. http://eros.science.ankara.edu.tr/~ozbek/model.htm (Accessed: December 2002).
16. Sokolowski J., Banks, C.: "Modeling and Simulation Fundamentals: Theoretical Underpinnings and Practical Domains", John Wiley & Sons Inc., Suffolk, (2010).
17. Law, A.M., Kelton, W.D.: "Simulation Modeling and Analyis", McGraw-Hill, USA, (1991).

18. Carrie, A.: “Simulation of Manufacturing Systems”, Department of Design, Manufacture and Engineering Management, University Of Strathclyde, John Wiley & Sons, pp. 1-13, (1998).

19. Gupta, N., Bhura, K.: “Introduction to Modeling and Simulation”, International Journal of IT, Engineering and Applied Sciences Research (IJIEASR), 2, (4), pp. 45–50, (2013).

20. Shannon, R.: “Introduction to the Art and Science of Simulation”, Proceedings of the 1998 Winter Simulation Conference, Washington, (13-16 Dec 1998)

21. Sánchez P.: “As Simple As Possible, But No Simpler: A Gentle Introduction to Simulation Modeling”, WSC 06. Proceedings of the 2006 Winter Simulation Conference, Monterey, CA., (3-6 Dec. 2006).

22. http://www.yildiz.edu.tr/~oeyeci/drsDosya/sat/BTP209_SAT_d1.pdf (Accessed: 20.August 2014).

23. Blanchard, B.S., Fabrycky, W.J.: “System Engineering and Analysis”, Prentice Hall, USA, pp. 143-149, (1998).

24. Altiok, T., Melamed B.: “Simulation Modeling and Analysis with Arena”,1, Elsevier Inc., New Jersey, (2007).

25. Beamon, B.M.: “Supply Chain Design and Analysis : Models and Methods”, International Journal of Production Economics, 55, pp. 281 – 294, (1998).

26. Gürkan, P.: “Dokuma İşletmelerinde Simülasyon Modelleme Tekniğinin Uygulanması”, MSc Thesis,, Ege University, Graduate School of Naturel and Applied Science, İzmir, (2004).

27. Pidd, M.: “Computer Simulation in Management Science”, 5th Edition, Johnson & Wiley Books, USA, (2004).

28. Robinson, S.: “Simulation: The Practice of Model Development and Use”, 1st Edition, Wiley, New York, (2004).

29. Fritzson, P.: “Introduction to Modeling and Simulation of Technical and Physical Systems with Modelica”, A John Wiley & Sons, Inc. Publication, New Jersey, (2011).

30. Wayne L. Winston: “Operations Research Applications And Algorithms”, Pws - Kent Publishing Company, Boston, pp. 1155, (1991).

31. Centeno, M., A.: “An Introduction to Simulation Modeling”, Proceedings of the 1996 Winter Simulation Conference, Coronado, (8-11 December 1996).

32. Cocks, S., Harlock, S.: “Computer-Aided Simulation of Production in the Sewing Room of A Clothing Factory”, Journal of Textile Institute, Vol. 80, pp. 455-463, (1989).

33. Fozzard, G., Spragg, J., Tyler, D.: "Simulation of Flow Lines in Clothing Manufacture, Part 1: Model Construction", International Journal of Clothing Science And Technology, Vol. 8, No. 4, pp. 17-27. (1996).

34. Zielinski, J., Czacherska, M.: "Optimisation of the Work of a Sewing Team by Using Simulation", Fibres&Textiles in Eastern Europe, Vol. 12, No: 4(48), pp. 78-83, (2004).

35. Rajakumar, S., Arunachalam, V., Selladurai, V.: "Simulation of Workflow Balancing in Assembly Shopfloor Operations", Journal of Manufacturing Technology Management, Vol.16, pp. 265-281, (2005).

36. Kursun, S., Kalaoglu, F.: "Line Balancing By Simulation in a Sewing Line", Tekstil ve Konfeksiyon, Vol. 3, pp. 257-261, (2010).

37. Kursun, S., Kalaoglu, F.: "Simulation of Production Line Balancing in Apparel Manufacturing", Fibers&Textiles in Eastern Europe, Vol. 17, pp. 68-71, (2009).

38. Kursun, S., Dincmen, M., Kalaoglu, F.: "Production Line Modelling in Clothing Industry by Simulation", Tekstil ve Konfeksiyon, Vol. 58, No. 5, pp. 186-195, (2009).

39. Eryuruk, S.H.: "Clothing Assembly Line Design Using Simulation and Heuristic Line Balancing Techniques", Tekstil ve Konfeksiyon, Vol. 4, pp. 360-368, (2012).

40. Guner M., Unal C.: "Line Balancing in the Apparel Industry Using Simulation Techniques", Fibres& Textiles in the Eastern Europe, Vol. 16, No.2, pp. 75-78, (2008).

41. Md. Mominul Islam, H.M. Mohiuddin, Syimun Hasan Mehidi, Nazmus Sakib: "An Optimal Layout Design in an Apparel Industry by Appropriate Line Balancing: A Case Study", Global Journal of Researches in Engineering, Vol. 14, Issue:5, Version 1.0 pp. 35-43, (2014).

42. Kayar, M., Akalin, M.: "Comparing the Effects of Automat Use on Assembly Line Performance in the Apparel Industry by Using a Simulation Method", Fibres & Textiles in Eastern Europe, 23, 5(113), pp. 114-123, (2015).

43. Kayar, M., Akalın, M.: "Comparing Heuristic and Simulation Methods Applied to the Apparel Assembly Line Balancing Problem", Fibres & Textiles in Eastern Europe 24, 2(116), pp. 131-137, (2016).

44. El-Hawary, I.I., El-Gholmy, S.H., Momtaz, H.M.: "Balancing the Multi-product Garment Production Line Using the Simulation Technique", Textile Bioengineering and Informatics Symposium Proceedings, (2019).

45. Bongomin, O., Mwasiagi, J.I., Nganyi, E.O., Nibikora, I.: "Complex Garment Assembly Line Balancing Using Simulation-Based Optimization", Engineering Reports. 2:e12258, (2020).

46. Bongomin, O., Mwasiagi, J.I., Nganyi, E.O., Nibikora, I.: "Simulation Metamodeling Approach To Complex Design Of Garment Assembly Lines". PLoS ONE 15(9): e0239410, (2020).

47. Eunyoung, L., Huiju, P.: "3D Virtual Fit Simulation Technology: Strengths And Areas Of Improvement For Increased Industry Adoption", International Journal of Fashion Design, Technology and Education, 10:1, pp. 59-70, (2017).

48. Porterfield, A., Traci A.M.L.: "Examining the Effectiveness of Virtual Fitting with 3D Garment Simulation", International Journal of Fashion Design, Technology and Education, 10:3, pp. 320-330, (2017).

49. Ernst, M., Anke, R.: "Comparability Between Simulation and Reality in Apparel: A Practical Project Approach from 3D-Body Scan to Individual Avatars and from 3D-Simulation in Vidya to Fitted Garments", 2nd International Conference on 3D Body Scanning Technologies, Lugano, Switzerland, (25-26 October 2011).

50. Kim, D-E., LaBat, K.: "An Exploratory Study of Users' Evaluations of the Accuracy and Fidelity of a Three-Dimensional Garment Simulation". Textile Research Journal, 83(2), pp. 171–184, (2013).

51. Kim, D-E., LaBat, K.: "Consumer Experience İn Using 3D Virtual Garment Simulation Technology", The Journal of The Textile Institute, 104:8, pp. 819-829, (2013).

52. Kim, M., Cheeyong, K.: "Augmented Reality Fashion Apparel Simulation Using a Magic Mirror", International Journal of Smart Home Vol. 9, No. 2, pp. 169-178, (2015).

53. Adikari, S.B., Ganegoda, N.C., Meegama, R.G.N., Wanniarachchi, I.L.: "Applicability of a Single Depth Sensor in Real-Time 3D Clothes Simulation: Augmented Reality Virtual Dressing Room Using Kinect Sensor", Advances in Human-Computer Interaction, Vol. 2020, pp. 1-10, (2020).

54. Park, J., Kim, D.E., Sohn, M.: "3D Simulation Technology as an Effective Instructional Tool for Enhancing Spatial Visualization Skills in Apparel Design", International Journal of Technology and Design Education, Vol. 21, pp. 505–517 (2011).

55. Baytar, F.: "Apparel CAD Patternmaking with 3D Simulations: Impact of Recurrent Use of Virtual Prototypes on Students' Skill Development", International Journal of Fashion Design, Technology and Education, 11:2, pp. 187-195, (2018).

56. Efendioglu, N.O., Mutlu, M.M., Pamuk, O.: "An Investigation on Usability of 3D Visualization and Simulation Programs in Leather Apparel", The Journal of The Textile Institute, (2021).

57. Zhenbin, J., Juan, G., Xinyu, Z.: " Fast Custom Apparel Design and Simulation for Future Demand-Driven Manufacturing", International

Journal of Clothing Science and Technology, Vol. 32 No. 2, pp. 255-270, (2020).

58. Satam, D., Liu, Y., Lee, H.J.: "Intelligent Design Systems for Apparel Mass Customization", The Journal of The Textile Institute, 102:4, pp. 353-365, (2011).

59. Kang, Z.Y., Cassidy, T.D:, Li, D., Cassidy, T.: "Historical Costume Simulation". In: 2014 international Textiles & Costume Culture Congress, Chonbuk National University, South Korea, (25-26 October 2014).

60. Kang, Z.Y., Cassidy, T.D:, Cassidy, T., Li, D.: "Historic Costume Simulation and its Application". In: 15th Autex World Textile Conference, Bucharest, Romania, (10-12 June 2015).

61. Lim, H-S.: "Analysis of Utilization of Virtual Try on Simulation and Consumers' Preference in Apparel Online Shopping", Fashion & Textile Research Journal, Vol. 14(1), pp. 83-89, (2012).

62. Wong, S-K.: "8 - Modeling and Simulation Techniques for Garments", Editor(s): Jinlian Hu, In Woodhead Publishing Series in Textiles, Computer Technology for Textiles and Apparel, Woodhead Publishing, pp. 173-199, (2011).

63. Backs, S., Jahnke, H., Lüpke, L., Stücken, M., Stummer, C.: "Traditional Versus Fast Fashion Supply Chains in the Apparel Industry: An Agent-Based Simulation Approach". Annals of Operational Research, (2020).

64. Ma, K., Wang, L., Chen, Y.A.: "Collaborative Cloud Service Platform for Realizing Sustainable Make-To-Order Apparel Supply Chain". Sustainability, Vol. 10, No. 11, pp. 1-21, (2018).

65. Mehrjoo, M., Zbigniew J.P: "Impact of Product Variety on Supply Chain in Fast Fashion Apparel Industry", Procedia CIRP, Vol. 17, pp. 296-301, (2014).

66. Aihua, D., Liangxing, Y., Tangyou, l., Qingying, M.: "A Simulation Study of a Two-Echelon Apparel Supply Chain with Forecasting Error", 8th International Conference on Supply Chain Management and Information, pp. 1-6, (2010).